

# ABSTRACTS

(854-1000)

GYNECOLOGIC AND OBSTETRIC PATHOLOGY

32  
24  
2021



**854 Human Epidermal Growth Factor (HER2) Expression in FIGO3 High-Grade Endometrial Endometrioid Adenocarcinoma: Clinicopathologic Characteristics and Future Directions**Evi Abada<sup>1</sup>, Kamaljeet Singh<sup>2</sup>, M. Ruhul Quddus<sup>1</sup><sup>1</sup>*Women & Infants Hospital/Alpert Medical School of Brown University, Providence, RI, <sup>2</sup>Women and Infants Hospital, Providence, RI***Disclosures:** Evi Abada: None; Kamaljeet Singh: None; M. Ruhul Quddus: None

**Background:** Prior studies have shown significant differences in disease specific and overall survival between FIGO 1/2 & FIGO 3 endometrioid carcinomas. The HER2 protein has emerged as a potential anti-tumor target in carcinomas of the breast, gastrointestinal tract, and endometrial serous carcinomas, with combinations of the anti-HER2 agent, trastuzumab significantly improving outcomes for these patients. HER2 expression has been scarcely studied in high-grade endometrial endometrioid adenocarcinoma, and its potential as a possible therapeutic target is currently unknown. We, therefore, aimed to study the expression of HER2 in FIGO3 endometrioid carcinomas and to correlate our findings with the clinicopathologic characteristics of this tumor.

**Design:** All high-grade endometrial carcinomas diagnosed between 2016 & 2021 were reviewed. Cases diagnosed as FIGO2 endometrioid carcinoma, high-grade serous carcinoma, clear cell & carcinosarcomas were excluded. Only cases diagnosed as FIGO3 endometrioid carcinomas were included. HER2 expression by IHC was performed on 10% formalin-fixed paraffin embedded tissue and subjected to routine processing. Four micrometer sections of tissue were prepared and stained with hematoxylin and eosin (R; Polyclonal, c-erbB-2, Dako). Adequate positive and negative controls were employed. HER2 expression was interpreted as negative (0), low (1+ and 2+) or positive (3+) using the current ASCO/CAP guidelines as in the breast. Additional clinical information was obtained from the electronic medical records after IRB approval.

**Results:** Seventy-five cases of FIGO3 endometrioid carcinomas (Fig 1) were identified. HER2 was negative in 23 (30.7%) cases, low in 50 (66.7%) cases and positive in 2 (2.7%) cases (Fig 2). p53 by IHC was performed in 28 cases, with 78.6% of those showing a wild-type pattern of expression. p53 wild-type tumors were less likely to be HER2 low and more likely to be HER2 negative ( $p=0.047$ ). There was no association between HER2 expression and Endometrial Intraepithelial Neoplasia (EIN), FIGO stage, microcystic, elongated and fragmented (MELF) pattern of invasion, mismatch repair (MMR) status or other endometrial pathology (Table 1). During a mean follow-up of 28 months (range:1-68), there was one reported death (1.3%).

Table 1: Patient Characteristics and Correlation of Clinicopathologic Parameters with HER2 Status

	All (n=75, except p53*)	P value**
<b>Age at diagnosis, mean (range)</b>	65 (43,92)	
<b>Follow up, months, mean (range)</b>	28 (1-68)	
<b>Race, no. (%)</b>		
White	69 (92)	
Black/African American	3 (4)	
Others	3 (4)	
<b>Other endometrial pathology, no. (%)</b>		0.157
None	43 (57.3)	
Polyps	8 (10.7)	
Endometrial intraepithelial neoplasia (EIN)	15 (20.0)	
EIN + Polyps	2 (2.7)	
Adenomyosis	7 (9.3)	
<b>Lymphovascular invasion, no. (%)</b>		0.771
Absent	34 (45.3)	
Present	41 (54.7)	
<b>Lymph node metastasis, no (%)</b>		0.677
Negative	55 (73.3)	
Positive	11 (14.7)	
Not removed	9 (12.0)	
<b>Necrosis, no. (%)</b>		0.613
Absent	61 (81.3)	
Present	14 (18.7)	
<b>HER2 Results, no. (%)</b>		
Negative	23 (30.7)	
HER 2 low	50 (66.7)	
HER 2 Positive	2 (2.7)	
<b>MELF Invasion, no. (%)</b>		0.121
Absent	70 (93.3)	
Present	5 (6.7)	
<b>FIGO Stage, no. (%)</b>		0.426
1	49 (65.3)	
2	6 (8.0)	
3	18 (28.0)	

4	2 (2.7)	
<b>MMR status, no (%)</b>		0.778
Deficient/loss	34 (45.3)	
Intact	35 (46.7)	
Not done	6 (8.0)	
<b>Deceased status, no. (%)</b>		
Alive	74 (98.7)	
Dead	1 (1.3)	
<b>*p53 IHC, (N=28), no. (%)</b>		0.047
Wild type	22 (78.6)	
Mutated (null/over-expressed)	6 (21.4)	

\*\*Chi-Square test as appropriate using SPSS (version 27)

Figure 1 – 854

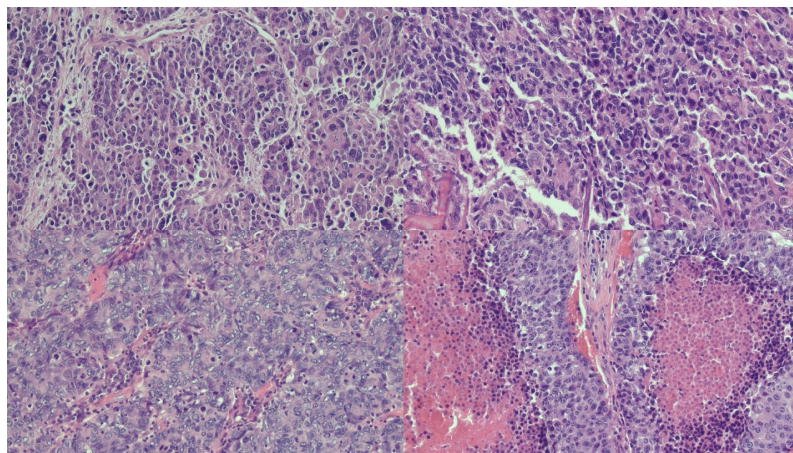
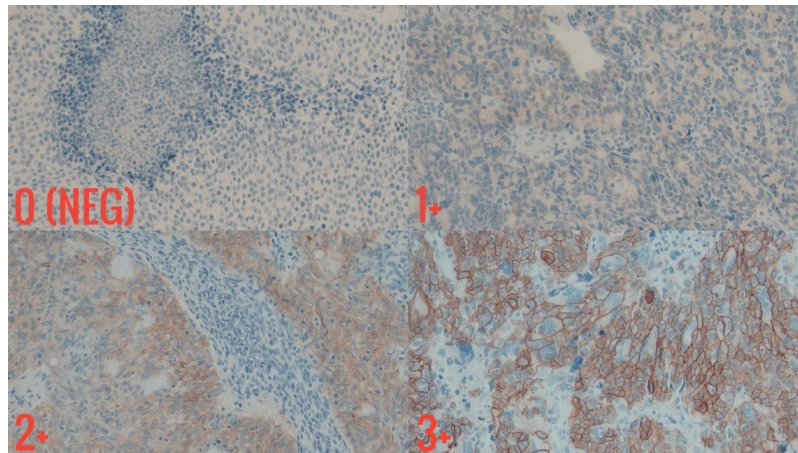


Figure 2 – 854



**Conclusions:** Based on our findings, two-thirds of FIGO3 endometrial endometrioid adenocarcinoma express the HER2/neu protein with varying intensities and anti-HER2 agents may be explored as potential therapeutic options in these patients.

**855 Low Level Expression of Human Epidermal Growth Factor-2 (HER2) in High-Grade Mullerian Tumors: Implications for Therapy Decision Making**
Evi Abada<sup>1</sup>, Jessica Claus<sup>2</sup>, Kamaljeet Singh<sup>3</sup>, Katrine Hansen<sup>4</sup>, M. Ruhul Quddus<sup>1</sup><sup>1</sup>*Women & Infants Hospital/Alpert Medical School of Brown University, Providence, RI*, <sup>2</sup>*Warren Alpert Medical School of Brown University, Providence, RI*, <sup>3</sup>*Women and Infants Hospital, Providence, RI*, <sup>4</sup>*Brown University Pathology, Providence, RI***Disclosures:** Evi Abada: None; Jessica Claus: None; Kamaljeet Singh: None; Katrine Hansen: None; M. Ruhul Quddus: None

**Background:** Reclassification of HER2 negative breast cancers to HER2 low-level expression (defined as immunohistochemistry (IHC) 1+ or 2+/Fluorescent in situ (FISH) non-amplified) allowed targeted treatment with trastuzumab- deruxtecan, anti-HER2 therapy (DESTINY-Breast04 Trail) in about 60% of patients improving their progression-free and overall survival. The high recurrence rates, ranging from 10-95% depending on the stage, unresectability, metastasis, and dismal outcomes with current therapies of high-grade Mullerian adenocarcinomas, has made it imperative to explore the utility of trastuzumab-dependent therapy for these patients. We, therefore, aimed to describe the expression of HER2 in high-grade Mullerian carcinomas, with a particular emphasis on HER2 low expression as currently defined in breast carcinomas.

**Design:** We searched our institution's database from January 2016 to December 2021 to identify all high-grade gynecologic cancers in which HER2 by IHC and/or FISH tests were previously performed. Additional clinical information was obtained from the electronic medical records after Institutional Review Board (IRB) approval. Statistical analysis was performed using SPSS (version 27).

**Results:** We identified 81 high-grade gynecologic cancers during the study time frame with previous HER2 and FISH reports. The patient demographics, type of tumor, disease stage, site of the primary tumor, clinical management, Mismatch Repair (MMR) status when appropriate, Her2 immunohistochemistry, FISH status, and follow-up data are presented in Table 1. In brief, the cohort consists of seventy (86.4%) cases that were high-grade serous carcinomas, eight (9.9%) carcinosarcomas, and three (3.7%) high-grade endometrioid carcinomas. Thirty-one (38.3%) cases were HER2 low, 17 (21%) were HER2 positive, 3 (3.7%) were HER2 2+ on IHC but had no FISH performed, and 30 (37%) were HER2 negative. HER2 expression had a significant association with primary tumor location ( $p=0.002$ ) but had no significant association with the type of cancer, race, MMR expression, FIGO stage, or deceased status. During a mean follow-up of 13.1 months (range: 1-34), 5% of the patients were deceased. Figure 1 represents Her2 score 1+, 2+, and 3+ levels of expression.

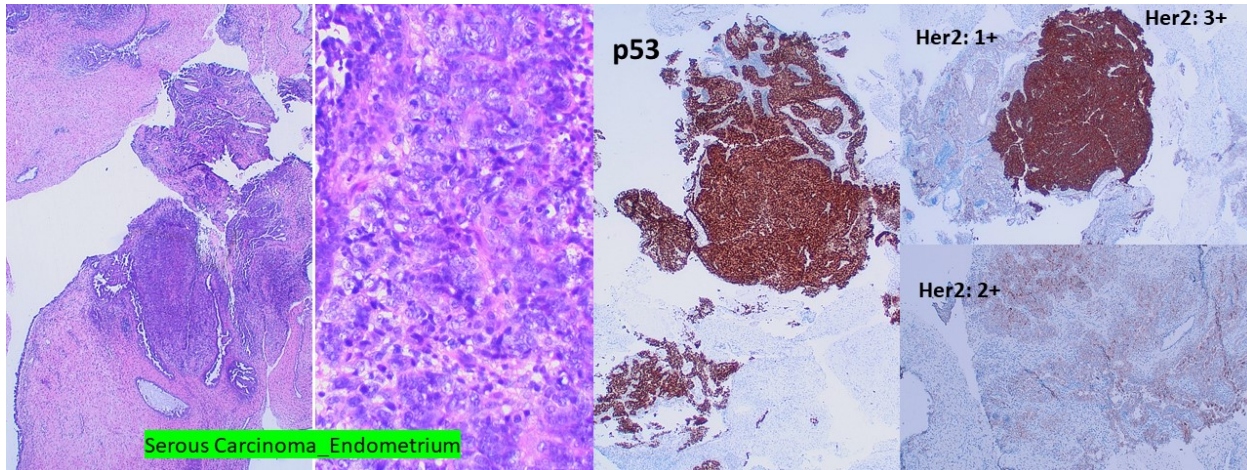
Table 1: Patient Characteristics and Hazard Ratios of Clinicopathologic Parameters with HER2 Status

	All (n=81)	Likelihood Ratio	P value*
<b>Age at diagnosis, mean (range)</b>	66.4 (43,85)		
<b>Follow up, months, mean (range)</b>	13.2 (1-34)		
<b>Race, no. (%)</b>		4.975	0.547
White	63 (77.8)		
Black/African American	7 (8.6)		
Others	11 (13.6)		
<b>Primary Tumor Location, no. (%)</b>		28.215	<b>0.001</b>
Ovary	20 (24.7)		
Fallopian tube	16 (19.8)		
Endometrium	40 (49.4)		
Peritoneum	5 (6.2)		
<b>Procedure, no. (%)</b>			
Biopsy	46 (56.8)		
Resection	35 (43.2)		
<b>Diagnosis, no (%)</b>		5.971	0.426
Serous	70 (86.4)		
Carcinosarcoma	8 (9.9)		
Endometrioid FIGO3	3 (3.7)		
<b>HER2 Results, no. (%)</b>			
Negative	30 (37.0)		
HER 2 low	31 (38.3)		
HER 2 Positive	17 (21.0)		
HER 2+ and no FISH results	3 (3.7)		
<b>FISH Results, no. (%)</b>			
Not amplified	13 (16.0)		
Amplified	7 (8.6)		
Not applicable	61 (75.3)		
<b>FIGO Stage, no. (%)</b>		8.153	0.519
1	10 (12.3)		
2	7 (8.6)		
3	23 (28.4)		
4	5 (6.2)		
Not applicable (biopsy)	36 (44.4)		

MMR status, no (%)		4.145	0.246
Intact	27 (33.3)		
Deficient	2 (2.5)		
Not done	52 (64.2)		
Deceased status, no. (%)		0.658	0.883
Alive	77 (95.1)		
Dead	4 (4.9)		

\*Chi-Square test as appropriate

Figure 1 – 855



**Conclusions:** Based on the current HER2 low recommendations in the breast, about a third of patients with high-grade Mullerian cancers might qualify for anti-HER2 therapy with a potential for improved progression-free and overall survival.

## 856 Novel Biomarkers of Immune Architecture for Predicting the Added Benefit of Adjuvant Chemotherapy Following Surgery in Early-Stage Endometrial Cancer

Arpit Aggarwal<sup>1</sup>, Sepideh Azarianpour<sup>2</sup>, Germán Corredor<sup>1</sup>, Can Koyuncu<sup>1</sup>, Pingfu Fu<sup>2</sup>, Stefanie Avril<sup>2</sup>, Haider Mahdi<sup>3</sup>, Anant Madabhushi<sup>2</sup>

<sup>1</sup>Emory University, Atlanta, GA, <sup>2</sup>Case Western Reserve University, Cleveland, OH, <sup>3</sup>University of Pittsburgh Medical Center, Pittsburgh, PA

**Disclosures:** Arpit Aggarwal: None; Sepideh Azarianpour: None; Germán Corredor: None; Can Koyuncu: None; Pingfu Fu: None; Stefanie Avril: None; Haider Mahdi: None; Anant Madabhushi: None

**Background:** Previous work has shown that features derived from the architecture of tumor-infiltrating lymphocytes (ArcTIL) are prognostic in three gynecologic cancer types (ovarian cancer, cervical cancer, endometrial cancer) and across three treatment types (chemotherapy, radiotherapy, immunotherapy). However, whether ArcTIL features suggest predictive benefit of adjuvant chemotherapy (AC) in early-stage endometrial cancer (EC) patients is not yet studied. In this work, we use ArcTIL features from H&E slides of early-stage EC and evaluate its predictive role in determining the added benefit of AC in women undergoing surgical-resection.

**Design:** Whole-Slide-Images (WSIs) of H&E surgically-resected samples from early-stage EC patients were obtained from TCGA (N=261) and University Hospitals (N=58). For training, samples from TCGA treated with AC following surgery were used (St, N=261). The added benefit of AC using ArcTIL features was validated on samples from UH by comparing patients who received AC following surgery (Sv1, N=32) against patients who underwent surgery alone (Sv2, N=26). The ArcTIL model previously developed by our group, was used for this study and a prognostic subset having 7 features was selected using the LASSO method. ArcTIL features were derived from cell cluster graphs of nuclei (epithelial TILs, epithelial non-TILs, stromal TILs and stromal non-TILs). Using these features, a Random survival forest model was trained to assign a risk of death to each patient in St. The mean risk score obtained in St was used to stratify patients as low or high-risk in Sv1 and Sv2.

**Results:** ArcTIL features were found to be associated with OS (Hazard-Ratio= 3.44 (1.14-10.4), p= 0.004 for Sv1 and Hazard-Ratio= 3.43 (1.02-12), p= 0.03 for Sv2). The high-risk patients in Sv1 and Sv2 were observed to have significantly longer survival with AC than patients who underwent surgery alone (Hazard-Ratio= 0.38 (0.08-0.98), p= 0.04 for Sv1+Sv2).

**Conclusions:** Our results found that ArcTIL features are predictive in determining the added benefit of AC in early-stage EC patients undergoing surgical-resection. Independent multi-site validation should allow for deployment of ArcTIL as a predictive decision support tool.

## 857 Does Timing of SARS-CoV-2 Infection During Pregnancy Affect Placental Pathology?

Muhammad Ahmad<sup>1</sup>, Olivier Michaud<sup>2</sup>, Hnin Ingyin<sup>2</sup>, Jiangling Tu<sup>3</sup>, Annacarolina da Silva<sup>1</sup>, Nina Schatz-Siemers<sup>1</sup>

<sup>1</sup>New York-Presbyterian/Weill Cornell Medicine, New York, NY, <sup>2</sup>New York-Presbyterian/Weill Cornell Medical Center, New York, NY, <sup>3</sup>Weill Cornell Medical College, New York, NY

**Disclosures:** Muhammad Ahmad: None; Olivier Michaud: None; Hnin Ingyin: None; Jiangling Tu: None; Annacarolina da Silva: None; Nina Schatz-Siemers: None

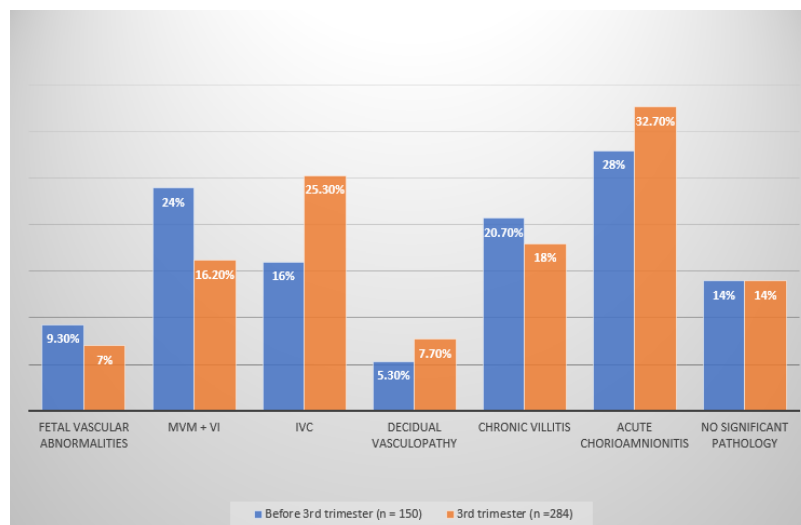
**Background:** The significance of SARS-CoV-2 infection timing during pregnancy on placental pathology is not well known. We reviewed placental pathology and clinical outcomes with reference to timing of SARS-CoV-2 infection.

**Design:** 500 placenta pathology reports from August 2021 – June 2022 with a clinical history of COVID-19 infection were reviewed and corresponding clinical data was collected.

**Results:** Of the 500 cases, 150 (30%) were positive for SARS-CoV-2 before the 3<sup>rd</sup> trimester, and 284 (57%) were positive in the 3<sup>rd</sup> trimester. Infection timing for the remaining cases was unknown. 97 (19%) patients were SARS-CoV-2 positive at delivery, all infected in the 3<sup>rd</sup> trimester. 55 (11%) patients were unvaccinated at the time of delivery. The average gestational age at delivery (39 weeks) did not differ with timing of SARS-CoV-2 infection. The rate of preterm (32-37 weeks) and very preterm (<=32 weeks) births was not significantly different between SARS-CoV-2 infection before and during the 3<sup>rd</sup> trimester (p=0.439 & 0.663, respectively). The prevalence of maternal vascular malperfusion (MVM) or villous infarction (VI) was slightly higher in placentas of patients infected before the 3<sup>rd</sup> trimester, which showed a trend toward statistical significance (p=0.054). The prevalence of ischemic vascular changes (IVC) not diagnostic of MVM was higher in placentas of patients infected in the 3<sup>rd</sup> trimester (p=0.029); the proportion of unvaccinated patients was not significantly higher in this group (p=0.487). The proportion of patients infected in the 3<sup>rd</sup> trimester who were positive at delivery was not significantly different in placentas with IVC compared to MVM or VI (p=0.685). The incidence of other placental pathology was not affected by the timing of SARS-CoV-2 infection.

Placental Pathology	Infection Before 3rd Trimester (n=150)	Infection During 3rd Trimester (n=284)	p-Value
MVM or VI, n (%)	36 (24.0)	46 (16.2)	0.054
IVC, n (%)	24 (16.0)	72 (25.3)	0.029
Gestational age at delivery	Infection Before 3rd Trimester (n=150)	Infection During 3rd Trimester (n=284)	p-Value
32-37 weeks, n (%)	4 (2.7)	13 (4.6)	0.439
<=32 weeks, n (%)	1 (0.7)	4 (1.4)	0.663

Figure 1 - 857



**Conclusions:** Timing of SARS-CoV-2 infection during pregnancy does not appear to affect the rate of preterm or very preterm delivery. SARS-CoV-2 infection earlier in pregnancy may slightly increase the risk of more severe maternal vascular abnormality (MVM or VI) over infection in the 3<sup>rd</sup> trimester. SARS-CoV-2 infection later in pregnancy appears to result in more non-specific mild maternal vascular abnormality (IVC). Neither the proportion of unvaccinated patients nor the proportion of active infection at delivery explained why mild and severe maternal vascular abnormalities were associated with different timing of SARS-CoV-2 infection during pregnancy.

## 858 Gastric-Type Carcinoma of the Endometrium: Clinicopathologic and Molecular Characteristics in a Series of Eight Cases

Douglas Allison<sup>1</sup>, Britta Weigelt<sup>1</sup>, Amir Momeni Boroujeni<sup>1</sup>, Kay Park<sup>1</sup>

<sup>1</sup>Memorial Sloan Kettering Cancer Center, New York, NY

**Disclosures:** Douglas Allison: None; Britta Weigelt: None; Amir Momeni Boroujeni: None; Kay Park: None

**Background:** Endometrial gastric-type carcinoma (EGC) is a rare histotype of endometrial carcinoma, with fewer than a dozen cases reported to date. We describe the clinicopathologic and molecular profiles of 8 cases to gain better understanding of this rare tumor.

**Design:** Cases were identified from in-house surgical specimens and consults. Pathology reports and select slides were reviewed and clinical data was retrieved from the electronic medical record. Several cases underwent molecular testing with an in-house next generation sequencing (NGS) platform as part of clinical care, for which the results were reviewed.

**Results:** Of the 8 cases, patients ranged from 43 to 80 years of age (mean 65) with follow-up of 3-40 months (Table 1). Six of 8 (75%) were stage I at the time of hysterectomy (4 IA, 2 IB), while one had nodal and adnexal metastasis at the time of surgery (IIIC1). One patient had lung metastases at presentation and did not undergo surgical treatment (IVB). One stage IA case recurred within a month and the patient died 6 months after diagnosis. The other 5 stage I patients remain alive with no evidence of disease at last follow up (6-40 months). Histologically, the cases exhibited at least some classic gastric-type differentiation, characterized by cells with clear to pale eosinophilic cytoplasm and distinct cell borders with well-formed glandular architecture, though features of low grade endometrioid carcinoma were also often present and posed diagnostic challenges. The background endometrium was variable, but frequently contained endometrial polyps, atypical hyperplasia, and mucinous metaplasia. Immunohistochemically, the tumors were consistently positive for CK7 and CEA, but otherwise showed variable expression of CK20, PAX8, ER, and PR. All cases tested were p53 aberrant (6/6) and proficient for DNA mismatch repair proteins (6/6). All four cases (50%) with available NGS data showed pathogenic mutations in TP53. Other common alterations included KRAS hotspot (3/4) and STK11 mutations (2/4), while one case was notable for HER2 amplification (confirmed by FISH).

Table 1. Characteristics of individual cases. NED-no evidence of disease; AWD-alive with disease; DOD-dead of disease				
Case #	Age	FIGO Stage	Select Molecular Findings	Outcome
1	77	IA		NED, 40mo
2	43	IA	TP53 R175H KRAS G12A	NED, 30mo
3	72	IA	TP53 R175H STK11 E223K ERBB2 amplification	Recurred <1mo DOD, 6mo
4	66	IVB		AWD, 3mo
5	80	IB		NED, 27mo
6	47	IA	TP53 R175H KRAS G13C	NED, 27mo
7	79	IB	TP53 E258_S261delinsD KRAS G13D STK11 multiple mutations	NED, 6mo
8	52	IIIC1		Recurred 18mo AWD, 24mo

Figure 1 - 858

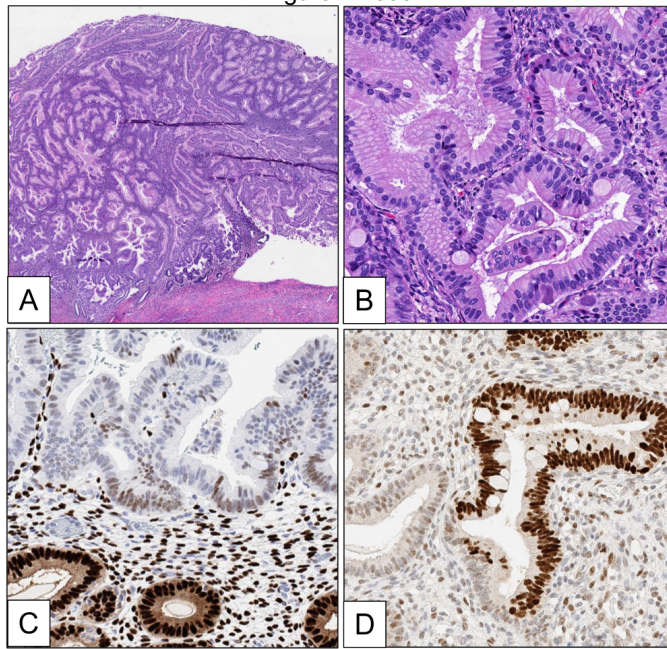


**Figure 1.** (A) A representative case shows a polypoid tumor with glandular architecture. (B) Cells are columnar with pale eosinophilic cytoplasm and distinct borders. Occasional goblet cells are seen. (C) IHC for ER shows weak/mixed expression and (D) p53 shows aberrant overexpression, distinct from the adjacent endometrial glands.

**Conclusions:** EGC is a distinct type of endometrial carcinoma morphologically and molecularly similar to the cervical counterpart, including TP53 and KRAS mutations, which has histologic overlap with endometrioid carcinoma. While the follow up period in our series is short, the rapid recurrence and death in a stage I patient suggests these may also behave more aggressively than conventional endometrioid carcinomas.

## 859 Incidence and Clinicopathologic Characteristics of HPV-Independent Squamous Cell Carcinomas of the Cervix

Douglas Allison<sup>1</sup>, Aaron Praiss<sup>1</sup>, Basile Tessier-Cloutier<sup>2</sup>, Jessica Flynn<sup>1</sup>, Alexia Iasonos<sup>3</sup>, Andrei Patrichi<sup>4</sup>, Lien Hoang<sup>5</sup>, Cristina Terinte<sup>6</sup>, Anna Pesci<sup>7</sup>, Claudia Mateiu<sup>8</sup>, Ricardo Lastra<sup>9</sup>, Lucian Puscasiu<sup>4</sup>, Takako Kiyokawa<sup>10</sup>, Mira Kheil<sup>11</sup>, Rouba Ali-Fehmi<sup>11</sup>, Kyle Devins<sup>12</sup>, Esther Oliva<sup>13</sup>, Nadeem Abu-Rustum<sup>1</sup>, Simona Stolnicu<sup>4</sup>, Robert Soslow<sup>14</sup>  
<sup>1</sup>Memorial Sloan Kettering Cancer Center, New York, NY, <sup>2</sup>McGill University Health Centre, Montreal, QC, <sup>3</sup>New York, NY, <sup>4</sup>UMFST GE Palade, Targu Mures, Romania, <sup>5</sup>The University of British Columbia, Vancouver, BC, <sup>6</sup>Regional Institute of Oncology, Iasi, Romania, <sup>7</sup>IRCCS Ospedale Sacro Cuore Don Calabria, Negrar, Verona, Italy, <sup>8</sup>Sahlgrenska University Hospital, Gothenburg, Sweden, <sup>9</sup>University of Chicago, Chicago, IL, <sup>10</sup>The Jikei University School of Medicine, Minato-ku, Japan, <sup>11</sup>Wayne State University, Detroit, MI, <sup>12</sup>Massachusetts General Hospital, Boston, MA, <sup>13</sup>Massachusetts General Hospital, Harvard Medical School, Boston, MA, <sup>14</sup>Memorial Sloan Kettering Cancer Center/Weill Medical College of Cornell University, New York, NY

**Disclosures:** Douglas Allison: None; Aaron Praiss: None; Basile Tessier-Cloutier: None; Jessica Flynn: None; Alexia Iasonos: None; Andrei Patrichi: None; Lien Hoang: None; Cristina Terinte: None; Anna Pesci: None; Claudia Mateiu: None; Ricardo Lastra: None; Lucian Puscasiu: None; Takako Kiyokawa: None; Mira Kheil: None; Rouba Ali-Fehmi: None; Kyle Devins: None; Esther Oliva: None; Nadeem Abu-Rustum: None; Simona Stolnicu: None; Robert Soslow: None

**Background:** Squamous carcinoma of the cervix (SCC) is among the most common gynecologic cancers worldwide. While the vast majority of cases can be attributed to infection with high-risk subtypes of Human Papilloma Virus (HPV), HPV-independent (HPVI) cases are known to occur. We aimed to determine the incidence of HPVI SCC and describe the clinicopathologic characteristics of these tumors.

**Design:** Drawing on a previously established multi-institutional cohort of 670 patients with surgically treated SCC, we identified 376 cases with readily available tissue to construct tissue microarrays. These were studied by *in situ* hybridization for high-risk HPV RNA and immunohistochemistry for p16 and p53. Cases were considered HPVI if they were both negative by HPV ISH and failed to show diffuse p16 positivity by IHC and considered HPV-associated (HPVA) if they were positive by HPV ISH. All other cases were considered equivocal.

# ABSTRACTS | GYNECOLOGIC AND OBSTETRIC PATHOLOGY

**Results:** A total of 6 HPVI SCCs and 361 HPVA SCCs were identified; another 9 cases were equivocal excluded from the current analysis. Despite the small numbers, patients with HPVI SCC showed important differences, being significantly older (mean age 72 vs 50, p<0.001) and with higher stage (33%, 17%, 33%, and 17% for stage I, II, III, and IV respectively vs. 69%, 13%, 17%, and 1%, p=0.031). While the overall rate of HPVI SCC was low (1.6%) the incidence was increased among older patients, accounting for 6.3% of patients over 60. Expression of p53 was varied, with 2 cases showing null expression, 2 cases showing wild-type expression, and 2 cases being equivocal. Histologically, HPVI SCCs were heterogeneous, with both keratinizing and non-keratinizing morphologies seen. Notably, several cases showed an apparent precursor lesion reminiscent of differentiated vulvar intraepithelial neoplasia, with prominent basal atypia and hypereosinophilia (Fig. 1). Of the 6 patients with HPVI SCC, 2 had distant recurrences within 12 months and 2 died within the follow up period. However, the small number of HPVI tumors precluded meaningful comparison of progression free and overall survival.

Table 1. Individual Characteristics of HPVI SCCs

Case #	Age	Stage (FIGO 2018)	Tumor Size (mm)	Histology	LVI	Precursor Lesion	Outcome
1	68	IIIA	50	Keratinizing	No	Yes	ANED, 35mo
2	71	IA2	0.1	Non-keratinizing	Focal	No	ANED, 7yr
3	67	IVB	40	Non-keratinizing	Extensive	Yes	DOD, 29mo
4	76	IIIC2	30	Keratinizing	Extensive	No	Distant recurrence, 12mo; AWD, 42mo
5	88	IIA2	70	Keratinizing	Yes (not quantified)	No	Distant recurrence, 5mo; DOD 8mo
6	74	IB2	14	Keratinizing	No	Yes	ANED, 29mo

Figure 1 – 859

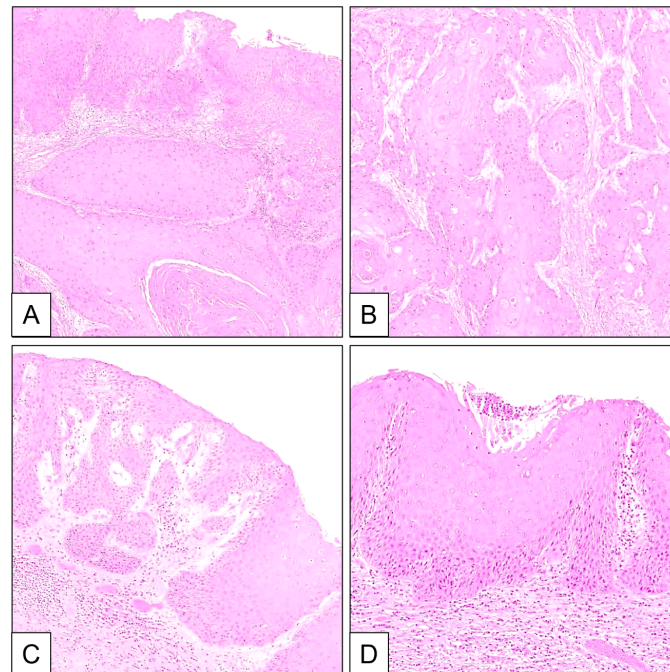


Figure 1. Morphology of an HPV-independent squamous carcinoma of the cervix. The invasive tumor shows a well-differentiated keratinizing appearance (A,B). An adjacent in situ lesion is seen (C) with morphology reminiscent of differentiated vulvar intraepithelial neoplasia (D).

**Conclusions:** HPVI SCCs are rare tumors, but with important clinical and histologic differences from their HPVA counterparts. Their predilection for older patients with higher stage disease suggests the need for increased awareness and testing within these populations. We posit that the true frequency of HPVI tumors may be even higher, as they may be underrepresented in this cohort of surgically treated patients.

## 860 Maximizing the Utility and Cost-Effectiveness of Targeted RNA Sequencing in the Diagnosis of Uterine Mesenchymal Tumors

Douglas Allison<sup>1</sup>, Leonel Maldonado<sup>2</sup>, Akisha Glasgow<sup>3</sup>, Eric Klein<sup>1</sup>, Amir Momeni Boroujeni<sup>1</sup>, Emeline Aviki<sup>1</sup>, Sarah Chiang<sup>1</sup>

<sup>1</sup>Memorial Sloan Kettering Cancer Center, New York, NY, <sup>2</sup>Vanderbilt University Medical Center, Nashville, TN, <sup>3</sup>Beth Israel Deaconess Medical Center, Boston, MA

**Disclosures:** Douglas Allison: None; Leonel Maldonado: None; Akisha Glasgow: None; Eric Klein: None; Amir Momeni Boroujeni: None; Emeline Aviki: None; Sarah Chiang: None

**Background:** Fusions in uterine mesenchymal tumors (UMT) can be detected by targeted RNA sequencing (RNAseq), aiding diagnosis. However, high cost and application of RNAseq only after immunohistochemistry (IHC) are common preconceptions. We review our institution's experience with RNAseq and IHC to identify cost-effective approaches in evaluating UMT.

**Design:** We reviewed 130 UMT profiled by RNAseq as part of clinical work up to identify 1) classifiable cases where a definitive diagnosis was reached by IHC and 2) initially unclassifiable cases where the diagnosis was descriptive or deferred until RNAseq results were obtained. Final diagnosis incorporating RNAseq results and number of IHC stains performed were recorded. The total cost to achieve a diagnosis was calculated for each case (costs at time of study: RNAseq=\$2309; IHC=\$647 initial, \$607 each additional). Cost-effectiveness of 2 diagnostic approaches was determined by calculating total and per-case cost of the normal workflow (IHC with reflex to RNAseq if inconclusive) and comparing it with total and per-case cost of an alternative workflow (RNAseq with reflex to IHC if inconclusive).

**Results:** IHC alone classified 76 (58%) UMT. Fusions were detected in 38 (50%) classifiable cases, of which 35 were disease-defining and 5 resulting in a change in diagnosis (Fig. 1). Among 54 initially unclassifiable UMT, 31 (57%) were classified after RNAseq (Fig. 2), including 11 (35%) found to have a disease-defining fusion and 20 (65%) where a negative RNAseq result excluded differential diagnoses. After IHC and RNAseq, 23 UMT (43%) remained unclassifiable. The total cost of RNAseq and IHC in 130 UMT was \$1,251,563 (\$9627/case) resulting in classification of 82% of UMT (\$117.40/% accuracy/case) (Table 1). RNAseq with reflex to IHC if inconclusive would achieve the same rate of classification and cost \$999,759 (\$7,690/case; \$93.78/% accuracy/case), which is an overestimation if fusion-specific IHC was excluded. IHC only testing would have similarly cost \$951,313 (\$7,318/case), but correctly classifying only 55% of UMT (\$133.05/% accuracy/case).

**Table 1.** Comparisons of different work up strategies in cost and efficacy.

Assay	*5 "classifiable" cases were reclassified after RNAseq results.				
	Total cost	Average cost per case	# (%) Classifiable cases	# (%) Unclassifiable cases	Cost per case per % accuracy
IHC followed by RNAseq if inconclusive (normal workflow)	\$1,251,563	\$9,627	107 (82)	23 (18)	\$117.40
RNAseq followed by IHC if inconclusive	\$999,759	\$7,690	107 (82)	23 (18)	\$93.78
IHC alone	\$951,393	\$7,318	71* (55)	59* (45)	\$133.05
RNAseq alone	\$300,170	\$2,309	46 (35)	84 (65)	\$65.97

**Figure 1 - 860**

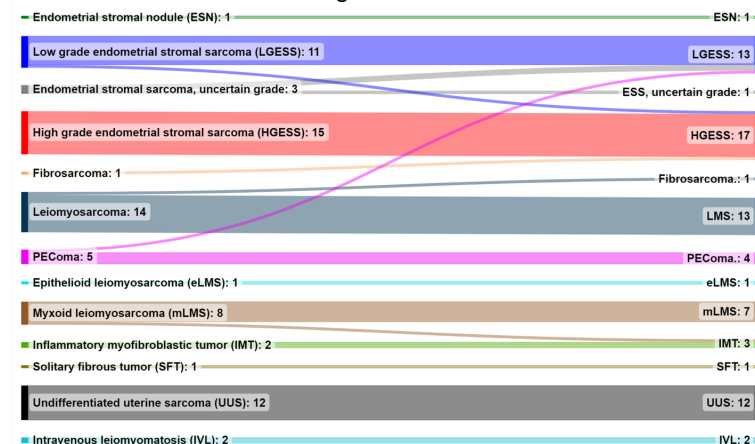


**Figure 1.** Sankey diagram showing initial (left) and RNAseq integrated (right) diagnoses of initially classifiable tumors (n=76).

Figure 2 - 860

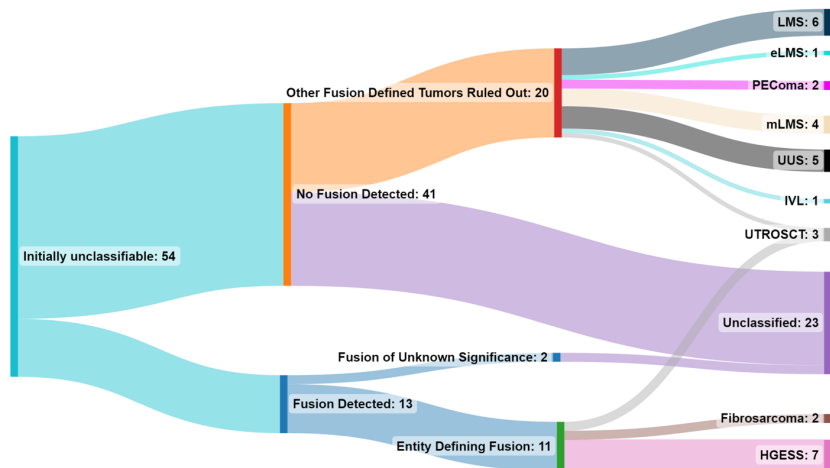


**Figure 2.** Sankey diagram showing the diagnostic integration of RNAseq results for initially unclassifiable tumors (n=54).

**Conclusions:** RNAseq is helpful in diagnosing UMT, providing utility even with a negative result. Performing RNAseq followed by IHC in inconclusive cases is a cost-effective strategy with savings of >20%, while still maximizing tumor classification. IHC only testing is the least efficient diagnostic approach.

## 861 PRAME Protein Expression in Uterine and Ovarian Carcinosarcoma

Alaaeddin Alrohaibani<sup>1</sup>, Yun Yu<sup>1</sup>, Lina Gao<sup>1</sup>, Kimberly McLean<sup>1</sup>, Jonathon Hetts<sup>1</sup>, Ozlen Saglam<sup>1</sup>

<sup>1</sup>Oregon Health & Science University, Portland, OR

**Disclosures:** Alaaeddin Alrohaibani: None; Yun Yu: None; Lina Gao: None; Kimberly McLean: None; Jonathon Hetts: None; Ozlen Saglam: None

**Background:** Carcinosarcoma (CS) is a biphasic tumor with epithelial and mesenchymal components. Overall survival rates did not improve in decades despite combined treatment modalities. PRAME (PREFERentially Expressed Antigen in MElanoma) is a member of cancer testis antigens and a promising immunotherapy target. We explored PRAME protein expression in uterine and ovarian CS cases by immunohistochemistry.

**Design:** Histologically confirmed archival uterine (n=17) and pelvic (n=12) CS cases (n=29) were queried at our institutional files. Following slide review and selection of representative tissue blocks, immunostained slides with PRAME antibody was scored in epithelial and mesenchymal components of CS separately by H-score (percent of positively stained tissue multiplied by staining intensity). The mean H-scores from components of CS were compared with each other by paired t-test for the entire cohort and then results from uterine and pelvic CS cases with each other by two sample pooled paired t-test. In addition, mean H-scores of epithelial component of CS and low-grade endometrioid adenocarcinoma (LGEC) (n=13), and mean H-scores of mesenchymal component of CS and uterine leiomyosarcoma (LMS) cases (n=14) were compared in a separate analysis. Finally, MLH-1 promoter hypermethylation status was tested against marker expression in LGEC group.

**Results:** The mean H-scores for carcinomatous and sarcomatous components were 156 and 160 respectively without any significant difference ( $p=0.81$ ) (Figure 1 and 2). There was also no PRAME expression difference between uterine and pelvic CS cases ( $p=0.087$ ). All CS cases had high-grade carcinomatous components. The mean H-score of LGEC was not significantly different from the mean H-score of carcinomatous component of CS group ( $p=0.572$ ). The median PRAME expression was only 10 in LMS and it was significantly different from the sarcomatous component of CS ( $p < 0.001$ ). There was no PRAME expression difference among 6 LGEC with MLH-1 promoter hypermethylation against 7 LGEC with intact MLH-1 ( $p = 0.466$ ).

Figure 1 - 861

Box plot for H-scores of the CS group

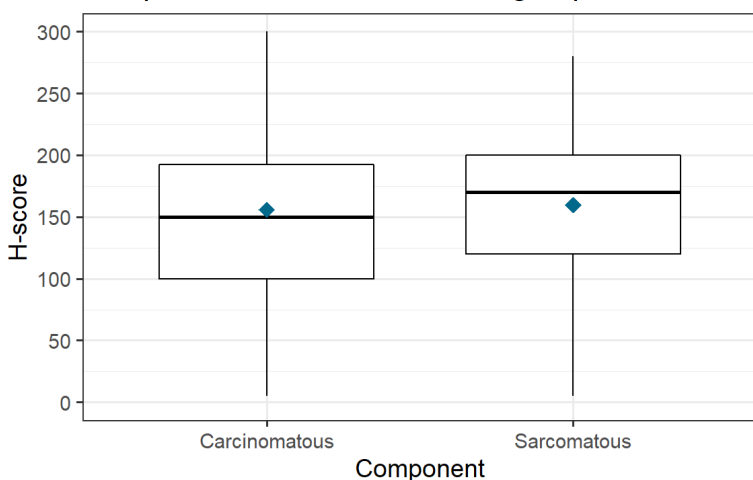
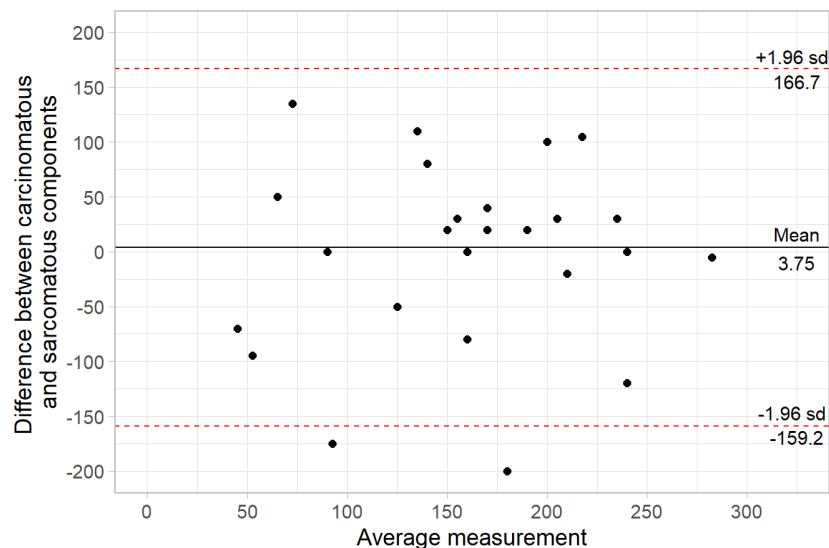


Figure 2 - 861

Bland-Altman plot for H-score of the CS group



**Conclusions:** PRAME is a promising target for the treatment of uterine and pelvic CS. The protein expression levels are similar in carcinomatous and sarcomatous components of CS supporting single cell origin. There is no PRAME expression difference between high-grade and low-grade carcinomas in this small cohort. Uterine LMS has overall low-PRAME protein expression levels. PRAME protein overexpression seems to be not associated with MLH-1 methylation status.

## 862 Methylation Profiling of High-Grade Ovarian Carcinomas and Comparison with High Grade Endometrial Carcinomas

Rofieda Alwaqfi<sup>1</sup>, Gulisa Turashvili<sup>2</sup>, Varshini Vasudevaraja<sup>3</sup>, Ivy Tran<sup>4</sup>, Jonathan Serrano<sup>5</sup>, M. Herman Chui<sup>1</sup>, Britta Weigelt<sup>6</sup>, Robert Soslow<sup>6</sup>, Lora Ellenson<sup>1</sup>, Nadeem Abu-Rustum<sup>1</sup>, Matija Snuderl<sup>5</sup>, Sarah Chiang<sup>1</sup>

<sup>1</sup>Memorial Sloan Kettering Cancer Center, New York, NY, <sup>2</sup>Emory University, Atlanta, GA, <sup>3</sup>New York University Medical Center, New York, NY, <sup>4</sup>NYU Langone Health, New York, NY, <sup>5</sup>New York University, New York, NY, <sup>6</sup>Memorial Sloan Kettering Cancer Center/Weill Medical College of Cornell University, New York, NY

**Disclosures:** Rofieda Alwaqfi: None; Gulisa Turashvili: None; Varshini Vasudevaraja: None; Ivy Tran: None; Jonathan Serrano: None; M. Herman Chui: None; Britta Weigelt: None; Robert Soslow: None; Lora Ellenson: None; Nadeem Abu-Rustum: None; Matija Snuderl: None; Sarah Chiang: None

**Background:** The most common high-grade ovarian carcinomas (HGOCs) consist of high-grade serous (oSC), grade 3 endometrioid (oEC3), and clear cell (oCCC) carcinomas. These tumors share overlapping histologic, immunophenotypic and genetic features with high-grade endometrial carcinomas (HGECS) of serous (eSC), endometrioid (eEC3), and clear cell (eCCC) histotypes. Here we sought to define the methylation profiles of HGOCs and epigenetic differences between HGOCs and HGECS.

**Design:** DNA methylation status of 850K CpG sites in 20 HGOCs (8 oSC, 4 oEC3, 8 oCCC) and 24 HGECS (9 eSC, 7 eEC3, 8 eCCC) were analyzed. DNA was extracted from microdissected formalin-fixed paraffin-embedded tumor tissue and profiled using the Illumina MethylationEPIC array. Methylation data were analyzed with R package minfi. Raw idats were quantile normalized and most variable probes were used for downstream analysis.

**Results:** Unsupervised hierarchical clustering, which groups samples based on their similarity/differences in methylation patterns, separated HGOCs into 2 major groups (Fig. 1). HGOC cluster 1 consisted of 2/4 oEC3 (50%), with all the remaining cases in HGOC cluster 2. Within HGOC cluster 2 were three subclusters, with i) the remaining oEC3 (2/4, 50%), ii) all oCCC (8/8, 100%) and 1 oSC (1/8, 12%), and iii) oSC (7/8, 88%). The comparison of HGOC and HGECS showed 2 major clusters, with oEC3 (1/4, 25%) in HGOC/EC cluster 1 (Fig. 2). HGOC/EC cluster 2 separated into two HGOC/EC subclusters, with 1) oCCC (6/8, 75%) and eCCC (7/8, 87%), and 2) three further sub-subcluster, including 2a) eEC3 (3/7, 43%), oEC3 (2/4, 50%) and eSC (1/9, 11%), 2b) only eSC (1/9, 11%), and 2c) oEC3 (1/4, 25%), eEC3 (4/7, 57%), eCCC (1/8, 12%), eSC (7/9, 78%), oSC (8/8, 100%) and oCCC (2/8, 25%).

Figure 1 - 862

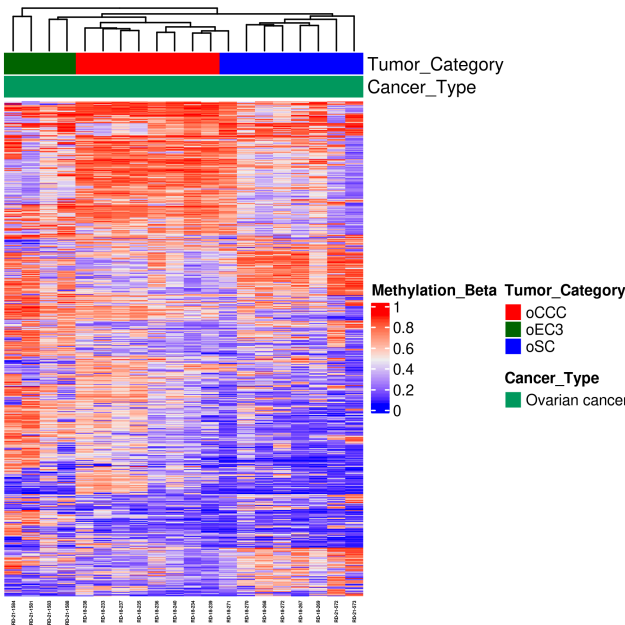
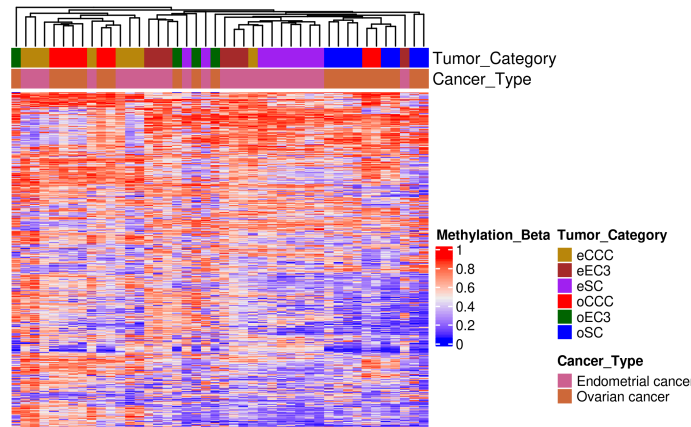


Figure 2 - 862



**Conclusions:** DNA methylation analysis of HGOC revealed that oCCC and oSC are distinct epigenetic subgroups, and that a subset of oEC3 appears to be epigenetically related to oCCC and oSC. Comparison of high-grade ovarian and endometrial lesions further showed that most oCCC and eCCC share similar methylation patterns, and that a small subset of oCCC is epigenetically related to oSC.

## 863 Growth-based Grading and Tumor Proportion Are Independent Prognostic Factors of Overall Survival in Metastatic Ovary Mucinous Carcinomas

Jie Bai<sup>1</sup>, Luyuan Li<sup>2</sup>, Lihong Li<sup>2</sup>, Yan Song<sup>2</sup>

<sup>1</sup>Tanshan, China, <sup>2</sup>National Cancer Center, National Clinical Research Center for Cancer, Cancer Hospital, Chinese Academy of Medical Sciences and Peking Union Medical College, Beijing, China

**Disclosures:** Jie Bai: None; Luyuan Li: None; Lihong Li: None; Yan Song: None

**Background:** Growth-Based Grade (GBG): low-grade (GBG-LG, confluent/expansile growth, or  $\leq 10\%$  infiltrative invasion) or high-grade (GBG-HG, infiltrative growth in  $> 10\%$  of tumor) is recently recommended and validated the prognostic value for both disease-free survival and disease-specific survival in primary mucinous ovarian cancer (MOC), which outperformed Silverberg and FIGO grades in multivariate analysis. Around 80% of mucinous carcinomas of the ovary are metastatic. The main objective of the present study is to identify the morphological characteristics and their prognostic value for patients with surgically confirmed ovarian

metastatic mucinous carcinomas and if microscopic morphology in metastatic ovary carcinoma can serve as an independent validation as a predictor of outcome.

**Design:** The medical records of patients who received ovary surgery were reviewed and a postoperative pathological evaluation of the morphological features (tumor gross features, proportion of tumor cells, the proportion of mucus, histologic grade, nuclear grade, the pattern of invasion(GBG), necrosis, tumor infiltrating lymphocytes (TILs)) and their relationship with prognosis were evaluated.

**Results:** 111 metastatic ovarian mucinous carcinomas diagnosed between 2010 and 2020 were included at our center. The median age was 50 years old. The median OS of all patients with ovarian metastases was 28.5 months. Metastases were found before the primary tumor in 35 (31.5%) patients. 76(68.5%) cases were diagnosed synchronously or after the primary tumor. Ovarian tumors in 60(54.1%) of 111 women are unilateral. The most frequent primary sites were gastrointestinal tract (80.2%) and female reproductive organs (16.2%). Log-rank analysis showed high tumor density (proportion of tumor cells $\geq$ 40%), poor differentiation, high-grade nucleus, and infiltrative invasion predicted more shorter overall survival ( $p=0.002$ ,  $0.026$ ,  $0.008$ , and  $0.015$ , respectively). Multivariate analysis demonstrated that high tumor density (HR,2.280;95% CI,1.029-5.052,  $p=0.042$ ) and GGB-HG (HR,3.759;95%CI,1.122-12.591,  $p=0.032$ ) were independent prognostic factors of overall survival.

Table 1. Univariate analysis of prognostic factors for 111 patients			
Prognostic factors		MST (months)	P
Age[median(range)]			0.547
≥50	55/111 (49.5%)	38.1	
<50	56/111 (50.5%)	44.6	
Size[median(range)]			0.668
≥9.3cm	43/111 (38.7%)	43.5	
<9.3cm	68/111 (61.3%)	54.5	
Laterality			0.254
Bilaterality	50/111 (45%)	31.6	
Unilaterality	61/111 (55%)	44.5	
Proportion of tumor cells			0.002
≥40%	75/111 (67.6%)	30.3	
<40%	36/111 (32.4%)	73.1	
Proportion of mucus			1.000
≥25%	38/111 (37.4%)	44.5	
<25%	73/111 (65.8%)	43.5	
Histologic grade			0.026
Well/moderately differentiated	73/111 (65.8%)	54.5	
Poorly differentiated	38/111 (34.2%)	21.5	
Nuclear grade			0.008
Low grade	19/111 (17.1%)	73.1	
High grade	92/111 (82.9%)	38.7	
Signet ring cells	30/111 (27.0%)		
Areas of MBT and/or mucinous cystadenoma			0.534
Yes	52/111 (46.8%)	43.2	
No	59/111 (53.2%)	44.6	
Pattern of invasion			0.015
GBG-HG	96/111 (86.5%)	38.7	
GBG-LG	15/111 (13.5%)		
Necrosis			0.257
Yes	56/111(50.5%)	31.6	
No	55/111(49.5%)	54.7	
Lymphocyte infiltration			0.886
Grade 2/3	20/111(18.0%)	44.5	
Grade 0/1	91/111(82.0%)	38.7	
Prominent stroma			0.525
Yes	40/111(36.0%)	43.5	
No	71/111(64.0%)	44.6	

**Conclusions:** Metastatic ovarian mucinous carcinomas mean at least T3 state for patients with unfavorable overall survival, and the proportion of tumor cells $\geq$ 40% and infiltrative invasion pattern(GBG-HG) predicted more unfavorable overall survival.

## 864 Prognostic Indicators of Tubal Free-Floating Intraluminal Cells for Patients with Endometrial Cancer

Julieta Barroeta<sup>1</sup>, David Warshal<sup>1</sup>, Courtney Griffiths<sup>1</sup>, Marie Gabriel<sup>1</sup>, Konstantinos Totolos<sup>2</sup>

<sup>1</sup>Cooper University Hospital, Camden, NJ, <sup>2</sup>Cooper Medical School of Rowan University, Camden, NJ

**Disclosures:** Julieta Barroeta: None; David Warshal: None; Courtney Griffiths: None; Marie Gabriel: None; Konstantinos Totolos: None

**Background:** Free-floating intraluminal cancer cells (FFICC) have been recently reported to be associated with lower survival in high risk endometrial cancer (EC). The mechanism of action proposed involves exfoliation through the fallopian tubes (FT) and spillage into the peritoneal cavity leading to widespread metastatic potential. Although the significance of peritoneal cytology has historically been called into question and has since been removed from surgical staging, a positive correlation has been noted among patients who have FFICC with positive washings. Our study aims to determine the incidence of FFICC, risk factors, and their prognostic significance.

**Design:** Retrospective analysis was performed including all patients with a diagnosis of EC who underwent surgical management between 2015-2018. Demographic and histopathologic variables were collected including stage, grade, lesion size, histologic subtype, and fluid cytology. Slides of the EC and FT were reviewed by a gynecological pathologist.

**Results:** A total of 576 patients were included. FFICCs were detected in 12.5% of patients with EC (endometrioid, n=54 vs non-endometrioid histologies, n=18). Robotic hysterectomy was performed in 81.9% of patients with FFICC versus 18.1% of patients who underwent abdominal hysterectomy with an odds ratio of 2.85. Grade 1 tumors were associated with 39.4% of positive FFICC, while grades 2 and 3 were associated with 36.6% and 23.9% respectively ( $p=0.012$ ). Among patients with positive cytology, 23.7% were associated with presence of FFICC ( $p<0.001$ ). A statistically significant decrease in overall survival was noted with patients with FFICC ( $p = 0.066$ ), however progression free survival in 1st and 2nd recurrence was not found to be statistically significant. We did not observe a statistically significant difference in presence of FFICC among histologic subtype or FIGO stage.

**Conclusions:** The presence of FFICC may provide important prognostic information specifically with regard to determining adjuvant treatment in those with positive cytology and/or high risk histology. Our findings suggest that FFICC are associated with age, tumor grade, positive peritoneal cytology, and surgical approach. The higher incidence of FFICC among robotic hysterectomies suggests a potential role of mode of uterine manipulation. Lack of difference in progression free survival with statistical significance in overall survival suggests a difference in the pattern of recurrence or possibly in postoperative adjuvant therapy.

## 865 Mutations in Homologous Recombination Genes and Loss of Heterozygosity Status in Epithelial Ovarian Carcinoma

Brooke Bartow<sup>1</sup>, Jeffrey Chang<sup>1</sup>, Gene Siegal<sup>1</sup>, Rebecca Arend<sup>1</sup>, Andrea Kahn<sup>1</sup>, Sameer Al Diffalha<sup>1</sup>, Alexander Mackinnon<sup>1</sup>, Christine Pesoli<sup>1</sup>, Shuko Harada<sup>1</sup>, Xiao Huang<sup>1</sup>

<sup>1</sup>The University of Alabama at Birmingham, Birmingham, AL

**Disclosures:** Brooke Bartow: None; Jeffrey Chang: None; Gene Siegal: None; Rebecca Arend: None; Andrea Kahn: None; Sameer Al Diffalha: None; Alexander Mackinnon: None; Christine Pesoli: None; Shuko Harada: None; Xiao Huang: None

**Background:** Ovarian cancers with homologous recombination deficiency (HRD), specifically mutations in *BRCA1/2*, have increased sensitivity to poly-ADP ribose inhibitors (PARPi). Recently, PARPi has been found to be efficacious in BRCA wild-type carcinomas with high genomic loss of heterozygosity (LOH) or other mutations in HR genes. Thus, the goal of this study was to investigate tumor mutations in HR genes in epithelial ovarian cancer (EOC).

**Design:** Patients diagnosed with EOC at our institution (2013 - 2021) having targeted next-generation sequencing analysis (NGS) were identified. Pathological genomic alterations and LOH score were collected. The cohort was divided into three groups: *BRCA1/2*, BRCA wild-type HR-mutated (BRCAwt-HRmt), and HR wild-type (HRwt). A LOH score of  $\geq 16\%$  was defined as LOH-high.

**Results:** Of the 138 EOC identified, 46(33%) had HR mutations, including 13(28%) in *BRCA1*, 9(20%) in *BRCA2*, and 24(52%) in BRCAwt-HRmt. HR gene mutation rates by histological subtypes are shown in figure 1A. HR mutations were present in all subtypes of EOC besides mucinous carcinoma. 35 of 92(38%) high grade serous carcinoma (HGSC) showed HR mutation, as compared to 11 of 46(24%) non-high grade serous carcinoma (NHGSC) ( $p=0.185$ ) (figure 1B). Among HR mutations in HGSC, 64%(7/11) were in BRCAwt-HR, compared to 49%(17/35) in HGSC ( $p=0.032$ ) (figure 1C). LOH data was available for 87 cases; 28 were LOH-high. 42%(24/57) of HGSC were LOH-high, while 14% (4/24) of NHGSC ( $p=0.00002$ ) were LOH-high. 27 of 87(31%) had a HR mutation, including 7(8%) in *BRCA1*, 5(6%) in *BRCA2*, and 15(17%) in BRCAwt-HRmt. Of the 28 LOH-high cases, 12(43%) showed HR mutation, including 10 (36%) in *BRCA1/2* and 2(7%) in BRCAwt-HRmt; 15 of 59(25%) LOH-low cases showed a HR mutation, including 2 (3%) in *BRCA1/2* and 13(22%) in BRCAwt-HRmt ( $p=0.000146$ ) (figure 2A). In LOH-high cases

with HR mutations, 83% (10/12) were in BRCA1/2, compared to 13% (2/15) in LOH-low cases ( $p<0.00001$ ) (figure 2B). LOH-low cases showed wider distribution of mutation in *BRCAwt-HR* genes, including *ATRX*, *C11ORF30*, *CDK12*, *MLH1*, *MUTYH*, and *RAD54L* that were not seen in LOH-high cases.

Figure 1 – 865

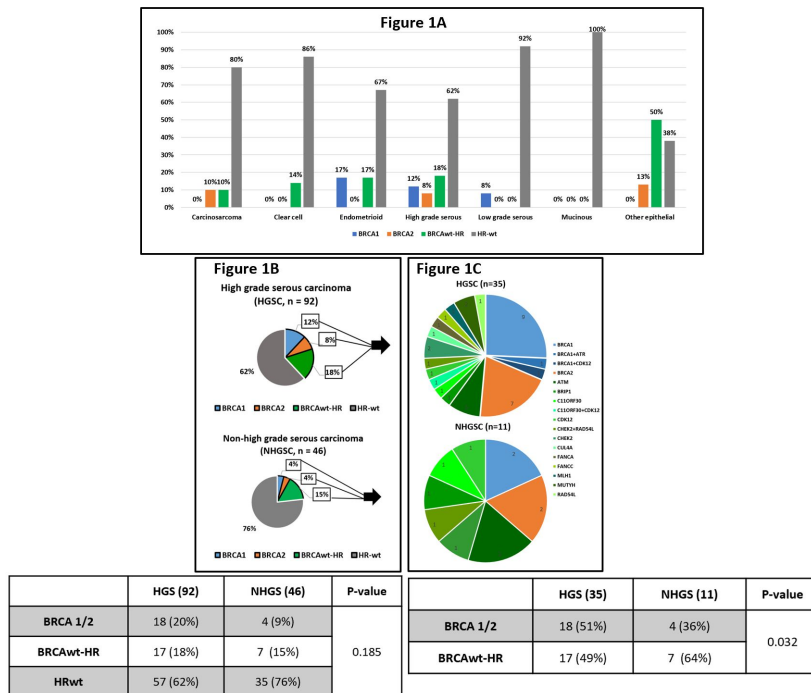
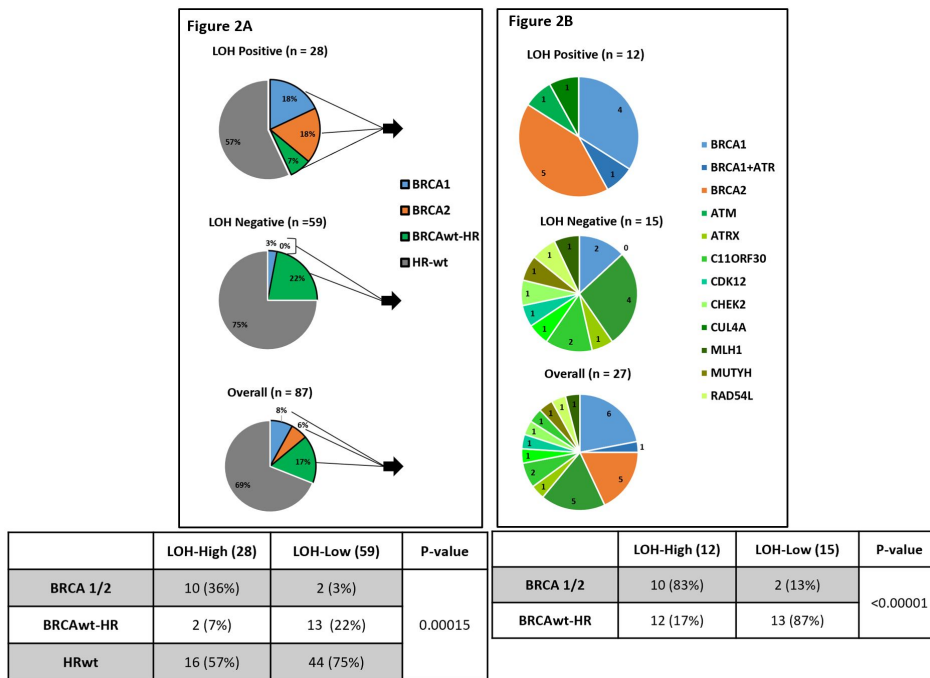


Figure 2 – 865



**Conclusions:** HGSC cases showed a higher rate of LOH positivity; however, NHGSC cases showed a higher rate of mutations in *BRCAwt-HR* genes. LOH-high cases showed a higher rate of *BRCA* mutation and LOH-low cases showed a higher rate of HR gene mutations other than *BRCA*. NGS with HRD analysis in EOC should be considered to help guide treatment options.

**866 Punctate Pattern Nuclear MLH1 Immunoexpression Without Classic Nuclear MLH1 Staining is an Artifact in MMR Deficient Endometrial Cancer that Merits MLH1 Promoter Methylation Testing**Swati Bhardwaj<sup>1</sup>, Joseph Rabban<sup>2</sup><sup>1</sup>Icahn School of Medicine at Mount Sinai, New York, NY, <sup>2</sup>University of California, San Francisco, San Francisco, CA**Disclosures:** Swati Bhardwaj: None; Joseph Rabban: None

**Background:** Punctate pattern nuclear MLH1 immunohistochemical staining (punctate MLH1), accompanied by complete loss of PMS2 IHC, has been reported as a putative antibody clone-related technical artifact in rare *MLH1/PMS2* deficient endometrial cancers with MLH1 promoter methylation. Punctate MLH1 may be misinterpreted as intact, leading to misclassification of the apparent isolated PMS2 loss as evidence of probable *PMS2* germline mutation. Herein we present morphologic and molecular correlation of the largest series to date of punctate MLH1 in endometrial cancer and highlight features to mitigate against misinterpretation.

**Design:** Punctate MLH1 was defined as discrete dot-like staining in the nucleus (one or more dots) of tumor cells. MLH1 IHC was otherwise interpreted using current ISGyP recommendations. 21 biopsy cases were collected from the practice of one of us (JTR) (Jan 2020-Aug 2022). For outside cases, MLH1 IHC was repeated inhouse on the biopsy for comparison (Cell Marque clone G168-728) and also performed on subsequent hysterectomy when available. *MLH1* promoter methylation and a 500+ gene next generation sequencing panel (NGS) with MSI Sensor testing were performed in selected cases.

**Results:** Punctate MLH1 without classic nuclear MLH1 occurred in 13/21 patients (all PMS2 deficient), while classical nuclear MLH1 co-existed in 8/21 (all PMS2 intact). Repeat inhouse IHC was concordant with outside biopsy IHC in all cases tested but IHC on hysterectomy showed completely negative MLH1 in 5/6 tested cases. In 11/13 biopsies without classic nuclear MLH1, punctate staining occurred in at least 80% of tumor cells. 12/13 were low grade endometrioid carcinoma, 1 was dedifferentiated carcinoma, all of which were MSI-high by NGS. Two somatic *MLH1* mutations were present in 1/13; the other 12 were *MLH1/PMS2* wild type by NGS and showed *MLH1* promoter methylation in all tested cases. Classic nuclear MLH1 co-existed in 8/21; 4 were p53 aberrant, CN-high grade 3 carcinoma; 3 were low grade CN-low endometrioid carcinoma and 1 grade 3 endometrioid carcinoma.

**Conclusions:** MLH1 promoter methylation testing. If classic nuclear staining is also present, MLH1 should be reported as intact, as supported by intact PMS2. The etiology of punctate MLH1 is unclear but may be a clone-related artifact and/or related to biopsy processing since this pattern was infrequently observed in the subsequent hysterectomy.

**867 Does 'One Size Fits All'? Rethinking FIGO Invasion Depth Measurement Methods in Vulvar Cancer**Maaike Bleeker<sup>1</sup>, Tjalling Bosse<sup>2</sup>, Koen Van de Vijver<sup>3</sup>, Joost Bart<sup>4</sup>, Hugo Horlings<sup>5</sup>, Trudy Jonges<sup>6</sup>, Nicole Visser<sup>7</sup>, Loes Kooreman<sup>8</sup>, Patricia C Ewing-Graham<sup>9</sup>, Johan Bulten<sup>10</sup><sup>1</sup>Amsterdam UMC, Amsterdam, Netherlands, <sup>2</sup>Leiden University Medical Center, Leiden, Netherlands, <sup>3</sup>Ghent University Hospital, Gent, Belgium, <sup>4</sup>University Medical Center Groningen, <sup>5</sup>Antoni van Leeuwenhoek Hospital, <sup>6</sup>UMCU, Utrecht, Netherlands, <sup>7</sup>Eurofins PAMM, Eindhoven, Netherlands, <sup>8</sup>Maastricht UMC+, Maastricht, Netherlands, <sup>9</sup>Erasmus MC, Netherlands, <sup>10</sup>Radboud University Medical Center**Disclosures:** Maaike Bleeker: None; Tjalling Bosse: None; Koen Van de Vijver: None; Joost Bart: None; Hugo Horlings: None; Trudy Jonges: None; Nicole Visser: None; Loes Kooreman: None; Patricia C Ewing-Graham: None; Johan Bulten: None

**Background:** In 2021, the International Federation of Gynecology and Obstetrics (FIGO) made several adaptions in the definitions of the FIGO staging system of vulvar cancer. One important adaptation is the altered recommendation on depth of invasion (DOI) measurement. Following the new FIGO 2021, this study was initiated by the Dutch Working Group Gynecological Pathology (NWGP) in order to study current practice variability among gynecopathologists concerning the used DOI method in vulvar cancer.

**Design:** In this explorative study, a series of 26 vulvar cancers were selected by 3 gynecopathologists during the day-to-day work between March 2022 and June 2022. The selection of cases was made when DOI was expected to change from >1 mm to ≤ 1 mm when applying the different DOI measurement methods (DOI-FIGO 2009 versus 2021) and/or when DOI measurement was challenging. For each case, DOI measurements were annotated for the distinct methods via a digital platform. Subsequently, one gynecopathologist from each gynecologic oncology center in the Netherlands (n=9) and one from Belgium were asked i) to indicate the feasibility of DOI-FIGO 2009 and DOI-FIGO 2021 and ii) to indicate the preferred DOI method (i.e. FIGO 2009, FIGO 2021, tumor thickness or no invasion) for each cancer case via the digital platform.

**Results:** As 26 vulvar cancer cases were assessed by 10 pathologists, 260 assessments were available for each study question. The feasibility of applying the DOI-FIGO 2009 method was found to be 'easy/reasonable' in 225 (86.5%) assessments, 'moderate' in 17 (6.5%) and 'difficult/not possible' in 18 (6.9%). For the DOI-FIGO 2021 method, these figures were respectively

138 (53.0%), 66 (25.4%) and 56 (21.5%). Figure 1 The DOI-FIGO 2009 method was preferred in 134 (51.5%) assessments, the DOI-FIGO 2021 in 95 (36.5%), tumor thickness in 19 (7.3%), no invasion in 8 (3.1%) and no preferred method in 4 (1.5%). Of the 26 vulvar cancer cases, a high agreement (> 80%) on the preferred method was present for 6 cases (4 FIGO 2009; 2 FIGO 2021), a moderate agreement (60-70%) was present in 8 cases (4 FIGO 2009; 4 FIGO 2021) and no agreement ( $\leq 50\%$ ) in 12 cases. Figure 2

Figure 1 - 867

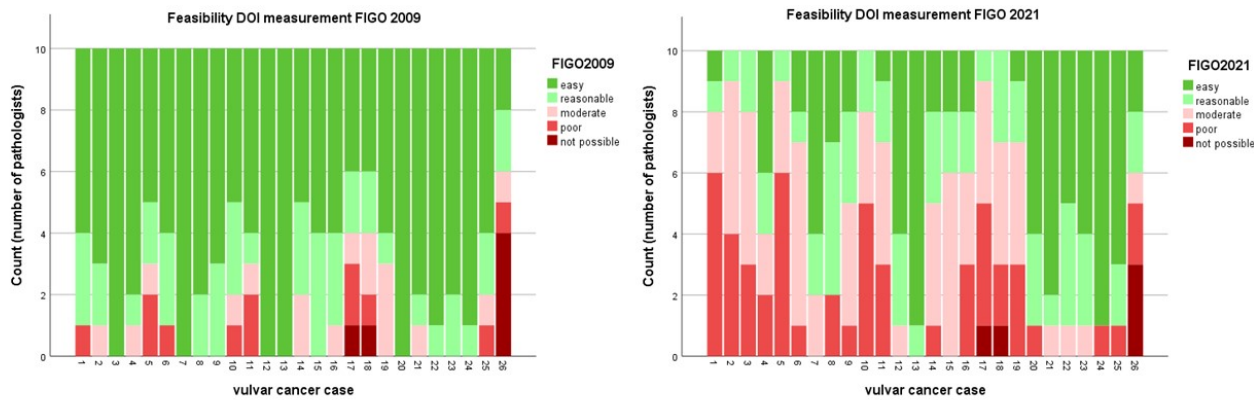


Figure 1: Feasibility of the DOI measurement according to the FIGO 2009 and FIGO 2021 definitions\*

\*The FIGO 2009 method to measure depth of invasion (DOI) is defined by the distance between the epithelial-stromal junction of the most superficial adjacent stromal papillae and the deepest point of invasion. The FIGO 2021 method to measure DOI is defined by the distance between the most adjacent dysplastic epithelium and the deepest point of invasion

Figure 2 – 867

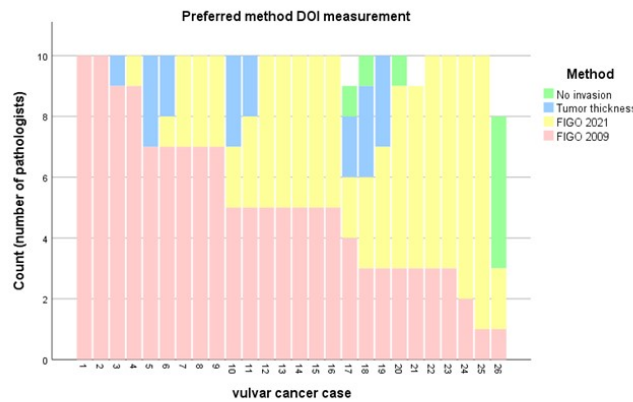


Figure 2: Preferred method\* of DOI measurement in vulvar cancer

\*The FIGO 2009 method is defined by the distance between the epithelial-stromal junction of the most superficial adjacent stromal papillae and the deepest point of invasion. The FIGO 2021 method is defined by the distance between the most adjacent dysplastic epithelium and the deepest point of invasion. The tumor thickness is defined by the distance between the surface of the dysplastic epithelium and the deepest point of invasion

**Conclusions:** The introduction of the FIGO 2021 depth of invasion measurement is difficult to apply in a subset of vulvar cancers. The FIGO 2009 DOI measurement was intuitively the preferred method in selected vulvar cancer cases. We may need to rethink this as "one method does not appear to fit all" vulvar cancers.

**868 Anaplastic Juvenile Granulosa Cell Tumors: A Variant Characterized by Recurrent TP53 Mutations, Frequent MYC Amplification and Aggressive Behavior**

Baris Boyraz<sup>1</sup>, Zehra Ordulu<sup>2</sup>, Jaclyn Watkins<sup>3</sup>, Rishikesh Haridas<sup>4</sup>, Pankhuri Wanjari<sup>5</sup>, Robert Young<sup>6</sup>, Esther Oliva<sup>3</sup>, Jennifer Bennett<sup>7</sup>

<sup>1</sup>Massachusetts General Hospital, Boston, MA, <sup>2</sup>University of Florida, Gainesville, FL, <sup>3</sup>Massachusetts General Hospital, Harvard Medical School, Boston, MA, <sup>4</sup>University of Chicago Medicine, Chicago, IL, <sup>5</sup>University of Chicago Medical Center, Chicago, IL, <sup>6</sup>Harvard Medical School, Boston, MA, <sup>7</sup>University of Chicago, Chicago, IL

**Disclosures:** Baris Boyraz: None; Zehra Ordulu: None; Jaclyn Watkins: None; Rishikesh Haridas: None; Pankhuri Wanjari: None; Robert Young: None; Esther Oliva: None; Jennifer Bennett: None

**Background:** Cytologic atypia and brisk mitoses including atypical forms are well-known features of juvenile granulosa cell tumors (JGCT), and in the largest study to date, Young et al. noted these features to be associated with decreased survival in JGCTs with extra-ovarian spread. In addition to these features, tumors also showing loss of the typical orderly architecture have been designated "anaplastic" JGCTs. Similar features have been described in adult granulosa cell tumors, which were shown to harbor *TP53* mutations. Herein, we report the first series of anaplastic JGCTs focusing on their morphology, molecular profile, and clinical behavior.

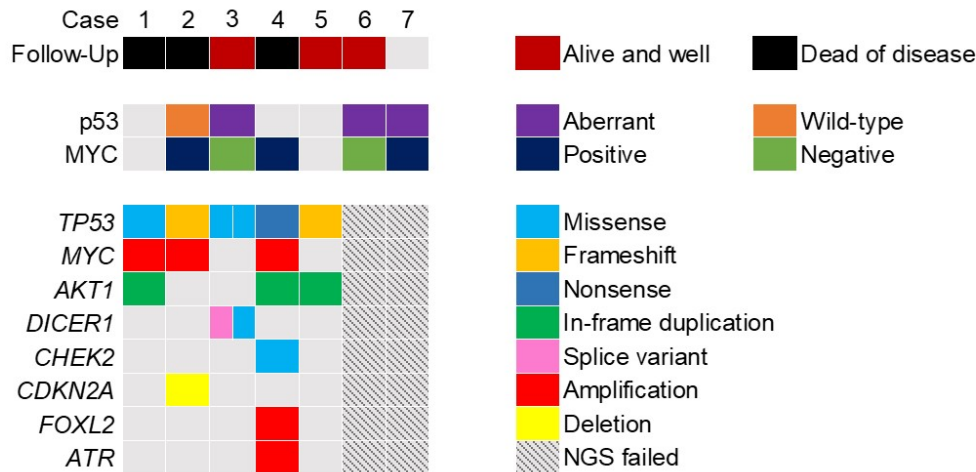
**Design:** 7 anaplastic JGCTs were identified from consultation files. An average of 26 H&E slides were reviewed (range 18-40). All tumors underwent next-generation sequencing on a 168 gene panel. p53 and MYC IHC were performed in selected tumors.

**Results:** Patients ranged from 9 to 22 (mean 13.7) years. Tumors ranged from 15.5 to 28 (mean 21.1) cm; they were solid and cystic with necrosis seen in 2. Conventional JGCT with diffuse/nodular, follicular, and/or papillary growths were seen in all and anaplastic areas constituted 10 to 90% (mean 42%). The components were vaguely demarcated from each other in 6 while admixed in 1 tumor. In the conventional areas, cytologic atypia was typically 2+ (with 3 showing foci of 3+) and mitoses ranged from 7-18 (mean 12.4)/10 HPFs. Anaplastic areas showed 4+ atypia and 19-41 (mean 30.8) mitoses/10 HPFs. Multinucleated (non-bizarre) tumor cells were identified in all (extensive in 3, rare in 1), tumor cell necrosis in 5, and lymphovascular invasion in 1. Sequencing was successful in 5 tumors and all harbored *TP53* mutations, with aberrant p53 expression noted in the remaining 2 by IHC. Other recurring alterations included *MYC* amplification (n=3, all patients dead of disease) and *AKT1* in-frame duplications (n=3). FIGO stage was IA (n=1), IC3 (n=2), II (n=1), IIIA (n=2), and unknown (n=1). Follow-up was available for 6 patients (mean 30 months); 3 died of disease and 3 were alive and well (range: 10-108 months, all stage I). Clinicopathological and molecular features summarized in Table and Figure.

Case	Age	Presentation	Size (cm)	FIGO Stage	Conventional			Anaplastic			Multinucleated Cells	Necrosis	LVI	Follow-Up (months)
					%	Atypia	Mitoses/10 HPF	%	Atypia	Mitoses/10 HPF				
<b>1</b>	12	Bloating, abdominal distension	22	IIIA	50	2-3	9	50	4	41	+	+	+	DOD, 7
<b>2</b>	22	Abdominal pain	28	IIIA	75	2-3	16	25	4	35	+	+	-	DOD, 22
<b>3</b>	13	NA	19	IC3	90	1-4*	25*	10	1-4*	25*	+	-	-	NED, 26
<b>4</b>	9	Intestinal occlusion	20	II	10	2	CBD	90	4	31	Rare	+	-	DOD, 8
<b>5</b>	12	NA	15.5	IC3	90	2-3	18	10	4	Rare	+	-	-	NED, 10
<b>6</b>	14	NA	21.8	IA	50	2	7	50	4	19	+	+	-	NED, 108
<b>7</b>	NA	NA	NA	NA	40	2	12	60	4	34	+	+	-	NA

HPF: High-power field, LVI: Lymphovascular invasion, +: Present, -: Absent, DOD: Dead of disease, NA: Not available, NED: No evidence of disease, CBD: Cannot be determined, \*: Merging components.

Figure 1 - 868



**Conclusions:** Anaplastic JGCTs are characterized by recurrent *TP53* mutations, often with concurrent *MYC* amplifications. These novel findings may have prognostic and therapeutic implications as tumors with *MYC* amplifications are associated with poor outcome but patients may benefit from *MYC* inhibitors.

### 869 Endometrial/oid Stromal Tumors with Extensive Whorling and *CTNNB1* Translocation: A Report of Three Cases

Baris Boyraz<sup>1</sup>, Arnaud Da Cruz Paula<sup>2</sup>, Kelly Devereaux<sup>3</sup>, Ivy Tran<sup>4</sup>, Edaise M. da Silva<sup>2</sup>, Robert Young<sup>5</sup>, Matija Snuderl<sup>6</sup>, Britta Weigelt<sup>2</sup>, Esther Oliva<sup>7</sup>

<sup>1</sup>Massachusetts General Hospital, Boston, MA, <sup>2</sup>Memorial Sloan Kettering Cancer Center, New York, NY, <sup>3</sup>NYU Grossman School of Medicine, NY, <sup>4</sup>NYU Langone Health, New York, NY, <sup>5</sup>Harvard Medical School, Boston, MA, <sup>6</sup>New York University, New York, NY, <sup>7</sup>Massachusetts General Hospital, Harvard Medical School, Boston, MA

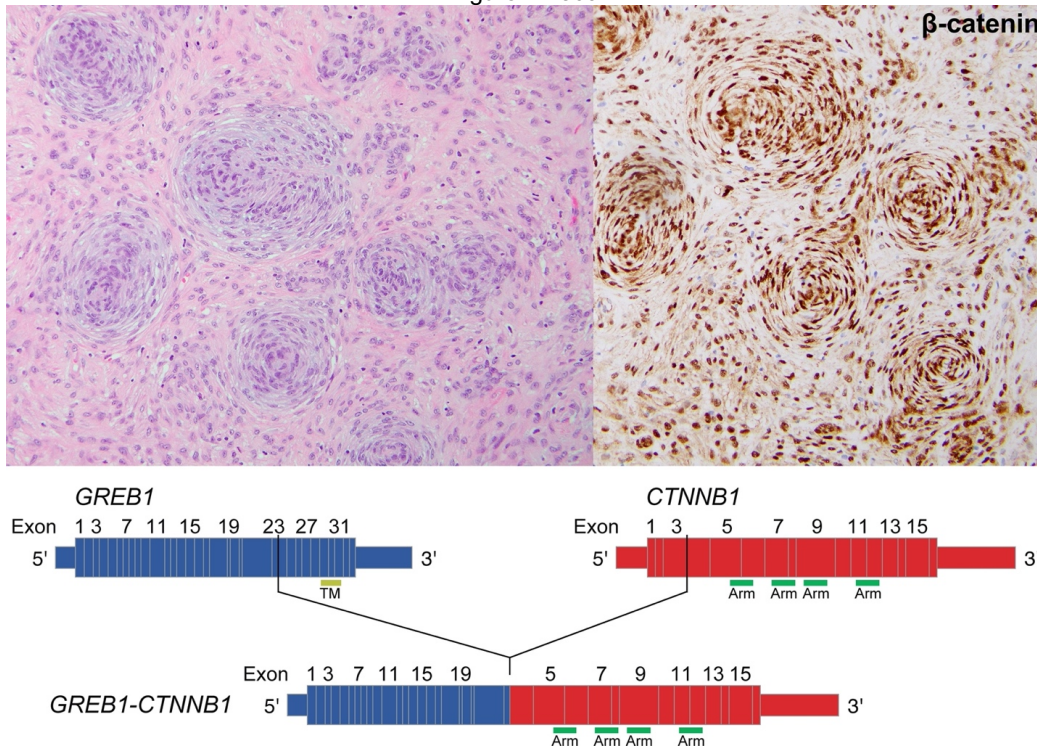
**Disclosures:** Baris Boyraz: None; Arnaud Da Cruz Paula: None; Kelly Devereaux: None; Ivy Tran: None; Edaise M. da Silva: None; Robert Young: None; Matija Snuderl: None; Britta Weigelt: None; Esther Oliva: None

**Background:** Endometrial stromal tumors are morphologically heterogenous and their diagnosis may especially be difficult when they show variant morphology and lack typical areas of endometrial stromal neoplasia. We identified three endometrial/oid stromal tumors with identical and previously undescribed histologic features and herein report their morphologic, immunohistochemical, and molecular profile.

**Design:** Clinical and gross characteristics were obtained from the consultation correspondence. An average of 16 (range 12-20) H&E slides was examined. CD10, β-catenin, calretinin, WT1, SMA, desmin and ER immunostains were performed. All 3 cases were subjected to RNA sequencing and *CTNNB1* split-apart FISH. Whole genome DNA methylation analysis was performed using Illumina EPIC array and data were analyzed by the DKFZ sarcoma classifier. Copy number analysis was performed using the conumee package.

**Results:** Patients were 53-, 62-, and 79-year-old. Tumors were completely resected, well-circumscribed, tan-yellow solid masses measuring 10.0, 11.0 and 18.7 cm, and were intramyoemtrial (n=2) or arose from the broad ligament (n=1). All showed a fibroblastic background with small and tight whorls of epithelioid to slightly spindled tumor cells with minimal cytoplasm and negligible mitosis, multifocally associated with hyalinization and myxoid changes and small, delicate vessels. This morphology was seen throughout in two and in ~20% of the other with the remaining areas showing cords, hollow tubules, and nests of tumor cells. CD10 (3/3, 1 focal), calretinin (3/3 diffuse), WT1 (3/3 diffuse), ER (1/1, diffuse) were positive while SMA (0/3), desmin (0/1), SF1 (0/1) and inhibin (0/2) were negative in the tumor cells. RNA sequencing was successful in one, and revealed a *GREB1-CTNNB1* in-frame fusion with a driver probability of 99%. All three tumors showed a *CTNNB1* translocation by FISH correlating with nuclear β-catenin positivity. All tumors fell under the low-grade endometrial stromal sarcoma reference class by methylation analysis with flat copy number profiles. One patient (79-year-old) died of unrelated causes two months after surgery and the other two were alive without disease after 9 and 72 months.

Figure 1 - 869



**Conclusions:** We have identified a rare subset of endometrial/oid stromal nodules/tumor with extensive whorling and *CTNNB1* translocation, a genetic alteration previously not described, expanding the morphologic and molecular spectrum of these neoplasms.

#### 870 Malignant Uterine Tumors Resembling Ovarian Sex Cord Tumors Lack *ESR1::NCOA1/2/3* Fusions

Baris Boyraz<sup>1</sup>, Fleur Cordier<sup>2</sup>, Mark Sabbagh<sup>1</sup>, Koen Van de Vijver<sup>3</sup>, Robert Young<sup>4</sup>, Jochen Lennerz<sup>5</sup>, Esther Oliva<sup>5</sup>

<sup>1</sup>Massachusetts General Hospital, Boston, MA, <sup>2</sup>UZ Gent, Gent, Belgium, <sup>3</sup>Ghent University Hospital, Gent, Belgium, <sup>4</sup>Harvard Medical School, Boston, MA, <sup>5</sup>Massachusetts General Hospital, Harvard Medical School, Boston, MA

**Disclosures:** Baris Boyraz: None; Fleur Cordier: None; Mark Sabbagh: None; Koen Van de Vijver: None; Robert Young: None; Jochen Lennerz: None; Esther Oliva: None

**Background:** Uterine tumors resembling ovarian sex cord tumors (UTROSCTs) are rare and most have been molecularly defined by *ESR1::NCOA1/2/3* fusions with only a minor subset harboring *GREB1* fusions. Despite these molecular findings, it has not yet been fully investigated whether different molecular alterations underlie tumors with different behavior. Five malignant UTROSCTs have been reported in a large cohort with >3 of 5 of the following features predictive of aggressive behavior: size >5 cm, infiltrative borders, at least moderate cytologic atypia, mitotic rate >3/10HPF, and tumor cell necrosis. Herein we study the molecular landscape of 13 UTROSCTs.

**Design:** 10 benign and 3 malignant UTROSCTs were identified. An average of 4 (range 2-11) H&E slides were examined. All tumors were submitted for solid fusion assay (SFA; 59 genes including *ESR1*, *JAZF1*) and 1 underwent RNA sequencing.

**Results:** Patients ranged from 32 to 73 (mean 52), and tumors from 1 to 11.5 (mean 5.2) cm. 10 were well-circumscribed, 3 minimally infiltrative. Predominant patterns (>50%) included diffuse (4), nests (2) and cords (1), and were intermixed with other patterns. 10/13 had smooth muscle pseudoinfiltration (range 10-60%, 3 extensive). Cytologic atypia was mild (8), moderate (3), moderate to severe (2) and 1 showed extensive rhabdoid morphology. Mitoses were negligible in 7, and 2-9 /10HPF in the others. 1 tumor showed necrosis. Follow-up was available for all, ranged from 10 to 144 (mean 60) months. 3 patients developed metastasis at 30-144 months and tumors showed 4/5 described features. Benign tumors showed 0 (n=7), 1 (n=1; size), 2 (n=1; size and borders), 3 (n=1; atypia, mitosis, necrosis; tumor with rhabdoid morphology) features. SFA only detected *ESR1::NCOA3* in 5/10 benign tumors (4 with 0 features, 1 with 3; 3/5 with extensive smooth muscle) but in none of the malignant tumors. No morphologic differences were identified between fusion-positive and negative benign tumors, and architectural patterns were similar between benign and malignant UTROSCTs. *JAZF1* fusion was not identified in any tumors. RNA sequencing revealed *GREB1::NCOA1* fusion in one malignant UTROSCT.

**Conclusions:** *ESR1::NCOA3* fusion was identified only in a subset of UTROSCTs (5/13) all being benign. However, in this very limited cohort, all 3 malignant tumors lack this fusion and likely show different genetic alterations as highlighted by *GREB1* fusion in one. Further molecular studies are in progress.

## 871 SARS-CoV2 Placental Infections and Relationship to Distal Villous Fetal Vascular Malperfusion

Andrea Breaux<sup>1</sup>, Faizan Malik<sup>2</sup>, Anas Bernieh<sup>1</sup>, Jerzy Stanek<sup>1</sup>

<sup>1</sup>Cincinnati Children's Hospital Medical Center, Cincinnati, OH, <sup>2</sup>Hospital of the University of Pennsylvania, Philadelphia, PA

**Disclosures:** Andrea Breaux: None; Faizan Malik: None; Anas Bernieh: None; Jerzy Stanek: None

**Background:** SARS-CoV2 placentitis features the triad of histiocytic and neutrophilic intervillitis, perivillous fibrin deposition, and trophoblast necrosis. We have also noticed features of fetal vascular malperfusion (FVM) in such cases. The CD34 immunohistochemical stain is a sensitive detector of recent/on-going FVM. Its utility has not been explored in COVID-infected placentas, however. Consequently, this study analyzes the rate of FVM in a cohort of cases with placentas positive for SARS-CoV2 by immunohistochemistry and a comparative group of women prenatally positive for SARS-CoV2 by serology but without placental evidence of SARS-CoV2 infection by immunohistochemistry.

**Design:** This is a retrospective analysis of cases of our institution from years 2020-2022. Group 1 contained 15 cases with SARS-CoV2 placentitis and Group 2 contained 18 mothers, positive prenatally for SARS-CoV2 by serology, but placentas negative by immunohistochemistry. All cases were stained by hematoxylin-eosin and immunohistochemistry for SARS-CoV2 and CD34 (for recent FVM featuring villous endothelial fragmentation). 23 independent clinical and 55 placental phenotypes were compared by Chi-square or analysis of variance where appropriate.

**Results:** Histologic features are shown in figures 1 and 2. Statistically significant differences ( $p<0.05$ ) were found in gestational age ( $28.9\pm7.7$  vs 36.0 weeks), perinatal mortality (80% vs 11%), macerated stillbirth (80% vs 6%), cesarean section rate (0% vs 28%), congenital malformations (0% vs 72%), placental weight (224 vs 446 gm), and increased extravillous trophoblasts in chorionic disc (0% vs 28%), in Group 1 and 2 respectively. Although not statistically significant, distal villous FVM was 80% and 89% in Group 1 and 2, respectively. In particular, the recent/on-going FVM with temporal heterogeneity was particularly high in Group 1 (47% vs 33%). Large vessel/proximal FVM was higher in Group 2 (7% vs 28%).

Figure 1 - 871

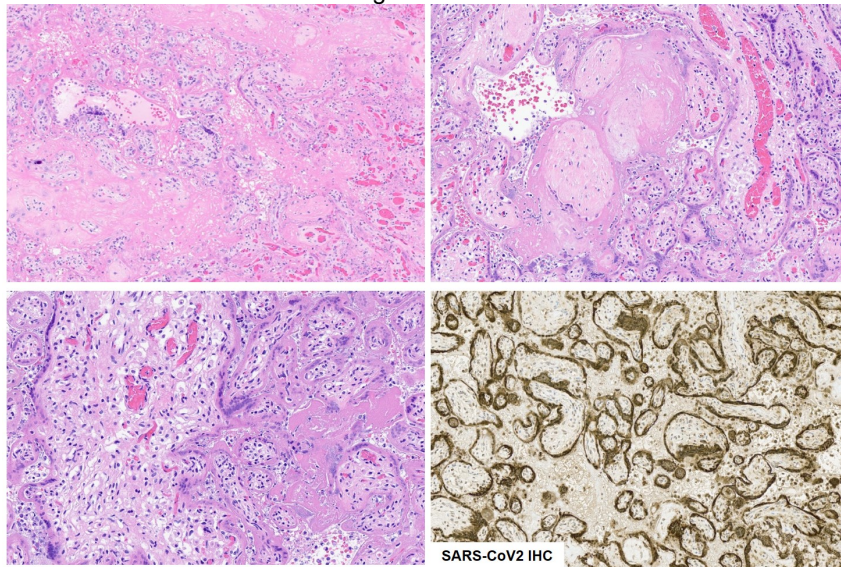


Figure 1. Classic histopathologic features of SARS-CoV2 placentitis with circumferential staining around villi with SARS-CoV2 immunostain

Figure 2 - 871

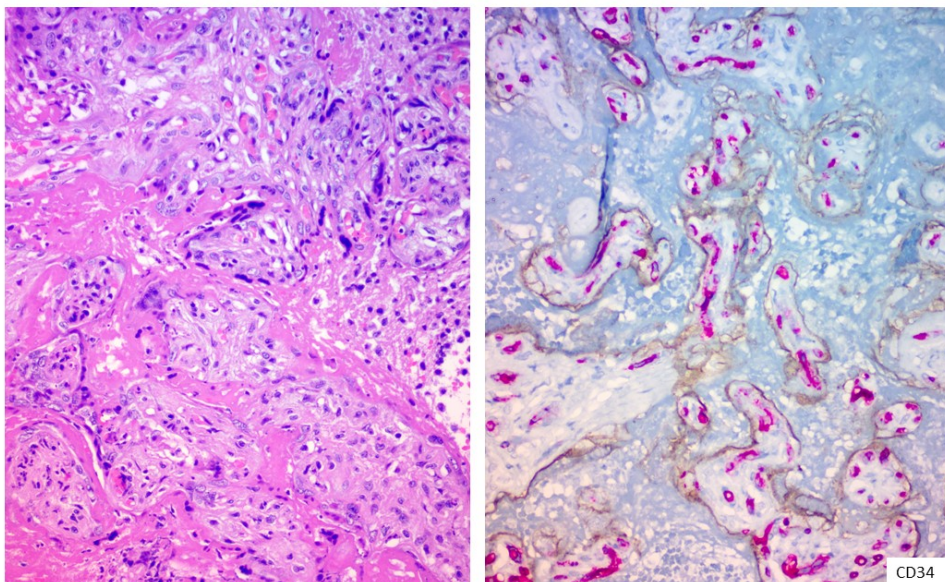


Figure 2. Examples of H&E and CD34 IHC staining demonstrating classic triad of SARS-CoV2 placentitis and endothelial fragmentation by CD34 stain consistent with fetal vascular malperfusion.

**Conclusions:** FVM was higher in SARS-CoV2 positive placentas than in any other clinically defined placental populations known to us, and much higher than the incidence of FVM in other perinatal infections. The high incidence of FVM in the comparative group may be explained by the high percentage of fetal congenital malformations in Group 2. Therefore, the high stillbirth rate in Group 1 may be explained by an additive effect of FVM resulting from massive perivillous fibrin deposition, intervillitis, and trophoblastic necrosis.

## 872 Expression of H3K27me3, a Histone Repressor Mark, in Serous Tubal Intraepithelial Carcinoma

Yen-Wei Chien<sup>1</sup>, Chi-Long Chen<sup>2</sup>, Brant Wang<sup>3</sup>, Russell S. Vang<sup>1</sup>, Tian-Li Wang<sup>4</sup>, Ie-Ming Shih<sup>5</sup>

<sup>1</sup>Johns Hopkins University School of Medicine, Baltimore, MD, <sup>2</sup>Taipei Medical University, <sup>3</sup>Inova Fairfax Hospital, Falls Church, VA, <sup>4</sup>Johns Hopkins Medical Institutions, Baltimore, MD, <sup>5</sup>Johns Hopkins Hospital, Baltimore, MD

**Disclosures:** Yen-Wei Chien: None; Chi-Long Chen: None; Brant Wang: None; Russell S. Vang: None; Tian-Li Wang: None; Ie-Ming Shih: None

**Background:** Chromatin remodeling is essential for a multitude of pathobiological processes including tumor initiation and progression. Modification in histone either by methylation or acetylation drives the remodeling. The updated paradigm in the genesis of ovarian high-grade serous carcinomas (HGSCs) posits that most of HGSCs originate from the precursor lesions on the fallopian tube epithelium. Serous tubal intraepithelial carcinomas (STICs) represent the earliest morphologically recognizable lesions in the development of HGSCs. How histone modifications alter in STICs remains an important question to be answered. In this study, we applied H3K27me3 immunohistochemistry on fallopian tubes containing STICs and HGSCs to compare their expression patterns.

**Design:** A total of 30 STICs and 26 HGSCs from 31 women were analyzed for H3K27me3 immunoreactivity. A rabbit monoclonal antibody against H3K27me3 was used. In addition, 3 normal fallopian tube epithelial (NFTE) samples, one NFTE cell line, 2 HGSC cell lines and one HGSC tissue were studied for H3K27me3 expression by immunoblotting using the same antibody. We employed a semi-quantitative H-score system for staining and the Kruskal-Wallis test for statistical analysis. This study was approved by the institutional review board.

**Results:** By comparing STIC, NFTE, and HGSC groups, we found that the H-scores of the STICs were lower than NFTEs, but higher than HGSCs ( $P$ -value < 0.0001). Among the same patients, we found 21 (70%) of 30 cases showing progressive decrease in the H-score from NFTE, STIC and HGSC. There was no correlation between the H-scores of the STICs and the following features: ages of patients, Ki-67 proliferation index, and papillary vs. flat STICs. Based on the Western blot analysis, we detected a single 17 kDa band corresponding to H3K27me3, indicating the high specificity of the antibody. In the Western blot analysis, we also observed that the 4 NFTE samples expressed significantly higher levels of H3K27me3 protein than HGSC samples.

Figure 1 - 872

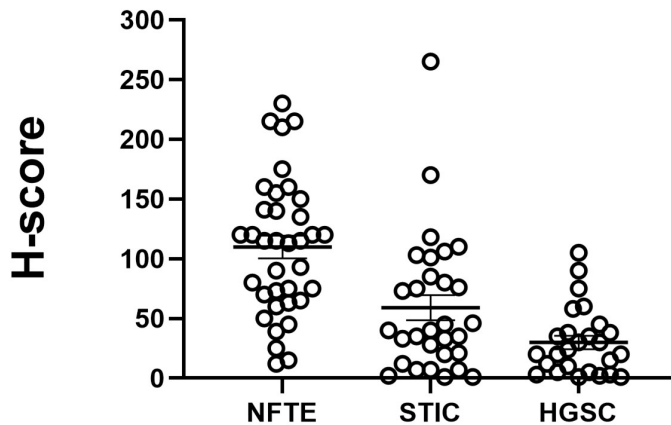


Figure 1. The scatter plot depicting the H-score (y axis) of each NFTE, STIC, and HGSC (x axis).

Figure 2 – 872

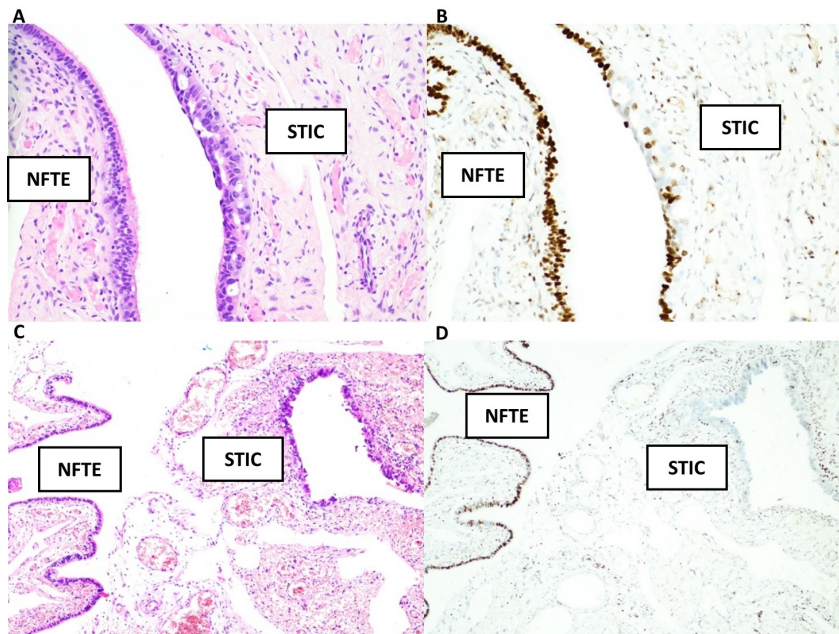


Figure 2. The H&E-stained images (A, 20X, C, 10X) and H3K27me3 immunohistochemical-stained images (B, 20X, D, 10X) of two STICs and the adjacent NFTEs in two patients.

**Conclusions:** Our results show a progressive decrease in H3K27me3 from NFTE, STIC to HGSC, suggesting that a decrease of this histone repressor mark occurs in HGSC precursors. These findings provide new insights into a possible role of chromatin configuration in the development of HGSC.

### 873 Early Genetic Divergence of High-grade Serous Carcinomas Originating from Low-grade Serous Ovarian Neoplasms

M. Herman Chui<sup>1</sup>, Qianqian Song<sup>2</sup>, Brant Wang<sup>3</sup>, Tian-Li Wang<sup>4</sup>, Russell S. Vang<sup>5</sup>, Ie-Ming Shih<sup>6</sup>

<sup>1</sup>Memorial Sloan Kettering Cancer Center, New York, NY, <sup>2</sup>Cancer Hospital Chinese Academy of Medical Sciences, Beijing, China, <sup>3</sup>Inova Fairfax Hospital, Falls Church, VA, <sup>4</sup>Johns Hopkins Medical Institutions, Baltimore, MD, <sup>5</sup>Johns Hopkins University School of Medicine, Baltimore, MD, <sup>6</sup>Johns Hopkins Hospital, Baltimore, MD

**Disclosures:** M. Herman Chui: None; Qianqian Song: None; Brant Wang: None; Tian-Li Wang: None; Russell S. Vang: None; Ie-Ming Shih: None

# ABSTRACTS | GYNECOLOGIC AND OBSTETRIC PATHOLOGY

**Background:** The current paradigm implicates a fallopian tube precursor as the origin for most ovarian high-grade serous carcinomas (HGSC). However, a rare subset of HGSCs develop via a distinct pathway from low-grade serous ovarian neoplasms, specifically low-grade serous carcinoma (LGSC) or serous borderline tumor (SBT). The molecular pathogenesis and evolutionary trajectory of this low-grade to high-grade transformation is unclear.

**Design:** Histomorphologic review was performed on 7 cases of SBT or LGSC associated with a synchronous or metachronous high-grade carcinoma (HGSC or poorly-differentiated carcinoma). Whole exome sequencing analyses was performed on microdissected low-grade and high-grade components from individual cases. Phylogenetic trees were constructed from single nucleotide variants and LOH events.

**Results:** Low-grade tumor components were morphologically indistinguishable from conventional SBTs/LGSCs. The degree of nuclear pleomorphism in high-grade tumors from the 7 patients was variable (grade 2 nuclear atypia, n=2, and up to grade 3, n=5). Notably, 1 patient initially presented with ovarian LGSC, which progressed to HGSC (nuclear grade 2, 23 mitoses per 10 HPF), followed by a subsequent LGSC recurrence. Truncal mutations, present across all tumor samples from a given patient, included known drivers of low-grade serous neoplasms: *KRAS* (n=4), *BRAF* (G469A, n=1), *NF2* (n=1), and *USP9X* (n=1). High-grade transformation was associated with a *TP53* mutation in 3 cases, all with grade 3 nuclear atypia and genome-wide allelic imbalances. Interestingly, a heterozygous *TP53* mutation was detected in an SBT, with loss-of-heterozygosity upon progression to HGSC. Immunohistochemical analysis revealed aberrant p53 expression only with bi-allelic inactivation of *TP53* and confirmed ATRX and p16/CDKN2A loss in tumors harboring these genetic alterations. Phylogenetic analyses revealed relatively few shared mutations between matched low-grade and high-grade tumors compared to private mutations specific to each component (i.e. trees with short trunks and long branches).

Figure 1 - 873

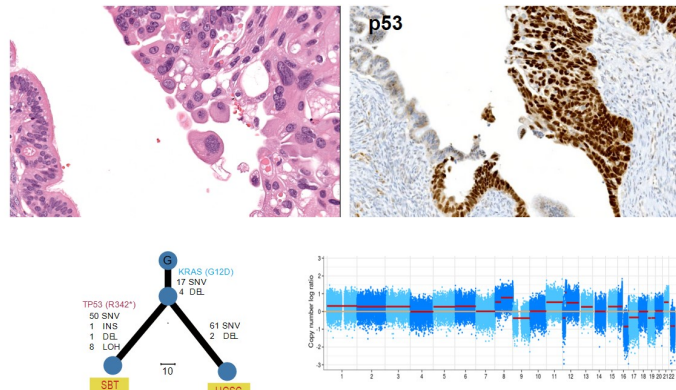


Figure 1: TP53-mutated HGSC arising from SBT.

Figure 2 - 873

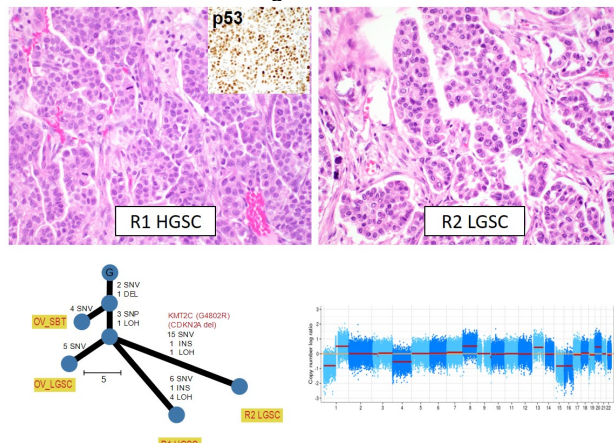


Figure 2: TP53-wildtype HGSC recurrence (R1) in patient with prior ovarian LGSC, followed by subsequent LGSC recurrence (R2)

**Conclusions:** Synchronous and metachronous low-grade serous neoplasms and high-grade carcinomas are clonally related but show early genetic divergence, suggesting that high-grade transformation may be a relatively early molecular event. *TP53* wild-type HGSCs are morphologically and molecularly distinct from conventional *TP53*-mutated HGSCs.

## 874 Mixed Ovarian Neoplasms with Gastrointestinal-Type Mucinous and Müllerian Epithelial Components: A Rare Group of Tumors Demonstrating the Phenotypic Plasticity of the Müllerian Epithelial Cell

M. Herman Chui<sup>1</sup>, Lora Ellenson<sup>1</sup>

<sup>1</sup>Memorial Sloan Kettering Cancer Center, New York, NY

**Disclosures:** M. Herman Chui: None; Lora Ellenson: None

**Background:** Primary mucinous ovarian neoplasms, gastrointestinal-type (GI-type), are composed of mucin-producing tumor cells resembling intestinal goblet cells or gastric foveolar epithelium. In contrast to seromucinous tumors, which exhibit endocervical-type mucinous differentiation and thought to be derived from endometriosis, the cell/tissue-of-origin of most GI-type mucinous ovarian tumors is unknown.

**Design:** We identified 7 GI-type mucinous ovarian tumors (cystadenomas, n=3; borderline tumor/carcinoma, n=4) with spatially distinct areas showing morphologic features of Müllerian-type epithelial differentiation (ciliated cells or endometrioid-type glands). Immunohistochemistry for cell lineage markers and PAS/Alcian Blue staining were performed. Morphologically distinct components were isolated by microdissection, from which extracted DNA was analyzed by targeted next generation sequencing.

**Results:** In all cases, immunohistochemistry demonstrated mucin-producing cells to be positive for at least one GI marker (CK20 or CDX2), while areas with morphologic features of Müllerian differentiation were positive for PAX8, ER and/or PR, and lacked expression of CK20 and CDX2; CK7 was strongly and diffusely positive in all tumor cells. Tumor cells with a gastric-type phenotype produced neutral mucin, while acidic mucin was present within intestinal-type goblet cells. Targeted sequencing revealed *ARID1A* mutations in all mixed borderline/malignant tumors (n=4); other recurrent genetic alterations included *KRAS* (n=2) and *TP53* mutations (n=2). Shared mutations were present in paired Müllerian and GI-type mucinous tumor components, consistent with their derivation from a common ancestor, with more shared mutations between components than private mutations specific to each component. All mixed borderline/malignant tumors were associated with endometriosis (n=3) or Müllerian inclusion cysts (n=1), and mutation or loss of *ARID1A* expression was seen in these putative precursor lesions in 2 cases.

Figure 1 – 874

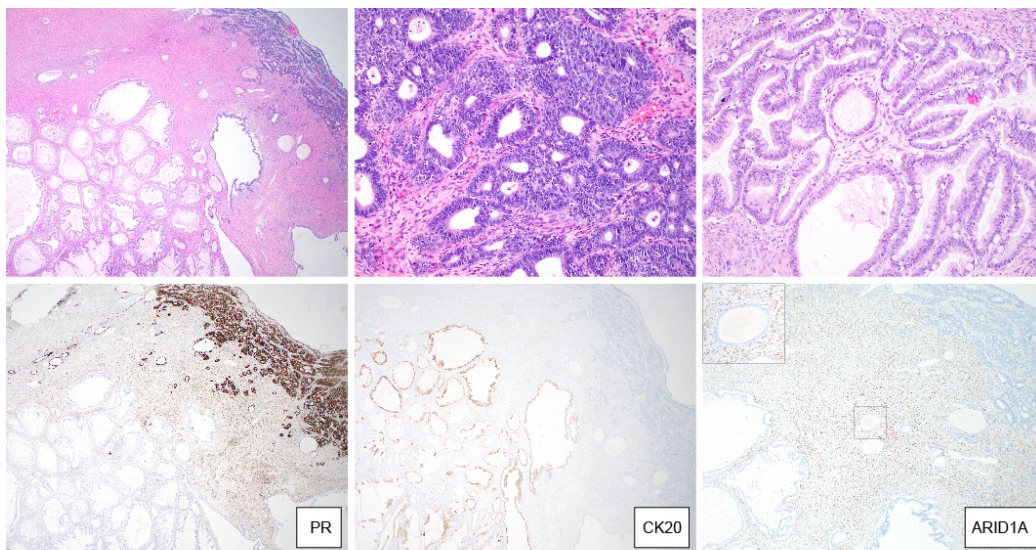


Figure 1: Representative case of mixed endometrioid and GI-type mucinous carcinoma.

Figure 2 – 874

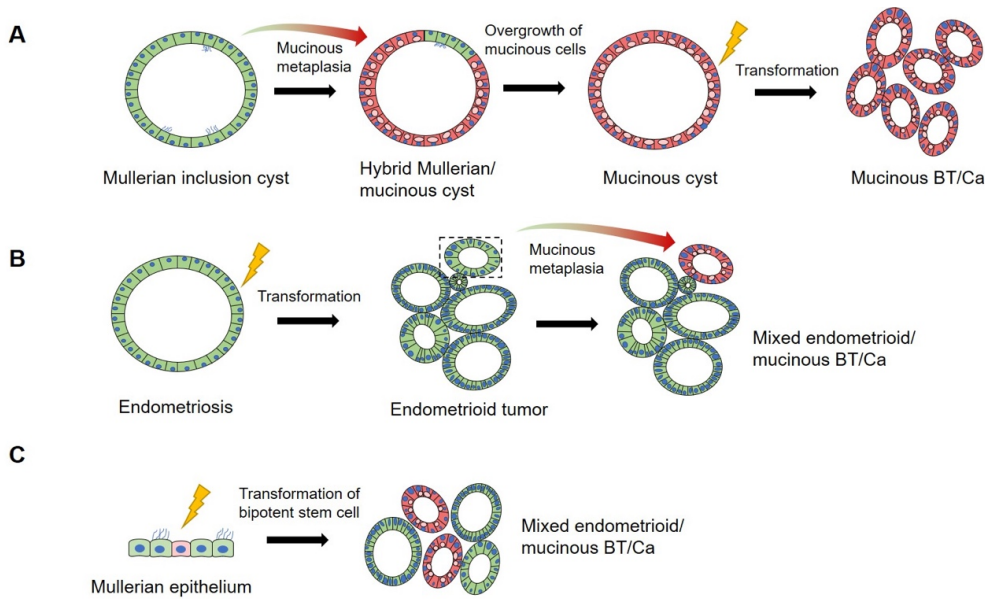


Figure 2: Proposed pathogenic models for pure and mixed GI-type mucinous ovarian tumors originating from Mullerian epithelial precursors.

**Conclusions:** Ovarian neoplasms composed of clonally related GI-type mucinous and Müllerian-type epithelial components harbor *ARID1A* mutations and are frequently associated with endometriosis. The existence of a Müllerian stem/progenitor cell with the capacity to differentiate towards cell lineages within the GI-tract may be involved in the pathogenesis of at least a subset of GI-type mucinous ovarian neoplasms.

## 875 Homologous Recombination Deficiency (HRD) Status in Rare Histotypes of Ovarian Carcinomas: A Single-Center Experience

Riccardo Ciudino<sup>1</sup>, Francesca Rosini<sup>2</sup>, Angelo Corradini<sup>3</sup>, Alessia Costantino<sup>2</sup>, Sara Coluccelli<sup>4</sup>, Thais Maloberti<sup>1</sup>, Dario de Biase<sup>5</sup>, Giovanni Tallini<sup>6</sup>, Donatella Santini<sup>3</sup>, Antonio De Leo<sup>5</sup>

<sup>1</sup>Alma Mater Studiorum-University of Bologna, Bologna, Italy, <sup>2</sup>IRCCS Azienda Ospedaliero-Universitaria di Bologna, Bologna, Italy, <sup>3</sup>S.Orsola-Malpighi Hospital, University of Bologna, Bologna, Italy, <sup>4</sup>Gynecologic Oncology Unit, S.Orsola-Malpighi Hospital, University of Bologna, Bologna, Italy, <sup>5</sup>University of Bologna, Bologna, Italy, <sup>6</sup>University of Bologna School of Medicine, Bologna, Italy

**Disclosures:** Riccardo Ciudino: None; Francesca Rosini: None; Angelo Corradini: None; Alessia Costantino: None; Sara Coluccelli: None; Thais Maloberti: None; Dario de Biase: None; Giovanni Tallini: None; Donatella Santini: None; Antonio De Leo: None

**Background:** HRD status has recently emerged as a predictive factor for response to PARP inhibitors in patients with ovarian carcinoma. This molecular parameter has been studied in high-grade serous carcinomas, but little is known in rare histotypes of ovarian carcinoma. The aim of the study is to investigate HRD status in rare histotypes of ovarian carcinoma such as so-called Indeterminate-Grade Serous Carcinomas (IGSCs)/serous carcinoma with mixed morphologic features of high-grade and low-grade and Mesonephric-Like Carcinomas (MLCs) and to correlate it with clinicopathologic features.

**Design:** Clinicopathologic and immunohistochemical (IHC) characteristics were evaluated in 323 consecutive cases of ovarian carcinoma between 2019 and 2022. Next-generation sequencing (NGS) analysis including *BRCA1/2* status was evaluated in all histotypes excluding mucinous carcinoma. The molecular analysis was expanded in 90 cases with evaluation of HRD status by using MyChoice HRD Plus assay. HRD status was considered positive if deleterious mutations in *BRCA1/2* were detected and/or Genomic Instability Score (GIS) was positive (GIS ≥ 42).

**Results:** Histotypes distribution: 203 (62.8%) high-grade serous (HGSC) carcinomas, 45 (13.9%) endometrioid carcinomas, 24 (7.4%) mucinous carcinomas, 17 (5.2%) low-grade serous ovarian carcinomas, 11 (3.4%) carcinosarcomas, 10 (3.1%) clear cells carcinomas, 9 (2.9%) MLCs, 7 (2%) IGSCs, 1 (0.3%) undifferentiated carcinoma. HRD status was positive in 33/90 cases: 24 HGSC, 3 CS, and 6 IGSC. As regards IGSC, NGS analysis identified TP53 mutation in 3/7 (42.8%) cases, PIK3CA and NRAS in 2 cases. Within HRD positive IGSC cases, 1 case was mutated in *BRCA2*, and 1 showed concomitant mutations in *BRCA1* and

ERBB2. The only IGSC HRD negative case featured NRAS and TP53 concomitant mutations. 2 HRD positive IGSCs presented with disease recurrence and, after the treatment with PARPi, showed an indolent clinical course. Conversely, all the MLCs were HRD and BRCA1/2 negative, revealing pathogenic variants of KRAS in 8 cases (8/9) and BRAF in 1 case (1/9). Mutations in TP53, POLE and MMR deficiency were not identified in MLCs. 7 MLCs cases had early disease recurrence with lung metastases and aggressive clinical behaviour.

**Conclusions:** In our cohort, rare histotypes of ovarian carcinomas are characterized by morphological and molecular heterogeneity resulting in different clinical behaviour. The evaluation of molecular markers could improve potential novel target therapy for these uncommon tumors.

**876 HPV-Independent p53 Wild-Type Verruciform Acanthotic Vulvar Intraepithelial Neoplasia (vaVIN): Comprehensive Analysis Reveals Frequent CK17 positivity and a Wider Spectrum of Genomic Alterations**

Eleanor Cook<sup>1</sup>, Koen Van de Vijver<sup>2</sup>, Marisa Nucci<sup>3</sup>, Carlos Parra-Herran<sup>3</sup>

<sup>1</sup>Brigham and Women's Hospital, Boston, MA, <sup>2</sup>University Hospital Ghent, Liège, Belgium, <sup>3</sup>Brigham and Women's Hospital, Harvard Medical School, Boston, MA

**Disclosures:** Eleanor Cook: None; Koen Van de Vijver: None; Marisa Nucci: None; Carlos Parra-Herran: None

**Background:** The term verruciform acanthotic Vulvar Intraepithelial Neoplasia (vaVIN) has been recently coined to describe Human Papillomavirus-independent (HPVi), p53 wildtype lesions with characteristic clinical and morphologic correlates. Currently, p16 and p53 stains have little role beyond excluding other VIN types. Our aim is to expand the pathologic and molecular landscape of vaVIN and to explore the use of CK17, a marker expressed by HPVi lesions, in its diagnosis.

**Design:** Cases with Vulvar Acanthosis with Altered Differentiation, Differentiated Exophytic Vulvar Intraepithelial Lesion, and other verruciform atypias were retrieved; vaVIN diagnosis was confirmed by slide review. Clinical and pathologic features were documented. Immunohistochemistry for p16, p53 and CK17 was performed. Sequencing using a panel with 447-gene coverage was used to survey for single-nucleotide variants (SNV), copy number alterations and structural variants.

**Results:** Sixteen vaVIN samples from 12 patients were included (Table 1); 3 had a concurrent vSCC. Median patient age was 69 (range 56-85) years. All lesions were positive for CK17 (9 with full-thickness, 3 with middle-superficial staining). Adjacent unininvolved mucosa was present in 9 cases; all showed negative or discontinuous CK17 (Fig 1). Genomic aberrations were noted in 11 cases (92%). These included SNVs involving PIK3CA (n=6, 50%), NOTCH1-2 and FAT1 (each n=5, 42%), HRAS (n=3, 25%), ARID2 and KRAS (each n=1, 8%). CDKN2A alterations were also noted (n=4, 33%; 2 with biallelic 9p21.3 loss and 2 with SNVs). Follow-up information was found in 9 patients (mean period 28 [range 6-50] months). Seven patients were alive free of disease (2 had concurrent vSCC). One patient with vaVIN and vSCC had recurrence and is alive with disease at 6 months after diagnosis. Remaining vaVIN patient presented 22 months later with vSCC and died of disease 6 months later.

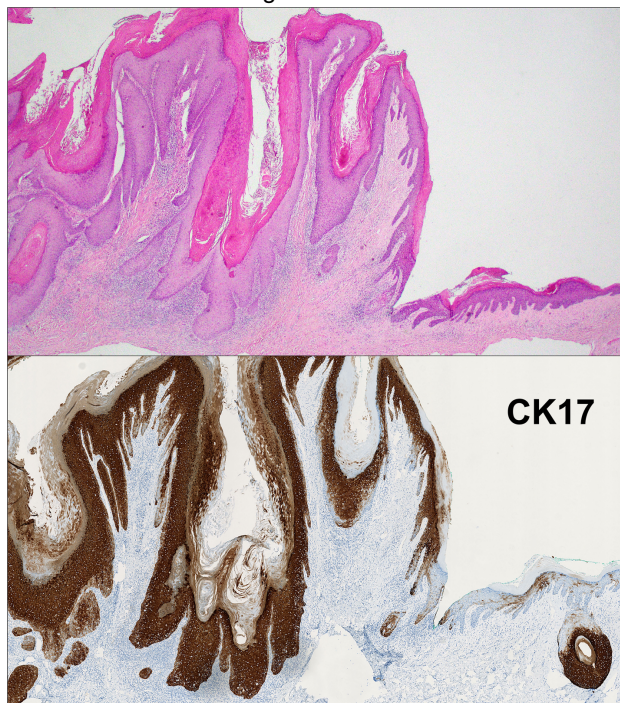
TABLE 1. Clinical, Pathologic and Molecular Findings

Case No. (n=12)	Age (years)	Diagnosis	p16 / p53 IHC in vaVIN / vSCC	CK17 IHC in vaVIN / vSCC	CK17 IHC in unininvolved mucosa	Pathogenic variants	Status at follow-up (period in months)
1	62	vaVIN	Negative / Wildtype	Positive (Full thickness)	N/A	NOTCH1 c.839A>G; TSC2 c.4468G>A	Unavailable
2	57	vaVIN	Negative / Wildtype	Positive (Full thickness)	Negative (Patchy)	None	Unavailable
3	64	vaVIN	Negative / Wildtype	Positive (Full thickness)	N/A	PIK3CA c.1624G>A; CDKN2A biallelic loss; FAT1 c.3286C>T	Unavailable
4	60	vaVIN and vSCC	vaVIN: Negative / Wildtype vSCC: Negative / Wildtype	vaVIN: Positive (Full thickness) vSCC: Positive (Full thickness)	Negative (Patchy)	HRAS c.35G>C; FAT1 c.8689C>T; NOTCH1 c.1057C>T; TSC2 c.2492C>T	Alive free of disease (34)
5	69	vaVIN	Negative / Wildtype	Positive (Full thickness)	Negative (Patchy)	PIK3CA c.1624G>A	Alive free of disease (28)
6	56	vaVIN	Negative / Wildtype	Positive (Full thickness)	Negative (Patchy)	FAT1 c.2017C>T; NOTCH1 c.1180G>T	Alive free of disease (18)
7	76	vaVIN	Negative / Wildtype	Positive (Full thickness)	Negative (Patchy)	PIK3CA c.3140A>G; HRAS c.173C>T; CDKN2A biallelic loss; NOTCH2 c.1298G>A	Subsequent vSCC; dead of disease (28)

# ABSTRACTS | GYNECOLOGIC AND OBSTETRIC PATHOLOGY

8	85	vaVIN and vSCC	vaVIN: Negative / Wildtype  vSCC: Negative / Wildtype	vaVIN: Positive (Full thickness)  vSCC: Positive (Full thickness)	Negative (Patchy)	<i>PIK3CA</i> c.1633G>A; <i>CDKN2A</i> c.151-2A>G; <i>FAT1</i> c.7666C>T; <i>NOTCH1</i> c.1363G>A; <i>ARID2</i> c.5260C>T	Alive with disease (6)
9	71	vaVIN	Negative / Wildtype	Positive (Mid-superficial)	N/A	<i>PIK3CA</i> c.1624G>A	Alive free of disease (36)
10	85	vaVIN	Negative / Wildtype	Positive (Full thickness)	Negative (Patchy)	<i>HRAS</i> c.182A>G	Alive free of disease (28)
11	76	vaVIN and vSCC	vaVIN: Negative / Wildtype  vSCC: Negative / Mutant	vaVIN: Positive (Mid-superficial)  vSCC: Positive (Full thickness)	Equivocal (Patchy, focally continuous)	<i>PIK3CA</i> c.1624G>A; <i>FAT1</i> c.2653C>T; <i>CDKN2A</i> c.151-1G>A; <i>TP53</i> c.473G>A; <i>TP53</i> c.733G>A	Alive free of disease (50)
12	70	vaVIN	Negative / Wildtype	Positive (Mid-superficial)	Negative (Patchy)	<i>KRAS</i> c.35G>A	Alive free of disease (24)

Figure 1 - 876



**Conclusions:** Our study shows a wider molecular spectrum in vaVIN, beyond known alterations in *PIK3CA*, *HRAS* and *ARID2* to now include *NOTCH1*, *FAT1* and *CDKN2A*, which are characteristic of HPV+ vSCC (PMID 34650187). Strong, continuous CK17 staining, either full-thickness or mid-superficial, is consistently seen in vaVIN. Since uninvolved mucosa is usually negative, CK17 can serve in assessing lesion extent and margin status. vaVIN can occur with concurrent or subsequent vSCC, sometimes with fatal outcome. These findings support the concept of vaVIN as a neoplastic process within the family of HPV+ vulvar neoplasia.

## 877 Impact of Molecular Signature on Outcomes of Endometrial Biopsies with Atypical Hyperplasia

Logan Corey<sup>1</sup>, Sharon Wu<sup>2</sup>, Kurt Hodges<sup>2</sup>, Matthew Oberley<sup>2</sup>, Premal Thaker<sup>3</sup>, Rami Musallam<sup>4</sup>, Mira Kheil<sup>5</sup>, Omar Kazziha<sup>5</sup>, Sudeshna Bandyopadhyay<sup>5</sup>, Robert Morris<sup>6</sup>, Rouba Ali-Fehmi<sup>5</sup>

<sup>1</sup>Barbara Ann Karmanos Center and Wayne State University School of Medicine, Detroit, MI, <sup>2</sup>Caris Life Sciences, Phoenix, AZ, <sup>3</sup>Washington University School of Medicine, St. Louis, MO, <sup>4</sup>Detroit Medical Center/Wayne State University, Detroit, MI,

<sup>5</sup>Wayne State University, Detroit, MI, <sup>6</sup>Karmanos Cancer Institute, Detroit, MI

**Disclosures:** Logan Corey: None; Sharon Wu: None; Kurt Hodges: None; Matthew Oberley: None; Premal Thaker: None; Rami Musallam: None; Mira Kheil: None; Omar Kazziha: None; Sudeshna Bandyopadhyay: None; Robert Morris: None; Rouba Ali-Fehmi: None

**Background:** Atypical Hyperplasia is difficult to manage, thus interest exists in identifying factors that may improve pre-operative risk prediction of EC, triaging of patients and providing necessary treatment. Data exists regarding molecular signatures that can predict the presence of concurrent EC in patients with AH on biopsy. We aim to characterize molecular landscapes of endometrial samples diagnosed with AH with EC on final hysterectomy.

**Design:** Our database was queried for patients with AH on endometrial curettage or biopsy who had a hysterectomy within 6 months. 59 tissue samples from 34 patients were included: 15 AH biopsy samples, 18 AH final hysterectomy samples (13 matched pairs), 13 EC biopsies and 13 samples that were EC on final hysterectomy samples (12 matched pairs) that were analyzed by WES or WTS (NovaSeq). Tumor mutational burden (TMB) was measured by totaling somatic mutations found per tumor (High:  $\geq 10$  mt/MB). Immune cell infiltrates were estimated by Quantiseq. Significance was determined by Fisher exact and Mann-Whitney U test and adjusted for multiple comparisons:  $p < 0.05$  but  $q > 0.05$  was considered a trend.

**Results:** 15/34 patients with AH initially had EC on final hysterectomy. 2 of 15 patients were  $\geq$  stage II at time of surgery. Decreased PTEN mutations were seen between AH ( $n=7/10$ ) and EC ( $n=7/8$ ) on biopsy (70% vs 88%,  $p=0.03$ ). Samples of EC origin were MSI-H by NGS-MSI ( $n=3/18$ ) and had no mutations in PPP2R1A ( $n=0/16$ ) (Fig 1a; Table 1). In hysterectomy samples, AH samples were all TMB low (Fig 1b). EC samples had trends of increased CTLA4 (FC: 6.97-fold) expression and immune cell infiltration of Macrophage M1 (+1.19%), NK (+2.13%), CD8+ T (+1.27%), regulatory T (+2.17%) and Dendritic (+2.87%) cells compared to AH samples (all  $p < 0.05$ ). Similarly, when comparing biopsies, EC samples had trends toward increased expression of CTLA4 (12.6-fold), HAVCR2 (FC: 2.59-fold) and IFNG (FC: 17.8-fold) and increased immune cell infiltration of Neutrophils (+11.7%), CD8+ T (+2.39%) and regulatory T (+2.43%) cells compared to AH samples (all  $p < 0.05$ ) (Fig 2a-b).

Biomarker	D&C, AH		Hysterectomy, AH		D&C, EMCA		Hysterectomy, EMCA		p-value	q-value
	Pos/Total	AH-D %	Pos/Total	AH-H %	Pos/Total	Cancer-D %	Pos/Total	Cancer-H %		
NGS-PTEN	7/10	70%	2/8	25%	7/8	87.5%	14/17	82.4%	0.025	1
NGS-PPP2R1A	2/10	20%	0/8	0%	0/8	0%	0/16	0%	0.117	1
NGS-ARID2	0/10	0%	0/8	0%	1/7	14.3%	0/15	0%	0.175	1
NGS-DICER1	0/10	0%	1/8	12.5%	1/8	12.5%	0/16	0%	0.192	1
NGS-KRAS	4/10	40%	4/8	50%	1/8	12.5%	3/18	16.7%	0.196	1
NGS-CTNNB1	0/10	0%	0/8	0%	0/8	0%	3/16	18.8%	0.298	1
NGS-SOS1	0/6	0%	0/3	0%	1/3	33.3%	0/6	0%	0.333	1
NGS-MSI	0/10	0%	0/6	0%	1/5	20%	3/16	18.8%	0.336	1
NGS-EZH2	1/10	10%	1/8	12.5%	0/8	0%	0/16	0%	0.377	1
NGS-MUTYH	1/10	10%	1/8	12.5%	0/8	0%	0/16	0%	0.377	1
NGS-FH	1/10	10%	1/8	12.5%	0/8	0%	0/16	0%	0.377	1
NGS-FAT1	0/10	0%	0/8	0%	1/8	12.5%	0/16	0%	0.381	1
NGS-CTNNA1	0/10	0%	0/8	0%	1/7	14.3%	1/16	6.25%	0.502	1
NGS-PIK3R1	1/10	10%	0/8	0%	1/7	14.3%	4/16	25%	0.550	1
CNA-SOX10	1/8	12.5%	0/6	0%	2/6	33.3%	2/13	15.4%	0.581	1
CNA-FGFR3	1/8	12.5%	0/6	0%	2/6	33.3%	2/13	15.4%	0.581	1
NGS-CCND1	1/10	10%	0/8	0%	0/8	0%	0/16	0%	0.619	1
NGS-TNFRSF14	1/10	10%	0/8	0%	0/8	0%	0/16	0%	0.619	1
NGS-SMAD2	1/10	10%	0/8	0%	0/8	0%	0/16	0%	0.619	1
NGS-NF1	1/10	10%	0/8	0%	0/7	0%	0/15	0%	0.625	1
TMB High	1/10	10%	0/7	0%	1/6	16.7%	2/17	11.8%	0.896	1
NGS-FBXW7	1/10	10%	0/8	0%	1/8	12.5%	2/17	11.8%	1	1
NGS-ESR1	0/10	0%	0/8	0%	0/8	0%	1/17	5.88%	1	1
NGS-RNF43	1/10	10%	0/8	0%	1/8	12.5%	1/16	6.25%	1	1
NGS-MSH6	0/10	0%	0/8	0%	0/8	0%	1/16	6.25%	1	1
CNA-FLT4	1/8	12.5%	0/5	0%	1/6	16.7%	1/13	7.69%	1	1
NGS-SPEN	0/10	0%	0/8	0%	0/8	0%	1/16	6.25%	1	1
CNA-PDCD1	1/8	12.5%	0/6	0%	1/6	16.7%	2/13	15.4%	1	1
NGS-SMARCB1	0/10	0%	0/8	0%	0/8	0%	1/16	6.25%	1	1
NGS-APC	0/10	0%	0/8	0%	0/7	0%	1/16	6.25%	1	1
NGS-SDHB	0/10	0%	0/8	0%	0/8	0%	1/16	6.25%	1	1
NGS-BCOR	1/10	10%	1/8	12.5%	1/8	12.5%	2/16	12.5%	1	1
NGS-EIF1AX	1/10	10%	0/8	0%	0/7	0%	2/18	11.1%	1	1

Table 1. Genomic Features of matched AH vs EC samples

Figure 1 - 877

**Figure 1.** Genomic Features of matched AH vs EC samples

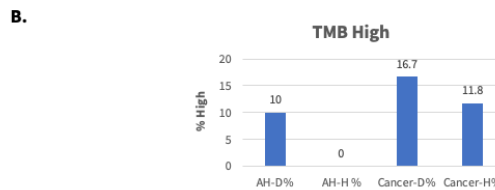
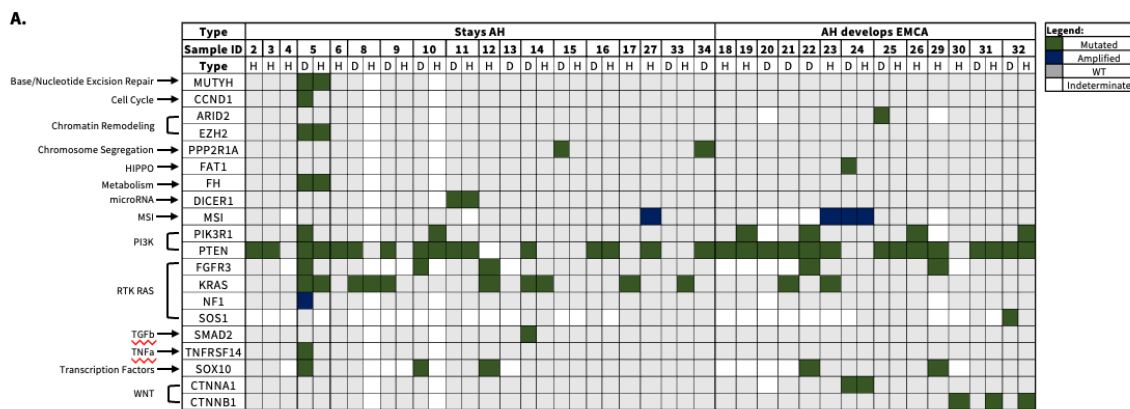
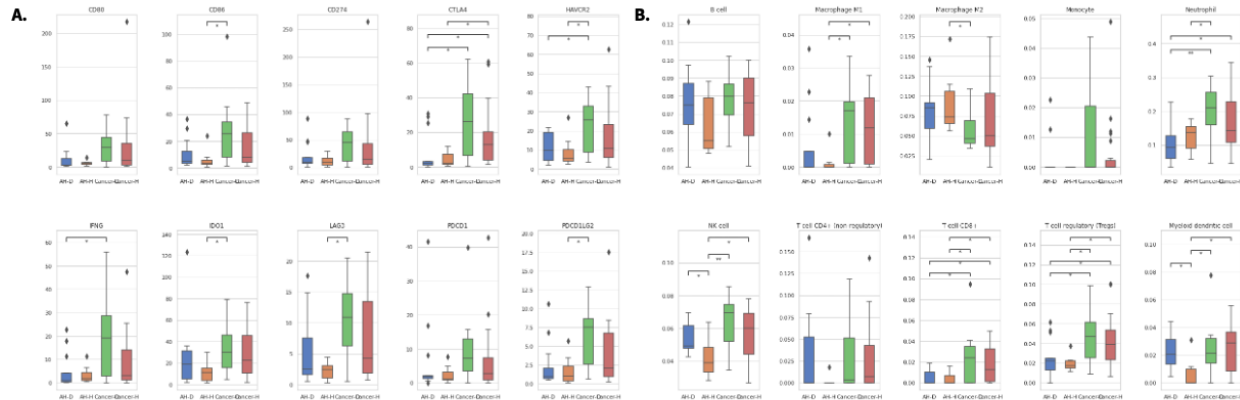


Figure 2 - 877

**Figure 2.** Immune Features of matched AH vs EC samples



**Conclusions:** Our analysis reveals molecular and immune differences between AH biopsies with concurrent EC compared to those without. These differences may lead to advances in identifying appropriate patients for fertility sparing treatments vs those that can be managed surgically.

## 878 High-grade Serous Carcinoma with Transitional-like Morphology: A Homologous Recombination-deficient Tumor

Emanuela D'Angelo<sup>1</sup>, Iñigo Espinosa<sup>2</sup>, Jaime Prat<sup>3</sup>

<sup>1</sup>Cagliari, Italy, <sup>2</sup>Hospital de la Santa Creu i Sant Pau, Barcelona, Spain, <sup>3</sup>Autonomous University of Barcelona, Barcelona, Spain

**Disclosures:** Emanuela D'Angelo: None; Iñigo Espinosa: None; Jaime Prat: None

**Background:** Thirteen years ago we pointed out that ovarian transitional cell carcinoma (TCC) and conventional high-grade serous carcinoma (HGSC) had similar genetic alterations and clinical behavior. Consequently, ovarian TCC is now classified as a morphologic variant of HGSCs. Defective homologous recombination, resulting from genetic or epigenetic inactivation of DNA damage repair genes, such as *BRCA1/2*, occurs in approximately 50% of the HGSCs. However, little is known about the role of these genes in HGSCs with transitional-like morphology.

**Design:** By next-generation sequencing, we study mutations of DNA damage repair genes including *BRCA1/BRCA2*, *PALB2*, *RAD51C*, *RAD51D*, *BRIP1*, *ESMY*, *ATR*, *PTEN*, *CHEK1/2*, and other genes involved in the ovarian carcinogenesis, in 6 HGSCs with transitional-like morphology, 1 typical HGSC, and 1 malignant Brenner tumor.

**Results:** One case of HGSC with transitional-like morphology developed as a component of a recurrent serous borderline tumor. All HGSCs had *p53* mutations and 3 HGSCs with transitional-like morphology also showed *BRCA1/2* mutations. No genomic aberrations in other homologous genes were found. Interestingly, in the case of HGSC with transitional-like morphology that arose from a recurrent serous borderline tumor, *p53* and *BRCA1/2* mutations were encountered in the HGSC component but were not identified in the serous borderline tumor. Also, one HGSC with transitional-like morphology and signet-ring cells had *APC* mutation. In contrast, the malignant Brenner tumor had *PIK3CA* mutation and neither *p53* nor *BRCA1/2* mutations were detected.

**Conclusions:** Our results show that many HGSCs with transitional-like morphology are homologous recombination deficiency tumors secondary to *BRCA1/2* mutations and confirm that HGSCs and malignant Brenner tumor follow different tumorigenic pathways.

## 879 Mutational Signatures (SIG) in Primary Endometrial Carcinomas (EC) and Correlation with Histological Subtypes: a Whole Genome Sequencing (WGS) Approach

Annacarolina da Silva<sup>1</sup>, Hnin Ingyin<sup>1</sup>, Majd Al Assaad<sup>1</sup>, Jiangling Tu<sup>2</sup>, Kevin Hadi<sup>3</sup>, Aditya Deshpande<sup>3</sup>, Ahmed Elsaed<sup>4</sup>, Jyothi Manohar<sup>4</sup>, Michael Sigouros<sup>4</sup>, Andrea Sboner<sup>4</sup>, Juan Medina-Martínez<sup>3</sup>, Olivier Elemento<sup>4</sup>, Juan Miguel Mosquera<sup>4</sup>

<sup>1</sup>New York-Presbyterian/Weill Cornell Medicine, New York, NY, <sup>2</sup>Weill Cornell Medical College, New York, NY, <sup>3</sup>New York, NY, <sup>4</sup>Weill Cornell Medicine, New York, NY

**Disclosures:** Annacarolina da Silva: None; Hnin Ingyin: None; Majd Al Assaad: None; Jiangling Tu: None; Kevin Hadi: Employee: Isabl, Inc.; Aditya Deshpande: Employee: Isabl Inc; Ahmed Elsaed: None; Jyothi Manohar: None; Michael Sigouros: None; Andrea Sboner: None; Juan Medina-Martínez: Employee: Isabl Inc.; Olivier Elemento: None; Juan Miguel Mosquera: None

**Background:** SIG help to shape tumor genomes and can be used as predictive markers as well as to inform patient eligibility for targeted therapies. Understanding and gaining more experience on handling the biological traits of EC, especially when correlated with traditional histological findings, is fundamental in the precision medicine era. We aimed to identify SIG of primary EC using a WGS approach correlating with histological subtypes (HS) and FIGO grading while attempting to stratify the tumors into the four TCGA molecular categories (TCGAmol).

**Design:** WGS analysis was performed in 32 primary non-treated EC by using state-of-the-art Isabl GxT platform. Through manual curation, total single nucleotide variants (SNVs), tumor mutational burden (TMB) and SIG were annotated. Driver gene mutations (mut) and copy number (CN) plots were manually reviewed to identify defining alterations and to establish the CN status as low or high, following TCGA classifiers. Clinical-pathologic features were reviewed and correlated with molecular findings (MOL).

**Results:** Median age was 68 years (range 30-82). HS comprised 23 endometrioid carcinomas (EMCA); 2 mesonephric-like carcinomas (MLC); 2 serous, 4 mixed (MC) and 1 clear cell (CCC). Figures 1 and 2 show HS and MOL. The average number of SIG was 5.2/case. Within relevant mutational signatures, MMR was the most prevalent (31%). APOBEC SIG, rarely described in EC, was seen in 46% of high-grade EC. 5 EC could not be placed into TCGAmol due to ambiguous features. CN high cases showed *CDK12* alterations (50% of cases) and enriched tandem duplications. No significant HRD SIG nor *BRCA* mut were identified. Table 1 reveals additional MOL with corresponding clinical outcomes.

Table 1. Clinical features and interesting molecular and histological findings. AW (alive and well); AWD (alive with disease); DOD (died of disease); NA (not available); UNK (unknown)					
ID and TCGA	FU (months)	Recurrence	Patient status	FIGO	Interesting findings
<b>POLE</b>					
1	30		AW	IA	<i>POLE p.V411L</i>
2	302		AW	IA	<i>POLE p.P286R</i>
<b>MSI-H</b>					
3	60	Peritoneal carcinomatosis, liver	AWD	IB	
4	34		AW	IB	
5	24		AW	IA	MMR intact by IHC; Mucinous features; MSI-H by SIG
6	17		AW	IA	
7	17		AW	IB	
8	15		AW	IA	
9	250		AW	IA	
10	NA	NA	NA	IA	
11	100	NA	AW	IIIA	
12	236	NA	AW	IA	<i>MSI-H; TP53 p.R273C</i>

# ABSTRACTS | GYNECOLOGIC AND OBSTETRIC PATHOLOGY

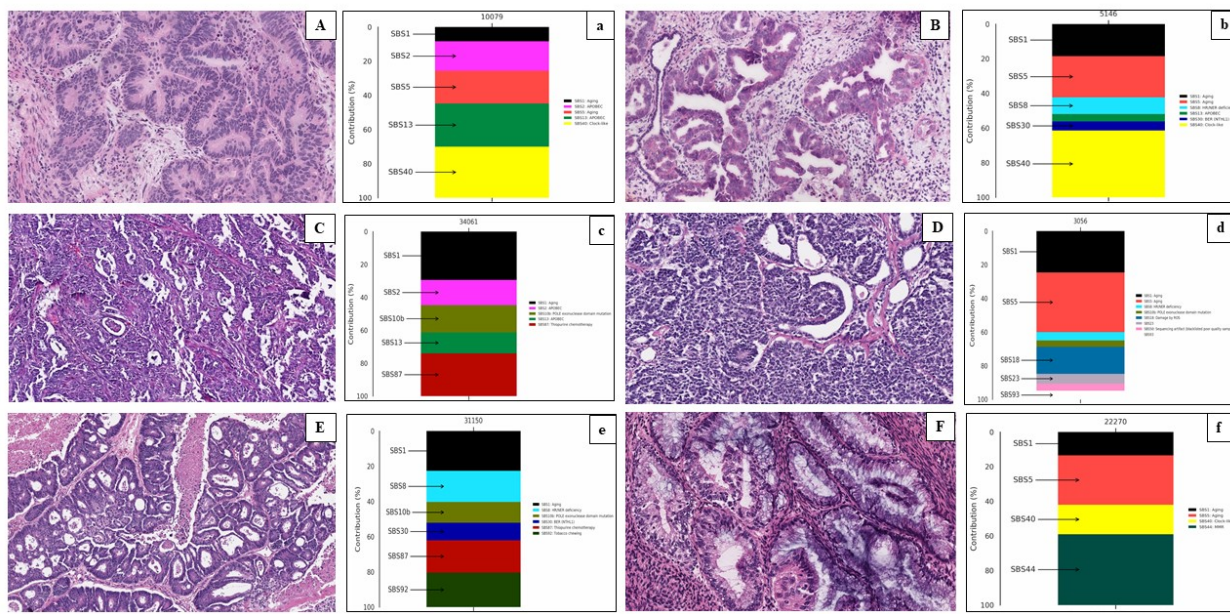
CN LOW						
13	98	Lymph nodes, peritoneum, liver, vaginal cuff	AWD	IIIC	<i>CTNNB1 p.S37C</i>	
14	41		AW	II	<i>CTNNB1 p.S37F</i>	
15	34		AW	IIIC1		
16	14		AW	IIIA		
17	288		AW	IA	FIGO grade 1; <i>TP53 p.R248G</i>	
18	NA	NA	NA	IA		
19	152	Para-aortic lymph nodes	AWD	IA		
CN HIGH						
20	27	Pleural effusions	DOD	IIIC		
21	66	Lymph nodes	AWD	IIIC2		
22	16		AW	IA		
23	201		AW	IB	<i>HER2 amplification</i>	
24	15	Unknown site	AWD	IIIC		
25	169	Unknown site	AWD	IA	Multiple primaries (lung, colon), <i>CHEK2 p.R562L (VUS germline)</i>	
26	26		AW	IA		
27	NA	NA	NA	IB		
TCGA UNK						
28	126		AW	IA	TMB: 15; <i>TP53 p.R273C; CTNNB1 p.S37F; unclassifiable CNV plot</i>	
29	83	Lung, vagina	AWD	IVB	Mesonephric Like carcinoma TTF1+, PAX8+, ER and PR neg, <i>BRAF p.N581S; RRAS2 p.Q72L</i>	
30	126	Unknown	AWD	IIIC	Aneuploid tumor with no <i>TP53</i> SNVs. <i>MYCL</i> and <i>MPL</i> amplification	
31	26	Liver	AWD	IA	Mesonephric Like carcinoma TMB: 12.5 and aneuploid CN plot. Unusual SNVs including: <i>RAD50 p.R1239*</i> , <i>STK11 p.S216F</i>	
32	NA	NA	NA	II	TMB:10; Aneuploid CN plot	

Figure 1 – 879

ID	Primary signature	Secondary signature	Tertiary signature	Signatures Total	SNVs	TMB	Histology	FIGO Grade
1	SBS14 MMR	SBS14 MMR deficiency + POLE	SBS10a POLE exonuclease domain mutation	3	2M	695	EMCA	3
2	SBS10a POLE exonuclease domain mutation	SBS28 POLE exonuclease domain mutation	SBS10b POLE exonuclease domain mutation	3	480K	165.3	EMCA	2
3	SBS44 MMR	SBS6 MMR	SBS8 HR/NER deficiency	8	120K	43	EMCA	3
4	SBS44 MMR	SBS26 MMR	SBS1 Aging	4	280K	98.2	EMCA	3
5	SBS44 MMR	SBS5 Aging	SBS40 Clock-like	4	49K	16.8	EMCA	2
6	SBS44 MMR	SBS92 Tobacco chewing	SBS1 Aging	3	180K	61	EMCA	1
7	SBS44 MMR	SBS92 Tobacco chewing	SBS1 Aging	4	190K	64.2	EMCA	2
8	SBS44 MMR	SBS26MMR	SBS4 Tobacco smoking	5	100K	35.8	EMCA	2
9	SBS44 MMR	SBS1 Aging	SBS26MMR	5	110K	39.1	EMCA	1
10	SBS44 MMR	SBS1 Aging	SBS12	4	120K	42.9	EMCA	3
11	SBS44 MMR	SBS1 Aging	SBS26 MMR	6	110K	38.5	EMCA	2
12	SBS44 MMR	SBS1 Aging		2	140K	47.9	EMCA	3
13	SBS40 Clock-like	SBS5 Aging	SBS18 Damage by ROS	5	71K	2.4	EMCA	2
14	SBS5 Aging	SBS1 Aging	SBS18 Damage by ROS	5	5.5K	1.9	EMCA	2
15	SBS5 Aging	SBS40 Clock-like	SBS1 Aging	4	5.9K	2	EMCA	1
16	SBS40 Clock-like	SBS5 Aging	SBS18 Damage by ROS	4	7.4K	2.6	EMCA	1
17	SBS40 Clock-like	SBS5 Aging	SBS1 Aging	4	7.4K	2.6	EMCA	1
18	SBS5 Aging	SBS1 Aging	SBS10 Clock-like	11	4.7K	1.6	EMCA	1
19	SBS40 Clock-like	SRS5Aging	SBS1 Aging	8	9K	3.1	EMCA	1
20	SBS40 Clock-like	SBS5 Aging	SBS1 Aging	4	6.1K	2.1	EMCA	3
21	SBS5 Aging	SBS3 HRD	SBS1 Aging	8	19K	6.7	MIXED	3
22	SBS40 Clock-like	SBS13 APOBEC	SBS5 Aging	5	11K	4	MIXED	3
23	SBS40 Clock-like	SBS1 Aging		2	6.6K	2.3	SEROUS	3
24	SBS5 Aging	SBS40 Clock-like	SBS1 Aging	7	6.3K	2.2	MIXED	3
25	SBS40 Clock-like	SBS5Aging	SBS1 Aging	6	6.1K	2.1	MIXED	3
26	SBS40 Clock-like	SBS5Aging	SBS1 Aging	3	4.6K	1.6	EMCA	3
27	SBS5 Aging	SBS13 APOBEC	SBS2 APOBEC	5	9K	3.1	SEROUS	3
28	SBS1 Aging	SBS92 Tobacco chewing	SBS87 Thiopurine chemotherapy	6	36K	12.3	EMCA	1
29	SBS5 Aging	SBS1 Aging	SBS18 Damage by ROS	7	4.3K	1.5	MLC**	3
30	SBS5 Aging	SBS1 Aging	SBS8 HR/NER deficiency	5	4.1K	1.4	EMCA	1
31	SBS1 Aging	SBS87 Thiopurine chemotherapy	SBS10b POLE exonuclease domain mutation	5	36K	12.5	MLC**	3
32	SBS13 APOBEC	SBS2 APOBEC	SBS8 HR/NER deficiency	4	27K	9.2	CCC	3

Figure 1. Mutational signatures of 32 endometrial carcinomas sorted according to molecular subtypes (TCGA classification), histological subtypes and FIGO grade. Cases demonstrating any contribution of APOBEC signatures are color-coded in aqua. Total number of signatures, primary, secondary, and tertiary signatures, total number of somatic mutations and mutational burden are also disclosed. Cases highlighted with \*\*\* correspond to two Mesonephric-Like carcinomas (MLC), re-classified histologically. EMCA (endometrioid carcinoma); CCC (clear cell carcinoma).

Figure 2 - 879



**Figure 2.** Morphology (capital letter ID) and its paired SIG contributions (lower case ID). Examples of histological findings of cases with APOBEC SIG (A; B; C) and cases with uncommon histological features when considering the predominant SIG (D,E,F). A/a- EMCA with mixed features; B/b- serous carcinoma; C/c and D/d- mesonephric like-carcinoma (originally endometrioid G3); E/e- EMCA grade 1 with unusual SIG pattern; F/f- EMCA grade 1 with mucinous features, pathogenic p53 mutation and MMR SIG (MMR retained by IHC).

**Conclusions:** The mutational processes in EC vary among tumor types and distinct SIG are observed. Using WGS, the cases were easily placed in the TCGA categories, including POLE and MSI-H which can be targetable by immune-checkpoint blockers. We observed that APOBEC SIG, although uncommon, was seen in high-grade tumors and might represent a distinct category. It is important to note that APOBEC SIG are not exclusive of cervical uterine cancers and might represent a pitfall for primary site definition. Targeting CDK12 alterations is an emerging therapeutic tool and could be of significance in CN high tumors. No relevant HRD SIG or BRCA mut were identified thus, potential for PARP inhibitor therapy in EC still needs to be explored.

## 880 MYB and MYBL1 Fusion Genes in Adenoid Cystic Carcinomas of the Bartholin Gland

Edaise M. da Silva<sup>1</sup>, Jacqueline Feinberg<sup>1</sup>, Arnaud Da Cruz Paula<sup>1</sup>, Fresia Pareja<sup>1</sup>, Juber Patel<sup>1</sup>, Yingjie Zhu<sup>1</sup>, Pier Selenica<sup>1</sup>, Mario Leitao<sup>1</sup>, Nadeem Abu-Rustum<sup>1</sup>, Jorge Reis-Filho<sup>1</sup>, Amy Joehlin-Price<sup>2</sup>, Britta Weigelt<sup>1</sup>

<sup>1</sup>Memorial Sloan Kettering Cancer Center, New York, NY, <sup>2</sup>Cleveland Clinic, Cleveland, OH

**Disclosures:** Edaise M. da Silva: None; Jacqueline Feinberg: None; Arnaud Da Cruz Paula: None; Fresia Pareja: None; Juber Patel: None; Yingjie Zhu: None; Pier Selenica: None; Mario Leitao: None; Nadeem Abu-Rustum: None; Jorge Reis-Filho: None; Amy Joehlin-Price: None; Britta Weigelt: None

**Background:** Adenoid cystic carcinoma (AdCC) of Bartholin's gland (AdCC-BG) is a rare gynecologic vulvar malignancy. Although AdCC-BGs are slow growing, they are locally aggressive and associated with high recurrence rates. Here we sought to characterize the molecular landscape of AdCC-BGs and define whether AdCC-BGs harbor *MYB* and *MYBL1* alterations akin to AdCCs of the breast and salivary glands.

**Design:** We subjected six AdCC-BGs to a combination of RNA-sequencing, targeted DNA-sequencing, fluorescence *in situ* hybridization (FISH) and reverse-transcription PCR. Somatic mutations, copy number alterations and chimeric transcripts were defined using validated bioinformatics methods. AdCC-BGs were also subjected to *MYB* immunohistochemistry.

**Results:** Of the six AdCC-BGs assessed, three were underpinned by the *MYB-NFIB* fusion gene with varying breakpoints and displayed high levels of *MYB* expression by immunohistochemistry. Two AdCC-BGs harbored *MYBL1* fusion genes with different gene partners, including *MYBL1-RAD51B* and *MYBL1-EWSR1* gene fusions. By immunohistochemistry, *MYB* protein expression was high in one, and focal and weak in the other *MYBL1*-rearranged AdCC-BG. The last case showed *MYB* protein overexpression and transcriptional *MYB* pathway activation based on RNA-sequencing analysis, however no gene fusion was detected, likely due to poor nucleic acid quality.

**Conclusions:** Akin to salivary and breast AdCCs, AdCC-BGs are underpinned by *MYB* and *MYBL1* chimeric fusions. Our data demonstrate that AdCCs, irrespective of organ site, provide an example of genotypic–phenotypic correlation and a convergent phenotype, whereby activation of *MYB* and *MYBL1* can be driven by the *MYB-NFIB* fusion gene, *MYBL1* rearrangements, and

likely other mechanisms. Assessment of *MYB* or *MYBL1* rearrangements, or potentially *MYB* overexpression, may be used as an ancillary marker for the diagnosis of AdCC-BGs.

**881 Spectrum of Molecular Alterations in Struma Ovarii and their Clinicopathologic Significance**

Sandhyarani Dasaraju<sup>1</sup>, Robert Freund<sup>2</sup>, Andrew Nelson<sup>1</sup>, Mahmoud Khalifa<sup>1</sup>, Khalid Amin<sup>1</sup>

<sup>1</sup>University of Minnesota, Minneapolis, MN, <sup>2</sup>University of Minnesota Medical School, Minneapolis, MN

**Disclosures:** Sandhyarani Dasaraju: None; Robert Freund: None; Andrew Nelson: None; Mahmoud Khalifa: None; Khalid Amin: None

**Background:** The histologic criteria for categorizing struma ovarii is the same as their thyroid counterparts. However, classifying cases with follicular architecture can be challenging. Recent advances in molecular diagnostics have allowed for greater characterization of pathologic mutations in thyroid tumors. However, no large-scale studies investigating the molecular landscape of struma ovarii have been published. This study aims to examine the spectrum of molecular aberrations in struma ovarii that can provide diagnostic and prognostic information.

**Design:** After a retrospective search of our archival database, 22 cases of struma ovarii (20 benign and 2 malignant) diagnosed from 2003-2022 were identified. Cases were reviewed and a representative area was marked on a representative slide from each case. Sections from the corresponding paraffin embedded block were then subjected to mutational analysis using next generation sequencing with a panel of 61 genes. Molecular results were correlated with clinicopathologic features.

**Results:** Of the 22 cases, 5 (23%) had detectable pathogenic or likely pathogenic mutations (Table 1). PTEN mutations were seen in 3 cases (14%) while RAS mutations were seen in 2 of 22 cases (9%). One case had a likely pathogenic EIF1AX mutation. One case of malignant struma ovarii with microfollicular architecture exhibited two mutations, PTEN and HRAS in a patient who presented with advanced disease. One case of papillary thyroid carcinoma (PTC) did not reveal any mutations. One case diagnosed as benign revealed an NRAS mutation and, on further review, had focal papillary architecture and cytologic features of PTC. Excluding the malignant case at presentation, none of the remaining 4 cases with mutations demonstrated evidence of disease progression on follow up.

Table 1: Clinicopathologic feature and mutational status

Case	Age	Size of tumor (cm)	Histology	Mutations
1	43	5.5	Follicular	PTEN
2	54	26.1	Follicular/microfollicular/ adenomatoid	PTEN
3	62	5.0	Follicular	EIF1AX
4	53	2.2	Focal papillary with cytologic features of PTC	NRAS
5	60	8.5	Malignant Struma ovarii with microfollicular architecture and advanced disease	HRAS and PTEN

**Conclusions:** This study demonstrates that a significant proportion of struma ovarii cases that appear benign on histology carry pathogenic mutations. Molecular testing can provide valuable information that can be used to more accurately diagnose and potentially better manage these cases. We suggest considering molecular testing on all struma ovarii cases irrespective of histologic diagnosis.

**882 Gynecologic-Tract Leiomyosarcomas in Young Premenopausal Women: Genetic Profiling and Clinicopathologic Characteristics**

Nooshin Dashti<sup>1</sup>, Eric Vail<sup>1</sup>, Elias Makhoul<sup>1</sup>, Bonnie Balzer<sup>1</sup>, Allan Silberman<sup>1</sup>

<sup>1</sup>Cedars-Sinai Medical Center, Los Angeles, CA

**Disclosures:** Nooshin Dashti: None; Eric Vail: Speaker: Illumina; Elias Makhoul: None; Bonnie Balzer: None; Allan Silberman: None

**Background:** Leiomyosarcoma (LMS) is the most common uterine sarcoma (40-50%), comprising 1-2% of all uterine malignancies. Gynecologic LMS (GYN-LMS) is a highly aggressive tumor typically occurring in patients older than 50 years with incremental age-associated risk and carries an overall poor prognosis. The molecular landscape of GYN-LMS is complex and data regarding young patients is sparse. Current data focused on post-menopausal GYN-LMS implicates mutations in *p53*, *ATRX*, *RB1*, *ATM*, *PTEN*, *CHEK2* and *MED12*, often with widespread chromosomal structural instability. Generally, tumors occurring in older patients show a more significant genomic complexity in contrast to their younger counterparts. We sought to explore molecular and clinicopathologic features of GYN-LMS in a well-annotated cohort of young premenopausal patients.

# ABSTRACTS | GYNECOLOGIC AND OBSTETRIC PATHOLOGY

**Design:** Institutional pathology archive was searched for GYN-LMS including uterus, adnexa, broad ligament and lower GYN tract. Clinicopathologic data was retrieved from clinical charts, pathology reports and comprehensive slide review: age, menopausal status, tumor site and size, histologic features and follow up data. DNA and RNA was extracted from FFPE blocks for sequencing (OCAPlus, Thermo Fisher Scientific, Waltham, MA) and data was compared to a cohort of 6 postmenopausal GYN-LMS tumors.

**Results:** Upon rereview 20 tumors were classified as LMS (n=20), while 4 tumors were excluded: 3 reclassified as smooth muscle tumor of uncertain malignant potential (STUMP) and 1 cervical tumor with *TPM3::NTRK1* fusion. The age range was 29-49 years (median 41yo, average 40.1yo). Tumors occurred in uterus (n=18, 90%) and ovary (n=2, 10%), with size range of 1.8 -25cm (median 8.5cm). Follow up information was available in 17 cases (range 6-18 months, median 48 months). 13 patients experienced locoregional recurrence and/or distant metastasis (76%) and 4 patients died of disease (23%). Sequencing was successful in 17 cases (85%) (Table1). Widespread chromosomal structural changes were seen in 8 tumors (47%).

Case	Age(Years)	SNVs	CNVs (Isolated Amplifications and Deep Deletions)	Fusions
1	30	KDM5C p.K1023R	None	None
2	41	None	RB1 deletion	None
3	36	TP53 p.Q192*, RB1 p.P21Rfs*44	None	None
4	40	PTEN p.N323Mfs*21	TP53 deletion	None
5	42	None	None	None
6	45	TP53 p.H179R	None	None
7	37	TP53 splice site	RB1 deletion	None
8	41	TP53 splice site, ATRX splice site	None	None
9	45	TSC1 splice site	MTAP, CDKN2A/B deletions	None
10	42	TP53 p.R175H, ATRX K1583Nfs*22	RB1 deletion	None
11	29	Poor quality	Poor quality	Poor quality
12	33	TP53 p.L145P, RB1 p.Q850*	None	None
13	47	MSH6 E645*, RB1 splice site	None	None
14	49	ATRX R907*	IGF1R amplification, RB1 deletion, RNASEH2B deletions, INPP4B deletion exons 16-27	None
15	36	Poor quality	Poor quality	Poor quality
16	47	Poor quality	Poor quality	Poor quality
17	30	TP53 p.R175H, RB1 p.R661W	None	None
18	47	FANCA p.F1263del	RAD51B, MLH3, ATRX deletions	None
19	49	TP53 p.R273H, PARP1 p.R282*	IL7R amplification	None
20	36	TP53 p.T256P	None	None

**Conclusions:** *TP53* was the most frequently mutated gene (10 tumors, 58%), followed by *Rb1* (8 tumors, 47%) and *ATRX1* (4 tumors, 23%). Most tumors had complex genetic makeup and numerous copy number changes. Our data highlights alterations in tumor suppressor genes and suggests significant overlap with molecular alterations often seen in post-menopausal GYN-LMS. This is in contrast to most other non-fusion driven tumors, which show incremental genomic complexity with age.

## 883 Outcome-Based Risk Stratification Model for the Diagnosis of Placental Maternal Vascular Malperfusion

Dale Davis<sup>1</sup>, Adam Lechner<sup>2</sup>, Jonathan Slack<sup>3</sup>, Chrystalle Carreon<sup>3</sup>, Bradley Quade<sup>4</sup>, David Chapel<sup>5</sup>, Carlos Parra-Herran<sup>1</sup>

<sup>1</sup>Brigham and Women's Hospital, Harvard Medical School, Boston, MA, <sup>2</sup>University of Missouri School of Medicine, Columbia, MO, <sup>3</sup>Boston Children's Hospital, Harvard Medical School, Boston, MA, <sup>4</sup>Brigham and Women's Hospital, Boston, MA, <sup>5</sup>Michigan Medicine, University of Michigan, Ann Arbor, MI

**Disclosures:** Dale Davis: None; Adam Lechner: None; Jonathan Slack: None; Chrystalle Carreon: None; Bradley Quade: None; David Chapel: None; Carlos Parra-Herran: None

**Background:** The Amsterdam Consensus Statement introduced the term maternal vascular malperfusion (MVM) to group a constellation of findings associated with impaired maternal-placental circulation. There remains uncertainty on how many, and which, findings are required for a pathologic diagnosis of MVM, and the diagnostic criteria are variably applied in practice. We aim to establish correlations between lesions associated with MVM and obstetric outcomes in a modern, well-characterized series of placentas, in order to determine criteria essential for the diagnosis of MVM.

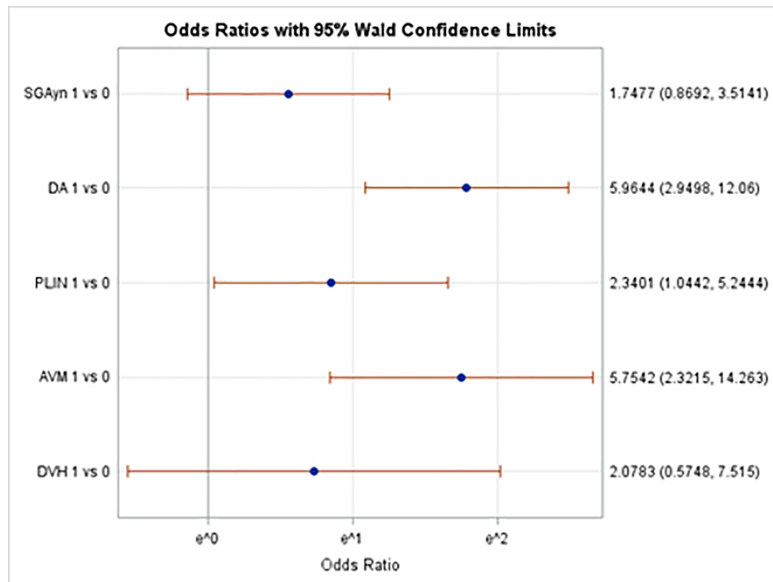
**Design:** Placentas reviewed at our institution within a 5-year period were retrieved. All material was reviewed to document MVM features including placental weight, accelerated villous maturation (AVM), decidual arteriopathy (DA), retroplacental hematoma (RPH), placental infarcts (PI) and distal villous hypoplasia (DVH). Obstetric outcomes in the current pregnancy were recorded included chronic hypertension, pre-eclampsia with or without severe features, gestational diabetes, prematurity, fetal growth

restriction, and intrauterine fetal demise. Correlation between pathologic features (and their combination) and any obstetric / fetal outcome was obtained.

**Results:** 200 cases were included (100 with a reported diagnosis of MVM, and 100 controls matched by maternal age and GPA status). On univariate logistic regression analysis, adverse maternal or fetal outcome was associated low placental weight (LPW, <10% percentile for gestational age), DA, PI, PI volume, AVM, and DVH (all  $p<0.01$ ). In a multivariable model, DA, PI, and AVM were significantly associated with adverse fetal and/or maternal outcomes (Fig 1 shows odds ratio for each variable in multivariate model). A ROC curve including LPW, DA, PI and AVM showed good predictive ability (AUC 0.8256). A nomogram was used to calculate the probability of adverse outcome based on these pathologic features (Table 1).

PATHOLOGIC FEATURE(S)	LOG(ODDS)
LPW only	0.23
PI only	0.30
PI + LPW	0.42
DA only	0.51
AVM only	0.52
DA + LPW	0.65
AVM + LPW	0.65
DA + PI	0.72
AVM + PI	0.73
DA + LPW + PI	0.82
AVM + LPW + PI	0.82
DA + AVM	0.87
DA + AVM + LPW	0.92
DA + AVM + PI	0.94
DA + AVM + LPW + PI	0.97

Figure 1 – 883



**Conclusions:** In our series DA, AVM, PI, and LPW had the strongest association with obstetric or fetal outcomes in the index gestation. Based on our analysis, we recommend consistent reporting of these features, summarizing them as “diagnostic of MVM” if there is DA or AVM plus any other of these features (yielding a probability of 65-97% for adverse obstetric outcomes) and “suggestive of MVM” if only one feature, or PI + LPW only (probability of up to 52%). Other features such as DVH and RPH can also be reported, although their correlation with MVM-related outcomes is less certain.

**884 Clinicopathological Evaluation of Tumor Buddings in Endometrial Carcinomas as a Prognostic Factor**

Louise De Brot<sup>1</sup>, Luan Furtado<sup>2</sup>, Samuel Buniatti<sup>3</sup>, Marcelo Corassa<sup>1</sup>, Bruna Gonçalves<sup>1</sup>, Glauco Baiocchi<sup>1</sup>, Graziele Bovolim<sup>1</sup>

<sup>1</sup>A.C.Camargo Cancer Center, São Paulo, Brazil, <sup>2</sup>São Paulo, Brazil, <sup>3</sup>Instituto de Anatomia Patológica, AC Camargo Cancer Center, São Paulo, Brazil

**Disclosures:** Louise De Brot: None; Luan Furtado: None; Samuel Buniatti: None; Marcelo Corassa: None; Bruna Gonçalves: None; Glauco Baiocchi: None; Graziele Bovolim: None

**Background:** Endometrial cancer (EC) is the most common malignant neoplasm of the female genital tract. Despite a good overall prognosis, it has a significant morbidity associated with treatment and a dismal prognosis when the disease recurs. Tumor budding, a common finding in colorectal cancer, can be associated with prognosis and can aid the multidisciplinary team in making better decisions regarding the patient's treatment.

**Design:** In this project a total of 143 patients with endometrial cancer who underwent hysterectomy with or without lymph node evaluation were selected, and their surgical specimens were evaluated for tumor budding. Buddings were defined as groups of at least 5 neoplastic cells. The most common prognostic features were evaluated in relation to the presence or absence of tumor buddings.

**Results:** Median follow-up for the population was 36 months; the presence of tumor budding was associated with higher histological grade, angiolympathic invasion, and lymph node spread ( $p = 0.011$ ,  $p < 0.001$ , and  $p = 0.040$ , respectively). There was no difference in the overall survival between the groups ( $p = 0.610$ ).

Table 1. Association between tumor buddings and histopathological characteristics of the endometrial carcinomas.

Variable	Budding status		$p^*$
	Absent	Present	
Stage	I+II	110	6 (5.2%)
	III+IV	18	8 (30.8%)
Mismatch repair gene <sup>a</sup>	Negative	29	5 (14.7%)
	Positive	92	7 (7.1%)
P53 <sup>b</sup>	Negative	115	11 (8.7%)
	Positive	7	1 (12.5%)
Histology	Endometrioid	114	10 (8.1%)
	Non-endometrioid	14	4 (22.2%)
Grade	Grades 1 and 2	92	5 (5.2%)
	Grade 3	36	9 (20%)
Lymphovascular space invasion	Absent	97	1 (1%)
	Present	31	13 (29.5%)
MELF <sup>c</sup> pattern	Absent	106	8 (7%)
	Present	18	5 (21.7%)
Myometrial invasion	<50%	82	3 (3.5%)
	≥50%	41	10 (19.6%)
Adnexal metastasis	No	124	12 (8.8%)
	Yes	4	2 (33.3%)
Parametrial invasion	No	124	11 (8.1%)
	Yes	4	3 (42.9%)
Cervical invasion	No	109	9 (7.6%)
	Yes	19	5 (20.8%)
Peritoneal implants	No	99	6 (5.7%)
	Yes	0	2 (100%)
Positive lymph node	No	95	6 (5.9%)
	Yes	14	7 (33.3%)

<sup>a</sup>Immunohistochemical protein expression of any mismatch repair gene; <sup>b</sup>immunohistochemical expression; MELF<sup>c</sup>: microcystic, elongated, and fragmented.

\*Qui-square and Fischer tests.

Figure 1 – 884

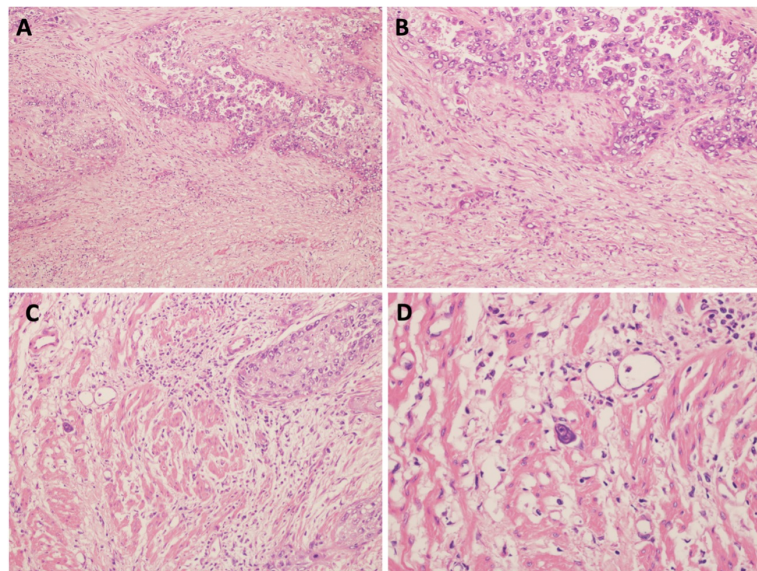
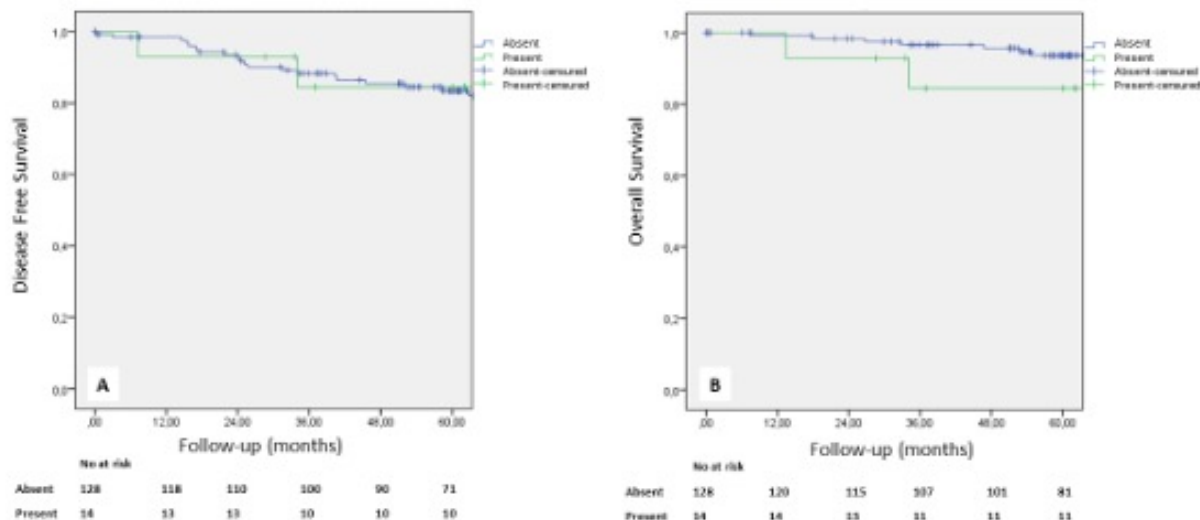


Figure 2 - 884



**Conclusions:** In conclusion, tumor budding is associated with worse prognosis in endometrial cancer and can represent a novel feature for the histological evaluation of patients that can aid physicians in making better treatment decisions.

### 885 L1CAM Expression in Endometrial Cancer: Is It Really a Prognostic Factor?

Louise De Brot<sup>1</sup>, Gabriel Oliveira<sup>1</sup>, Marcelo Corassa<sup>1</sup>, Bruna Gonçalves<sup>1</sup>, Glauco Baiocchi<sup>1</sup>, Graziele Bovolim<sup>1</sup>

<sup>1</sup>A.C.Camargo Cancer Center, São Paulo, Brazil

**Disclosures:** Louise De Brot: None; Gabriel Oliveira: None; Marcelo Corassa: None; Bruna Gonçalves: None; Glauco Baiocchi: None; Graziele Bovolim: None

**Background:** Endometrial carcinoma (EC) is classified by the Bokhman system in types I (low grade) and II (high grade). Many biomarkers are necessary to improve prognostic evaluation, such as L1 cell adhesion molecule (L1CAM), a membrane glycoprotein frequently detected in solid tumors. L1CAM performs an essential role in epithelial-mesenchymal transition in tumor cells. EC with high L1CAM expression displays a more aggressive phenotype.

**Design:** Retrospective cohort study evaluating 356 EC cases from Jan/2007 to Dec/2017. Tissue Microarray (TMA) blocks were prepared with and immunohistochemistry (IHC) for L1CAM and p53 was performed. L1CAM expression was considered negative

(completely negative membrane staining) or positive (at least 10% of positive membrane staining). p53 expression was also evaluated by IHC, and considered aberrant (*null*, strong and diffuse positivity or cytoplasmatic expression) or non-aberrant. DNA mismatch-repair protein expression was evaluated by IHC for PMS2, MLH1, MSH2, MSH6. Statistical analysis was performed by parametric tests (chi-square test for categorical variables) to determine relation between L1CAM expression and clinico-pathological factors. Survival analyses were performed by the Kaplan Meier method using the logrank test.

**Results:** Final sample consisted of 295 cases. 282 (95.5%) were negative and 13 (4.5%) positive (staining 10-90%). L1CAM expression associated with non-endometrioid histology (n=11 – 84.6% – p value < 0.0001). FIGO stage 3 was predominant (n=10 – 76.9% – p value < 0.0001). Other parameters (myometrial invasion, angiolympathic invasion, MELF pattern and lymph node metastasis) are listed on table 1, and albeit with numerical difference, did not demonstrate statistical significance for the interaction. L1CAM expression was evaluated in 44 p53 aberrant cases and 9 (20.5%) were L1CAM positive – p value < 0.0001. 8 (61.5%) L1CAM positive cases were mismatch-repair proficient (p value = 0.414). There was no difference in overall survival (OS) and progression free survival (PFS) among L1CAM positive and negative patients.

Table 1: Relationship between clinico-pathological variables and L1CAM expression.

Variable	Category	N (%)	P Value
<b>Histology</b>	Endometrioid	2 (15.4%)	<0.0001
	Non-endometrioid	11 (84.6%)	
<b>FIGO grade</b>	G1/G2	3 (23.1%)	<0.0001
	G3	10 (76.9%)	
<b>Myometrial invasion</b>	<50%	6 (46.2%)	0.062
	≥50%	7 (53.8%)	
<b>Vascular lymphatic invasion</b>	Present	5 (38.5%)	0.949
	Absent	8 (61.5%)	
<b>MELF pattern</b>	Present	2 (50%)	0.527
	Absent	2 (50%)	
<b>Lymph Node Involvement</b>	Present	2 (18.2%)	0.734
	Absent	9 (81.8%)	
<b>P53 status</b>	Wild Type	4 (30.8%)	<0.0001
	Mutant	9 (69.2%)	
<b>Mismatch Repair status</b>	Proficient	8 (61.5%)	0.414
	Deficient	5 (38.5%)	

**Conclusions:** L1CAM expression is associated with factors of worse prognosis that are intrinsic to the tumor. It is a simple biomarker, evaluated by IHC, and a potentially valuable tool in the clinical setting. However, there was no correlation between L1CAM expression and survival, and further studies are necessary to demonstrate what is the factual role of L1CAM as a biomarker in EC.

## 886 HLA Class I Loss in Endometrial Carcinoma: Differences in the Immunosurveillance Pattern in Molecular Subtypes

Antonio De Leo<sup>1</sup>, Angelo Corradini<sup>2</sup>, Francesca Rosini<sup>3</sup>, Camelia Alexandra Coada<sup>4</sup>, Marco Grillini<sup>2</sup>, Alessia Costantino<sup>3</sup>, Thais Maloberti<sup>4</sup>, Sara Coluccelli<sup>5</sup>, Dario de Biase<sup>1</sup>, Claudio Ceccarelli<sup>2</sup>, Donatella Santini<sup>2</sup>, Giovanni Tallini<sup>6</sup>

<sup>1</sup>University of Bologna, Bologna, Italy, <sup>2</sup>S.Orsola-Malpighi Hospital, University of Bologna, Bologna, Italy, <sup>3</sup>IRCCS Azienda Ospedaliero-Universitaria di Bologna, Bologna, Italy, <sup>4</sup>Alma Mater Studiorum-University of Bologna, Bologna, Italy, <sup>5</sup>Gynecologic Oncology Unit, S.Orsola-Malpighi Hospital, University of Bologna, Bologna, Italy, <sup>6</sup>University of Bologna School of Medicine, Bologna, Italy

**Disclosures:** Antonio De Leo: None; Angelo Corradini: None; Francesca Rosini: None; Camelia Alexandra Coada: None; Marco Grillini: None; Alessia Costantino: None; Thais Maloberti: None; Sara Coluccelli: None; Dario de Biase: None; Claudio Ceccarelli: None; Donatella Santini: None; Giovanni Tallini: None

**Background:** Human leukocyte antigen class I (HLA-I) molecules play an important role in regulating immune response. Loss of HLA-I expression results in tumor immune escape from cytotoxic T lymphocytes. The aim of the study is to investigate HLA-I expression in a consecutive series of endometrial carcinoma (EC) and to correlate it with immune cell markers, molecular subtypes, pathologic features, and prognosis.

# ABSTRACTS | GYNECOLOGIC AND OBSTETRIC PATHOLOGY

**Design:** Immunohistochemistry (IHC) and Next-Generation Sequencing (NGS) are used to assign TCGA molecular EC subgroups: POLE mutant (POLE), mismatch repair deficient (MMRd), p53 mutant (p53abn), and no specific molecular profile (NSMP). IHC expression of HLA-I, CD20, CD3, CD8, PD-1, PD-L1, CD68 has been assessed and quantified by digital image analysis on whole tumor tissue sections.

**Results:** 199 ECs have been stratified into 4 molecular subtypes: 16 (8.4%) POLE, 66 (33.2%) MMRd, 39 (19.6%) p53abn and 78 NSMP (39.2%). Loss of HLA-I expression is associated with several pathologic features such as high grade ( $p=0.01$ ), extensive tumor necrosis ( $p<0.001$ ), high mitotic activity ( $p<0.001$ ), substantial lymphovascular invasion ( $p<0.001$ ), budding ( $p=0.029$ ), absence of tumoral PD-L1 expression ( $p=0.001$ ), and high peri-tumoral expression of CD68 ( $p<0.001$ ), PD-L1 ( $p=0.001$ ) and CD20 ( $p=0.001$ ). The percentage of cases with HLA-I loss is different in the four molecular subgroups: 12 (75%) POLE, 29 (43.9%) MMRd, 9 p53abn (23.1%), 13 NSMP (20%) subtypes. In our cohort, EC molecular subtypes are statistically associated with different clinical outcomes (see Figure 1). In addition, the integration of pathologic features, HLA-I expression and immune markers distribution has improved prognostic stratification of NSMP tumors (see Figure 2). Specifically, high grade, substantial lymphovascular invasion and HLA-I loss revealed a strong correlation with disease recurrence ( $p<0.001$ ). Loss of HLA-I expression is associated with aggressive pathologic features in EC. In particular, evaluation of HLA-I may represent an additional prognostic parameter in identifying disease recurrence in the NSMP subgroup. Our findings highlight the role of HLA-I alterations in the immune evasion mechanisms and in the progression of endometrial carcinoma.

Figure 1 - 886

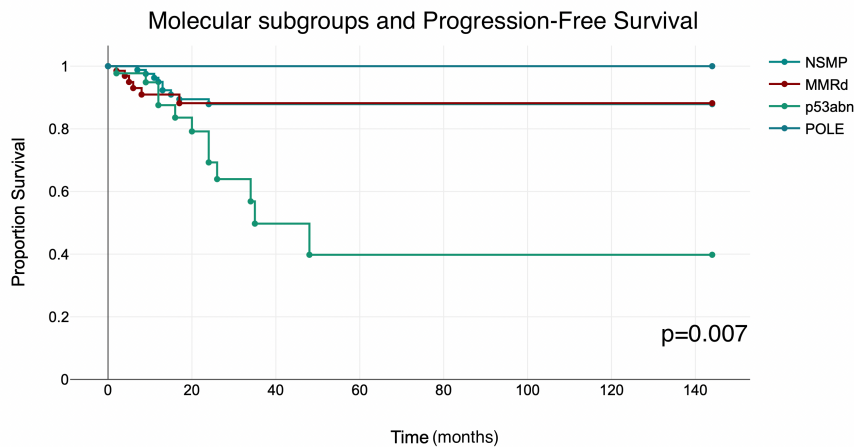
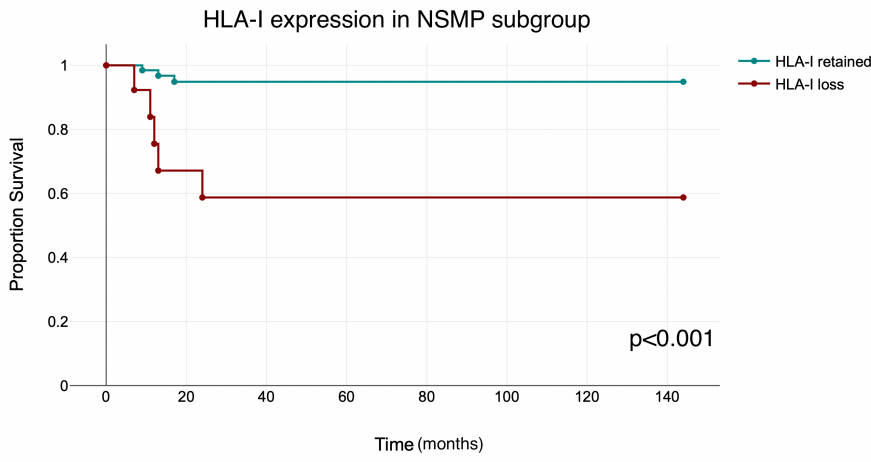


Figure 2 - 886



**Conclusions:** Loss of HLA-I expression is associated with aggressive pathologic features in EC. In particular, evaluation of HLA-I may represent an additional prognostic parameter in identifying disease recurrence in the NSMP subgroup. Our findings highlight the role of HLA-I alterations in the immune evasion mechanisms and in the progression of endometrial carcinoma.

**887 STK11 (LKB1) Immunohistochemistry is a Sensitive and Specific Marker for STK11 Adnexal Tumors**

Amir Dehghani<sup>1</sup>, Chrystalle Carreon<sup>2</sup>, Fabiola Medeiros<sup>3</sup>, Marisa Nucci<sup>1</sup>, Christopher Crum<sup>4</sup>, Jason Hornick<sup>1</sup>, W. Glenn McCluggage<sup>5</sup>, David Kolin<sup>4</sup>

<sup>1</sup>Brigham and Women's Hospital, Harvard Medical School, Boston, MA, <sup>2</sup>Boston Children's Hospital, Harvard Medical School, Boston, MA, <sup>3</sup>Cedars-Sinai Medical Center, Los Angeles, CA, <sup>4</sup>Brigham and Women's Hospital, Boston, MA, <sup>5</sup>The Royal Hospitals/Queen's University of Belfast, Birmingham, United Kingdom

**Disclosures:** Amir Dehghani: None; Chrystalle Carreon: None; Fabiola Medeiros: None; Marisa Nucci: None; Christopher Crum: None; Jason Hornick: None; W. Glenn McCluggage: None; David Kolin: None

**Background:** STK11 adnexal tumor is a rare recently described entity, which is important to recognize because of its strong association with Peutz-Jeghers syndrome. However, it is challenging to correctly diagnose because it shows significant morphologic variability, has a non-specific immunoprofile, and currently requires molecular studies for diagnosis. We sought to investigate the diagnostic utility of STK11 immunohistochemistry (IHC) in a cohort of STK11 adnexal tumors and its morphologic mimics.

**Design:** STK11 adnexal tumors [n=7] and potential mimics were retrospectively identified from the files of 4 institutions. Molecular profiling of tumors was performed when possible. IHC was performed on formalin-fixed paraffin-embedded tissue using an anti-STK11 monoclonal antibody (clone D60C5F10; 1:1000 dilution). STK11 staining was scored as either positive/intact (positive cytoplasmic staining in all tumor cells) or negative/lost (complete loss of cytoplasmic staining in tumor cells with intact staining in internal controls).

**Results:** The clinicopathologic, IHC and molecular findings are summarized in Table 1, and representative cases are illustrated in Figure 1. All 7 STK11 adnexal tumors showed complete loss of expression of STK11. All 50 mimics of STK11 adnexal tumor showed retained expression of STK11 (adult granulosa cell tumor [n=10], ovarian endometrioid carcinoma [n=8], tubo-ovarian high grade serous carcinoma [n=8], female adnexal tumor of Wolffian origin [FATWO, n=7], sex-cord tumor with annular tubules [SCTAT, n=7], Sertoli-Leydig cell tumor [n=4], steroid cell tumor [n=1], extraovarian sex-cord stromal tumor [n=2], ovarian clear cell carcinoma [n=1], microscopic extraovarian sex-cord proliferation [n=1], and periovarian plexiform leiomyoma [n=1]). Molecular testing was performed on 24 non-STK11 adnexal tumors, and none showed STK11 alterations.

Table 1. Clinicopathologic features of STK11 adnexal tumors and their morphologic mimics.

Tumor type (n)	Age range (median)	Positive/intact LKB1 IHC staining (n, %)	STK11 mutations (n)
STK11 adnexal tumor (7)	16-74 (33)	0/7 (0%)	Point mutation (n=4)  2 copy deletion (n=1)  Negative* (n=1)  NA (n=1)
AGCT (10)	28- 87 (52)	10/10 (100%)	None (0/5)  NA (5)
Ovarian endometrioid carcinoma (8)	41-72 (55)	8/8 (100%)	None (0/8)
High grade serous carcinoma (8)	50-81 (69)	8/8 (100%)	None (0/8)
Female adnexal tumor of Wolffian origin (FATWO) (7)	23-74 (52)	7/7 (100%)	NA (n=7)
Sex-cord tumor with annular tubules (SCTAT) (7)	Unknown	7/7 (100%)	NA (n=7)
Ovarian Sertoli-Leydig cell tumor (4)	22-57 (55)	4/4 (100%)	NA (n=4)
Steroid cell tumor (1)	38	1/1 (100%)	NA (n=1)
Extraovarian sex-cord stromal tumor (2)	53-77 (65)	2/2 (100%)	NA (n=2)
Ovarian clear cell carcinoma (1)	73	1/1 (100%)	None (0/1)
Microscopic extraovarian sex-cord proliferations (1)	57	1/1 (100%)	NA (n=1)
Periovarian plexiform leiomyoma (1)	43	1/1 (100%)	NA (n=1)

\*No point mutations in STK11 detected in this case; the assay could not detect copy number loss. NA: not available.

Figure 1 - 887

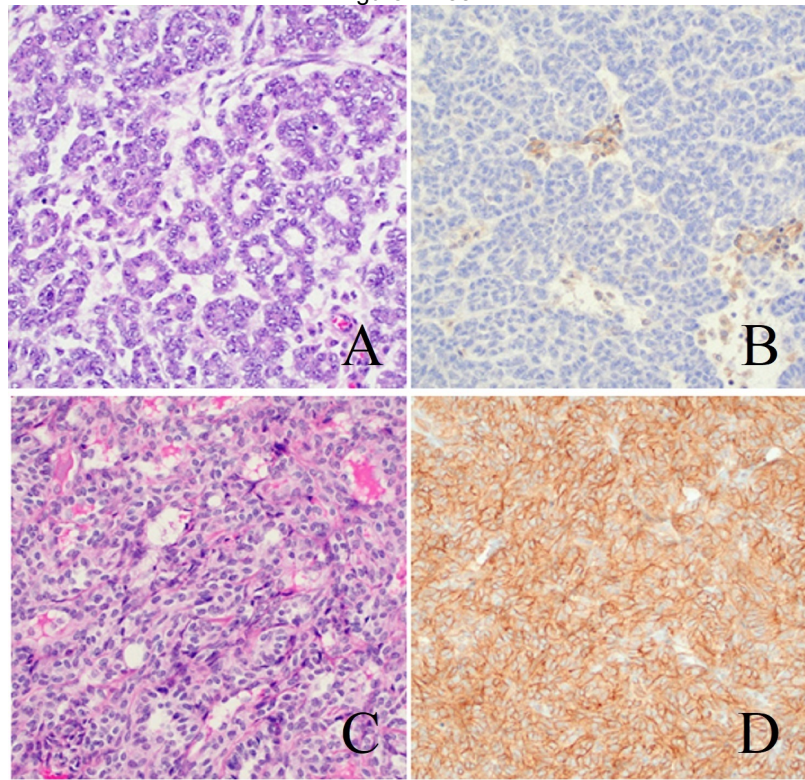


Figure 1. A) H&E of STK11 adnexal tumor, with B) complete loss of STK11 staining in tumor cells. C) H&E of FATWO, with D) intact STK11 staining.

**Conclusions:** STK11 IHC is a sensitive and specific marker for STK11 adnexal tumor. Compared to STK11 sequencing, STK11 IHC is more cost-effective and is potentially more sensitive since there is loss of expression in tumors with copy number loss, and this alteration is not assessed/reported on all molecular assays. Loss of expression of STK11 appears to be a reliable surrogate for molecular studies to differentiate STK11 adnexal tumor from its morphologic mimics, and our data suggests that sequencing is no longer required for the diagnosis of STK11 adnexal tumor if STK11 IHC is supportive of the diagnosis in the appropriate morphologic context.

## 888 Malignant Uterine Inflammatory Myofibroblastic Tumors are Characterized by Aberrant p16 Expression and Frequent CDKN2A Deletions

Kyle Devins<sup>1</sup>, Zehra Ordulu<sup>2</sup>, Sabrina Croce<sup>3</sup>, Rishikesh Haridas<sup>4</sup>, Andre Pinto<sup>5</sup>, Esther Oliva<sup>6</sup>, Jennifer Bennett<sup>7</sup>

<sup>1</sup>Massachusetts General Hospital, Boston, MA, <sup>2</sup>University of Florida, Gainesville, FL, <sup>3</sup>Institut Bergonié, Bordeaux, France, <sup>4</sup>University of Chicago Medicine, Chicago, IL, <sup>5</sup>University of Miami Health System, Miami Beach, FL, <sup>6</sup>Massachusetts General Hospital, Harvard Medical School, Boston, MA, <sup>7</sup>University of Chicago, Chicago, IL

**Disclosures:** Kyle Devins: None; Zehra Ordulu: None; Sabrina Croce: None; Rishikesh Haridas: None; Andre Pinto: None; Esther Oliva: None; Jennifer Bennett: None

**Background:** Uterine inflammatory myofibroblastic tumors (IMT) are rare mesenchymal neoplasms with a relatively low risk of malignancy. Although tumor size > 7 cm, moderate to severe atypia, frequent mitoses, necrosis, and LVI are associated with malignancy, even histologically banal IMTs may recur. A recent study noted a correlation among complete loss of p16 immunohistochemistry, CDKN2A deletions, and malignancy, independent of tumor morphology. Herein, we evaluate the morphology, p16 status, and genomic profile of a cohort of malignant IMTs (mIMT).

**Design:** 10 mIMTs, all with ALK fusions and metastases at diagnosis (n=5) or recurrences (n=5), as well as 3 benign IMTs (bIMT, median follow-up: 53 months) were retrospectively evaluated. For 2 mIMTs, only the recurrence was available for review. p16 was performed on all tumors, with aberrant expression defined by positivity in < 1% or > 90% of tumor cells. Next-generation sequencing using a 1004-gene panel or comparative genomic hybridization was performed on IMTs with available tissue (n=11).

**Results:** Patients with mIMTs ranged from 8–65 (median: 53) years and tumors from 3.5–20 (median: 13.8) cm. In the primary mIMTs (n=8), 6 were predominantly spindled and 2 epithelioid, with at least moderate atypia in 6. Necrosis was noted in 5, LVI in 4, and mitoses ranged from 0–18 (median 5.5) per 10 HPFs. In contrast, all bIMTs had mild atypia, < 3 mitoses/10 HPFs, lacked

# ABSTRACTS | GYNECOLOGIC AND OBSTETRIC PATHOLOGY

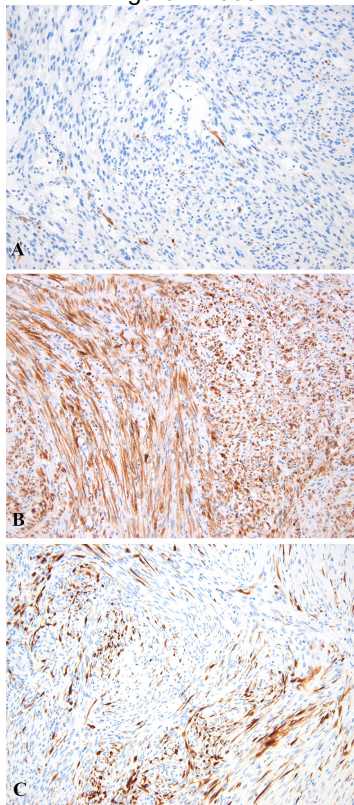
necrosis and LVI, and only 1 was > 7 cm. Clinicopathological features are summarized in table. Aberrant p16 expression was noted in all mIMTs, with < 1% positivity seen in 7 and > 90% in 3; all bIMTs had non-specific staining (30%, 40%, 50%) (Figure 1). *CDKN2A* deletions were detected in 6 mIMTs, all characterized by < 1% p16 expression. Two also harbored concurrent *CDKN2B* deletions. No alterations were detected in mIMTs with > 90% p16 expression as well as all bIMTs. Molecular findings are highlighted in Figure 2.

Case	Behavior	Age	Extrauterine Disease at Dx	Recurrence	Follow-Up	Size (cm)	Cell Type	Moderate/Severe Atypia	Mitoses/10 HPFs	Tumor Cell Necrosis	LVI	Fusion
1	M	56	Ovaries, fallopian tubes, pelvic lymph nodes, abdomen/pelvis	Persistent disease	DOD, 7 mo	12.5	Epithelioid	+	7	+	+	<i>IGFBP5-ALK</i>
2	M	56	Abdomen/pelvis	Persistent disease	AWD, 3 mo	3.5	Epithelioid	+	4	-	+	<i>IGFBP5-ALK</i>
3	M	49	Ovaries, abdomen/pelvis, lung	Persistent disease	DOD, 34 mo	15	Spindled	+	8	+	-	<i>TNC-ALK</i>
4	M	50	Lung, abdomen/pelvis	Persistent disease	AWD, 6 mo	8.1	Spindled	+	10	+	+	<i>FN1-ALK</i>
5*	M	61	None	Abdomen/Pelvis, 39 mo	AWD, 54 mo	N/A	Spindled	N/A	N/A	N/A	N/A	<i>PDLM7-ALK</i>
6*	M	59	None	Abdomen/Pelvis, 116 mo	NED, 186 mo	N/A	Spindled	N/A	N/A	N/A	N/A	FISH only
7	M	65	None	Lung, 24 mo	DOD, 48 mo	18	Spindled	-	2	-	-	<i>IGFBP5-ALK</i>
8	M	42	None	Lung, Abdomen/Pelvis, 8 mo	NED, 38 mo	7	Spindled	+	0	-	-	<i>ZBTB20-ALK</i>
9	M	36	Abdomen/pelvis	Persistent disease	DOD, 4 mo	15	Spindled	+	18	+	+	<i>SEC31-ALK</i>
10	M	8	None	Abdomen/Pelvis, 1 mo	AWD, 11 mo	20	Spindled	-	1	+	-	<i>TPM3-ALK</i>
11	B	29	None	None	NED, 53 mo	3.5	Spindled	-	0	-	-	<i>THBS1-ALK</i>
12	B	45	None	None	NED, 114 mo	4.5	Spindled	-	2	-	-	<i>IGFBP5-ALK</i>
13	B	54	None	None	NED, 31 mo	8	Spindled	-	3	-	-	FISH only

HPF = high-power field; LVI = lymphovascular invasion, M = malignant, DOD = dead of disease, + = present, AWD = alive with disease, - = absent, N/A = not available, NED = no evidence of disease, B = benign

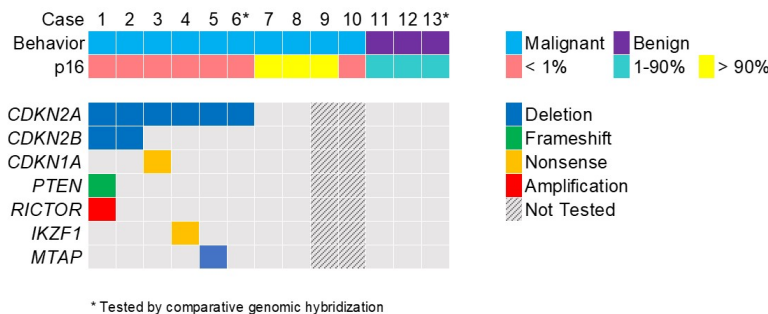
\*Only recurrence available for review

Figure 1 - 888



Aberrant p16 expression defined by positivity in < 1% (A, case 6) or > 90% (B, case 9) of tumor cells. Non-specific p16 staining (C, case 11).

Figure 2 - 888



**Conclusions:** mIMTs are associated with aberrant p16 expression and commonly *CDKN2A* deletions, independent of tumor morphology. Use of p16 immunohistochemistry is recommended in all uterine IMTs for risk stratification and management. Further studies are warranted to explore the pathobiology of mIMTs with diffuse (> 90%) p16 expression.

## 889 Novel PGR::NR4A2 Fusion Expands the Molecular Spectrum of PGR-Rearranged Epithelioid Leiomyosarcomas

Juanhui Dong<sup>1</sup>, Yimin Li<sup>2</sup>, Qianlan Yao<sup>3</sup>, Xiaoyan Zhou<sup>3</sup>, Wentao Yang<sup>4</sup>

<sup>1</sup>Chongqing University Cancer Hospital, Chongqing, China, <sup>2</sup>Fudan University Shanghai Cancer Center, Fudan University Shanghai Medical College, Shanghai, China, <sup>3</sup>Fudan University Shanghai Cancer Center, Shanghai Medical College, Fudan University, Shanghai, China, <sup>4</sup>Fudan University Shanghai Cancer Center, Shanghai, China

**Disclosures:** Juanhui Dong: None; Yimin Li: None; Qianlan Yao: None; Xiaoyan Zhou: None; Wentao Yang: None

**Background:** Uterine epithelioid leiomyosarcoma is a morphologic variant of malignant smooth muscle tumors. Due to the rarity of epithelioid leiomyosarcomas, genetic abnormalities are seldom reported until the recent discovery of progesterone receptor (PGR) rearrangements. So far, NR4A3 and UBR5 are prime partners of PGR rearrangements in epithelioid leiomyosarcomas.

**Design:** In this report, we described a unique case of epithelioid leiomyosarcoma harboring a novel PGR:: NR4A2 (nuclear receptor subfamily 4 group A member 2) fusion, which occurred in a 42-year-old woman who had a mass in the myometrium. The patient underwent hysterectomy and then relapsed 29 months later with a large mass in the pelvic cavity.

**Results:** Histologically, the relapsed pelvic neoplasm was solid-cystic. The tumor was composed of round/polygonal or rhabdoid cells, spindle cells and large amount of myxoid matrix. Immunohistochemistry revealed diffuse staining of ER, PR, and Desmin and focal staining of h-caldesmon in tumor cells. CD10, ALK, and BCOR were all negative. Furthermore, next-generation sequencing (NGS) revealed PGR:: NR4A2 rearrangement that fused PGR exon 2 to NR4A2 exon 1.

Figure 1 - 889

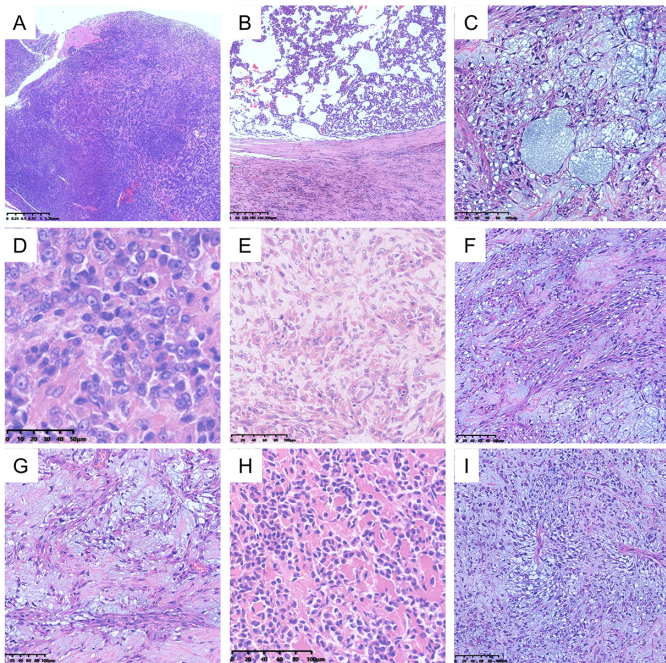


Fig. 1 Histologic features of PGR::NR4A2 fusion positive epithelioid leiomyosarcoma.  
 (A) The tumor cells were abundant in the solid area and distributed in nodularity.  
 (B) The tumor cells in cystic areas formed cystic chambers of varying size, as shown in the lower right corner where infiltration of inflammatory cells and hemosiderosis were observed in the tissue of cystiform.  
 (C) Cystic cavities were formed and surrounded by scattered tumor cells.  
 (D-E) The epithelioid/polygonal cells with eosinophilic granular cytoplasm were abundant, resembling "rhabdoid" cells, with slightly irregular and dislocated nuclei, clear karyotheca, centered or slightly deviated nucleoli, and rough chromatin.  
 (F-G) The spindle shaped cells with eosinophilic cytoplasm and oval or round nuclei arranged in fascicular or interlaced. Mild to moderate cell atypia was observed.  
 (H) Hyaline degeneration was observed in collagenous fibers.  
 (I) The structure of spindle shaped cells surrounding blood vessels resembled starburst.

**Conclusions:** In conclusion, we report a case of uterus epithelioid leiomyosarcoma showing a large amount of myxoid matrix and harboring PGR::NR4A2 rearrangement. PGR::NR4A rearrangement expands the molecular spectrum of PGR-rearranged epithelioid leiomyosarcomas.

## 890 Mosaic P53 Expression in Tubo-Ovarian High Grade Serous Cancer: A Report of 9 Cases

Rawda Elshennawy<sup>1</sup>, Jason Yap<sup>1</sup>, Raji Ganeshan<sup>2</sup>, Andrew Turnell<sup>1</sup>

<sup>1</sup>University of Birmingham, Birmingham, United Kingdom, <sup>2</sup>Birmingham Women's Hospital, Birmingham, United Kingdom

**Disclosures:** Rawda Elshennawy: None; Jason Yap: None; Raji Ganeshan: None; Andrew Turnell: None

**Background:** More than 96% of tubo-ovarian high grade serous carcinoma (HGSC) will harbor a *Tp53* mutation which can be detected by immunohistochemistry (IHC). About 66% of these are missense mutations affecting the DNA binding domain resulting in p53 overexpression by IHC. Another 25% are nonsense or frameshift mutations that result in complete absence of p53 expression in the tumor. Less common mutations include those affecting the nuclear localization signal resulting in cytoplasmic p53 expression and truncating mutations affecting the C-terminal domain resulting in wild type like staining. Mosaic or heterogeneous p53 expression has been reported in endometrial carcinoma but not in HGSC. We report 9 cases of HGSC with mosaic p53 expression by IHC and correlate with survival and clinicopathological parameters.

**Design:** Tissue blocks of 100 HGSC females were collected from a large Gynecologic Oncology tertiary referral centre in the United Kingdom. The DO-1 clone of p53 was applied on tissue sections after proper optimization and validation in an automated IHC platform. Clinicopathological data collected included age, FIGO stage, type of surgery, volume of residual disease after surgery, lymph node status, chemotherapy response score, platinum resistance, BRCA mutation, progression-free (PFS) and Overall survival (OS). Kaplan-Meier curves were used to compare survival differences between the p53 expression groups and clinicopathological parameters were compared for any prognostic significance.

**Results:** P53 overexpression was seen in 65 cases, null pattern in 23 cases, cytoplasmic in 3 and 9 showed a combination of overexpression and wild type like staining. (Figure 1) When comparing OS, the mosaic p53 cases exhibited the shortest median

Figure 2 - 889

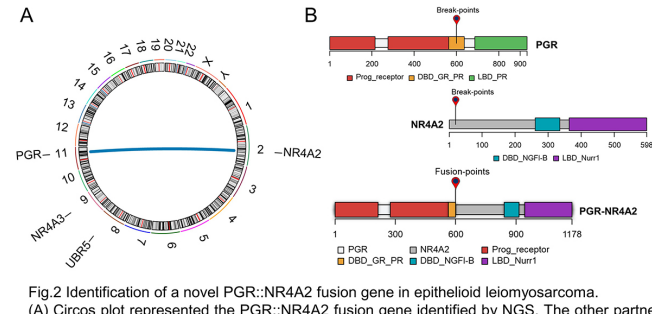


Fig.2 Identification of a novel PGR::NR4A2 fusion gene in epithelioid leiomyosarcoma.  
 (A) Circos plot represented the PGR::NR4A2 fusion gene identified by NGS. The other partners for PGR, NR4A3 and UBR5, were also displayed.  
 (B) Schematic diagram represented the PGR::NR4A2 fusion breakpoint. The domains retained in the fusion protein included prog\_receptor domain and part of DBD\_GR\_PR domain of PGR and almost the complete NR4A2 protein.

OS (28.2 months) followed by the null cases (37.4 months). The p53 overexpressing cases had an intermediate median OS (51.8 months), while the cytoplasmic showed the longest (80.5 months). The difference was not statistically significant (Log rank  $X^2=2.073$ ,  $p=0.557$ ). (Figure 2) PFS was not significantly different between the four groups (Log rank  $X^2=0.602$ ,  $p=0.896$ ). For statistical reasons, the null and cytoplasmic p53 cases were omitted. Clinicopathological parameters were compared in the mosaic and overexpression groups. (Table 1)

Patient characteristic	Mosaic p53 pattern	P53 Overexpression	Test of significance (p-value)
<b>Age, year</b> <i>Mdn</i> ( <i>Min</i> , <i>Max</i> )	64.5 (42, 74)	65 (40, 84)	Mann Whitney=245 $p=0.791$
<b>Type of surgery, n</b> PDS DDS	1/9 8/9	22/65 43/65	Fisher's exact 2-sided significance=0.096
<b>Cytoreduction, n</b> R0 & R1 R2	9/9 0/9	55/65 10/65	Fisher's exact 2-sided significance=0.588
<b>CRS, n<sup>a</sup></b> Minimal & Partial Complete	4/8 4/8	35/43 8/43	Fisher's exact 2-sided significance=0.059
<b>FIGO stage, n</b> Early (I, II) Late (III, IV)	0/9 9/9	4/65 61/65	Fisher's exact 2-sided significance=1
<b>LN status, n</b> Nx & N0 N1	4/9 5/9	37/65 28/65	Fisher's exact 2-sided significance=0.455
<b>Platinum resistance, n<sup>b</sup></b> Yes No	2/9 5/9	18/65 35/65	Fisher's exact 2-sided significance=1
<b>BRCA status, n<sup>c</sup></b> Mutant Wildtype	3/9* 2/9	11/65 11/65	Fisher's exact 2-sided significance=1

a data available for patients only undergoing DDS n=51, b data available for n=60 patients, c data available for n=27 patients.

DDS=delayed debulking surgery, PDS=primary debulking surgery.

R0=complete cytoreduction, R1=optimal cytoreduction, R2=suboptimal cytoreduction

CRS=chemotherapy response score

Nx=LN not submitted, N0=no LN involvement, N1=LN involvement

\* Two cases had BRCA-1 frameshift mutation in exon 11 and one had a germline BRCA-2 frameshift deletion

Figure 1 – 890

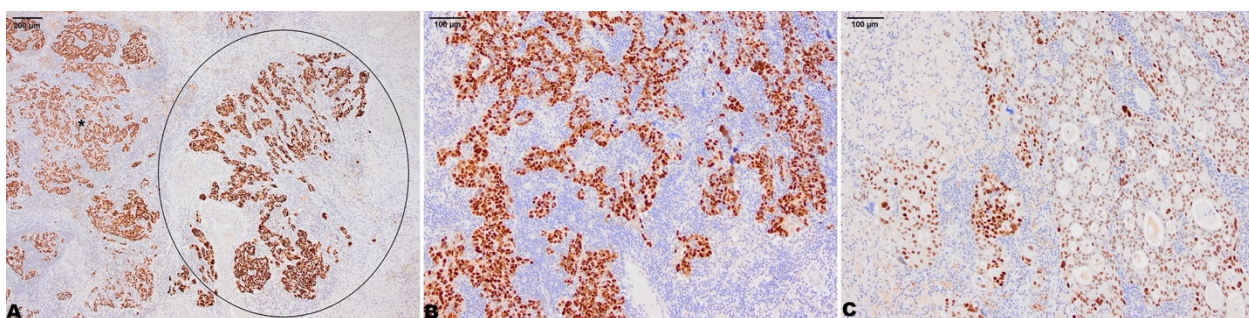
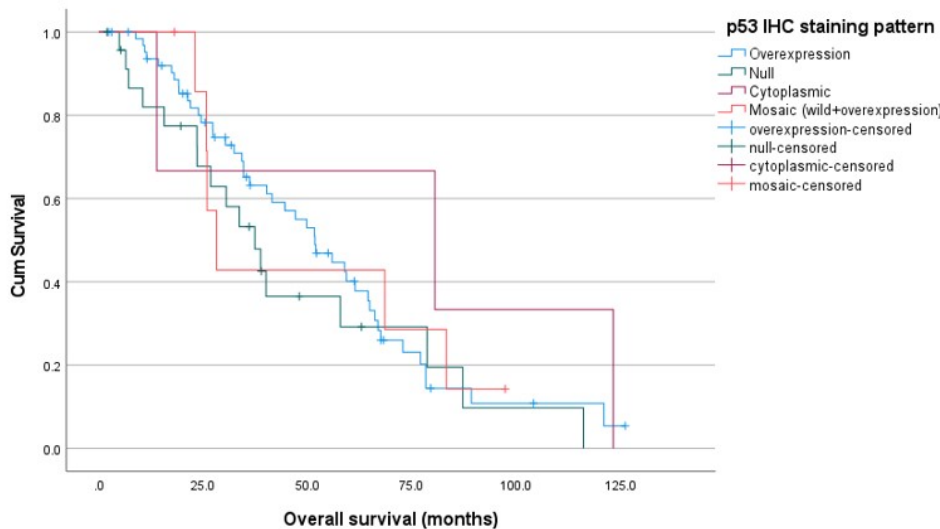


Figure 2 - 890



**Conclusions:** Mosaic p53 expression in HGSC is an under-reported IHC expression pattern. We believe a larger cohort and more detailed investigation into the biological nature of this pattern would have significant clinical implications.

### 891 UbcH10 Is a Proto-oncogene and Cell-Cycle Proliferation Marker of Borderline Prognostic Significance in Tubo-Ovarian High Grade Serous Cancer

Rawda Elshennawy<sup>1</sup>, Jason Yap<sup>1</sup>, Raji Ganeshan<sup>2</sup>, Andrew Turnell<sup>1</sup>

<sup>1</sup>University of Birmingham, Birmingham, United Kingdom, <sup>2</sup>Birmingham Women's Hospital, Birmingham, United Kingdom

**Disclosures:** Rawda Elshennawy: None; Jason Yap: None; Raji Ganeshan: None; Andrew Turnell: None

**Background:** Tubo-ovarian high grade serous carcinoma (HGSC) is the most common ovarian cancer whose genetic profile is marked by early *Tp53* mutation. It is the 5<sup>th</sup> leading cause of cancer-related deaths in females & a significant contributor to female morbidity worldwide. Despite advances in our understanding of the molecular pathology of HGSC, treatment modalities remain at a standstill & have not improved patient survival. Therefore, we continue to investigate the biological mechanisms that underpin the aggressive behaviour of these tumours to identify new molecular targets. UbcH10 is an E2-conjugating enzyme for the Anaphase-Promoting Complex/Cyclosome that regulates cell-cycle progression, by promoting the degradation of mitotic regulators through ubiquitin-mediated proteolysis. UbcH10 is also a proto-oncogene whose aberrant expression has been reported in numerous cancers, making it a potential cancer biomarker for the prognosis of HGSC.

**Design:** Multiplex immunohistochemistry (IHC) was used to investigate the expression of UbcH10 & p53 in HGSC. IHC was performed on three main HGSC cohorts: the 1<sup>st</sup> consisted of 100 cases of whole tumour sections; the 2<sup>nd</sup> of 81 cases of tumour constructed on tissue microarrays(TMA) for validation. The 3<sup>rd</sup> cohort included 24 cases with matched serous tubal intraepithelial carcinoma (STIC) samples to measure disease progression. In these cohorts, we investigated the relative protein expression of UbcH10, its relation to p53 mutation & Ki67 index, as well as its effect on patient outcome. We used 2 scoring systems for UbcH10 {IRS and H-score} & divided our patients into low and high UbcH10 expressors based on cut-off values generated by the bioinformatics tool X-tile; the data was analyzed & modelled using the Cox proportional hazards model.

**Results:** UbcH10 overexpression did not significantly impact survival nor correlate with p53 mutation & prognostic parameters in the 1<sup>st</sup> cohort (Table 1). In the TMA cohort, UbcH10 negatively impacted OS {HR=1.1, 95%CI(1.008, 1.223), *p*=0.032} (Figure 1) The trend was maintained in PFS but was not significant (Log rank  $\chi^2$ =1.591, *p*=0.163). UbcH10 expression in STICs were comparable to their matched HGSC (*U*=233, *p*=0.261). A significant positive correlation was detected between UbcH10 and Ki67 index (*p*=0.48, *p*=0.021) (Figure 2)

Clinicopathological feature of whole tumour section cohort (n=100)	UbcH10 expression (IRS-score)		Test of significance (p-value)	UbcH10 expression (H-score)		Test of significance (p-value)
	≤7	>7		≤120	>120	
<b>Age, year</b> ≤64 (Mdn) >64	40 31	11 18	Pearson $\chi^2=2.79$ ( $p=0.095$ )	38 29	13 20	Pearson $\chi^2=2.65$ ( $p=0.103$ )
<b>Cytoreduction</b> R0 & R1 R2	60 11	25 4	Fisher's exact ( $p=1$ )	58 9	27 6	Fisher's exact ( $p=0.56$ )
<b>CRS<sup>a</sup></b> Minimal & Partial Complete	47 9	7 5	Fisher's exact ( $p=0.108$ )	42 9	12 5	Fisher's exact ( $p=0.315$ )
<b>FIGO stage</b> Early (I, II) Late (III, IV)	4 68	3 25	Fisher's exact ( $p=0.356$ )	4 63	3 30	Fisher's exact ( $p=0.681$ )
<b>P53 IHC staining</b> Overexpression Null & Cytoplasmic	51 21	22 6	Pearson $\chi^2=0.612$ ( $p=0.434$ )	49 18	24 9	Pearson $\chi^2=0.002$ ( $p=0.96$ )
<b>LN status</b> N0 N1 Nx	9 28 35	2 11 15	Pearson $\chi^2=0.626$ ( $p=0.731$ )	8 27 32	3 12 18	Pearson $\chi^2=0.454$ ( $p=0.797$ )
<b>Platinum resistance <sup>b</sup></b> Yes No	20 37	4 18	Pearson $\chi^2=2.145$ ( $p=0.143$ )	19 35	5 20	Pearson $\chi^2=1.863$ ( $p=0.172$ )
<b>BRCA mutation <sup>c</sup></b> Wildtype Mutant	10 12	6 5	Pearson $\chi^2=0.243$ ( $p=0.622$ )	8 13	8 4	Pearson $\chi^2=2.456$ ( $p=0.114$ )
<b>Median OS, months</b>	44.6	59.3	Log rank $\chi^2=1.848$ ( $p=0.172$ )	44.6	59.3	Log rank $\chi^2=2.154$ ( $p=0.142$ )

a data available for patients only undergoing delayed debulking surgery n=68, b data available for n=79 patients, c data available for n=33 patients.

R0=complete cytoreduction, R1=optimal cytoreduction, R2=suboptimal cytoreduction

CRS=chemotherapy response score

Nx=LN not submitted, N0=no LN involvement, N1=LN involvement

IRS=immunoreactive score

OS=Overall survival

Figure 1 – 891

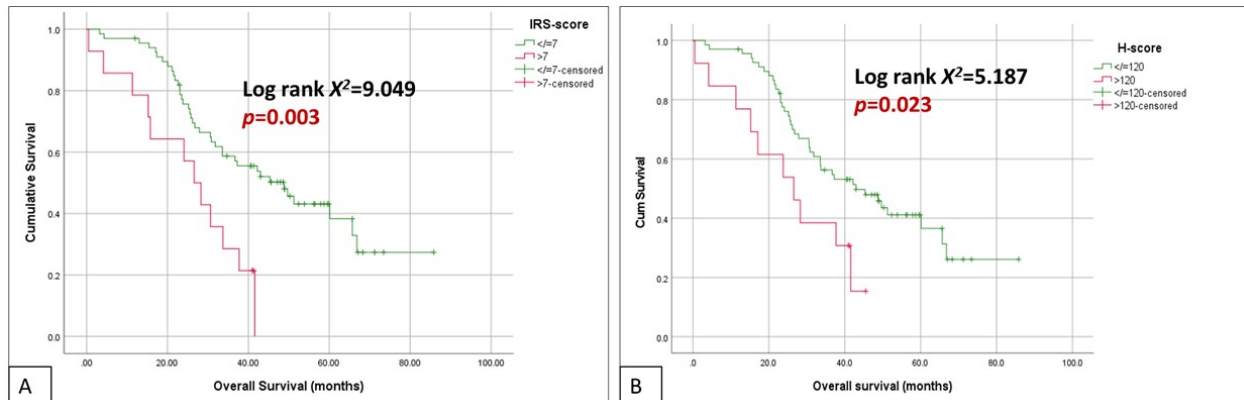
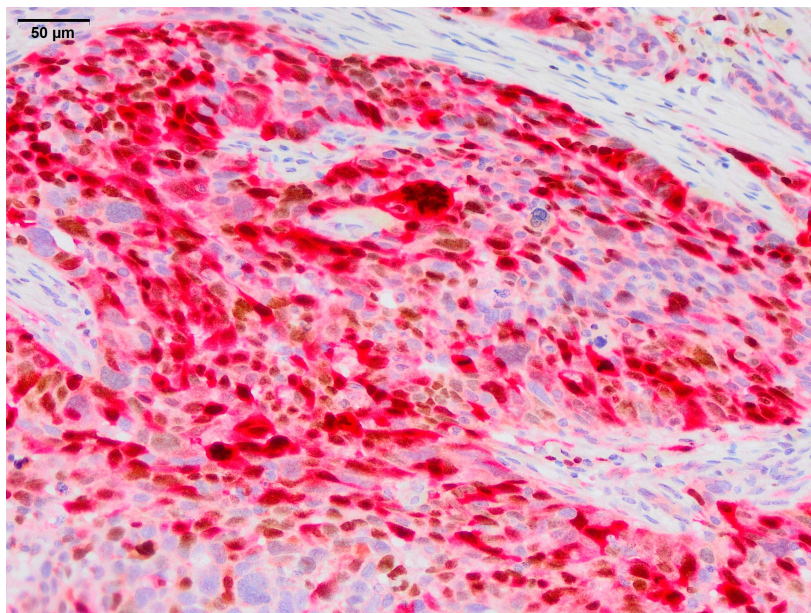


Figure 2 – 891



**Conclusions:** UbcH10 is expressed early in HGSC and their precursors lesions (STIC). It is significantly related to the proliferative state of the cell and has a weak poor prognostic impact on patient outcome.

## 892 Many Faces of Cellular Angiofibroma: Variable Morphology of Rare Sarcomatous Transformation

Anna Sarah Erem<sup>1</sup>, Sandra Gjorgova Gjeorgjievski<sup>1</sup>, Krisztina Hanley<sup>1</sup>, Gulisa Turashvili<sup>1</sup>

<sup>1</sup>Emory University, Atlanta, GA

**Disclosures:** Anna Sarah Erem: None; Sandra Gjorgova Gjeorgjievski: None; Krisztina Hanley: None; Gulisa Turashvili: None

**Background:** Cellular angiofibromas (CAFs) are benign mesenchymal neoplasms of the vulva and lower genitourinary tract. Recurrences, cytologic atypia, and sarcomatous transformation are extremely uncommon. We aimed to describe detailed clinicopathologic features of CAF with and without sarcomatous transformation in a female population.

**Design:** We are presenting complete resection specimens of CAFs, retrieved from our institution's surgical and consultation files between 2010 and 2022. Clinical data was obtained from the electronic medical records, and microscopic slides were reviewed.

**Results:** A total of 17 CAFs were identified. The median age at diagnosis was 49 years (32-68). All tumors were located within the subcutis, and ranged in size from 0.5 to 5 cm (median 3 cm). CAFs were histologically characterized by bland spindle cell proliferation, variable amounts of adipose tissue, mast cells and numerous medium-sized thick-walled vessels. Infiltrative borders were seen in 4, fascicular growth in 9, and chronic perivascular or stromal inflammation in 15 cases. Stromal edema (8) and fat entrapment (9) were common. Rare histologic features included myxoid changes (3), vascular thrombosis (1) and hemangiopericytoma-like vasculature (4). Cytologic atypia was seen in 3 cases, presenting as scattered multinucleated cells. CD34 and desmin were positive in 12 and 2 tumors, respectively, while Rb-1 was lost in 2 cases. Six CAFs had sarcomatous transformation, ranging from 10-80% of overall tumor volume. Abrupt transition between sarcoma and CAF was seen in 4 cases, gradual transition in 2 cases, and 1 CAF had multiple sarcomatous foci. Three of 6 cases showed increased mitotic activity (up to 28 per 10 HPF), whereas the remaining 3 had ≤3 mitoses per 10 HPF. Diffuse p16 expression was present in 2 cases with sarcomatous transformation, which was not seen in any of the CAFs lacking sarcomatous transformation. Only 1 case of CAF with sarcomatous transformation recurred upon re-excision.

**Conclusions:** Common histologic features of CAF include fascicular growth, stromal edema, and myxoid changes. Infiltrative borders are uncommon, while perivascular and stromal inflammation is frequently present. A subset of CAFs in female patients is associated with sarcomatous transformation (seen in 35% of our cases) with rare local recurrences but no distant metastases. Diffuse expression of p16 may have diagnostic significance in CAFs with sarcomatous transformation.

## 893 Malignant Rhabdoid Tumors of the Vulva: “In the Dark, Everything Looks Alike”: A Clinicopathologic, Immunohistochemical, and Molecular Genetics Study

Iñigo Espinosa<sup>1</sup>, Emanuela D'Angelo<sup>2</sup>, Louise De Brot<sup>3</sup>, Jaime Prat<sup>4</sup>

<sup>1</sup>Hospital de la Santa Creu i Sant Pau, Barcelona, Spain, <sup>2</sup>Chieti, Italy, <sup>3</sup>A.C.Camargo Cancer Center, Sao Paulo, Brazil, <sup>4</sup>Autonomous University of Barcelona, Barcelona, Spain

**Disclosures:** Iñigo Espinosa: None; Emanuela D'Angelo: None; Louise De Brot: None; Jaime Prat: None

**Background:** It has been suggested that most, if not all, extrarenal rhabdoid tumors of the vulva represent “proximal-type” epithelioid sarcomas.

**Design:** To better understand rhabdoid tumors of the vulva, we studied the clinicopathologic, immunohistochemical (IHC), and molecular features of 5 of these tumors and 6 extragenital epithelioid sarcomas. IHC analysis for cytokeratin AE1/AE3, EMA, S100, CD34, smooth muscle actin, desmin, and SMARCB1 (INI1) was performed. Ultrastructural study was done in one rhabdoid tumor. Next generation sequencing of the SMARCB1 gene was performed in all cases.

**Results:** The 5 vulvar tumors occurred in adult women (mean age 52). They were poorly differentiated neoplasms with a rhabdoid morphology. The ultrastructural study showed large amounts of intermediate filaments (10 nm). All cases had loss of expression of INI1 and were negative for CD34. No SMARCB1 mutations were found. Follow-up revealed that 3 patients died of disease, 1 was alive with disease, and 1 was alive without evidence of disease. The epithelioid sarcomas occurred in young adults (mean age 33). Three cases arose in the distal extremities and the other three had a proximal location. They showed the characteristic “granulomatous” arrangement of the neoplastic cells. The recurrent tumors were more proximal and often showed a rhabdoid morphology. All cases had loss of expression of INI1. CD34 was expressed by 3 of 6 cases. No SMARCB1 mutations were encountered. Follow-up revealed that 2 patients died of disease, 1 was alive with disease, and 3 were alive without evidence of disease.

**Conclusions:** Based on their different morphology and biologic behavior, we conclude that rhabdoid tumors of the vulva and epithelioid sarcomas are different diseases with distinct clinicopathologic features. Undifferentiated vulvar tumors with rhabdoid morphology should be classified as malignant rhabdoid tumors, rather than “proximal-type” epithelioid sarcomas. The term “proximal-type” epithelioid sarcoma is artificial even if malignant rhabdoid tumors of the vulva may overlap morphologically with recurrent epithelioid sarcomas exhibiting a rhabdoid phenotype.

## 894 The Cancer Genome Atlas Classification of Endometrial Carcinoma: Is It Really Useful?

Iñigo Espinosa<sup>1</sup>, Irmgard Costa<sup>2</sup>, Alberto Gallardo<sup>1</sup>, Emanuela D'Angelo<sup>3</sup>, Fabiana Aguirre Neira<sup>2</sup>, Armando Reques<sup>2</sup>, Ruben Carrera<sup>4</sup>, Jaime Prat<sup>5</sup>, Enrique Lerma Puertas<sup>6</sup>

<sup>1</sup>Hospital de la Santa Creu i Sant Pau, Barcelona, Spain, <sup>2</sup>Hospital Parc Taulí, Sabadell, Spain, <sup>3</sup>Chieti, Italy, <sup>4</sup>Hospital Parc Taulí, Spain, <sup>5</sup>Autonomous University of Barcelona, Barcelona, Spain, <sup>6</sup>Hospital Sant Pau, Barcelona, Spain

**Disclosures:** Iñigo Espinosa: None; Irmgard Costa: None; Alberto Gallardo: None; Emanuela D'Angelo: None; Fabiana Aguirre Neira: None; Armando Reques: None; Ruben Carrera: None; Jaime Prat: None; Enrique Lerma Puertas: None

**Background:** The Cancer Genome Atlas (TCGA) Research Network identified four molecular subgroups of endometrial carcinomas with different prognosis: ultramutated (POLE mut); hypermutated (MMRd); low degree of copy-number (NSMP); and high degree of copy-number (p53abn). The aim of this study is to know the incidence of the molecular subgroups in a Spanish population and evaluate the utility of TCGA classification in the diagnosis and management of the patients.

**Design:** We studied 220 consecutive endometrial carcinomas diagnosed between 2015-2022 at the Sant Pau Hospital and Taulí Hospital (Barcelona). IHC for p53 and the mismatch repair proteins was performed. All patients were also tested for POLE-EDM by Sanger sequencing.

**Results:** Patient age ranged from 33 to 99 (median 69) years. 184 cases (84%) were endometrioid and 36 cases (16%) non-endometrioid. Grade distribution of the endometrioid carcinomas included 79 (43%) G1, 66 (36%) G2, and 39 (21%) G3 tumors. Molecular classification yielded 11 (5%) POLE mut, 56 (26%) MMRd, 117 (53%) NSMP, and 36 (16%) p53abn. POLE mut cases included 1 DDC, 2 G1 EECs, 4 G2 EECs, and 4 G3 EECs. 5 patients had stage IA disease and 5 patients had stage IB. Four tumors had also p53 aberrant expression and two cases had loss of MLH1 and PMS2 proteins. Adjuvant chemotherapy was given to one patient while the rest of the patients did not receive adjuvant treatment. Follow-up revealed that all patients were alive without evidence of disease. MMRd cases included 53 EECs, 2 DDC, and 1 CS. Four cases of Lynch Syndrome were detected. NSMP cases included 115 EECs, 1 MC (EEC+CCC), and 1 CCC. p53 mut cases comprised 15 SCs, 6 G3 EECs, 11 CSs, 2 UCs, and 2 MCs.

**Conclusions:** The only novel and exclusive contribution of the TCGA classification is the discovery of the POLE mut ECs. These patients, if they carry pathogenic mutations, have a very good prognosis and could benefit from a de-escalating adjuvant

treatment. However, the incidence of these tumors is low. Multiple classifier endometrial carcinomas having both POLE-mutated tumors and abnormal p53 expression or MMRd, should be classified as POLE. Grade 1 and 2 EECs with aberrant expression of p53 are extremely rare. Our results show that morphology (H&E) is still the best method for the diagnosis/classification of endometrial carcinomas and even provides valuable prognostic information.

## 895 Pathologic Evaluation of Sentinel Lymph Nodes in Endometrial Carcinoma: What Have We Learned in 10 Years?

Elizabeth Euscher<sup>1</sup>, Preetha Ramalingam<sup>1</sup>, Anais Malpica<sup>1</sup>

<sup>1</sup>The University of Texas MD Anderson Cancer Center, Houston, TX

**Disclosures:** Elizabeth Euscher: None; Preetha Ramalingam: None; Anais Malpica: None

**Background:** Sentinel lymph node (SLN) mapping targets LNs most likely to harbor metastases (MT) providing staging information in endometrial carcinoma (ECa) without the morbidities associated with LN dissection. We present the results of LN pathology in ECa since SLN mapping became routine at our institution 10 years ago.

**Design:** We identified ECa with at least one mapped SLN (n=1073; 2013 to 2022); for comparison we retrieved consecutive ECa with LN dissection (LND) (n=695; 2002-2012). SLNs negative by initial hematoxylin&eosin (H&E) exam underwent ultrastaging (US) by one of two methods: 5 sets of 1 H&E + 2 unstained slides (USS) at 250 µm intervals with pankeratin immunohistochemistry (IHC) on level 1 (2013-2014) or 1 H&E + 2 USS cut 250 µm into the block and pankeratin IHC (2015-2022). We recorded tumor histotype, SLN status, MT size, if MT detected by US, and presence of MT in unmapped LN with negative SLNs. For LND cases we recorded presence and size of largest LN MT.

**Results:** ECa with SLN MT had the following histotypes: endometrioid FIGO 1-2, 86; endometrioid FIGO 3, 13; clear cell, 4; serous, 24; carcinosarcoma, 22; high grade mixed, 20; high grade NOS, 9; undifferentiated, 6; mesonephric-like, 3. 187(17%) ECa with SLN mapping and 142(20%) with LND had LN MTs. Table 1 shows the MT size distribution for SLN and LN dissection cases. In SLN cases, 98(52%) cases had MTs detected by routine H&E; 78(42%) by US; and 11(6%) had negative SLN with LN MTs in an unmapped LN. 8 SLNs with microMT or ITC had a positive nonSLN: 6 at the same ipsi- or contralateral level; 2 had ITC in aortic LNs. 6 ECa (4 serous, 1 carcinosarcoma, 1 endometrioid FIGO 2) without myometrial invasion had SLN MT (4 on initial H&E; 2 by US).

Metastasis Size in ECa with SLN or LN Dissection					
	MacroMT (>2 mm)	MicroMT (>0.2 to 2 mm)	ITC (up to 0.2 mm)	Size Unknown	% Low + Ultralow Volume LN MT
SLN (n=176)	55	59	63	10	69%
LN dissection (n=142)	71	13	13	45	18%

**Conclusions:** MT rate in ECa is similar between SLN mapping (17%) and LND (21%). Low or ultralow volume MTs were more common in SLN (69% vs 23% for LND) possibly due to utilization of US. US increased LN MT detection by just over 1.5 times above that detected by routine H&E examination emphasizing the need to incorporate US into routine practice. Much of the increase is due to detection of low and ultralow volume MTs. The significance of ITCs requires further study; but 8 SLNs with ITCs had tumor in nonSLN, including 2 cases with positive para-aortic LNs. Six (3%) ECa had a SLN MT in the absence of myometrial invasion with 2 cases detected by US. These findings underscore the need for US as a part of SLN examination even in the absence of myoinvasive ECa.

## 896 Leiomyosarcoma from Leiomyoma with Bizarre Nuclei: Histologic, Molecular, and Digital Analysis

Christopher Felicelli<sup>1</sup>, Melissa Mejia-Bautista<sup>1</sup>, Mei Lin<sup>1</sup>, Brian Vadasz<sup>1</sup>, Jorge Novo<sup>1</sup>, Amanda Strickland<sup>1</sup>, Xinyan Lu<sup>1</sup>, Lawrence Jennings<sup>1</sup>, Jian-Jun Wei<sup>2</sup>

<sup>1</sup>Northwestern University Feinberg School of Medicine, Chicago, IL, <sup>2</sup>Northwestern University, Chicago, IL

**Disclosures:** Christopher Felicelli: None; Melissa Mejia-Bautista: None; Mei Lin: None; Brian Vadasz: None; Jorge Novo: None; Amanda Strickland: None; Xinyan Lu: None; Lawrence Jennings: None; Jian-Jun Wei: None

**Background:** Leiomyoma with bizarre nuclei (LMBN) is a rare variant of leiomyoma with a benign clinical course. In contrast, leiomyosarcoma (LMS) is a malignant neoplasm with poor survival. While LMBN and LMS show distinct histology, they show similar immunophenotype and molecular features. Rare cases of LMBN associated with LMS have been reported, however the relationship between them is unclear. We analyzed 10 cases of LMS arising in conjunction with LMBN to elucidate clinical, histologic, digital, and molecular characteristics.

# ABSTRACTS | GYNECOLOGIC AND OBSTETRIC PATHOLOGY

**Design:** Ten cases of LMS arising in conjunction with LMBN were included. Select slides were examined by IHC to confirm LMS and LMBN components and scanned by whole slide imaging. Virtual images were analyzed by automated intelligence with aid of QuPath software for cyto-histologic and distribution patterns of LMS, LMBN, and myometrium. DNA from LMS and adjacent LMBN was isolated from FFPE tissue for molecular analysis on Affymetrix OncoScan® CNA arrays (Table 1). Additionally, 10 LMS cases and 13 LMBN sporadic cases were selected as controls for CNA analysis.

**Results:** The 10 cases displayed presence of both LMBN and LMS areas. IHC and digital image analysis demonstrated that LMBN and LMS were physically separated in three growth patterns: adjacent, circumferential, and separate nodules (Figure 1A-C). Digital analysis of these lesions revealed LMBN had significantly increased nuclear hyperchromasia in comparison to LMS and myometrium ( $p=0.004$ ,  $p<0.001$ ). Higher nuclear: cytoplasmic ratios were seen in LMS ( $p<0.0001$ ) (Figure 1D). Both components had similar p16 and p53 IHC patterns, but LMS had higher Ki-67 index and lower ER/PR expression. Clonal analysis revealed 9 cases of LMS were from existing LMBN due to their identical genomic CNA and LOH. Common genomic losses of *TP53*, *RB1*, *PTEN* and *CDKN2A/B* were identified in LMS. In sporadic cases of LMS and LMBN, frequent CNA in 42 genomic regions were identified and 37 of them shared by both tumor types (Figure 2A-B).

#	Age	Size (cm)	Tumor type	Histology	ER	PR	p16	p53	Ki-67	Molecular	Clonality	FIGO	Recurrence	Survival	Pathways
1	43	27	LMBN	BN, LM 2M/10HP F	50%	50%	Patchy	Diffuse	5%	Loss: 1q, 11q, 14q, 15q	Loss: 1q, 11q, 14q	IIIB	No	Alive	<i>p53</i> , <i>PTEN</i> , <i>Rb</i> , <i>CDKN2A</i>
				LMS	NA, 24 M/10HPF, TN	50%	50%	Patchy	Diffuse	50%	Loss: Xp, 1p, 2p, 3q, 4q, 8q, 9q, 10q, 11p, 11q, 13q, 14q, 16q, 17p, 18p, 21q, 22q				
2	42	6	LMBN	BN, high density 6M/10HP F	90%	90%	Block positive	Focal	10- 20%	Loss: 4q, 5q, 7p, 7q, 13q, 14q, 16p, 16q, 17p, 19q	Loss: 4q, 5q, 7p, 7q, 13q, 14q, 16p, 16q, 17p,	IV	Yes	Dead	<i>p53</i> , <i>PTEN</i> , <i>Rb</i>
				LMS	NA, >15M /10HPF, necrosis	90%	90%	Block positive	Focal	30%	Loss: Xp, 2q, 4q, 5q, 6q, 7p, 7q, 9q, 10q, 13q, 14q, 16p, 17p, 19q, 21p, 22q				
3	48	7.8	LMBN	BN, 1M/10HP F	100%	100%	Block positive	Wild type	5%	Loss: 13q, 16q, 17p, Xq	Loss: 13q, 16q, 17p, Xq	1A	No	Alive	<i>p53</i> , <i>Rb</i>
				LMS	NA, 12 M/10HPF, necrosis	20%	0%	Block positive	Diffuse Mutant	30- 40%	Loss: 1p, 2p, 2q, 4p, 5p, 7q, 11q, 12p, 13q, 14q, 16p, 16q, 17p, 17q, Xq Gain: 12p, Xp				
4	41	3.7	LMBN	BN, 0M/10HP F	N/A	N/A	N/A	N/A	N/A	N/A	N/A	IA	No	Alive	N/A
				LMS	NA, 20 M/10HPF, necrosis	N/A	N/A	N/A	N/A	N/A					
5	54	10.5	LMBN	BN, 2M/10HP F	0%	0%	N/A	N/A	N/A	Loss: 11p, 11q, 12q, 13q, 17p	Loss: 11p, 11q, 12q, 13q, 17p	IA	Yes	Alive	<i>p53</i> , <i>Rb</i>
				LMS	NA, 40 M/10HPF, necrosis	0%	0%	N/A	N/A	N/A	Loss: 2q, 4q, 5q, 6q, 9p, 10, 11p, 11q, 12, 14q, 15q, 16, 17p, 17q, 18, 19, 20q Gain: X, 1p, 3, 4p, 6p, 7, 8, 9q, 20q, 21				
6	55	14.9	LMBN	BN, 0M/10HP F	100%	100%	Block positive	Null, mutant	5%	Loss: 6p, 6q, 13q	Loss: 6p, 6q, 13q	IA	Yes	Alive	<i>p53</i> , <i>PTEN</i> , <i>Rb</i>
				LMS	NA, >20 M/10HPF, necrosis	100%	100%	Block positive	Null, mutant	50%	Loss: Xp, Xq, 1p, 2q, 4q, 5q, 6q, 6q, 8q, 9q, 11q, 12p, 16p, 16q, 17p, 19q, 20p Gain: 3p, 10, 16q, 17p, 17q, 19q				
7	50	4.5	LMBN	BN, 1M/10hpF	80%	95%	Bock Positive	Null, mutant	5%	N/A	N/A	IA	No	Alive	N/A
				LMS	NA, 21 M/10HPF, necrosis	50%	20%	Block positive	Null, mutant	40%	N/A				
8	55	7.5	LMBN	BN, 1M/10HP F	N/A	N/A	Patchy	Diffuse mutant	5%	Loss: Xq, 3q, 4q, 5q, 6p, 6q 10q, 13q, 17p Gain: 13p	Loss: Xq, 3q, 4q, 5q, 6p, 6q 10q, 13q, 17p Gain: 19p	IA	No	Alive	<i>p53</i> , <i>PTEN</i> , <i>Rb</i>
				LMS	NA, 30 M/10HPF, necrosis	N/A	N/A	Block positive	Diffuse mutant	40%	Loss: Xq, 3q, 4q, 4q, 5q, 6p, 6q, 8p, 10p, 10q, 13q, 14q, 16q, 17p, 19q, 19q Gain: 2q, 9p, 9q, 11q, 13q, 17p, 15, 19q 19q				
9	34	3.5	LMBN	BN, 1M/10hpF	80%	80%	Block positive	Diffuse mutant	5-10%	Loss: 2q, 4p, 6p, 7p, 13q, 14q, 17p Gain: 11, 21	Loss: 2q, 6p, 13q, 14q Gains: 16p	IA	No	Alive	<i>p53</i> , <i>Rb</i>
				LMS	NA, 36 M/10HPF, necrosis	30%	30%	Block positive	Diffuse, mutant	50%	Loss: Xp, 2q, 5q, 6p, 7q, 10q, 11p, 13q, 14q, 16p, 17q, 19p, 19q Gain: 1q, 3p, 9q, 16p				
10	48	3.7	LMBN	BN, 2M/10HP F	80%	80%	Block positive	Wild type	10%	Loss: 1p, 2p, 6p, 6q, 13q	Loss: 1p, 2p, 6p, 6q, 13q	IA	No	Alive	<i>Rb</i>
				LMS	NA, 24 M/10HPF, necrosis	20%	20%	Block positive	Wild type	60%	Loss: 1p, 2p, 6p, 6q, 7q, 9p, 9q, 11q, 13q, 16q, 17p, 20q Gain: 1q				

Table 1 Summary of 10 LMS in association with LMBN

Figure 1 – 896

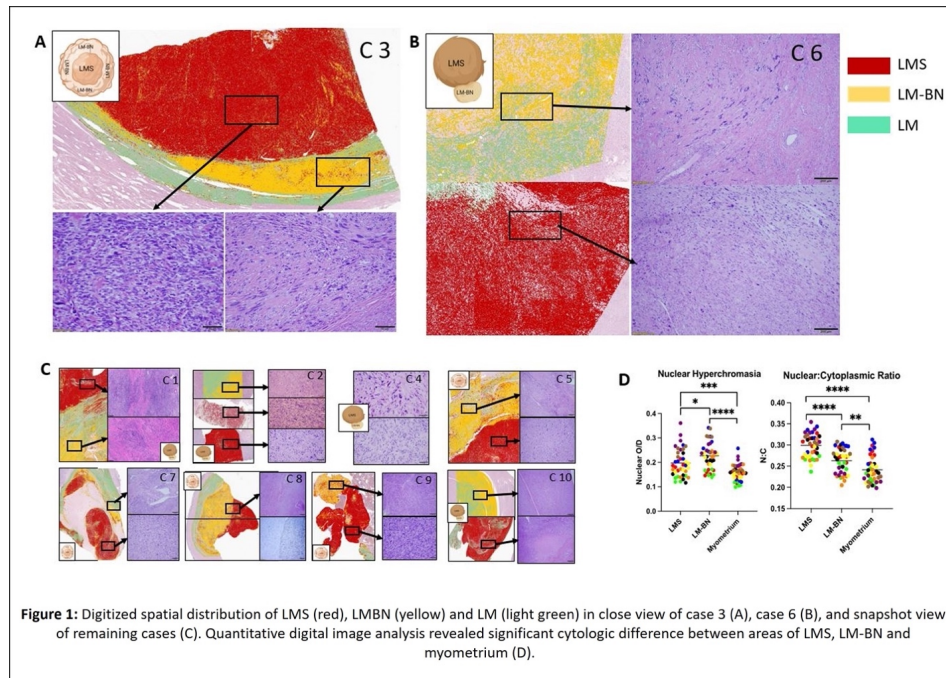
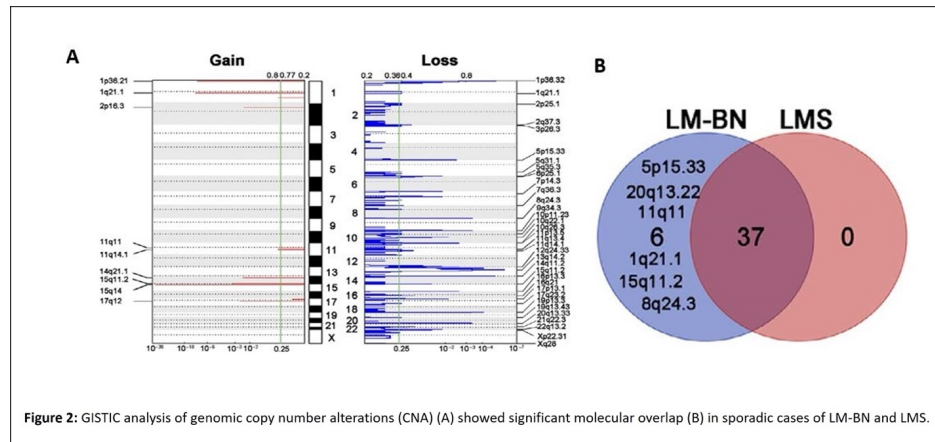


Figure 2 – 896



**Conclusions:** We present 10 cases of LMS arising in conjunction with LMBN. Molecular analysis demonstrated the same clonal origin of both tumor types in a majority of cases, with shared IHC and genomic alterations, suggesting that some LMS arise from existing LMBN. AI imaging analysis further reveals spatial relationships between LMS and LMBN, and digital image analysis demonstrates significant differences in nuclear size, shape, and chromatin patterns between LMBN and LMS, confirming their different tumor nature.

### 897 Methylation Profiling for Uterine Leiomyosarcoma: Potential Application for Tumor Classification

Christopher Felicelli<sup>1</sup>, Brian Vadasz<sup>1</sup>, Drew Duckett<sup>2</sup>, Timothy Blanke<sup>3</sup>, Lucas Santana dos Santos<sup>1</sup>, Farres Obeidin<sup>1</sup>, Borislav Alexiev<sup>4</sup>, Lawrence Jennings<sup>1</sup>, Jian-Jun Wei<sup>3</sup>

<sup>1</sup>Northwestern University Feinberg School of Medicine, Chicago, IL, <sup>2</sup>Northwestern Medicine, Chicago, IL, <sup>3</sup>Northwestern University, Chicago, IL, <sup>4</sup>Northwestern Memorial Hospital, Chicago, IL

**Disclosures:** Christopher Felicelli: None; Brian Vadasz: None; Drew Duckett: None; Timothy Blanke: None; Lucas Santana dos Santos: None; Farres Obeidin: None; Borislav Alexiev: None; Lawrence Jennings: None; Jian-Jun Wei: None

**Background:** Uterine leiomyosarcomas (LMS) are a rare malignancy with an overall poor survival. While conventional LMS can be graded low or high grade on a two-tier system, the adoption of such systems and application for clinical outcome produces mixed results. Global methylation profile (GMP) is a useful tool for tumor classification with most success in brain tumors. GMP in sarcomas is currently being explored, and its value in classification and diagnosis remains to be determined. We aimed to explore the clinical utility of GMP in LMS and explore its associations with histology and clinical outcomes.

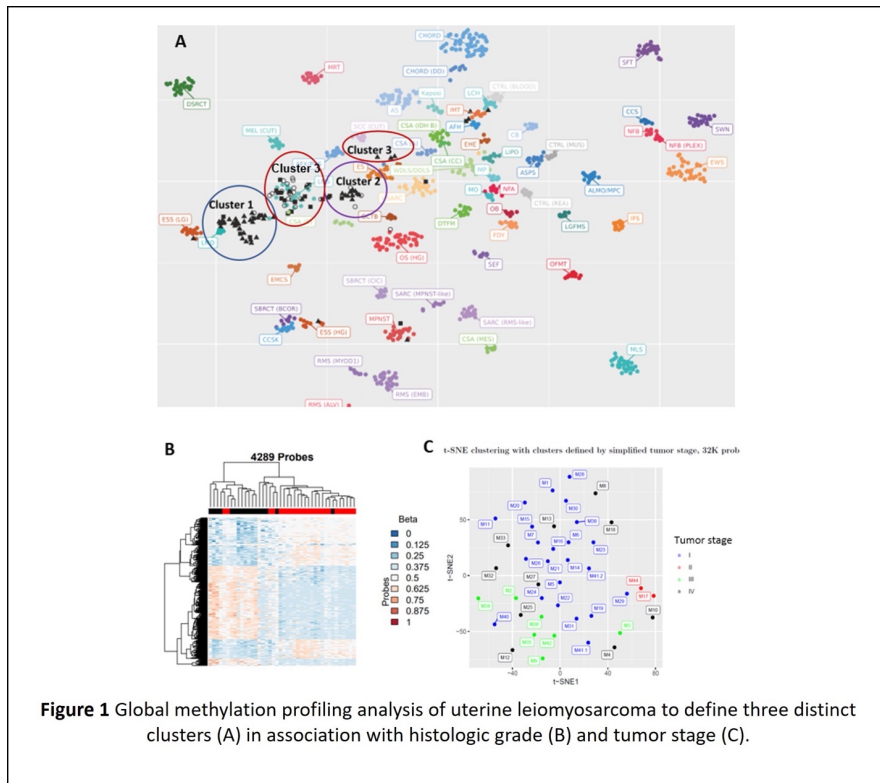
**Design:** 47 LMS cases were selected. Select slides for each case were reviewed to define histologic findings, and the patient's clinical information was reviewed. Tumor DNA was prepared, and GMP was conducted using 850k probes with the Illumina Infinium Methylation EPIC array. Unsupervised clustering analysis was performed with t-Distributed Stochastic Neighbor Embedding (tSNE) using  $\beta$  values from the 10k and 32k most variable probes. Differential methylation analysis was performed, and the probes identified were visualized using a heatmap. Statistical analysis was calculated utilizing the one-way ANOVA or Chi-square.

**Results:** Among 47 LMS, 41 cases yielded high quality GMP data for analysis. The clinical and histologic features of the cases are summarized in Table 1. t-SNE plot analysis showed LMS presented 3-4 aggregates of subclusters defined as clusters 1-3, separated from most reference sarcomas (Figure 1A). Further analysis revealed that LMS subclusters had significant differences in association with histologic and clinical characters (Table 1). Cluster 1 showed higher numbers of low grade cases ( $p=0.0332$ ) and stage I tumor ( $p=0.0218$ ), higher p53 (26%) and MED12 (17%) mutations, lower Ki-67 index (25%), and lower recurrence rates (47%). Both 10K and 32K CpG probes demonstrated the distinct clusters of low and high-grade LMS (Figure 1B). Additionally, different methylation patterns were seen in different tumor stages (Figure 1C).

Group (n)	All (41)	Cluster1 (23)	Cluster 2 (9)	Cluster 3 (9)	p-value
Age(yrs.)	53.83± 1.86	52.26± 2.41	55.67± 3.11	56.00± 5.09	0.6439
Race (%)					
White	25 (61.0)	11 (47.8)	6 (66.7)	8 (88.9)	
Black	11 (26.8)	9 (39.1)	2 (22.2)	0 (0)	0.2257
Others	5 (2.2)	3 (13)	1 (11.1)	1 (11.1)	
Tumor Size (cm)	10.89± 1.17	11.03± 1.55	10.44 ± 1.73	10.99± 3.33	0.9806
Histologic Type					
Spindle	36 (87.8)	18 (78.3)	9 (100)	9 (100)	
Epithelioid	5 (12.2)	5 (21.7)	0 (0)	0 (0)	0.1077
Necrosis					
Positive	26 (63.4)	13 (56.5)	7 (77.8)	6 (66.7)	
Negative	15 (36.6)	10 (43.5)	2 (22.2)	3 (33.3)	0.5188
Infiltrating Borders					
Positive	29 (70.7)	16 (69.6)	7 (77.8)	8 (88.9)	
Negative	12 (29.3)	7 (30.4)	2 (22.2)	1 (11.1)	0.5119
Mitoses (10hpf)	39.32± 5.22	35.30± 6.75	50.33±13.89	38.56± 9.27	0.5297
Bizarre Features					
Present	14 (34.1)	11 (47.8)	2 (22.2)	1 (11.1)	
Absent	27 (65.9)	12 (52.2)	7 (77.8)	8 (88.9)	0.0999
Histologic Grade					
Low	25 (61.0)	18 (78.3)	3 (33.3)	4 (44.4)	
High	16 (39.0)	5 (21.7)	6 (66.7)	5 (55.6)	0.0332 *
3 Tier Risk					
Intermediate	16 (39.0)	11 (47.8)	1 (11.1)	4 (44.4)	
High	18 (43.9)	7 (30.4)	8 (88.9)	3 (33.3)	0.0474 *
FIGO Stage					
I	23 (56.1)	17 (73.9)	2 (22.2)	4 (44.4)	
II-IV	18 (43.9)	6 (26.1)	7 (77.8)	5 (55.6)	0.0218 *
IHC					
ER	18.05± 4.64	28.35± 6.91	8.75 ± 8.25	0 ± 0	0.0281 *
PR	16.65± 5.08	23.52± 7.79	11.25±10.61	3.89 ± 3.31	0.2752
p16	65.28± 6.61	65.68±8.81	61.38±16.89	67.78± 13.2	0.9531
p53 Pos	11 (26.8)	7 (30.4)	1 (11.1)	3 (33.3)	0.4774
p53 Neg	30 (73.2)	16 (69.6)	8 (88.9)	6 (66.7)	
Ki-67	31.62± 3.93	25.09± 4.55	37.625±9.66	42.22±13.21	0.1726
Recurrence					
Yes	22 (53.7)	11 (47.8)	5 (55.6)	6 (66.7)	
No	19 (46.3)	12 (52.2)	4 (44.4)	3 (33.3)	0.1726
Survival					
Alive	22 (53.7)	12 (52.2)	6 (66.7)	4 (44.4)	
Dead	19 (46.3)	11 (47.8)	3 (33.3)	5 (55.6)	0.625
p53 mutations					
Yes	9 (22.0)	6 (26.1)	1 (11.1)	2 (22.2)	
No	35 (79.5)	17 (73.9)	8 (88.9)	7 (77.8)	0.6547
MED12 mutations					
Yes	4 (9.8)	4 (17.4)	0 (0)	0 (0)	
No	37 (90.2)	19 (82.6)	9 (100)	9 (100)	0.1765

Table 1 Methylation clusters in association with clinical and histologic features

Figure 1 – 897



**Conclusions:** GMP is emerging as a powerful tool for tumor classification, with Mullerian LMS readily classified in distinct clusters. While methylation can clearly distinguish and classify low and high grade LMS and FIGO stage, the power to classify histologic subtype and survival is currently limited. Additionally, the genetic heterogeneity of LMS can lead to methylation mapping differences, most commonly to undifferentiated sarcomas.

## 898 Integrating ProMisE into Daily Practice: Initial Insights from a Hybrid Academic-Community Practice

Elizabeth Ferreira<sup>1</sup>, Alexandra Schefter<sup>1</sup>, Abby Brustad<sup>1</sup>, Molly Klein<sup>1</sup>, Boris Winterhoff<sup>2</sup>, Mahmoud Khalifa<sup>1</sup>, Andrew Nelson<sup>1</sup>

<sup>1</sup>University of Minnesota, Minneapolis, MN, <sup>2</sup>University of Minnesota Medical Center, Minneapolis, MN

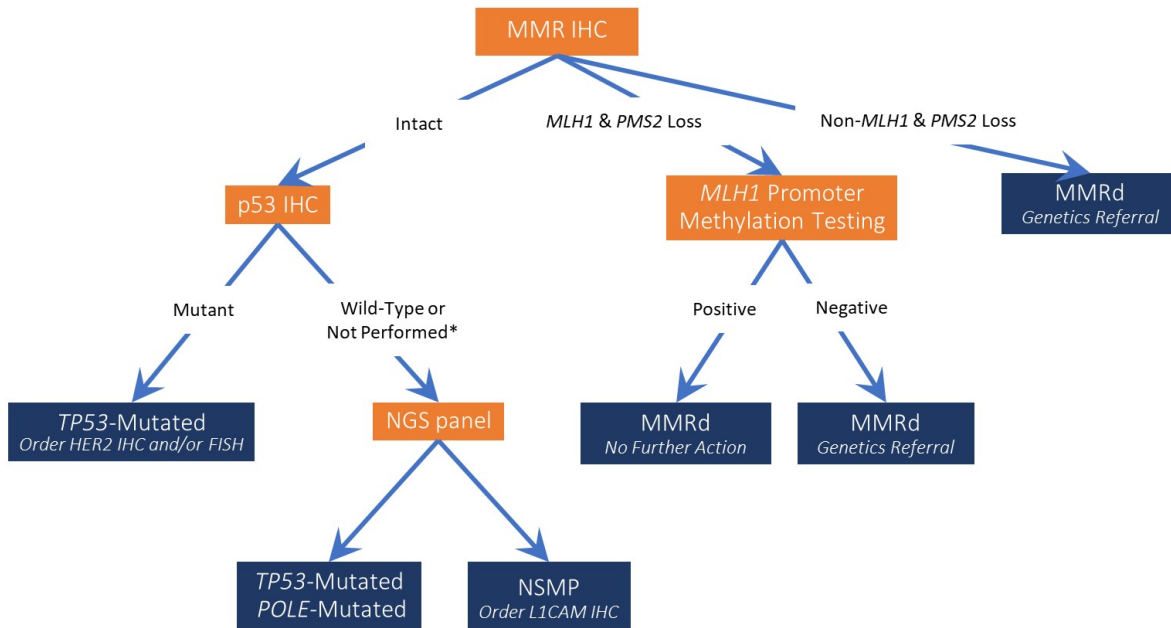
**Disclosures:** Elizabeth Ferreira: None; Alexandra Schefter: None; Abby Brustad: None; Molly Klein: None; Boris Winterhoff: None; Mahmoud Khalifa: None; Andrew Nelson: None

**Background:** The Proactive Molecular Risk Classifier for Endometrial Cancer (ProMisE) was developed as a practical method to improve patient prognostication over conventional histologic classification alone. Our institution, which provides hybrid academic-community care, was one of the first to develop and integrate a local ProMisE protocol (Figure 1) into our daily practice, which went live 10/01/2021. This study aimed to assess its initial performance and identify areas for process improvement.

**Design:** We conducted a retrospective search of all patients who underwent primary resection for an endometrial carcinoma in our institution from 10/01/2021-09/15/2022 and compared the distribution of molecular and traditional staging factors to available literature. Clinical risk stratification was designated using GOG-99 criteria.

**Results:** We identified 259 patients who underwent primary resection for endometrial cancer from 10/01/2021-09/15/2022, of which 136 (52.5%) were clinically classified as low risk (LR). Overall, 30.9% (80/259) of tumors were MMR-deficient, 13.1% (34/259) were TP53-mutated, 2.3% (6/259) were POLE-mutated, 27.8% (72/259) had no specific molecular profile (NSMP) and 25.9% (67/259) failed to receive full ProMisE protocol testing and were therefore classified as endometrioid, NOS (not otherwise specified). Of the 72 NSMP cases, 13 (18.1%) were beta-catenin-mutated and 9 (12.5%) were L1CAM positive, although only 52 (72.2%) NSMP cases received L1CAM testing. Ten and three LR patients were found to have beta-catenin-mutated and L1CAM positive NSMP tumors, respectively. In addition, seven endometrioid tumors were found to harbor TP53 mutations on NGS, two of which were LR.

Figure 1 - 898



**Conclusions:** Our ProMisE protocol identified 15 of 136 (11.0%) clinically low risk tumors following conventional histologic classification that are harboring incipient high risk molecular aberrations in beta-catenin, L1CAM, and TP53. After accounting for protocol non-adherence, the molecular distribution of our cohort is compatible with TCGA (The Cancer Genome Altas) statistics. Initiating L1CAM studies earlier in the protocol and improving protocol compliance, especially in the community setting, would increase detection of LR tumors with incipient high risk molecular aberrations. Overall, initial review of our protocol is encouraging; however, longterm survival data and results of ongoing trials assessing the role of molecular-based adjuvant therapy are required to confirm the protocol's clinical utility.

## 899 Primary Ovarian Carcinoid Tumors are Indolent Neoplasms with Variable Immunohistochemistry, Proliferation and Ki67 Index: A Comprehensive Clinicopathologic and Immunohistochemical Analysis

Madeline Fitzpatrick<sup>1</sup>, Bojana Djordjevic<sup>1</sup>, Carlos Parra-Herran<sup>2</sup>, Jelena Mirkovic<sup>1</sup>

<sup>1</sup>Sunnybrook Health Sciences Centre, University of Toronto, Toronto, ON, <sup>2</sup>Brigham and Women's Hospital, Harvard Medical School, Boston, MA

**Disclosures:** Madeline Fitzpatrick: None; Bojana Djordjevic: None; Carlos Parra-Herran: None; Jelena Mirkovic: None

**Background:** Grading of neuroendocrine tumors (NET) varies by anatomic site. However, markers of cell proliferation are common to most, as they are associated with patient outcome. Currently, there is no formal grading system for primary ovarian carcinoid tumors (pOCT). There is also limited data on prognosis and expected immunophenotype of these tumors. This study aims to provide a detailed clinicopathologic and immunohistochemical analysis of pOCTs and document the role of mitotic count and Ki67 proliferation index in prognosis and classification.

**Design:** Twenty-one pOCTs were retrieved from the archives of 2 institutions. Clinical, pathologic and follow-up data were obtained. Histologic sections were reviewed and pOCT subtype and mitotic index (per 2mm<sup>2</sup>) were recorded. A panel of immunohistochemistry (IHC) including Ki67, Chromogranin, Synaptophysin, TTF1, PAX8, CDX2, p53, MSH6, PMS2, ATRX, PTEN and PDL1 was performed. Ki67 index was determined by counting 500 cells in areas of increased labelling.

**Results:** Clinicopathologic and IHC findings are summarized in Table 1. The mean mitotic rate was 3.1 (range 0-23). The mitotic rate was <2 in 57.1% of cases (12/21), between 2 and 20 in 38.1% of cases (8/21) and >20 in 4.8% of cases (1/21). The mean Ki67 index was 9.6% (range 1-59%). The Ki67 index was <3% in 47.6% of cases (10/21), between 3 and 20% in 38.1% of cases (8/21) and >20% in 14.3% of cases (3/21). Most pOCTs presented as Stage IA disease (13/21; 61.9%), of which 5 had Ki67 indexes >3%. The overall range of Ki67 for Stage IA cases was 1-20%. There were 5 cases of Stage IC disease (23.8%), which

# ABSTRACTS | GYNECOLOGIC AND OBSTETRIC PATHOLOGY

showed a wide variation in Ki67 index (range 1-36%); of which none had disease recurrence. Extraovarian spread was noted in 3 cases (14.3%), all of which had Ki67 indexes >3% (range 4-59%). Local recurrence occurred in 1 case (4.8%), which had pelvic sidewall involvement at the time of diagnosis and a Ki67 index of 59%. Follow-up, ranging from 1.5 to 149 months (mean 67.5), showed no disease-related deaths.

TABLE 1. Clinicopathologic and Immunohistochemical Characteristics of Primary Ovarian Carcinoid Tumors (N=21)	
Age (in years), mean (range)	52 (22-75)
Clinical presentation	
Incidental	3 (14.3%)
Pelvic mass or related symptoms	18 (85.7%)
Stage at presentation	
IA	13 (61.9%)
IB	1 (4.8%)
IC	5 (23.8%)
IIB	1 (4.8%)
IIIB	1 (4.8%)
Extraovarian spread at time of diagnosis	
No	18 (85.7%)
Yes	3 (14.3%)
Disease recurrence	
No	20 (95.2%)
Yes	1 (4.8%); local recurrence to peritoneum
Alive at 5 years post diagnosis	
No	0 (0%)
Yes	11/11 (100%)
Alive at 10 years post diagnosis	
No	2/6 (33.3%); no disease related deaths
Yes	4/6 (66.7%)
Ovary size (gross measurement)	
<= 5 cm	6 (28.6%)
5.1-10 cm	8 (38.1%)
10.1-15 cm	1 (4.8%)
15.1-20 cm	4 (19.0%)
>20 cm	2 (9.5%)
Laterality	
Bilateral	2 (9.5%)
Left	12 (57.1%)
Right	6 (28.6%)
Not otherwise specified	1 (4.8%)
Ovarian surface involvement	
No	20 (95.2%)
Yes	1 (4.8%)
Background ovarian pathology	
Mature teratoma only	7 (33.3%)
Mucinous tumor	6 (28.6%)
Struma ovarii	2 (9.5%)
No diagnostic background pathology	4 (19.0%)
Other	2 (9.5%)
Carcinoid subtype	
Strumal	9 (42.3%)
Insular	6 (28.6%)
Trabecular	3 (14.3%)
Mucinous	1 (4.8%)
N/A	2 (9.5%)
Mitotic index (per 2 mm <sup>2</sup> ), mean (range)	
< 2	3.1 (0-23)
2 - 20	12 (57.1%)
> 20	8 (38.1%)
1 (4.8%)	
Ki67 index (in %), mean (range)	
<3	9.6 (1-59%)
3-20	10 (47.6%)
>20	8 (38.1%)
3 (14.3%)	
Chromogranin	
Positive	18 (85.7%)
Negative	3 (14.3%)
Synaptophysin	
Positive	21 (100%)
Negative	0 (0%)
TTF1	
Positive	6 (28.6%)
Negative	15 (71.4%)
PAX8	
Positive	3 (14.3%)
Negative	18 (85.7%)
CDX2*	
Positive	18 (90.0%)
Negative	2 (10.0%)
p53*	
Wild type	17 (89.5%)
Abnormal	2 (10.5%)
MSH6/PMS2*	
Intact	20 (100%)
Lost	0 (0%)
ATRX*	
Intact	20 (100%)
Lost	0 (0%)
PTEN*	
Intact	20 (100%)
Lost	0 (0%)
PDL1	
Positive	1 (10%), n=10 (additional stains pending)
Negative	9 (90%), n=10 (additional stains pending)

\* Cases non-contributory: tumor exhausted from block; lack of internal control

**Conclusions:** Most pOCTs behave in an indolent fashion; however, extraovarian spread and recurrence can be observed. Although local recurrence occurred in one case, disease-related death or distant metastases did not occur. Frequent staining with TTF1 and CDX2 was also observed, limiting their utility in the distinction between pOCT and metastatic NET. Our findings support the notion that most pOCTs behave as low grade neoplasms with excellent prognosis and show that Ki67 is highly variable and can be increased even in pOCTs with indolent follow-up.

## 900 Reflex Molecular Subtyping in 135 Cases of Endometrial Carcinoma: A Detailed Analysis with Impact on Patient Management

Madeline Fitzpatrick<sup>1</sup>, Kenneth Craddock<sup>1</sup>, Weei-Yuarn Huang<sup>2</sup>, Rashmi Goswami<sup>2</sup>, Anna Plotkin<sup>3</sup>, Sharon Nofech-Mozes<sup>1</sup>, Jelena Mirkovic<sup>1</sup>, Bojana Djordjevic<sup>1</sup>

<sup>1</sup>Sunnybrook Health Sciences Centre, University of Toronto, Toronto, ON, <sup>2</sup>Sunnybrook Health Sciences Centre, Toronto, ON, <sup>3</sup>University of Toronto, Toronto, ON

**Disclosures:** Madeline Fitzpatrick: None; Kenneth Craddock: None; Weei-Yuarn Huang: None; Rashmi Goswami: None; Anna Plotkin: None; Sharon Nofech-Mozes: None; Jelena Mirkovic: None; Bojana Djordjevic: None

**Background:** With the evolution of genomic tumor characterization of endometrial carcinoma (EC), universal molecular subtyping has been proposed to better define its prognostic subgroups. This is, however, a resource-intensive practice for a publicly funded healthcare system. This study's aim was to summarize our Canadian laboratory experience with reflex molecular subtyping of EC and to examine its impact on clinical management.

**Design:** *POLE* sequencing was performed on 135 biopsy or resection EC specimens from September 2021-present. All cases were initially tested by immunohistochemistry (IHC) for MMR and p53, as per our universal reflex EC testing policy. *POLE* testing criteria included: High grade (HG) EC; Low grade (LG) ECs (endometrioid gr 1 or 2) with an abnormal MMR and/or p53 result; Clinician request; Pathologist discretion.

**Results:** Pathogenic *POLE* mutations and EC molecular classification were designated as per current literature. Table 1 shows ECs categorized by histologic vs. molecular subtype. In 5 cases, p53 IHC was equivocal and presence of *TP53* pathogenic mutations was used to classify them. The pathogenic *POLE*mut rate in our cohort was 5.2% (7/135). 6 cases with *POLE* variant of uncertain significance were considered *POLE*wt when assigning the molecular subtype. Among the 118 HGEC, 58 (49.1%) were not further subclassified histologically (HGEC unclassified). 35(60.0%) of these were diagnosed on biopsy. *POLE* testing on LGECs was requested by radiation oncology in at least 6 cases with Stage ≥ 1b and/or extensive lymphovascular invasion (LVI); in 4 of these cases with *POLE*wt adjuvant radiation therapy (ART) was administered. In one endometrioid gr 1, stage 2, case with extensive LVI and *POLE*mut, ART was given but chemotherapy was withheld. Only 4 HGEC cases (1 serous, 3 HGEC unclassified) with pathogenic *POLE*mut were identified. In one case (HGEC unclassified, stage 1a), ART was withheld. 2 cases are recent and clinical management is pending.

Table 1. Molecular Classification of 135 Cases of Endometrial Carcinoma

	Total n=135	<i>POLE</i> mut 7 (5.2%)	MMRd 33 (24.4%)	NSMP 22 (16.3%)	p53abn 73 (54.1%)
Endometrioid gr 1	7 (5.2%)	2	3	2	0
Endometrioid gr 2	10 (7.4%)	1	5	4	0
Endometrioid gr 3	19 (14.1%)	0	11	6	2
Clear cell carcinoma	5 (3.7%)	0	0	3	2
Serous carcinoma	31 (23.0%)	1	0	0	30
HGEC unclassified	58 (43.0%)	3	10	6	39
Undiff/dediff carcinoma	4 (3.0%)	0	4	0	0
Mesonephric carcinoma	1 (0.7%)	0	0	1	0

**Conclusions:** Judicious resource utilization in a publicly funded healthcare system is key to its sustainability. For LGEC cases without p53 or MMR IHC abnormalities, it may be appropriate to withhold *POLE* testing from reflex testing, as radiation oncology will identify cases under ART consideration. For management of HGECs, more information is still needed. Interestingly, with molecular subtyping, a strong pathologist trend emerged to not further histologically subclassify HGEC, particularly on endometrial biopsies.

## 901 Single Cell Mapping of Whole Human Fallopian Tubes with Labeling of Deep Learning Secretory and Ciliated Epithelial Cells

André Forjaz<sup>1</sup>, Ashleigh Crawford<sup>1</sup>, Pei-Hsun Wu<sup>1</sup>, Ashley Kiemen<sup>1</sup>, Ie-Ming Shih<sup>2</sup>, Denis Wirtz<sup>1</sup>

<sup>1</sup>Johns Hopkins University, Baltimore, MD, <sup>2</sup>Johns Hopkins Hospital, Baltimore, MD

**Disclosures:** André Forjaz: None; Ashleigh Crawford: None; Pei-Hsun Wu: None; Ashley Kiemen: None; Ie-Ming Shih: None; Denis Wirtz: None

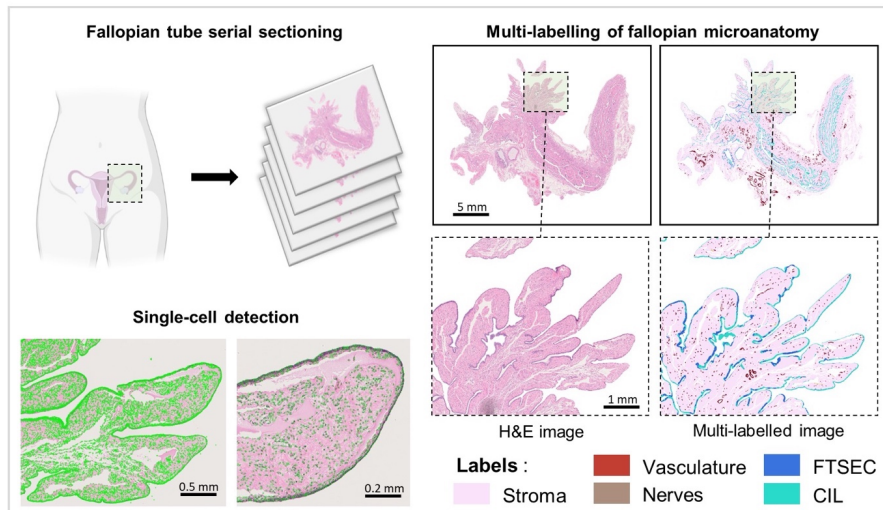
**Background:** High-grade serous ovarian carcinoma (HGSO) is the deadliest form of ovarian cancer. While cancers such as cervical cancer have clearly mapped developmental stages, the development of HGSO is not well understood. Recent theories suggest HGSO may develop from serous tubal intraepithelial carcinomas (STICs), precursor lesions in the fallopian tubes which migrate to and colonize the ovaries. STICs are believed to stem from fallopian tube secretory epithelial cells (FTSECs), one of two major classes of epithelial cell in the fallopian tubes. The spatial distribution, prevalence and change with age of FTSECs is yet not fully understood. While 3D microscopy has made great strides in mapping of soft organs such as the brain and lungs, tissue clearing techniques are not easily applied to study of STIC development in the large ( $\text{cm}^3$ ), fibrous structure of human fallopian tubes. Recent advances in 2D and 3D pathology approaches (including tissue clearing, immunofluorescence, and deep learning (DL) applications to standard histological slides) allow micrometer resolution visualization of tissue anatomy. Here, we present novel reconstruction of whole human fallopian tubes at single cell resolution and present the utility of this technique for spatial mapping of FTSECs.

**Design:** Two whole surgically removed human fallopian tube samples were cut to a length of ~3cm, formalin-fixed, paraffin embedded, and serially sectioned to a depth of ~3mm, collecting the fimbriated end. Sections were stained with hematoxylin and eosin and scanned at high resolution. A 3D rendering software named CODA was used to register the images, and DL was used to label at 1-micron resolution the fallopian epithelium (subdividing the epithelium into FTSECs and ciliated epithelial cells), nerves, vasculature and stroma.

**Results:** Using the CODA workflow, the serially sectioned tissue images transformed into a labelled, registered tissue volume (Fig 1). In visualizations of the fallopian tube, the distinct regions of the fimbriae and the ampulla are clear (Fig 2). Quantification reveals striking cellularity, with expectedly higher cell density in the epithelial layer than in the surrounding stroma (Table 1).

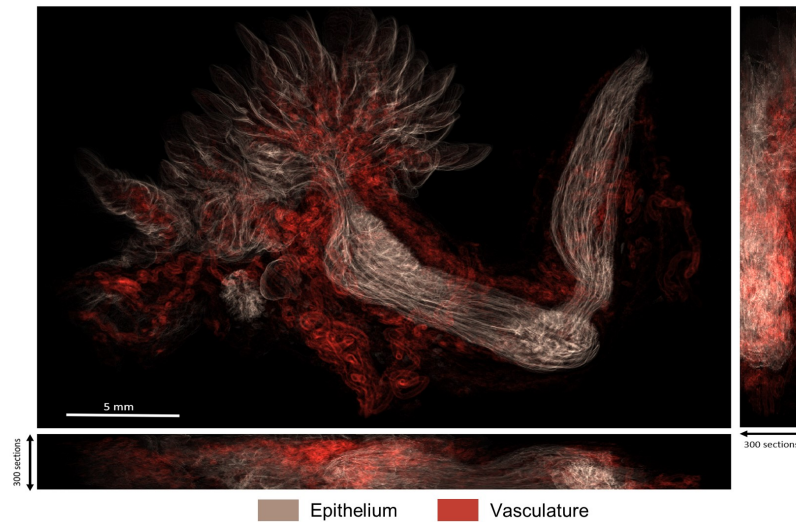
Component	Cell density (cells x 105 / mm <sup>3</sup> )
Fallopian tube secretory epithelial cells	19.23
Ciliated epithelial cells	22.10
Stroma	9.23
Vasculature	0.07
Nerves	10.24

Figure 1 - 901



**Figure 1.** Whole fallopian tubes were serially sectioned, stained with H&E, and scanned. Nuclear coordinates were generated using the hematoxylin channel of the images, and anatomical structures were labelled using a semantic segmentation algorithm. Here, we successfully distinguish between fallopian tube secretory epithelial cells (FTSECs) and ciliated epithelial cells (CILs), two epithelial cell types with morphological differences.

Figure 2 - 901

**Figure 2.** Epithelial and vasculature mapping of a whole human fallopian tube reveals spatial heterogeneity.

**Conclusions:** This project represents the first mapping of a whole human fallopian tube. We show feasibility of distinguishing in H&E FTSECs from ciliated epithelial cells, important for study of STIC development. By further mapping FTSECs, 3D projects have the potential to increase our knowledge of ovarian cancer development.

## 902 Molar and Nonmolar Hydropic Conceptions with Divergent p57 Expression: A Clinicopathologic Study of 29 Cases

Masaharu Fukunaga, Shin-Yurigaoka General Hospital, Kawasaki, Kanagawa, Japan

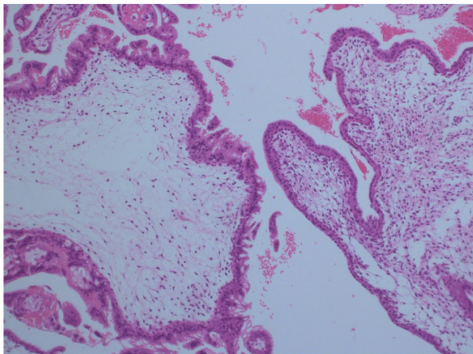
**Disclosures:** Masaharu Fukunaga: None

**Background:** A divergent p57 staining pattern is characterized by two populations of villi; each may have different morphologies and different staining patterns of p57. Conception with divergent p57 expression is very rare and always poses clinical and diagnostic challenges.

**Design:** Twenty-nine cases of molar and nonmolar hydropic conceptions with divergent p57 expression, all of which in the first trimester, were retrieved from 1025 cases with hydropic placental tissue, and clinicopathologically analyzed with immunostaining of p57 (Kip2) (p57), which is a product of paternally imprinted, maternally expressed genes.

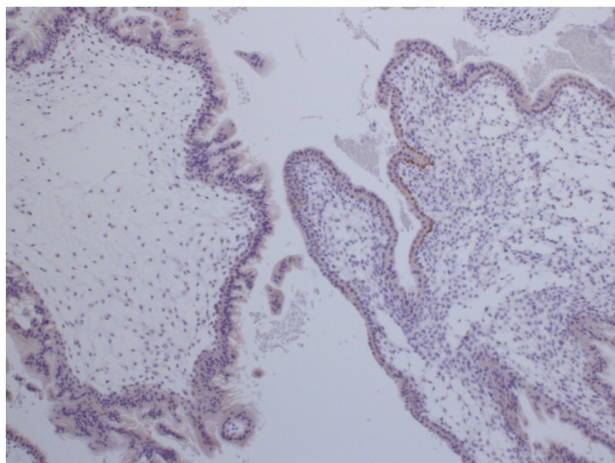
**Results:** p57 divergent expression was detected in 13 cases twin gestation comprised of a p57-negative complete mole (CM) and p57-positive nonmolar villi and in six cases of early stage placental mesenchymal dysplasia (PMD) and in five cases of CM with PMD, in which p57 positive cytotrophoblasts and p57 negative villous stromal cells were observed (Fig 1 and 2). PMD villi were histologically characterized by the presence of normal villi and enlarged villi, stromal cell hyperplasia and the absence of trophoblastic hyperplasia. Remaining five cases were nonmolar hydropic conceptions with normal villi and enlarged villi with focal trophoblastic hyperplasia showing focal p57 positive cytotrophoblasts and p57 positive/negative villous stromal cells. Two of 13 patients with twin with CM and one of 5 patients of CM with PMD had persistent trophoblastic disease and two patients of twin with CM developed lung metastasis.

Figure 1 - 902



Complete mole (left) and placental mesenchymal dysplasia (PMD) showing stromal cell hyperplasia (right)

Figure 2 - 902



p57-negative complete mole (left) and placental metaplasia dysplasia with p57-positive cytrophoblasts and p57-negative stromal cells (right)

**Conclusions:** This study showed hydropic placenta with divergent p57 expression is a diagnostic challenge for pathologists, and that most were associated with CM or PMD. The presence of two distinct populations of villi is a clue to clarifying divergent p57 expression. A thorough morphological examination with careful interpretation of p57 immunostaining is required to reach a definite diagnosis, and the presence or absence of an under-diagnosed early stage CM or PMD should be considered. These conceptions may be good candidates for genotyping analysis. Patients with twin with CM and those with CM and PMD components carry a risk for persistent trophoblastic disease, and require appropriate treatment and follow-up as with conventional CM patients.

### 903 Genomic Landscape of Endometrial Cancers in African American Women

Elmer Gabutan<sup>1</sup>, Andria Chen<sup>2</sup>, Absia Jabbar<sup>3</sup>, Rachelle Mendoza<sup>4</sup>, Ning Chen<sup>3</sup>, Daniel Levitan<sup>3</sup>

<sup>1</sup>SUNY Downstate Health Sciences University, Brooklyn, NY, <sup>2</sup>Great Neck, NY, <sup>3</sup>SUNY Downstate Medical Center, Brooklyn, NY, <sup>4</sup>University of Chicago, Chicago, IL

**Disclosures:** Elmer Gabutan: None; Andria Chen: None; Absia Jabbar: None; Rachelle Mendoza: None; Ning Chen: None; Daniel Levitan: None

**Background:** Recent studies have shown that African American (AA) women have a higher prevalence of uterine carcinomas with worse prognoses. Current literature proves that uterine carcinoma in AA patients differ from non-AA on socioeconomic factors and histologic grade and features, but genomic studies have been limited. In this study, we analyze the molecular profile of our cohort of uterine cancer patients and compare the results with published data.

**Design:** A preliminary cohort of 135 patients with uterine cancer were analyzed, 96 of which were AA and 49 were non-AA. 66 patients have type 1 cancers including 54 low grade endometrioid carcinomas (LGEC) and 12 high grade endometrioid carcinomas (HGEC). The remaining 69 patients have type 2 cancers including 40 serous carcinomas (SC), 7 clear cell carcinomas (CCC) and 22 carcinosarcomas (MMMT). Next-generation sequencing comprehensive tumor profiling by Caris Molecular Intelligence (MI) was performed on representative sections of the paraffin-embedded formalin-fixed tumors. The data were analyzed to assess the tumor genetic differences between the AA and non-AA patients.

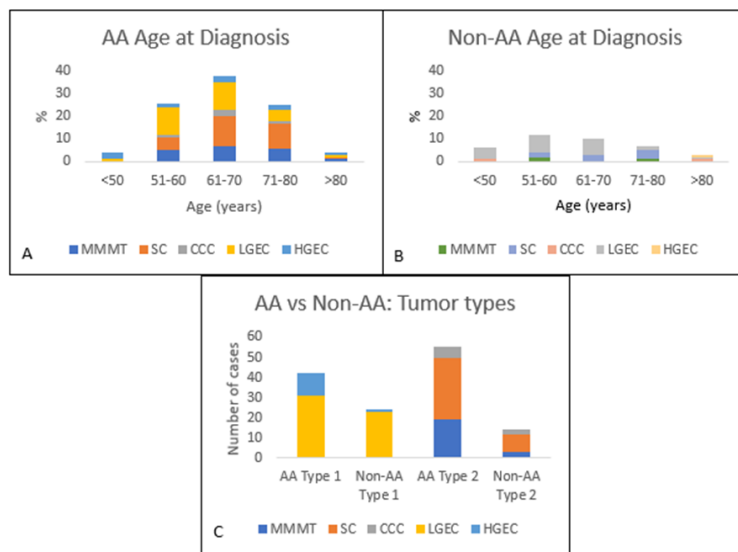
**Results:** The AA patients, who made up the bulk of the cohort, were found to have more type 2 than type 1 cancers (54 vs 42/135). Non-AA patients were more often diagnosed with type 1 than type 2 cancers (24 vs 14/135)(figure 1). 47.4% of non-AA patients were diagnosed at  $\leq$ 60 years of age, compared to 30.9% of AA patients. 93 total pathogenic mutations were identified across all cancer types. Type 1 cancers harbored more mutations in PTEN (58/66), PIK3CA (40/66), ARID1A (36/66), CTNNB1 (29/66), PIK3R1 (19/66), and RNF43 (15/66)(table 1). AA patients exhibited a greater frequency of ARID1A (35/66) and PIK3CA (27/66) mutations. Almost all of the type 2 carcinomas had TP53 mutations (63/69). Another mutation associated with higher grade tumors was FBXW7 (18/135), which was more frequent in type 2 cancers (11/69) than in type 1 cancers (7/66).

Table 1. Most common genetic mutations in Endometrial Carcinoma, 135 patients.

List of Common Pathogenic Variants/Mutations	Endometrioid adenocarcinoma (66)		Serous carcinoma (40)	Clear cell carcinoma (7)	Carcinosarcoma (22)
	LGEC	HGEC	SC	CCC	CS
PPP2R1A	1.85%	8.33%	22.50%	14.29%	9.09%
PTEN	92.59%	66.67%	2.50%	14.29%	0.00%
PIK3CA	59.26%	66.67%	15.00%	28.57%	13.64%
ARID1A	51.85%	66.67%	2.50%	14.29%	0.00%
TP53	0.00%	41.67%	97.50%	85.71%	95.45%
CTNNB1	46.30%	33.33%	2.50%	0.00%	4.55%
RNF43	20.37%	33.33%	0.00%	0.00%	0.00%
KMT2D	14.81%	33.33%	0.00%	14.29%	0.00%
JAK1	12.96%	33.33%	0.00%	0.00%	0.00%
PIK3R1	29.63%	25.00%	10.00%	0.00%	0.00%
CIC	9.26%	25.00%	0.00%	0.00%	0.00%
ATRX	3.70%	25.00%	0.00%	0.00%	0.00%
HNF1A	7.41%	16.67%	0.00%	0.00%	4.55%
BRCA2	7.41%	16.67%	0.00%	0.00%	0.00%
SETD2	3.70%	16.67%	0.00%	14.29%	0.00%
NSD1	1.85%	16.67%	0.00%	0.00%	0.00%
FBXW7	11.11%	8.33%	15.00%	14.29%	18.18%
MSH6	9.26%	8.33%	0.00%	14.29%	0.00%

Figure 1 - 903

Figure 1. A. Bar graph showing age at diagnosis of endometrial cancer in African American (AA) patients. B. Bar graph showing age at diagnosis of endometrial cancer in Non-African American (Non-AA) patients. C. Bar graph showing types of endometrial cancer in African American (AA) and Non-African American (Non-AA) patients. MMMT - Carcinosarcoma, SC - serous carcinoma, CCC - clear cell carcinoma, LGEC - low grade endometrial carcinoma, HGEC – high grade endometrial carcinoma.



**Conclusions:** Endometrial cancers in AA patients are diagnosed at an older age as compared to non-AA. Their molecular profile show more frequent targetable mutations like ARID1A, FBXW7, PIK3CA and PIK3R1 across all cancer types, suggesting a role for a multi-faceted approach to immunotherapy. Alterations in CTNNB1 in LGEC of AA patients are a poor prognostic indicator. Further studies investigating genomic disparities between endometrial cancers of AA and non-AA patients are needed to improve and tailor clinical management strategies for AA patients.

## 904 Aberrant p53 Staining is Seen Only in a Minority of FIGO Grade 2 Endometrioid Carcinomas but Correlates with Adverse Clinical Outcomes

Georgi Galev<sup>1</sup>, Amy Joehlin-Price<sup>1</sup>, Brian Rubin<sup>1</sup>, Kepeng Che<sup>1</sup>, Michelle Kuznicki<sup>1</sup>, Johanna Kelley<sup>1</sup>, Karuna Garg<sup>1</sup>

<sup>1</sup>Cleveland Clinic, Cleveland, OH

**Disclosures:** Georgi Galev: None; Amy Joehlin-Price: None; Brian Rubin: None; Kepeng Che: None; Michelle Kuznicki: None; Johanna Kelley: None; Karuna Garg: None

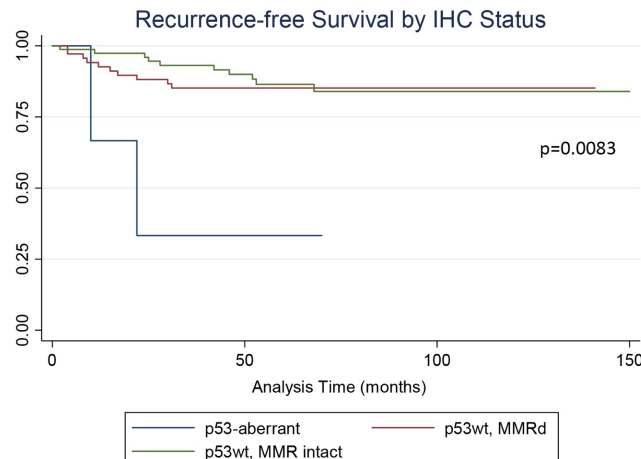
**Background:** Endometrial endometrioid carcinoma (EEC), FIGO grade 2 (G2), is a heterogeneous group of tumors with variable clinical outcome. Binary classification of EEC into low versus high-grade has been proposed which would eliminate the EEC G2 category. The distribution and impact of molecular classification on G2 tumors has not been systematically evaluated.

**Design:** After obtaining IRB approval, FIGO grade 2 EEC were identified. A panel of IHC stains (MLH1, PMS2, MSH2, MSH6, p53, PTEN, PAX8, ER, PR) was performed on TMAs or whole sections. POLE mutation analysis was performed by Sanger sequencing.

**Results:** 157 EECG2 were identified for inclusion. Patients had a median age of 64 (range 22-91) and most presented with low stage disease (129 FIGO stage I, 6 II, 19 stage III and 3 stage IV). MMR IHC data was available in 155 patients: 69 were MMR deficient 61 with MLH1/PMS2 and 8 with MSH2/MSH6 loss. Three of 155 tumors showed aberrant p53 (ab-p53). Three EC showed MMR loss and clonal ab-p53. PTEN was frequently lost (117/157 lost, 26/157 retained, 14/157 equivocal) and PAX8 was negative in 1 EC (100/141 diffuse, 36/141 patchy, 4/141 focal, 1/141 negative). ER was at least focal in all cases (87/128 diffuse, 33/128 patchy, 9/128 focal), and 4 were PR negative (86/153 diffuse, 49/153 patchy, 14/153 focal, 4/153 negative). POLE sequencing data was available for 25 EC (POLE mutation analysis underway in the remaining cases) and no pathogenic mutations were identified (2 EC with V360V and P476S each and 1 with P356S). Median follow up time was 63 months (range 1-150) and most patients (122/157, 78%) showed no evidence of disease (NED), 5 (3%) were alive with disease (AWD) and 11 (7%) dead of disease (DOD). The rest were dead of unknown or unrelated causes. Although the numbers are limited, 2 out of 3 (67%) MMR proficient, p53-aberrant patients recurred and were AWD (n=1) or DOD (n=1) compared to 20/148 (14%) p53 wild-type patients with recurrences. Logrank testing of recurrence free survival by p53 and MMR status are shown in Figure 1. Overall survival was not significant due to low numbers of deaths from disease.

IHC/POLE result	# of cases (%)
MMR deficient	69/155 (44.5%)
p53 aberrant	3/155 (1.9%)
MMR loss + ab p53	3/155 (1.9%)
Pathogenic POLE mutation	0/25 (0%)
PTEN loss	117/157 (74.5%)
ER focal (<10%) or negative	9/128 (7%)
PR focal (<10%) or negative	18/153 (12%)

Figure 1 - 904



**Conclusions:** In our cohort of FIGO grade 2 EEC, almost half of the cases showed MMR deficiency and a small subset (2%) were p53-aberrant. Although the numbers are small, the presence of aberrant p53 staining showed significant correlation with recurrence free survival. This data could support the use of universal p53 IHC in EEC G2 to identify potentially aggressive tumors.

## 905 Comparison of the Conventional and Alternative Method of Measuring Depth of Invasion of Vulvar Squamous Cell Carcinoma Using Whole Slide Digital Pathology Images

Cynthia Gasper<sup>1</sup>, Peyman Samghabadi<sup>1</sup>, Nikka Khorsandi<sup>1</sup>

<sup>1</sup>University of California, San Francisco, San Francisco, CA

**Disclosures:** Cynthia Gasper: None; Peyman Samghabadi: None; Nikka Khorsandi: None

**Background:** When vulvar squamous cell carcinoma is present at a depth > 1 mm, the tumor is upstaged from FIGO stage IA to IB. In the conventional method, depth of invasion is defined as the distance in millimeters from the epithelial-stromal junction of the adjacent, most superficial dermal papilla to the deepest point of invasion. An alternative method measures depth from the most adjacent dysplastic rete ridge to the deepest point of invasion. Using the alternative method of invasion may downstage a significant proportion of patients.

**Design:** Patients with a diagnosis of invasive squamous cell carcinoma of the vulva were identified. 40 patients with H&E slides were reviewed and measurements using the conventional and alternative method were documented using a measuring ocular. Of those, 19 patients also had whole slide images and measurements were documented using both a measuring ocular and the measurement ruler tool on the digital image.

**Results:** Depth of invasion changed in 36/40 patients (90%) with the alternative method. The median depth of invasion with the conventional method was 3.1 mm (range 0.7-18 mm) and with the alternative method it was 1.8 mm (range 0.5-6.5 mm). 8/40 patients (20%) were given a new FIGO stage due to change in depth of invasion. For the 19 patients with both H&E and digital images, the conventional method with ocular showed a median depth of invasion of 3.5 mm (range 0.4-9 mm) and using the digital ruler tool was 3.3 mm (range 0.5-8mm). For the alternative method the median depth of invasion using an ocular was 2.1 mm (range 0.3-6.5 mm) and using the digital ruler tool was 2 mm (range 0.3-6.6 mm). 4/19 patients in this group were given a new FIGO stage as a result of a change in depth of invasion. When using the conventional method or alternative method and comparing the measuring ocular to the digital ruler tool, 0 patients (0%) were given a new FIGO stage. Follow-up data was available for 19 patients with a median of 12 months (range 1-168 months). For patients who were down staged using the alternative method from FIGO IB to IA 0/6 (0%) recurred while for those who remained FIGO IB using the alternative method 3/19 (16%) recurred.

Figure 1 - 905



**Conclusions:** Measuring depth of invasion using an alternative method versus the conventional method will downstage a portion of patients with vulvar squamous cell carcinoma. Using a measuring ocular versus a digital ruler yields similar results. If the alternative method is adopted less patients might be treated with groin surgery.

**906 Poorly Differentiated Clusters and Tumor Budding in Uterine Endometrioid Carcinoma are Morphological Findings Associated with Decreased Recurrence Free Survival**Mariam Ghafoor<sup>1</sup>, Daniel Christensen<sup>1</sup>, Allison Goldberg<sup>1</sup>, Joanna Chan<sup>1</sup><sup>1</sup>Thomas Jefferson University Hospital, Philadelphia, PA**Disclosures:** Mariam Ghafoor: None; Daniel Christensen: None; Allison Goldberg: None; Joanna Chan: None

**Background:** Tumor budding (TB), and poorly differentiated clusters (PDCs) are associated with a poor prognostic outcome in many carcinomas. However, the association has rarely been investigated in uterine endometrioid carcinoma (UEC). Here, we evaluate TB and PDCs in UEC and correlate these findings with morphological features known to be associated with a poor clinical outcome and with recurrence free survival (RFS).

**Design:** We performed a 5-year retrospective search of our institution's EMR for cases of hysterectomy for UEC. We collected clinical data including disease recurrence and death as well as data associated with patient outcomes including lymphovascular invasion (LVI), lymph node status (LNS), depth of invasion (DI), FIGO grade, and surgical stage. Cases were evaluated for TB and PDCs by two pathologists. TB was defined as the presence of isolated single clusters of up to 4 cells at the invasive front and was graded as present or absent. PDCs were defined as solid nests of  $\geq 5$  cells at invasive front region. Ten 20x fields were examined. Of those 10 fields, the one with the most PDCs was graded as follows: grade 1=0 to 4 PDCs; grade 2=  $\geq 5$  PDCs. (Figure 1). Categorical data were evaluated using chi-squared tests; LogRank test was performed on the Kaplan Meier curves to evaluate RFS. P value was set at 0.05.

**Results:** 113 cases were evaluated. Presence of TB was associated with LVI (68% vs 41%, p=0.01), positive LNS (36% vs 5%, p<0.001), DI >50% (65% vs 24%, p<0.001), higher FIGO grade (p<0.001) and worse stage (p<0.001). Grade 2 PDCs was associated with LVI (87% vs 23%, p<0.001), positive LNS (42% vs 9%, p<0.001), DI >50% (69% vs 29%, p<0.001), higher FIGO grade (p<0.001) and worse stage (p<0.001) (Table 1). Kaplan Meier curves show decreased RFS for patients with TB present (p=0.03) and grade 2 PDCs (p=0.01) (Figure 2).

Table 1: Association between TB and PDCs at invasive front of carcinoma and morphologic findings known to be associated with poor prognosis

		TB present	TB absent	p-value	PDC grade 2	PDC grade 1	p-value
Lymphovascular invasion present		68%	41%	0.01	87%	23%	<0.001
Positive lymph node status		36%	5%	<0.001	42%	9%	<0.001
Depth of invasion >50%		65%	24%	<0.001	69%	29%	<0.001
FIGO Grade	1	20%	63%	<0.001	7%	59%	<0.001
	2	50%	29%		60%	31%	
	3	30%	7%		33%	10%	
Pathologic Stage	I	45%	84%	<0.001	40%	79%	<0.001
	II	6%	7%		13%	6%	
	III	48%	7%		47%	14%	
	IV	0%	1%		0%	1%	

Figure 1 - 906

Figure 1. PDCs (red arrows) and TBs (blue arrows) present at the invasive front.

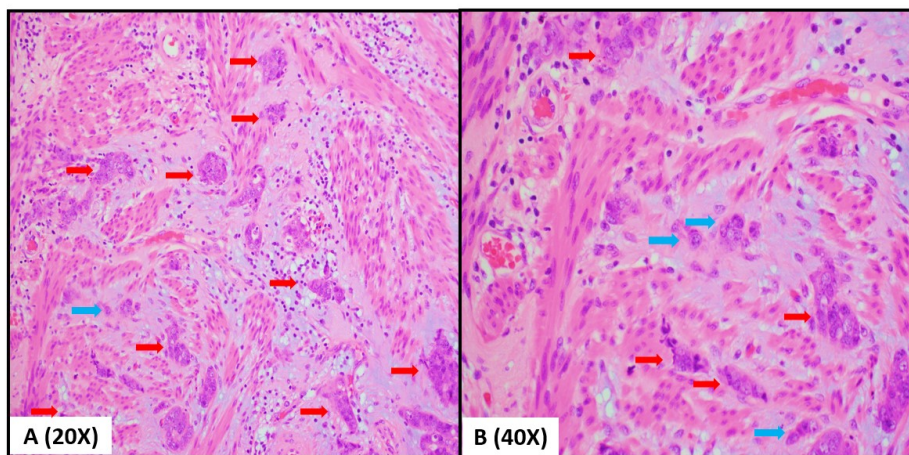


Figure 2 - 906

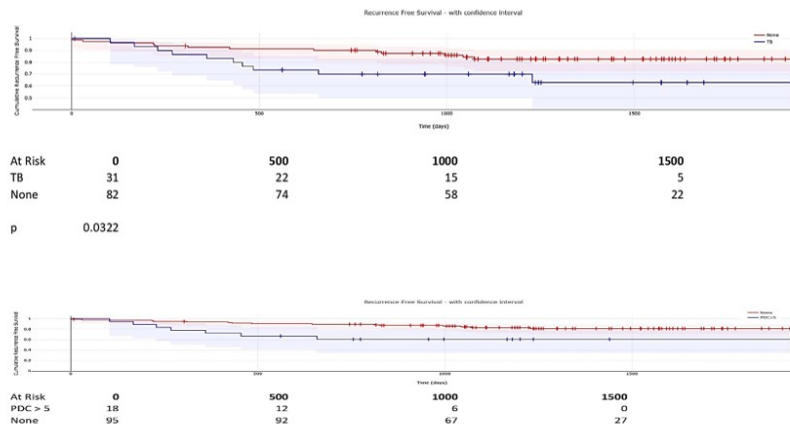


Figure 2: Kaplan Meier curves showing decreased recurrence free survival for patients with TB present ( $p=0.03$ ) and grade 2 PDCs.

**Conclusions:** We show a statistically significant association between TB presence and >5 PDCs and decreased RFS in UEC. We also show an association between TB presence and >5 PDCs and known poor prognostic factors such as LVI, positive LNS, increased DI, higher FIGO grade, and worse stage at presentation. We conclude that TB and PDCs are strong independent prognostic indicators in UEC and provide additional value to the currently used morphological assessment of UEC.

## 907 Evaluation of Intratumoral HER2 Heterogeneity in Endometrial Serous Carcinoma and Carcinosarcoma

Manisha Goel<sup>1</sup>, Jennifer Bennett<sup>2</sup>

<sup>1</sup>University of Chicago Medicine, Chicago, IL, <sup>2</sup>University of Chicago, Chicago, IL

**Disclosures:** Manisha Goel: None; Jennifer Bennett: None

**Background:** HER2 overexpression and/or amplification has been reported in 25-30% of endometrial serous carcinomas (ESC) and 15% of endometrial carcinosarcomas (ECS). Although intratumoral HER2 heterogeneity is well-recognized, it is unclear whether multiple tumor sections should be evaluated by immunohistochemistry (IHC) to avoid missing a HER2-overexpressed subclone.

# ABSTRACTS | GYNECOLOGIC AND OBSTETRIC PATHOLOGY

**Design:** Institutional archives were searched for all ESC and ECS diagnosed on hysterectomy within a 1-year period. HER2 IHC was performed on all tumor blocks and scored from 0 to 3+ based on the Fader et al recommendations. HER2 FISH results were documented if available.

**Results:** The study cohort included 15 tumors (10 ESC, 5 ECS). Patients ranged from 55 to 79 (median 66) years and tumors from 0.3 to 8.5 (median 4.2) cm. Recurrences occurred in 6 patients (median 8.4 months) and at last follow-up (median 23 months), 11 were alive and well, 2 were dead of disease, and 2 were alive with disease. Heterogeneous HER2 expression was identified in 9 (60%) tumors with a two-degree difference observed in 2. Among all tumors evaluated, no recurrent morphological features (architecture, degree of atypia, cytoplasmic features) were predictive of HER2 expression. However, occasionally within an individual tumor, specific appearances did show distinct HER2 scores. In one tumor, the solid component was consistently 1+, the cored areas 2+, and glands/papillae 3+. Another tumor showed decreased HER2 expression (0-1+) in the deeply invasive component, while the superficial areas were 3+. All ECS showed a lower HER2 score in the sarcoma compared to the carcinoma. For cases where HER2 was performed on a single slide during the original diagnostic work-up (n=12), heterogeneity was noted in 3 (25%) tumors (all ESC). All 3 received a score of 1+ and FISH was not performed. However, staining of additional slides yielded scores of 2+ and 3+. HER2 FISH is pending in these 3 tumors.

Figure 1 - 907

## HER2 Immunohistochemical Expression in Endometrial Serous Carcinoma and Carcinosarcoma

Case	Size (cm)	# Slides	Score (n=# of slides)		# Slides with Focal 3+*	Clinical Score	Clinical FISH	Possible Management Change
			Carcinoma	Sarcoma				
1	1.5	4	2+ (n=2) 1+ (n=2)		0	1+	NP	Yes
2	2.1	2	2+ (n=2)		2	2+	Amp	No
3	7.0	9	2+ (n=9)		5	NP	NP	N/A
4	5.5	17	3+ (n=16) 2+ (n=1)		1	NP	NP	N/A
5	5.4	5	2+ (n=3) 1+ (n=2)		0	1+	NP	Yes
6	3.2	2	1+ (n=2)		0	1+	NP	No
7	3.8	6	3+ (n=1) 2+ (n=3) 1+ (n=2)		1	1+	NP	Yes
8	6.0	13	3+ (n=2) 2+ (n=11)		9	3+	NP	No
9	4.2	4	2+ (n=4)		0	2+	Amp	No
10	0.3	6	2+ (n=6)		0	2+	Not Amp	No
11	2.7	5	2+ (n=4) 1+ (n=1)	1+ (n=2) 0 (n=2)	0	2+	Not Amp	No
12	8.5	7	3+ (n=4) 2+ (n=2) 1+ (n=1)	2+ (n=2) 1+ (n=2) 0 (n=1)	0	NP	NP	N/A
13	4.2	11	2+ (n=11)	1+ (n=1)	1	2+	Not Amp	No
14	7.0	7	1+ (n=7)	0 (n=1)	0	1+	NP	No
15	5.0	4	3+ (n=3) 2+ (n=1)	2+ (n=1) 0 (n=1)	1	3+	NP	No

\*Strong complete, basal, or basolateral staining in < 30% of cells

NP=not performed, Amp=amplified, N/A=not applicable

**Conclusions:** Intratumoral HER2 heterogeneity is frequent in ESC and ECS, which in a subset of patients may result in therapeutic implications if only 1 slide is evaluated. While it is not feasible to stain every tumor section for HER2, the results of this study suggest additional evaluation of 1-2 slides in the setting of a score of 0-1+ or not amplified 2+, has the potential to alter management. Furthermore, as clinical trials evaluating novel agents in patients with HER2 1+ and not amplified 2+ tumors are currently accruing, precise assessment of the HER2 score is crucial.

**908 TCGA Molecular Subgroup Shows Greater Prognostic Significance Than Histologic Diagnosis in High-Grade Endometrial Carcinomas with Spindled, Undifferentiated and Sarcomatous Components**

Phoebe Hammer<sup>1</sup>, Aihui Wang<sup>1</sup>, Sabrina Zdravkovic<sup>1</sup>, Lucas Heilbroner<sup>1</sup>, Emily Ryan<sup>2</sup>, Anne Mills<sup>3</sup>, Taylor Jenkins<sup>4</sup>, Brooke Howitt<sup>2</sup>

<sup>1</sup>Stanford Medicine/Stanford University, Stanford, CA, <sup>2</sup>Stanford University, Stanford, CA, <sup>3</sup>University of Virginia, Charlottesville, VA, <sup>4</sup>University of Virginia Health System, Charlottesville, VA

**Disclosures:** Phoebe Hammer: None; Aihui Wang: None; Sabrina Zdravkovic: None; Lucas Heilbroner: None; Emily Ryan: None; Anne Mills: None; Taylor Jenkins: None; Brooke Howitt: None

**Background:** Since The Cancer Genome Atlas (TCGA) established four molecular subclasses for endometrial carcinoma (EC), there has been increasing interest in determining the molecular subtype in the context of the histologic subtype. ECs with undifferentiated, spindled and/or sarcomatous components represent a diagnostically challenging subset of uterine tumors with overlapping clinical and histologic features. The prognostic differences among this group of aggressive ECs are not well established. We examined the morphologic, immunohistochemical, and molecular features of these tumors.

**Design:** High-grade ECs were identified in our institution's pathology database. Patient age, BMI, histologic diagnosis, tumor size, stage, and lymph node status were recorded, and immunohistochemistry for mismatch repair proteins, p53,  $\beta$ -catenin, estrogen receptor, and progesterone receptor was performed. We analyzed morphologic features, including nuclear grade, tumor heterogeneity, and presence of heterologous differentiation. TCGA subgroups were assigned when possible. Overall survival (OS) and progression-free survival (PFS) were analyzed using Kaplan-Meier curves and log rank test.

**Results:** The key clinicopathologic features are summarized in Table 1. The tumors occurred in adult women (median 67 years) and included carcinosarcomas (UCS) (n=75), de-differentiated (n=22), and undifferentiated (n=18) carcinomas, endometrioid carcinomas with spindled growth (n=16) and other high-grade ECs (n=4). All showed similar clinical characteristics. OS and PFS plots by histotype showed no difference in OS ( $p=0.664$ ) or PFS ( $p=0.708$ ) (Figure 1, a,b). However, prognostic differences in both OS ( $p=0.011$ ) and PFS ( $p=0.0005$ ) were seen when divided by TCGA subgroup (Figure 1, c,d). There was no difference in OS or PFS between UCS with heterologous or homologous differentiation. We also enriched for p53 wild type UCS (n=17), which showed a difference in PFS ( $p=0.043$ ) compared to p53 aberrant UCS (Figure 2); there was no difference in OS ( $p=0.378$ ).

Table 1. Clinical and key histologic features of the 135 high-grade endometrial carcinomas in our cohort.

Diagnosis & Molecular Subtype	FIGO Stage	Age (Yrs), Median	BMI, Median	Tumor Size (cm) Median	Lymph node involvement	Heterologous Differentiation
<b>Carcinosarcoma (n=75)</b> POLE = 0 MSI = 13 P53 abnormal = 36 NSMP = 11 Pending = 15	Stage I-II (n=38)	67 (38 – 85)	30.8	5.3 (1.0–17.0)	0% (0/35)	39% (15/38)
	Stage III-IV (n=37)	68 (44 – 91)	30.9	5.5 (1.2–17.0)	79% (19/24)	38% (14/37)
<b>Dedifferentiated (n=22)</b> POLE = 1 MSI = 13 P53 abnormal = 0 NSMP = 5 Pending = 3	Stage I-II (n=12)	66.5 (46-76)	31.1	5.5 (3.3–10.0)	0% (0/12)	0% (0/12)
	Stage III-IV (n=10)	70 (29-79)	30.0	5.8 (1.1-15.0)	43% (3/7)	0% (0/10)
<b>Undifferentiated (n=18)</b> POLE = 0 MSI = 5 P53 abnormal = 4 NSMP = 1 Pending = 8	Stage I-II (n=7)	61 (42-76)	30.7	5.5 (4.0-17.0)	0% (0/6)	14% (1/7)
	Stage III-IV (n=11)	60 (52-76)	31.0	8.5 (5.0-10.5)	100% (4/4)	0% (0/11)
<b>High-grade endometrioid (n=16)</b> POLE = 0 MSI = 5 P53 abnormal = 2 NSMP = 2 Pending = 7	Stage I-II (n=8)	70 (43-84)	29.4	4.0 (3.5-7.2)	0% (0/7)	0% (0/8)
	Stage III-IV (n=8)	61.5 (35-78)	34.6	9.1 (3.5-14.0)	75% (3/4)	0% (0/8)
<b>Other* (n=4)</b> POLE = 0 MSI = 1 P53 abnormal = 2 NSMP = 1	Stage I-II (n=1)	64	28.3	4.9	0% (0/1)	0% (0/1)
	Stage III-IV (n=3)	65 (52-73)	31.1	8.4	100% (1/1)	0% (0/3)

\*Other includes: high-grade endometrial carcinoma NOS (n=3), and favor mesonephric-like carcinoma (n=1)

Figure 1 - 908

**Figure 1. Overall survival and progression free survival by histologic diagnosis (a,b) and TCGA subgroup (c,d).**

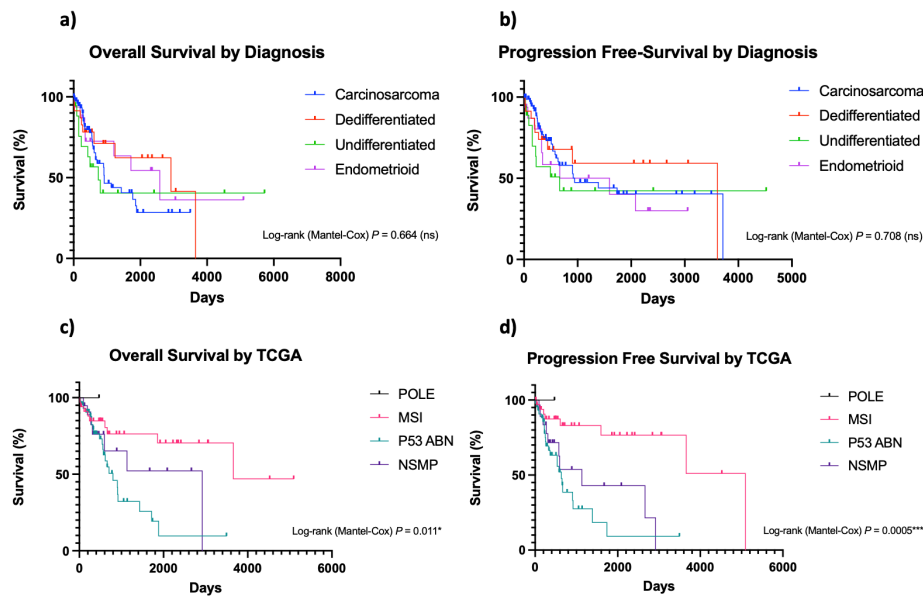
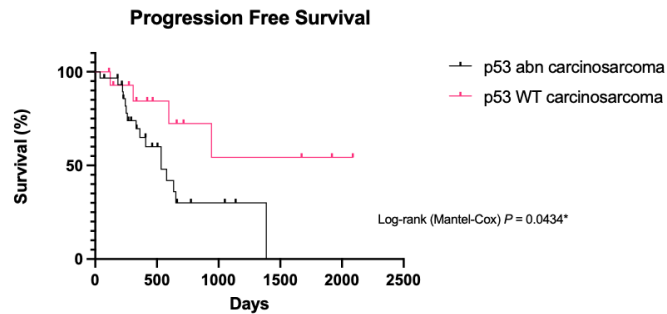


Figure 2 - 908

**Figure 2. Progression free survival of p53 wild-type carcinosarcomas compared to p53 aberrant (null/diffuse pattern) carcinosarcomas by immunohistochemistry**



**Conclusions:** There was no prognostic difference when stratified by histotype among UCS, dedifferentiated/undifferentiated carcinomas, and grade 3 endometrioid carcinomas with spindled growth. However, TCGA molecular subgroups showed prognostic differences similar to that seen in wider studies of EC.

## 909 Concordant Glandular PTEN and Progesterone Receptor Down-Regulation or Loss is a Physiologic Finding in Mid-To-Late Secretory Endometrium: A Pilot Assessment

Elham Hatami<sup>1</sup>, Omonigho Aisagbonhi<sup>1</sup>

<sup>1</sup>University of California, San Diego, La Jolla, CA

**Disclosures:** Elham Hatami: None; Omonigho Aisagbonhi: None

**Background:** Loss of PTEN immunoreactivity is recommended by the WHO as a diagnostic adjunct for atypical endometrial hyperplasia despite a 2019 meta-analysis that showed low diagnostic usefulness of PTEN in differentiating benign from pre-malignant endometrial hyperplasia. The reported low diagnostic usefulness of PTEN may be because PTEN loss/down-regulation physiologically occurs in the mid-to-late secretory phase of the normal menstrual cycle and can confound interpretation of PTEN immunohistochemical stain.

# ABSTRACTS | GYNECOLOGIC AND OBSTETRIC PATHOLOGY

**Design:** Following approval by our Institutional Review Board, formalin-fixed paraffin-embedded samples from endometrial biopsies diagnosed as secretory endometrium or atypical hyperplasia with secretory change or in a secretory background were chosen and re-reviewed and further classification was performed as early secretory endometrium, day 17-18 endometrium, mid-to-late secretory endometrium or atypical hyperplasia with secretory change. Immunohistochemical staining was performed for PTEN and Progesterone Receptor. PTEN immunohistochemistry was interpreted according to the following patterns as recently described by Wang et al: 1. Retained: moderate glandular cytoplasmic expression 2. Reduced: weak glandular cytoplasmic expression 3. Loss: completely absent staining in glands with positive staining in stromal cells as internal control.

**Results:** We evaluated the IHC expression pattern of PTEN and progesterone receptor in secretory endometrium: early (9 cases), day 17-18 (4 cases) mid-to-late (11 cases) and atypical hyperplasia with secretory change (6 cases). PTEN and PR expression patterns were generally concordant in normal endometrial glands, with retained cytoplasmic PTEN and positive nuclear PR in early secretory phase, and reduced to absent PTEN and PR in mid-to-late secretory phase. A discordant glandular PTEN and PR pattern – PTEN reduction/loss but moderate to strong PR – was observed within the atypical foci in all the cases of atypical hyperplasia.

**Conclusions:** In summary, in evaluating secretory endometrium and atypical hyperplasia with secretory change, our study shows that concordant PTEN and PR expression pattern is physiologic and can be reassuring in rendering a diagnosis of benign secretory endometrium, whereas, discordant PTEN and PR is more nuanced; though observed in all our cases of atypical hyperplasia, isolated benign glands also sporadically showed the discordant pattern.

## 910 Digital Spatial Profiling of Adenomyosis: A Proof of Concept Examination of Differentially Expressed Genes in Immune Cells and Epithelial Cells

Tahyna Hernandez<sup>1</sup>, Ie-Ming Shih<sup>1</sup>

<sup>1</sup>Johns Hopkins Hospital, Baltimore, MD

**Disclosures:** Tahyna Hernandez: None; Ie-Ming Shih: None

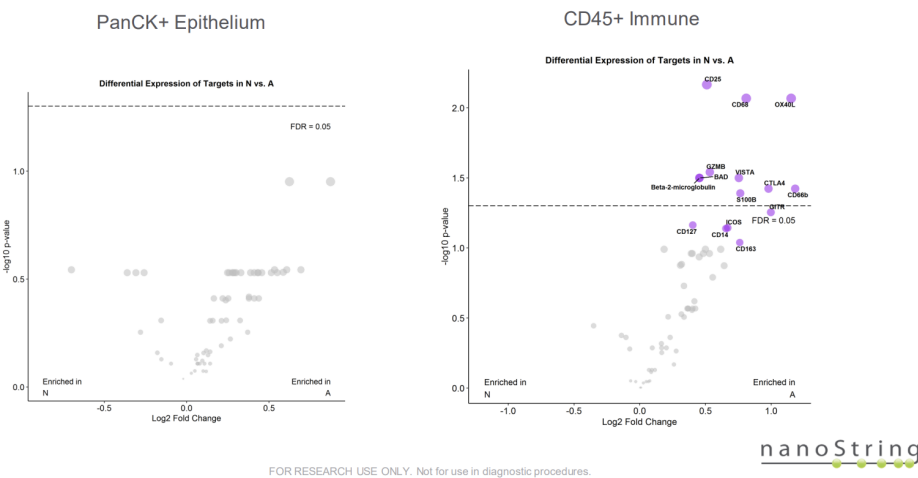
**Background:** Adenomyosis affects a significant number of women and is defined by presence of ectopic endometrial tissue within the myometrium that causes abnormal uterine bleeding, dysmenorrhea and subfertility and often co-occurs with endometriosis. The role of immune cells in adenomyosis is unclear. Digital spatial expression profiling is a powerful method of quantifying gene expression patterns in formalin fixed paraffin embedded tissue across specific areas of interest. The objective of this study was to characterize the expression profile of immune-related genes and genes pertaining to common cancer signaling pathways in adenomyosis lesions compared to matched eutopic endometrium.

**Design:** Formalin-fixed and paraffin-embedded archival tissues were retrieved from 21 patients undergoing hysterectomy for abnormal uterine bleeding. The sample size consisted of 22 adenomyosis lesions and 32 eutopic endometrial samples. Areas of interest were selected for analyzing 77 protein markers. The NanoString GeoMx™ Digital Spatial Profiling platform was used to profile the protein expressions in different spatial locations. We analyzed epithelial cells (Pan-Ck+) and associated immune cells (CD45+) surrounding the endometrial glands, separately. Housekeeping targets or IgG negative controls were used for normalization to account for sample variability and targets not detected above background noise were filtered out from downstream analysis.

**Results:** Ten markers were upregulated in immune cells in adenomyosis compared to eutopic endometrium ( $p<0.05$ ). OX40L, a ligand that is present on many antigen-presenting cells such macrophages, and activated B lymphocytes, was increased 2.3-fold. The Glucocorticoid-Induced TNFR-Related (GITR) protein found on T cells, natural killer cells and some myeloid cells was increased 2-fold. CD66b was increased 2.3-fold. We did not observe any statistically significant difference in expression profiles of epithelial cells between adenomyosis and eutopic endometrium.

Figure 1 - 910

## Differential Expression Example: N vs. A



**Conclusions:** This study demonstrates that immune cells in adenomyosis lesions have distinct immune profiles compared to eutopic endometrium, and suggest that the immune microenvironment may contribute to the pathogenesis of adenomyosis. CD66b, GITR, and OX40L, have not been previously described in adenomyosis and further spacial characterization of genes around regions of higher expression could offer potential novel immune-based interventions.

## 911 Immunohistochemical Biomarker Evaluation of Thyroid Proliferations and Neoplasms Arising in Ovarian Teratomas

Anjelica Hodgson<sup>1</sup>, Ozgur Mete<sup>2</sup>

<sup>1</sup>Toronto General Hospital, University Health Network, Toronto, ON, <sup>2</sup>University Health Network, University of Toronto, Toronto, ON

**Disclosures:** Anjelica Hodgson: None; Ozgur Mete: None

**Background:** Immunohistochemical biomarkers are not infrequently employed in the evaluation of native thyroid lesions when there is a morphological concern for a subtle malignant process. The finding of thyroid tissue in ovarian teratomas is not uncommon and definite classification and determination of malignancy is known to be, at times, notoriously difficult. In this study, we sought to retrospectively assess the performance of immunohistochemical biomarkers in thyroid proliferations and neoplasms arising in ovarian teratomas.

**Design:** Our institutional database was searched from the beginning of 2018 until present day, to identify cases of ovarian teratomas with thyroid proliferations and neoplasms which had been evaluated with an immunohistochemical biomarker work up including CK19, HBME1, galectin-3, CD56, Cyclin D1, p27, BRAF p.V600E-mutation specific VE1 and MIB1. CK19, HBME1, galectin-3 and VE1 were assessed for the presence of expression while CD56, cyclin D1 and p27 were assessed based on the amount of expression (decreased/loss or increased amount), depending on the marker. MIB-1 was assessed in hot spots using a digital nuclear counting algorithm. All of the cases were originally reviewed by a pathologist with subspecialist expertise in pathology of the thyroid. Data was taken from the pathology reports.

**Results:** A total of 16 cases were identified of which 3 were ultimately assigned a benign diagnosis (reactive atypia or follicular nodular disease, cases 1-3) while the remaining 13 were all assigned a malignant diagnosis (differentiated thyroid carcinoma, cases 4-16). The profiles of each case are shown in the Table. Proliferations ultimately classified as benign showed positivity for CK19 in 2/3 cases but otherwise showed no concerning immunohistochemical expression patterns. Cases with a malignant diagnosis, however, showed abnormal expression patterns of multiple markers simultaneously. In particular, CK19 was always positive while CD56 and p27 always showed abnormal reduced or loss of expression (in cases which were assessed).

# ABSTRACTS | GYNECOLOGIC AND OBSTETRIC PATHOLOGY

Case	Diagnosis	CK19	HBME1	Galectin-3	CD56	Cyclin D1	p27	VE1	MIB1 (%)
1	Thyroid tissue with focal mild atypia	Positive (near diffuse)	Negative	Negative	No loss of expression	Normal expression	N/A	N/A	N/A
2	Complex follicular nodular disease	Negative	Negative	N/A	No loss of expression	Normal expression	N/A	N/A	N/A
3	Complex follicular nodular disease	Positive (focal)	Negative	Negative	No loss of expression	Normal expression	N/A	N/A	N/A
4	Follicular thyroid carcinoma	Positive (focal)	Positive (focal)	Negative	Multifocal reduced to absent expression	Diffuse overexpression	Variable loss of expression	N/A	6.0
5	Follicular thyroid carcinoma	Positive (focal)	Negative	Negative	No loss of expression	Variable overexpression	Variable loss of expression	N/A	6.5
6	Follicular thyroid carcinoma and follicular variant of papillary carcinoma (2 foci)	Positive (focal)	Positive (focal)	Negative	Multifocal reduced to absent expression	Normal expression	N/A	N/A	6.1
7	Follicular variant of papillary carcinoma (multiple foci)	Positive (focal)	Negative	Positive (focal)	Multifocal reduced to absent expression	Variable overexpression	N/A	N/A	4.2
8	Follicular variant of papillary carcinoma	Positive (focal)	Positive (patchy)	Positive (focal)	No loss of expression	Variable overexpression	N/A	N/A	6.5
9	Follicular variant of papillary carcinoma	Positive (near diffuse)	Positive (patchy)	N/A	Near total loss of expression	N/A	N/A	Negative	3.6
10	Follicular variant of papillary carcinoma	Positive (patchy)	Positive (near diffuse)	N/A	N/A	Diffuse overexpression	N/A	Negative	N/A
11	Follicular variant of papillary carcinoma	Positive (patchy)	Positive (near diffuse)	Positive (focal)	Multifocal reduced to absent expression	N/A	N/A	Negative	10.6
12	Follicular variant of papillary carcinoma	Positive (near diffuse)	Negative	N/A	Multifocal reduced to absent expression	Diffuse overexpression	N/A	Negative	N/A
13	Papillary carcinoma (multiple foci)	Positive (near diffuse)	Positive (patchy)	N/A	Multifocal reduced to absent expression	N/A	N/A	Negative	N/A
14	Follicular variant of papillary carcinoma	Positive (near diffuse)	Negative	N/A	Multifocal reduced to absent expression	Diffuse overexpression	N/A	N/A	N/A
15	Follicular variant of papillary carcinoma	Positive (focal)	Positive (focal)	Positive (focal)	Multifocal reduced to absent expression	Variable overexpression	Variable loss of expression	N/A	8.4
16	Papillary carcinoma with predominant follicular growth	Positive (near diffuse)	Positive (near diffuse)	N/A	Focal reduced to absent expression	Variable overexpression	Variable loss of expression	Negative	N/A

**Conclusions:** In this study, we have shown that immunohistochemical biomarkers used in workup of native thyroid lesions can be applied to thyroid proliferations and neoplasms in ovarian teratomas, and that their expression patterns differ among lesions classified as benign vs. malignant (differentiated thyroid carcinoma).

**912 EPM2AIP1 Immunohistochemistry is Not a Sensitive Surrogate for MLH1 Promoter Methylation in Endometrial Carcinoma**

Robert Humble<sup>1</sup>, Andrew Bellizzi<sup>1</sup>, Jacob Kaplan<sup>2</sup>

<sup>1</sup>University of Iowa Hospitals & Clinics, Iowa City, IA, <sup>2</sup>University of Iowa Carver College of Medicine, Iowa City, IA

**Disclosures:** Robert Humble: None; Andrew Bellizzi: None; Jacob Kaplan: None

**Background:** Mismatch repair-deficient (MMRd) endometrial carcinoma (EC) is a distinct molecular subtype in the 5<sup>th</sup> Edition of the WHO Classification of Female Genital Tumors. Immunohistochemistry (IHC) for MMR proteins (MLH1, PMS2, MSH2, MSH6) is essential in identifying these tumors in addition to screening for Lynch syndrome. Most sporadic MLH1/PMS2-deficient ECs demonstrate MLH1 promoter methylation (PM), which suggests a tumor is not associated with Lynch syndrome. Recently EPM2AIP1 IHC has been proposed as a surrogate for MLH1 PM in EC (PMID: 34772843).

**Design:** MLH1 (clone ES05), PMS2 (clone EP51), MSH2 (clone FE11), MSH6 (clone EP49) and EPM2AIP1 (clone OTI2G3) IHC was performed on tissue microarrays (TMAs) constructed from consecutive EC resections (n=322) taking place between September 2019 and June 2021. Charts were reviewed for results of clinically performed MMR IHC and send out MLH1 PM testing (ARUP Laboratories, Salt Lake City, UT) by real time PCR with methylation levels  $\geq 10\%$  reported as positive. EPM2AIP1 IHC was assessed as intact, lost, or lost with cytoplasmic staining. EPM2AIP1 IHC was correlated with MMR IHC and MLH1 PM status.

**Results:** MMR results were interpretable in 319 cases (99.1%), 22% of which were MLH1-deficient (n=71). 80.3% of MLH1-deficient ECs received MLH1 PM testing (n=57); just two of the tested cases were negative for methylation (3.5%). Loss of nuclear EPM2AIP1 expression with or without cytoplasmic staining was seen in 58% (n=32) of MLH1-deficient methylated ECs. In ECs with other patterns of MMRd (n=15), 13.3% demonstrated loss of nuclear EPM2AIP1 expression without cytoplasmic staining (n=2). Among MMR intact ECs (n=233), 5.2% of cases demonstrated loss of nuclear EPM2AIP1 expression with or without cytoplasmic staining (n=12); Among MLH1-deficient ECs, EPM2AIP1 loss was 58.2% sensitive (and 100% specific) for MLH1 PM (though only two MLH1-deficient ECs were not methylated in the cohort). Detailed data are presented in the Table below.

Table 1. EPM2AIP1 IHC by MMR and promoter methylation status

MMR pattern	EPM2AIP1 IHC		
	Intact	Lost	Lost+Cyto
MLH1-deficient, MLH1 PM positive (n=55)	23	11	21
MLH1-deficient, MLH1 PM negative (n=2)	2	0	0
MLH1-deficient, MLH1 PM unknown (n=14)	9	0	5
MMR intact (n=233)	221	1	11
Other patterns of MMRd (n=15)	13	2	0
-MSH2/MSH6-deficient (n=5)	4	1	0
-PMS2-deficient (n=1)	1	0	0
-MSH6-deficient (n=4)	3	1	0
-Other MMR abnormal (n=5)	5	0	0
Total (n=319)	268	14	37

**Conclusions:** In our study, EPM2AIP1 IHC as a surrogate for MLH1 PM was less sensitive than in a previous studies (58.2% vs 94.5%). Additionally, loss of EPM2AIP1 was not specific to MLH1-deficient ECs with PM (ie, loss was occasionally seen with other patterns of MMRd and rarely in ECs with intact MMR). This diagnostic adjunct should be carefully optimized and validated before being placed into clinical service as a surrogate for MLH1 PM.

**913 Synaptophysin and Chromogranin Expression in Endometrial Carcinoma Are Associated with Different Histotypes/Molecular Subtypes, And Lack Prognostic Significance**

Jutta Huvila<sup>1</sup>, Amy Jamieson<sup>2</sup>, Jessica McAlpine<sup>3</sup>, C. Blake Gilks<sup>4</sup>

<sup>1</sup>University of Turku, Turku, Finland, <sup>2</sup>The University of British Columbia, Vancouver, BC, <sup>3</sup>The University of British Columbia, BC Cancer Agency, Vancouver, British Columbia, <sup>4</sup>Vancouver General Hospital/University of British Columbia, Vancouver, BC

**Disclosures:** Jutta Huvila: None; Amy Jamieson: None; Jessica McAlpine: None; C. Blake Gilks: None

**Background:** Neuroendocrine markers are used in clinical practice to confirm the diagnosis of neuroendocrine neoplasm when the morphology shows “typical” features, or to demonstrate neuroendocrine differentiation in a poorly differentiated neoplasm.

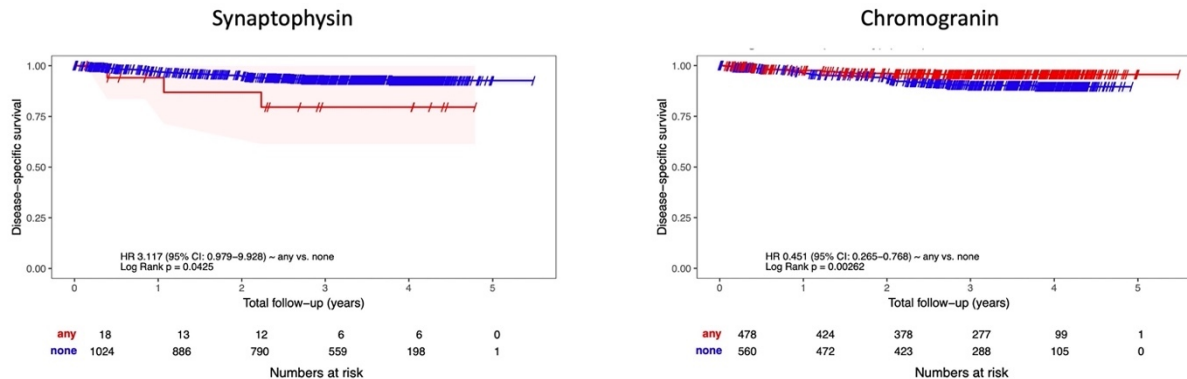
Neuroendocrine tumors in gynecological tract are rare, however, many carcinomas express neuroendocrine markers. Our aim was to assess the frequency of neuroendocrine marker expression in a large series of molecularly subtyped endometrial carcinomas and evaluate their diagnostic and prognostic significance.

**Design:** Tumor tissue from 1221 ECs identified across 29 centers and arranged on TMAs were immunohistochemically stained for chromogranin and synaptophysin. The staining was successful in 1051 and 1055 cases respectively and were scored using h-score and grouped into three groups: ≤10%, >10 – 50% and >50%. Over >10% staining was considered positive.

**Results:** Synaptophysin and chromogranin staining results and association with pathological features is presented in table 1. Only one tumor (a p53abn carcinosarcoma) showed positivity for both markers. Chromogranin positivity was more common, and most frequently seen in low-grade endometrioid tumors of NSMP subtype, whereas synaptophysin positive tumors were most often high-grade p53abn tumors. Chromogranin positivity was associated with better disease specific survival and synaptophysin with adverse survival across the whole cohort (figure 1), but not within the molecular subtypes, indicating that this association is due to correlation with clinicopathological factors.

Synaptophysin n= 1055					Chromogranin n= 1051								
	0 %	1-10%	11-50%	>50%		0 %	1-10%	11-50%	>50%	p-value			
<b>total</b>	1036 (98%)	13	3	3	566	54 %	273	26 %	162	15 %	50	5 %	
<b>Histotype</b>													
Endometrioid	788 (78%)	8	2	0	397	70 %	234	86 %	149	92 %	49	98 %	<0.001
Non-endometrioid	193 (19%)	5	1	3	154	27 %	35	13 %	11	7 %	1	2 %	
<b>Grade</b>													
Low-grade	720(72%)	7	0	0	329	58 %	210	77 %	142	88 %	44	88 %	<0.001
High-grade	286 (28%)	6	3	3	219	39 %	55	20 %	14	9 %	6	12 %	
<b>Molecular subtype</b>													
POLEmut	66 (6%)	1	0	0	39	7 %	14	5 %	11	7 %	3	6 %	<0.001
MMRd	302 (29%)	3	1	0	165	29 %	78	29 %	49	30 %	13	26 %	
NSMP	478 (46%)	6	1	0	214	38 %	145	53 %	92	57 %	33	66 %	
p53abn	190 (18%)	3	1	3	148	26 %	36	13 %	10	6 %	1	2 %	

Figure 1 - 913



**Conclusions:** Neuroendocrine markers synaptophysin and chromogranin show strikingly different and virtually non-overlapping expression profiles in endometrial carcinomas, with variable positivity. Chromogranin positivity was associated with low-grade NSMP tumors whereas synaptophysin was associated with high-grade histology and p53abn subtype. In conclusion, neuroendocrine markers do not add to the prognostic assessment of endometrial carcinomas and positivity for these markers without a neuroendocrine histology should not warrant the diagnosis of neuroendocrine carcinoma.

## 914 Placental Pathology in the Setting of Maternal Intrahepatic Cholestasis of Pregnancy

Anh Huynh<sup>1</sup>, Lauren Ray<sup>1</sup>, Drucilla Roberts<sup>1</sup>, Jaclyn Watkins<sup>2</sup>

<sup>1</sup>Massachusetts General Hospital, Boston, MA, <sup>2</sup>Massachusetts General Hospital, Harvard Medical School, Boston, MA

**Disclosures:** Anh Huynh: None; Lauren Ray: None; Drucilla Roberts: None; Jaclyn Watkins: None

**Background:** Intrahepatic cholestasis of pregnancy (ICP) is characterized by the onset of pruritus and elevated serum bile acid levels in the second or third trimester. In the United States, ICP affects up to 5.6% of all pregnancies. While ICP poses little risk to maternal health, it has been associated with adverse perinatal outcomes, including intrauterine fetal demise (IUFD), respiratory distress syndrome, and preterm delivery, due to the accumulation of bile acids in the placenta and amniotic fluid. However, there is limited knowledge of associated histopathologic features in the placentas of ICP patients, particularly in those with poor fetal outcomes.

**Design:** All placentas (from 2017-2021) from patients with a history of ICP were retrieved from the archives of the Massachusetts General Hospital. All H&E slides were reviewed with a particular focus on features of fetal vascular malperfusion (FVM) and possible bile pigment deposition. Clinical and laboratory data, including maternal serum bile acid levels, were obtained from the electronic medical record.

**Results:** 45 placentas (including 3 twins and one IUFD) were identified and reviewed. In 31 (69%, including the IUFD), pigment most compatible with bilirubin was found within macrophages of at least one intravillous vascular space or loose within the villous stroma. Two of these cases were notable for extensive bilirubin-laden macrophages (iron stain largely negative) within the vascular spaces of the terminal and stem villi (Figure 1). In 11 cases (24%), at least one feature of FVM was identified. Interestingly, developmental concerns were noted in childhood in 31% of cases. Average bile acid levels were calculated for the entire cohort, cases with identifiable pigment, and cases with childhood developmental concerns, averaging 30.5, 27.3, and 28.6 µmol/L, respectively.

Figure 1 - 914

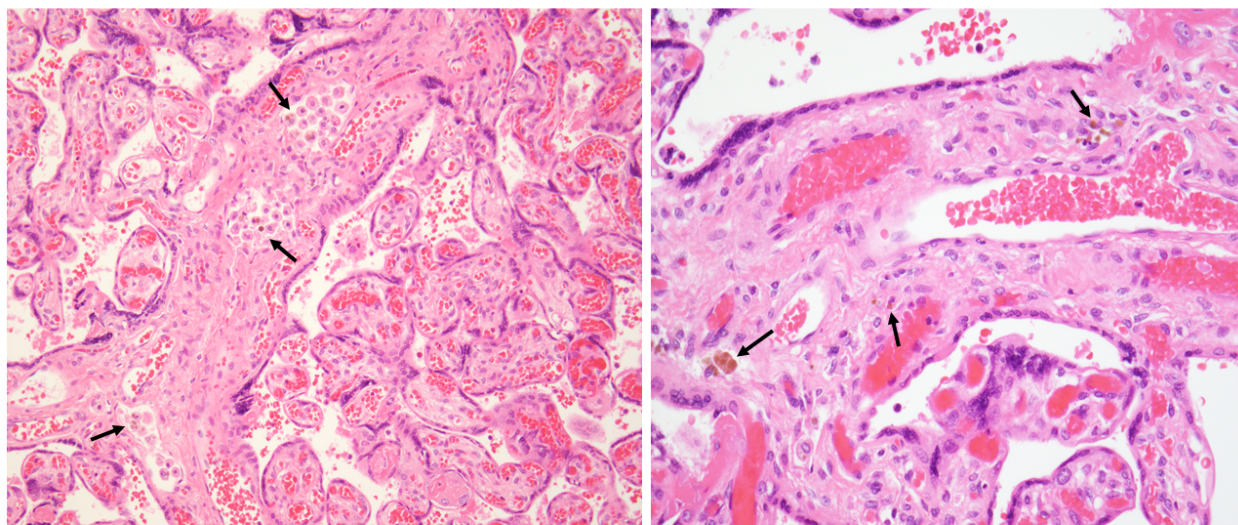


**Figure 1.** Photomicrograph of villi with pigment and pigment-laden macrophages (arrows).

**Conclusions:** Our results suggest distinct histomorphologic features of ICP including loose pigment deposition and/or bilirubin-laden macrophages in the villous vascular space as well as possible associated FVM. As these findings may be subtle and focal, additional stains, such as a Hall stain, may be useful for further characterization and quantification of these pigments. Future steps include cohort expansion, Hall stain in all cases, and correlation between histologic findings, maternal serum bile, and outcomes.

## 915 Utilization of Key Morphologic and Molecular Prognostic Parameters in Endometrial Malignancies: A Survey of Gynecologic Pathologists

Ekta Jain<sup>1</sup>, Shivani Kandukuri<sup>2</sup>, Sambit Mohanty<sup>3</sup>, Anandi Lobo<sup>4</sup>, Samriti Arora<sup>5</sup>, Nishat Afroz<sup>6</sup>, Rania Bakkar<sup>7</sup>, Bonnie Balzer<sup>8</sup>, Rupanita Biswal<sup>9</sup>, Luca Cima<sup>10</sup>, Danielle Costigan<sup>11</sup>, Mallika Dixit<sup>5</sup>, Deepti Dhall<sup>12</sup>, Preeti Diwaker<sup>13</sup>, Poonam Elhence<sup>14</sup>, Cynthia Gasper<sup>15</sup>, Yuna Gong<sup>16</sup>, Harveen Gulati<sup>17</sup>, Michelle Hirsch<sup>18</sup>, Deepika Jain<sup>1</sup>, Niraj Kumari<sup>19</sup>, Suseela Kodandapani<sup>20</sup>, Manoj Kahar<sup>21</sup>, Bhagat Lali<sup>22</sup>, Zaibo Li<sup>23</sup>, Vipra Malik<sup>5</sup>, Sandeep Mathur<sup>24</sup>, Divya Midha<sup>22</sup>, Santosh Menon<sup>25</sup>, Neda Moatamed<sup>26</sup>, Geetashree Mukherjee<sup>22</sup>, Vaishali Nagose<sup>27</sup>, Subhasini Naik<sup>28</sup>, Sandeep Ojha<sup>29</sup>, Immaneni Rao<sup>30</sup>, Shivani Sharma<sup>1</sup>, Sayali Shinde<sup>1</sup>, Hena Singh<sup>1</sup>, Christine Salibay<sup>31</sup>, Meenakshi Swain<sup>32</sup>, Nuzhat Khatoon Sayyed<sup>33</sup>, Rohan Sardana<sup>34</sup>, Ankur Sangoi<sup>35</sup>, Charanjeet Singh<sup>36</sup>, Juhi Varshney<sup>1</sup>, Lateef Zameer<sup>37</sup>, Oluwole Fadare<sup>38</sup>, Joseph Rabban<sup>39</sup>, W. Glenn McCluggage<sup>40</sup>, Saloni Walia<sup>41</sup>

<sup>1</sup>Core Diagnostics, Gurgaon, India, <sup>2</sup>University of Southern California, Keck School of Medicine of USC, Los Angeles, CA, <sup>3</sup>Advanced Medical and Research Institute, New Delhi, India, <sup>4</sup>Kapoor Centre of Urology and Pathology, Raipur, India, <sup>5</sup>Core Diagnostics, Gurugram, India, <sup>6</sup>Jawaharlal Nehru Medical College, Aligarh Muslim University, Aligarh, India, <sup>7</sup>City of Hope Cancer Center, Duarte, CA, <sup>8</sup>Cedars-Sinai Medical Center, Los Angeles, CA, <sup>9</sup>IMS & SUM Hospital, Bhubaneswar, India, <sup>10</sup>Santa Chiara Hospital of Trento, <sup>11</sup>The University of North Carolina at Chapel Hill, Chapel Hill, NC, <sup>12</sup>The University of Alabama at Birmingham, Birmingham, AL, <sup>13</sup>UCMS and GTB Hospital, Delhi, India, <sup>14</sup>All India Institute of Medical Sciences, JODHPUR, India, <sup>15</sup>UCSF Pathology, San Francisco, CA, <sup>16</sup>University of Southern California, CA, <sup>17</sup>Basavataarakam Indo American Cancer Hospital, Hyderabad, India, <sup>18</sup>Brigham and Women's Hospital, Boston, MA, <sup>19</sup>All India Institute of Medical Sciences, Raebareli, India, <sup>20</sup>Basavataarakam Indo-American Cancer Hospital and Research Institute, Hyderabad, India, <sup>21</sup>Bhanumati Clinical Laboratory, <sup>22</sup>Tata Medical Center, Kolkata, India, <sup>23</sup>The Ohio State University Wexner Medical Center, Columbus, OH, <sup>24</sup>All India Institute of Medical Sciences, New Delhi, India, <sup>25</sup>Tata Memorial Hospital, Mumbai, India, <sup>26</sup>David Geffen School of Medicine at UCLA, Los Angeles, CA, <sup>27</sup>Jalgaon, India, <sup>28</sup>Prolife Diagnostics and Apollo Hospitals, Bhubaneswar, India, <sup>29</sup>Balco Medical Centre, <sup>30</sup>Hyderabad, India, <sup>31</sup>Kaiser Permanente, Los Angeles, CA, <sup>32</sup>Apollo Hospitals, Hyderabad, India, <sup>33</sup>Ministry of Health, Sohar, MOH, Oman, <sup>34</sup>Sardana Labs, <sup>35</sup>El Camino Hospital, Mountain View, CA, <sup>36</sup>AdventHealth Orlando, FL, <sup>37</sup>Tata Medical Center, <sup>38</sup>UC San Diego School of Medicine, La Jolla, CA, <sup>39</sup>University of California, San Francisco, San Francisco, CA, <sup>40</sup>The Royal Hospitals/Queen's University of Belfast, Birmingham, United Kingdom, <sup>41</sup>Keck School of Medicine of USC, Los Angeles, CA

**Disclosures:** Ekta Jain: None; Shivani Kandukuri: None; Sambit Mohanty: None; Anandi Lobo: None; Samriti Arora: None; Nishat Afroz: None; Rania Bakkar: None; Bonnie Balzer: None; Rupanita Biswal: None; Luca Cima: None; Danielle Costigan: None; Mallika Dixit: None; Deepti Dhall: None; Preeti Diwaker: None; Poonam Elhence: None; Cynthia Gasper: None; Yuna Gong: None; Harveen Gulati: None; Michelle Hirsch: None; Deepika Jain: None; Niraj Kumari: None; Suseela Kodandapani: None; Manoj Kahar: None; Bhagat Lali: None; Zaibo Li: None; Vipra Malik: None; Sandeep Mathur: None; Divya Midha: None; Santosh Menon: None; Neda Moatamed: None; Geetashree Mukherjee: None; Vaishali Nagose: None; Subhasini Naik: None; Sandeep Ojha: None; Immaneni Rao: None; Shivani Sharma: None; Sayali Shinde: None; Hena Singh: None; Christine Salibay: None; Meenakshi Swain: None; Nuzhat Khatoon Sayyed: None; Rohan Sardana: None; Ankur Sangoi: None; Charanjeet Singh: None; Juhi Varshney: None; Lateef Zameer: None; Oluwole Fadare: None; Joseph Rabban: None; W. Glenn McCluggage: None; Saloni Walia: None

**Background:** Ever since the seminal Cancer Genome Atlas (TCGA) paper on genomic profiling of endometrial carcinoma (EC) came out, there has been increasing integration of morphology and molecular characteristics to stratify EC, predict prognosis and guide treatment. However, there is disparity on practice trend and molecular resource utilization even among gynecologic pathologists. This prompted us to conduct a multi-institutional survey to understand the global practice patterns of gynecologic pathologists and to evaluate the frequency of adoption of genomic profiling as well as recently recommended changes in morphologic assessments.

**Design:** A survey questionnaire was shared among 75 gynecologic pathologists using Survey Monkey software. Deidentified and anonymized respondent data was analysed (Figure 1).

**Results:** 56 of 75 participants completed the survey (75%). Morphologic assessment of EC: Most respondents routinely report lymphovascular invasion as focal or extensive (69%) and use a binary grading (low grade and high grade) for endometrioid subtype (51%). Only a minority always report exact percentages in mixed carcinoma or carcinosarcoma (42%), or a MELF pattern of invasion (25%). Intraoperative Assessment: Over 70% participants agreed that intraoperative assessment of depth of myometrial invasion is at least somewhat reliable. Ultrastaging for sentinel lymph nodes: 31% respondents always evaluate sentinel lymph nodes using ultrastaging. Molecular classification: About half (51%) are not performing complete molecular characterization of EC; combination of MMR and p53 IHC are done by 51% vs combined MMR, p53 and POLE testing by 24%. Low grade EC do not undergo POLE testing by majority (60%). Biomarker Studies: Universal MMR testing for ECs is done by just over half (54%) respondents, HER2 testing is performed by 49% for endometrial serous carcinoma and for all TP53 mutated tumors by additional 7%. Most respondents do not get requests for TMB, HRD or PD-L1 testing for ECs from their oncologists. The differences in practice patterns amongst pathologists in Asia vs. North America/ Europe are summarized in Table 1.

Parameter	Pathology practice in Asia (n=34)	Pathology practice in North America and Europe (n=22)
<b>Report LVI as focal/ extensive</b>	Yes (n=29, 85.3%)	Yes (n=22, 100%)
<b>Reliability of intraoperative assessment of EC</b>	Always or somewhat (n=25, 73.5%)	Always or somewhat (n=17, 77.3%)
<b>Use IHC for diagnosis of EIN in ambiguous cases</b>	Yes (n=10, 29.4%)	Yes (n=5, 22.7%)
<b>Perform ultrastaging for sentinel lymph nodes</b>	Yes (n=21, 61.2%)	Yes (n= 21, 95.5%)
<b>Use binary grading for endometrioid histology</b>	Yes (n=19, 55.9%)	Yes (n=4, 18.2%)
<b>Performing molecular characterization in all EC</b>	Yes (n=12, 35.3%)	Yes (n=8, 36.4%)
<b>Use of MMR+p53+POLE versus MMR+p53 IN EC</b>	all 3 (n=9, 26.5%)/ 2 (n= 17, 50%)	all 3 (n=4, 18.2%)/ 2 (n=15, 68.2%)
<b>Use of BRG1+MMR for undifferentiated/de-differentiated carcinoma</b>	Yes (n=8, 23.5%)	Yes (n=10, 45.5%)
<b>Universal testing of endometrial carcinoma for MMR deficiency</b>	Yes (n=10, 29.4%)	Yes (n=19, 86.4%)
<b>Use of IHC versus IHC+KRAS for mesonephric like carcinoma diag</b>	IHC (n=26, 76.5%)/ IHC+KRAS (n=2, 5.9%)	IHC (n=21, 95.5%)/ IHC+KRAS (n=1, 4.5%)
<b>Classify EC as multiple genomic classifier</b>	Yes (n=9, 26.5%)	Yes (n=6, 27.3%)
<b>TMB in endometrial carcinoma</b>	Yes (n=15, 44.1%)	Yes (n= 7, 32%)
<b>PD-L1 in endometrial carcinoma</b>	Yes (n=20, 58.8%)	Yes (n=9, 40.9%)
<b>HRD in endometrial serous carcinoma</b>	Yes (n=13, 38.2%)	Yes (n=6, 27.3%)
<b>HER2 in EC (mostly serous/ high grade endometrioid histology)</b>	Yes (n=26, 76.5%)	Yes (n=19, 86.4%)
<b>MELF pattern reporting</b>	Always or somewhat (n=16, 47.1%)	Always or somewhat (n=17, 77.3%)
<b>Percentage of mixed carcinoma components</b>	Always or somewhat (n=30, 88.2%)	Always or somewhat (n=20, 90.1%)

Figure 1 - 915

*Utilization of key morphologic and molecular prognostic parameters in endometrial malignancies: Results from a survey of pathologists practicing gynecologic pathology*

1. Do you routinely report lymphovascular space involvement as focal or extensive, while assessing lymphovascular space invasion in endometrial carcinoma?  
 a. Yes  
 b. No  
 c. Sometimes  
 Comment, please specify
2. In cases of mixed carcinoma and carcinosarcoma, do you report exact percentages of the components?  
 a. Never  
 b. Sometimes  
 c. Always  
 Comment, please specify
3. In cases of endometrial carcinoma, do you report the microcystic, elongated, fragmented (MELF) pattern of invasion specifically in the final diagnosis?  
 a. Never  
 b. Sometimes  
 c. Always  
 Comment, please specify
4. In your practice how reliable is the assessment of myometrial invasion during intraoperative consultation for endometrial carcinoma?  
 a. Very Reliable  
 b. Somewhat Reliable  
 c. Unreliable  
 Comment, please specify
5. How often do you perform ultrastaging of the sentinel nodes for endometrial carcinoma cases?  
 a. All cases  
 b. None  
 c. Some, only if the surgeon requests  
 Comment, please specify
6. In your practice do you use binary grading for endometrioid histology, as recommended by the WHO Classification of Tumours (5th Edition) whereby grades 1-2 tumors are classified as low-grade and grade 3 tumors as high-grade?  
 a. Yes  
 b. No  
 Comment, please specify
7. How often do you get a request for HER-2 in endometrial carcinomas from your oncologist?  
 a. Never  
 b. Only for TP53 mutated tumors  
 c. Always  
 Comment, please specify
8. In your practice, are you performing molecular characterization per the TCGA classification for all endometrial carcinomas across all tumor grades?  
 a. Yes  
 b. No  
 c. Sometimes  
 Comment, please specify
9. In your practice, which of the following markers do you routinely do for molecular characterization of endometrial carcinoma?  
 a. MMR testing by IHC  
 b. p53 IHC  
 c. POLE hot spot testing  
 d. MMR and p53  
 e. MMR, p53, and POLE  
 f. None  
 Comment, please specify
10. In cases of undifferentiated/de-differentiated endometrial carcinomas do you routinely test by immunochemistry for  
 a. BRG-1  
 b. MMR  
 c. BRG-1 and MMR  
 Comment, please specify
11. Do you currently perform POLE mutational assay in low-grade endometrial carcinoma?  
 a. Yes  
 b. No  
 c. Sometimes  
 Comment, please specify
12. At your institution, which of the following specimens are triaged for MMR testing (institutional protocol)?  
 a. All endometrial carcinoma cases  
 b. Endometrioid histology only  
 c. In women between the ages of 35-60 years  
 d. Based on family history  
 Comment, please specify
13. What is your experience with the accuracy and reliability of MMR protein and p53 immunohistochemistry as surrogate markers for molecular classifiers in endometrial carcinomas?  
 a. Complete concordance  
 b. High concordance  
 c. Low concordance  
 d. No utility  
 Comment, please specify
14. Which of the following diagnostic modalities do you use for the diagnosis of mesonephric-like adenocarcinoma of the endometrium?  
 a. Morphology alone  
 b. Morphology + IHC (PAX8+, GATA3+, CD10+, ER-, PR-)  
 c. Morphology + IHC + KRAS mutation analysis  
 Comment, please specify
15. Do you perform PD-L1 testing in endometrial carcinoma?  
 a. Yes  
 b. No  
 c. Only in metastatic setting  
 d. Comment, please specify
16. How often do you get a request for tumor mutational burden (TMB) in endometrial carcinomas from your oncologist?  
 a. Never  
 b. Sometimes  
 c. Always  
 Comment, please specify
17. How often do the oncologists request HRD mutation assay on high-grade serous carcinoma of the uterus?  
 a. Always  
 b. Sometimes  
 c. Never  
 Comment, please specify
18. In your practice, are you classifying endometrial tumors as multiple genomic classifier or carcinomas that harbor more than one molecular event i.e. MMR, POLE mutations and TP53  
 a. Yes  
 b. No  
 Comment, please specify
19. How often do you test mutations in CTNNB1 in endometrioid carcinoma with no special molecular profile (NSMP)?  
 a. Always  
 b. Sometimes  
 c. Never  
 Comment, please specify
20. Which of the following immunohistochemical markers do you use to confirm endometrial intraepithelial neoplasia (EIN) in ambiguous cases?  
 a. PAX2  
 b. PTEN  
 c. BETA CATENIN  
 d. PAX-2 AND BETA CATE  
 e. PAX-2, PTEN, AND BETA CATENIN  
 Comment, please specify

**Conclusions:** Despite clinically validated molecular algorithms, there is absence of well formulated testing guidelines for EC. The responses to survey represent a wide variation that is present in the practice patterns amongst gynecologic pathologists for EC and most of it is clinician-driven. Some variations are also regional and based on availability of resources.

## 916 H3K27 Trimethylation in Malignant and Benign Smooth Muscle Tumors of the Uterus: A Clinicopathologic and Immunohistochemical Study of 106 Cases

Terri Jones<sup>1</sup>, Rohit Bhargava<sup>2</sup>, Mirka Jones<sup>3</sup>

<sup>1</sup>University of Pittsburgh Medical Center, Pittsburgh, PA, <sup>2</sup>UPMC Magee-Womens Hospital, Pittsburgh, PA, <sup>3</sup>University of Pittsburgh, Pittsburgh, PA

**Disclosures:** Terri Jones: None; Rohit Bhargava: None; Mirka Jones: None

**Background:** The trimethylation of histone 3 lysine 27 (H3K27me3) is an epigenetic regulation in normal and neoplastic tissue leading to decreased expression of downstream genes. In some neoplasms, decreased expression of H3K27me3 by IHC has been associated with poorer survival and with decreased response to chemotherapy and radiotherapy. To our knowledge, expression of H3K27me3 has not been investigated in uterine smooth muscle tumors (uSMTs).

**Design:** Representative sections of 60 leiomyosarcomas (LMS), 11 smooth muscle tumors of uncertain malignant potential (STUMPs), 13 leiomyomas with bizarre nuclei (LBN), and 22 usual leiomyomas underwent immunostaining with H3K27me3. Expression was calculated and reported as a tiered H-score (low: 1-99; intermediate: 100-199; high: 200-300) and correlated with clinicopathologic features.

**Results:** Most LMS (40/60; 67%) showed low or absent reactivity for H3K27me3, with 48% showing complete loss of staining. The average H-score for LMS was 60 (range: 0-240). H3K27me3 expression in STUMPs was low for all positive cases (8/11; 73%) with an average H-score of 17 (range: 0-50). In cases of LBN, most cases were positive (10/13; 77%), with mostly low expression (7/10; 70%) and an average H-score of 37 (range: 0-180). Only 3/22 (14%) LMs were focally and weakly positive for H3K27me3 with an average H-score of <1 (range: 0-10). There did not appear to be correlations between survival, recurrence, tumor stage, tumor characteristics and expression of H3K27me3.

**Conclusions:** Complete loss of H3K27me3 expression was seen in a minority of LMS, STUMPs, and LBN (48%, 27%, and 23%, respectively). Most LMS and LBN showed low to intermediate H3K27me3 expression (87% and 100%, respectively), whereas all STUMPs with expression showed only low reactivity. Of the uSMTs subtypes in our cohort, only LMS cases showed high H3K27me3 reactivity. In a case where a diagnosis of LMS is challenging histologically, the presence of high H3K27me3 expression could be useful. Most (86%) of leiomyomas demonstrated complete loss of H3K27me3 expression as compared to the other uSMT subtypes. This suggests that H3K27me3 may play a role in tumorigenesis of this benign neoplasm and that LMs may have distinct epigenetic regulation compared with other uSMTs.

## 917 Evaluation of HER2 in Endometrial Serous Carcinomas: Is there a role for a HER2-Low Subgroup?

David Jou<sup>1</sup>, Jonathan Hecht<sup>2</sup>, Liza Quintana<sup>2</sup>, Marcos Lepe<sup>1</sup>

<sup>1</sup>Beth Israel Deaconess Medical Center, Harvard Medical School, Boston, MA, <sup>2</sup>Beth Israel Deaconess Medical Center, Boston, MA

**Disclosures:** David Jou: None; Jonathan Hecht: None; Liza Quintana: None; Marcos Lepe: None

**Background:** Serous endometrial carcinomas have a poor prognosis, with the majority of them having extrauterine metastases at presentation. Recent advances in molecular drivers of serous carcinomas have led to the use of targeted therapeutics such as the anti-HER2 therapy, trastuzumab, which when added with conventional chemotherapy is associated with improved survival. With the recent FDA approval of antibody drug conjugates (ADC) targeting HER2 in breast cancer, new targeted therapies exist for patients with HER2-low status disease (defined as IHC score 1+ or 2+ with negative FISH). As such, we sought to further elucidate HER2 categories in patients with high-grade serous endometrial carcinomas (HGSEC) to determine what proportion of patients might be eligible if treatment options for HER2-low become available for HGSEC.

**Design:** The pathology database at our institution was queried for cases of endometrial carcinomas where HER2 IHC was performed between 2013-2022. H&E and HER2-stained slides of endometrial biopsies and resection specimens were retrieved and evaluated. HER2 IHC was scored using the Fader et al Clinical Trial criteria for (HGSEC) and the ASCO/CAP 2018 breast criteria.

**Results:** 42 cases of HGSEC were identified; 9 biopsies (21%) and 33 resections (79%). The cohort was composed of 34 pure HGSEC (81%) and 8 carcinosarcomas with a HGSEC component (19%) (Table 1). By the Fader et al Clinical Trial criteria, the HER2 IHC score distribution was: score 0 (8 cases, 19%), 1+ (12 cases, 29%), 2+ (13 cases, 31%), and 3+ (9 cases, 21%). 5 cases (12%) were discrepant between the Fader et al Clinical Trial and ASCO/CAP 2018 cutoffs for HER2 positive tumors with 25 cases (60%) and 27 cases (64%) falling into the category of HER2-low tumors, respectively. HER2 FISH was performed in 17 cases where the IHC was equivocal; 2 cases (5%) were HER2-amplified and 15 cases (36%) were negative for HER2 amplification.

<b>Histological Type</b>		
Serous carcinoma	34 (81%)	
Carcinosarcoma	8 (19%)	
<b>Specimen Type</b>		
Biopsy	9 (21%)	
Resection	33 (79%)	
<b>HER2 Score</b>		
	Fader et al Clinical Trial criteria	ASCO/CAP 2018 Breast criteria
0	8 (19%)	8 (19%)
1+	12 (29%)	15 (36%)
2+	13 (31%)	12 (28%)
3+	9 (12%)	7 (17%)
<b>HER2 FISH</b>		
HER2 Amplified	2 (5%)	
HER2 Not Amplified	15 (36%)	

**Conclusions:** A majority of (HGSEC) at our institution (60%) would be classified as HER2-low by the Fader et al criteria. Currently at our institution, HER2 testing is performed when requested by the oncology team. With the approval of an ADC for treatment of HER2-low breast cancer, the routine identification of HER2-low (HGSEC) may be important as to recruit candidates for targeted therapy in combination with conventional chemotherapy. As the cutoff for positive HER2 is higher in the Fader et al criteria versus breast, a greater number of patients would potentially qualify.

## 918 PIK3CA Hotspot Mutation in Squamous Cell Carcinoma of the Uterine Cervix: A Single Institution Study

Harsimar Kaur<sup>1</sup>, Chien-Fu Hung<sup>2</sup>, T. C. Wu<sup>3</sup>, Deyin Xing<sup>2</sup>

<sup>1</sup>Johns Hopkins University, Baltimore, MD, <sup>2</sup>Johns Hopkins Hospital, Baltimore, MD, <sup>3</sup>The Johns Hopkins University School of Medicine

**Disclosures:** Harsimar Kaur: None; Chien-Fu Hung: None; T. C. Wu: None; Deyin Xing: None

**Background:** It has been reported that *PIK3CA* mutations are present in cervical cancers with the prevalence varying from 13% to 36%, suggesting their important role in cervical cancer development and progression. While several studies have investigated the impact of *PIK3CA* on tumor characteristics and patient survival of cervical cancer patients, there is no convincing data on the clinical utility of this biomarker in these patients. In a recent meta-analysis which comprised of 12 articles and 2,196 women with cervical cancer, the study concluded that current evidence concerning the impact of *PIK3CA* mutations on survival outcomes of patients with cervical cancer is inconclusive.

**Design:** To explore the role of *PIK3CA* in the development and prognosis of HPV-related cervical squamous cell carcinoma with minimal confounding factors, we planned to investigate the prevalence of *PIK3CA* hotspot mutations in these cancers at our institution. We collected 182 genomic DNA samples from formalin-fixed paraffin-embedded (FFPE) tumors which were pathologically confirmed as cervical squamous cell carcinoma. We performed polymerase chain reaction (PCR)-based Sanger sequencing to assess exons 9 and 20 hotspot mutations in the *PIK3CA* gene. The patients' age, clinical presentations, procedures, and specimen gross descriptions including tumor site and size were also retrieved and reviewed.

**Results:** Sequencing of the purified PCR products detected exon 9 *PIK3CA* mutations in 22 (16%) of 138 tested samples, including 17 cases with E545K mutation, 4 with E542K, and 1 with T544I. No somatic mutations were detected in exon 20 which harbors H1047R hotspot mutation. The patients with the mutations ranged in age from 27 to 79 years-old (mean, 54 years; median, 55 years). In the hysterectomy (10 cases) and conization (1 case) specimens, the tumors ranged in size from 0.4 to 8.5 cm (mean, 3.1 cm; median, 2.3 cm). Distant metastasis was present in 6 cases. Follow-up information was available in 20 cases with *PIK3CA* mutation, of which, 10 patients died (median follow-up, 29 months) and 10 patients were still alive at the time of study (median follow-up, 25 months).

**Conclusions:** Our study further demonstrates frequent activation of PIK3CA pathway in the oncogenesis of cervical squamous cell carcinoma, indicating a therapeutic potential by directly targeting PI3K. The impact of *PIK3CA* mutation on survival outcomes of patients with cervical cancer in our institution is under investigation.

**919 Concordance Between Biopsy and Resection Diagnoses of Uterine Cervical Adenocarcinoma According to the Updated World Health Organization 2020 Classification: A Multi Institutional Study in Japan**

Fumi Kawakami<sup>1</sup>, Hiroyuki Yanai<sup>2</sup>, Masanori Yasuda<sup>3</sup>, Takako Kiyokawa<sup>4</sup>, Norihiro Teramoto<sup>5</sup>, Sachiko Minamiguchi<sup>6</sup>, Yoshiki Mikami<sup>1</sup>

<sup>1</sup>Kumamoto University Hospital, Kumamoto, Japan, <sup>2</sup>Okayama University Hospital, Okayama, Japan, <sup>3</sup>Saitama Medical University International Medical Center, Hidaka, Japan, <sup>4</sup>The Jikei University School of Medicine, Minato-ku, Japan, <sup>5</sup>National Hospital Organization Shikoku Cancer Center, Matsuyama, Japan, <sup>6</sup>Kyoto University Hospital, Kyoto, Japan

**Disclosures:** Fumi Kawakami: None; Hiroyuki Yanai: None; Masanori Yasuda: None; Takako Kiyokawa: None; Norihiro Teramoto: None; Sachiko Minamiguchi: None; Yoshiki Mikami: None

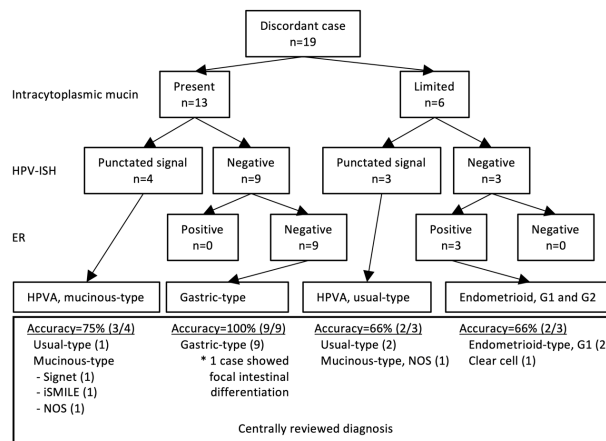
**Background:** World Health Organization (WHO) classification 2020 divides endocervical adenocarcinomas (ECAs) into two major categories, i.e., human papilloma virus (HPV)-associated and HPV-independent primarily based on morphology. However, in case of biopsy limited sampling can be challenging, and thus necessitates application of the algorithmic approach employing ancillary studies as proposed by the international group in 2018 (Stolnicu et al.). Aim of this study was: 1) demonstration of the real-world practice in Japan; and 2) validation of WHO2020 definition and criteria and utility of ancillary studies for biopsy diagnosis of ECAs.

**Design:** We retrieved a total of 217 cases of ECAs (patient age:  $47.9 \pm 0.8$ ) diagnosed according to WHO 4<sup>th</sup> (2014) and 5<sup>th</sup> (2020), with slides of both biopsy and resection specimens available (17 conizations and 200 hysterectomies) in 6 academic institutions in Japan between 2014 and 2021. The diagnoses according to WHO 4<sup>th</sup> were converted to the corresponding diagnostic categories in the WHO 5<sup>th</sup> for analysis. Concordance rate between the biopsy diagnosis and the resection specimen diagnosis was calculated. Cases with discordant diagnosis (discordant cases) were critically reviewed, and HPV in situ hybridization (ISH) and p16, ER, and GATA3 immunohistochemistry were performed on biopsy samples.

**Results:** Biopsy diagnosis matched the resected specimen diagnosis in 197 cases (concordance rate of 91%; kappa=0.75). The concordance for HPV-associated ECAs was significantly higher, compared with HPV-independent carcinoma (95% vs 81%,  $p$  value =0.001, Table). Ancillary studies for algorithmic approach proposed by Stolnicu et al. was applied to a total of 19 discordant cases with unstained sections available. All 19 cases could be correctly re-categorized as HPV-associated or HPV-independent using HPV ISH. On the other hand, p16 immunohistochemistry was positive in 3 of 9 HPV ISH-negative cases with intracytoplasmic mucin. Further subclassification of HPV-associated (mucinous and usual-type) and HPV-independent (gastric, clear cell, and endometrioid-type) ECAs was failed in 3 of 19 cases (16%) (Fig.), presumably due to: limited tissue sampling, marked intratumoral heterogeneity, or absence of appropriate clinical information provided by clinicians.

Institutional diagnosis of resected specimen	Case numbers	Concordant case numbers
<b>HPV-associated</b>	168	160 (95%)
<b>Usual-type</b>	157	153
<b>Mucinous (intestinal/NOS, signet)-type</b>	5	1
<i>iSMILE</i>	6	6
<b>HPV-independent</b>	42	34 (81%)
<b>Gastric-type</b>	37	30
<b>Clear cell-type</b>	5	4
<b>Unusual morphology</b>	7	3 (43%)
<b>Total</b>	217	197 (91%)

Figure 1 - 919



**Conclusions:** Most of the ECAs can be correctly diagnosed by the morphology-based WHO 5<sup>th</sup> criteria in cases of small biopsy, although a subset of challenging cases need HPV-ISH as a substitute for conforming association with HPV.

## 920 Prognostic Relevance and Reproducibility of Pattern-Based Immune Scoring in Endometrial Carcinoma

Merve Kaya<sup>1</sup>, Jan Jobsen<sup>2</sup>, Tessa Rutten<sup>1</sup>, Lisa Vermij<sup>1</sup>, Jan Oosting<sup>1</sup>, Carien Creutzberg<sup>1</sup>, Vincent Smit<sup>1</sup>, Carlos Parra-Herran<sup>3</sup>, Marisa Nucci<sup>3</sup>, Nanda Horeweg<sup>1</sup>, Tjalling Bosse<sup>1</sup>

<sup>1</sup>Leiden University Medical Center, Leiden, Netherlands, <sup>2</sup>Medisch Spectrum Twente, Enschede, Netherlands, <sup>3</sup>Brigham and Women's Hospital, Harvard Medical School, Boston, MA

**Disclosures:** Merve Kaya: None; Jan Jobsen: None; Tessa Rutten: None; Lisa Vermij: None; Jan Oosting: None; Carien Creutzberg: None; Vincent Smit: None; Carlos Parra-Herran: None; Marisa Nucci: None; Nanda Horeweg: None; Tjalling Bosse: None

**Background:** Tumor-infiltrating lymphocytes carry independent prognostic significance in endometrial carcinoma (EC) and have potential in predicting immunotherapy benefit. However, clinical implementation is hampered by the lack of a simple, reproducible scoring method. Here, we developed a pattern-based immune scoring method and studied its reproducibility, correlation with molecular EC classes and clinical outcome.

**Design:** In total, 245 (histologically defined) high-risk EC from a prospective clinical cohort were included. DNA-sequencing and immunohistochemistry (IHC) were performed to molecularly classify EC in *POLE*-ultramutated (*POLEMut*), mismatch repair deficient (MMRd), no specific molecular profile (NSMP) and p53-abnormal (p53abn) EC. Whole slides were stained for hematoxylin and eosin (H&E) and CD8 IHC and scored according to a predefined immune scoring method; no/few CD8+ T cells (desert), CD8+ T cells present but excluded from the tumor epithelium (excluded-inflamed) or CD8+ T cells included in the epithelium (included-inflamed) (Figure 1). Kaplan-Meier method and log-rank test were used for analysis of recurrence-free survival (RFS). For 60 randomly selected cases reproducibility of the method was tested by 3 gynaecopathologists. Agreement was calculated by Fleiss' kappa.

**Results:** Overall, 112 EC (46%) were assigned desert, 55 (22%) excluded-inflamed and 78 (32%) included-inflamed. The included-inflamed pattern was significantly more prevalent in *POLEMut* and MMRd EC compared to NSMP and p53abn EC, 55% versus 20% ( $p < 0.001$ ), respectively (Table 1). Furthermore, the excluded-inflamed pattern was predominantly (29%) found in MMRd EC. The 10-year RFS of included-inflamed EC was 80% versus 51% for excluded-inflamed and 55% for desert EC ( $p < 0.01$ , Figure 2). Across molecular EC classes, a significant survival benefit for the included-inflamed pattern was observed in NSMP EC ( $p < 0.001$ ), and a similar non-significant trend in MMRd and p53abn EC. The Fleiss' kappa was 0.68 for the 3-tiered immune scoring method, which improved when using a 2-tiered immune scoring method; 0.79 when tiered to desert versus inflamed, and 0.83 when tiered to included-inflamed versus others.

	Molecular endometrial carcinoma (EC) class				Total n = 245
	<i>POLEMut</i> EC n = 16	MMRd EC n = 70	NSMP EC n = 90	p53abn EC n = 69	
	n = 86		n = 159		
Desert	2 (13%) 16/86 (19%)	14 (20%)	55 (61%) 96/159 (60%)	41 (59%)	112 (46%)
Excluded-inflamed	3 (19%) 23/86 (27%)	20 (29%)	15 (17%) 32/159 (20%)	17 (25%)	55 (22%)
Included-inflamed	11 (69%) 47/86 (55%)	36 (51%)	20 (22%) 31/159 (20%)	11 (16%)	78 (32%)

Table 1: Prevalence of the three predefined immune patterns across the molecular classes of endometrial carcinoma (EC) and across the molecular EC classes with a mutator phenotype (*POLEMut* EC and MMRd EC) versus non-mutator phenotype (NSMP EC and p53abn EC). Abbreviations: EC, endometrial carcinoma; MMRd, mismatch repair deficient; NSMP, no specific molecular profile; p53abn, p53-abnormal; *POLE*, *POLE* exonuclease domain mutation.

Figure 1 - 920

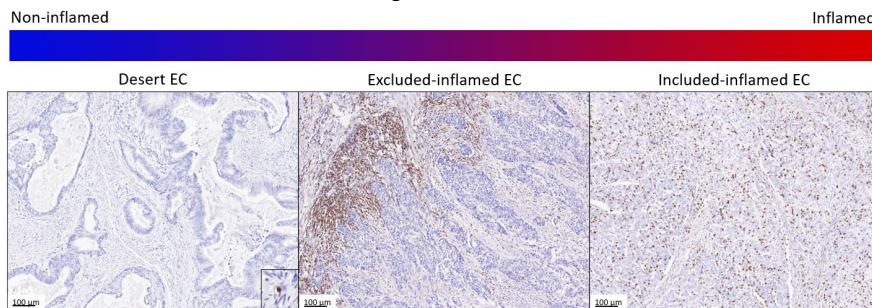


Figure 1: Pattern-based immune scoring in endometrial carcinoma (EC) based on whole slide H&E and CD8 IHC. First, the degree of inflammation was reported on H&E (inflamed versus non-inflamed, not shown). Second, T-cell infiltration was assessed on CD8 IHC and cases were classified into one of the three predefined immune patterns. Representative CD8 IHC images are shown: 1) desert EC (positive CD8+ T cells as internal control); low abundance of CD8+ T cells reflecting a non-inflamed tumor, 2) excluded-inflamed EC; increased density or clustering of CD8+ T cells in the stroma around tumor nests (usually at invasive border) without penetrating the tumor epithelium ('epithelium-excluded'), and 3) included-inflamed EC; presence of CD8+ T cells within the tumor epithelium ('epithelium-included') reflecting a highly inflamed tumor. Original magnifications 10x.

Figure 2 - 920

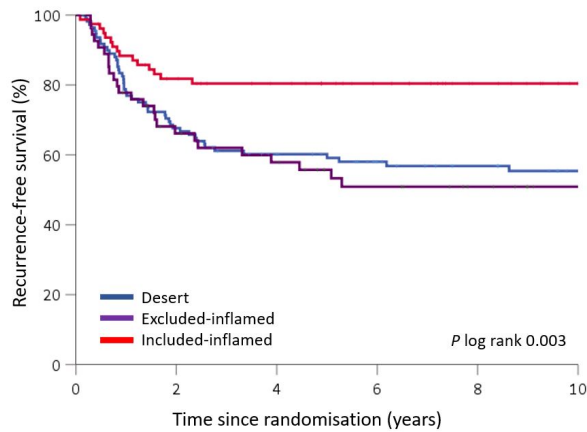


Figure 2: Prognostic value of pattern-based immune scoring in endometrial carcinoma (EC). Kaplan-Meier curves showing probability of EC recurrence according to the three predefined immune patterns: 'desert (n=112)', 'excluded-inflamed (n=55)' and 'included-inflamed (n=78)'.

**Conclusions:** Using a practical and good reproducible immune scoring method, we show that the included-inflamed pattern is associated with hypermutant molecular EC classes and improved RFS. Our novel approach is readily implementable in routine clinical use, and may be a helpful tool to inform therapeutic strategies in EC.

## 921 High Tumor Mutational Burden Predicts Recurrence in Copy Number Low Early Stage Endometrial Cancer and is Associated with ARID1A and TP53 Mutations: Practical Implications for ARID1A and P53 Immunostaining as a Triage Tool

Neslihan Kayraklıoglu<sup>1</sup>, Walter Devine<sup>1</sup>, Joseph Rabban<sup>1</sup>

<sup>1</sup>University of California, San Francisco, San Francisco, CA

**Disclosures:** Neslihan Kayraklıoglu: None; Walter Devine: None; Joseph Rabban: None

**Background:** Checkpoint inhibitors are promising treatment options for patients with endometrial cancer (EC) harboring high tumor mutational burden (TMB). Copy number low (CN-L) tumors are the most heterogeneous group of EC with variable prognosis and degree of TMB. Predicting recurrence in CN-L EC, especially in low grade and early stage disease, remains enigmatic and the significance of TMB in this group is unknown. This study employed next generation sequencing (NGS) to assess the prognostic significance of TMB in low grade, early stage, CN-L EC and further characterized the clinical and molecular features associated with high TMB.

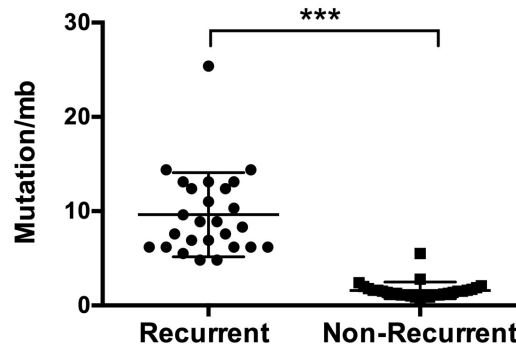
**Design:** The primary tumors of 21 recurrent low grade (grade 1-2), early stage (stage I-II) and CN-L EEC from a single institution were retrospectively analyzed using a clinically validated NGS panel that includes 529 cancer-related genes, quantitation of TMB and MSI Sensor evaluation. TMB was compared to non-recurrent low grade, low stage, CN-L EEC identified from the TCGA database with at least 24 months follow up (n=29). In a second cohort, EC from 263 patients were prospectively analyzed by NGS. Patients with CN-L tumors are identified and among them, molecular and clinical features of TMB-high (TMB-H, ≥10 mutations/Mb) cases are described in comparison with TMB-low (TMB-L, <10 mutations/Mb).

**Results:** TMB was significantly higher in recurrent low grade, early stage, CN-L EC when compared to their non-recurrent counterparts ( $p<0.001$ , Figure 1). Within the prospective patient cohort, 102 CN-L EC were identified; among those, 23% were TMB-H and 77% were TMB-L (Table 1). The average age was similar (63 vs 58,  $p>0.05$ ). No significant difference is observed in tumor histotype, grade and stage. Lymphovascular space invasion (LVSI) was slightly more common in TMB-H ( $p=0.05$ ). Both groups had similar and low MSI Sensor scores (1.5% vs 1%,  $p>0.05$ ). *PTEN* mutations were the most common molecular alteration in both groups (87% vs 78%,  $p>0.05$ ). *ARID1A*, *TP53* and *PIK3R1* mutation frequency were significantly higher in the TMB-H group whereas *CTNNB1* mutations were less frequent ( $p<0.05$ ).

	TMB high (n=23)	TMB low (n=79)	p val
<b>Average age (range)</b>	63 (57-74)	58 (31-76)	0.1
<b>Histotype</b>			
Endometrioid	100%	97%	1
Non-endometrioid	0%	3%	
<b>Grade</b>			
1-2	100%	90%	0.1
3	0%	10%	
<b>pT</b>			
1a/1b/2	96%	94%	1
3a/3b	4%	6%	
<b>pN</b>			
N0 or NX	96%	95%	1
N1 or more	4%	5%	
<b>pM</b>			
M0 or MX	100%	94%	0.5
M1 or more	0%	6%	
<b>FIGO Stage</b>			
I-II	91%	90%	1
III or more	9%	10%	
<b>LVSI</b>			
Present	39%	19%	0.054
<b>Molecular alterations</b>			
<i>ARID1A</i>	87%	47%	<b>0.0007***</b>
<i>TP53</i>	17%	0%	<b>0.002**</b>
<i>PIK3R1</i>	61%	32%	<b>0.01*</b>
<i>CTNNB1</i>	13%	35%	<b>0.04*</b>
<i>PTEN</i>	87%	78%	0.5
<i>PIK3CA</i>	48%	53%	0.8
<i>KRAS</i>	26%	18%	0.3
<i>FGFR2</i>	22%	13%	0.3
<b>Average MSI % (Range)</b>	1.5% (0-3.5%)	1% (0-5%)	0.1

Figure 1 - 921

### Tumor Mutational Burden (Copy Number Low Group)



**Conclusions:** High TMB is present in 23% of CN-L EC, associated with *ARID1A* and *TP53* mutations and recurrence in low grade, early stage disease. These results identify *ARID1A* and p53 immunohistochemistry as potential prognostic markers or triage tools for TMB testing via NGS in early stage endometrioid carcinoma.

## 922 Tumor Infiltrating Lymphocytes (TILs) and Tertiary Lymphoid Structures (TLS) as a Predictor of Immunotherapy Response in Endometrial Cancer

Aysenur Keske<sup>1</sup>, Taja Lozar<sup>2</sup>, Megan Fitzpatrick<sup>2</sup>

<sup>1</sup>University of Wisconsin-Madison Hospital and Clinics, Madison, WI, <sup>2</sup>University of Wisconsin School of Medicine and Public Health, Madison, WI

**Disclosures:** Aysenur Keske: None; Taja Lozar: None; Megan Fitzpatrick: None

**Background:** Response rate to immune checkpoint inhibitors (ICI) is highly variable in endometrial cancer (EC) despite relatively high PD-1 and PD-L1 expression. Mismatch repair status is currently regarded as a biomarker of response to ICI due to overall good response to therapy, however, a subset of the tumors in this group has poor response to ICI therapy. Currently, there are no reliable biomarkers to predict ICI response in EC. Tumor infiltrating lymphocytes (TILs) and tertiary lymphoid structures (TLS) have been shown to modulate response to ICI in various malignancies. In this study, we investigate the role of TILs and TLS in predicting ICI response among ICI-treated EC.

**Design:** Patients with advanced stage or recurrent EC who were treated ICI are included in this study. Clinical data was obtained from the medical records including the molecular classification of the tumors. All available diagnostic slides were evaluated for presence of TILs, the quantity and maturity of the TLS. Clinical outcomes were investigator-assessed with at least one post-treatment scan or evidence of clinical progression after treatment initiation. Objective response rate (ORR) was evaluated based on best documented response to ICI. Correlation between the presence of TLS and clinical outcomes was assessed using Fischer's exact test.

**Results:** We identified 10 cases of primary EC treated with Pembrolizumab (Table 1). The histologic types included endometrioid (n=4), serous (n=4), clear cell (n=1) and dedifferentiated carcinoma (n=1). ORR (40%, 4/10) in our cohort was associated with the presence of TLS ( $p=0.024$ ) and the presence of both TILs and TLS ( $p=0.005$ ), but not TILs only. Four of six (66%; 4/6) MSS (serous, dedifferentiated, or CCC) had either no TILs and/or TLS, and a lack of response to ICI (3 with progressive disease, 1 with stable disease). Two of these six EC (33%; 2/6) had both TILs and TLS, and a partial response to ICI. Of the MMRd endometrioid cases, all had TILs; the two of four cases with TILs and TLS showed response (complete or partial) to ICI, while those without TLS (2/4) showed lack of response (progressive or stable disease) to ICI.

Case Number	Histologic Subtype	Molecular subtype	Duration of treatment (months)	TILs	TLS	Best overall response	Duration of response (months)	Vital status
1	Undifferentiated	p53abn	1.80	N	N	PD	NA	DOD
2	CCC	NSMP	3.54	N	N	PD	NA	DOD
3	Serous	p53abn	1.38	N	Y	PD	NA	AWD
4	Serous	p53abn	14.92	Y	Y	PR	13	DOD
5	Serous	p53abn	9.18	N	N	SD	3	AWD
6	Serous	p53abn	4.92	Y	Y	PR	2 <sup>a</sup>	AWD
7	Endometrioid	MMRd	34.66	Y	Y	CR	37	NED
8	Endometrioid	MMRd	5.64	Y	N	PD	NA	AWD
9	Endometrioid	MMRd	5.38	Y	Y	PR	5	AWD
10	Endometrioid	MMRd	27.05	Y	N	SD <sup>b</sup>	4	AWD

AWD: Alive with disease, CCC: Clear cell carcinoma, CR: Complete response, DOD: Died of disease, N: No, NA: Not applicable, NED: No evidence of disease, NSMP: No specific molecular profile, PD: Progressive disease, p53abn: p53-abnormal, PR: Partial response, SD: Stable disease, Y: Yes.

<sup>a</sup>The patient is currently being treated with ICI

<sup>b</sup>Based on clinical response as the radiologic assessment is pending

**Conclusions:** The presence of TLS alone or with TILs was associated with objective response in our cohort. Our findings suggest that the presence of TILs and TLS may be predictive of ICI response in EC regardless of molecular subtype. The results of our expanded cohort will be reported as part of our poster.

## 923 BRCA1 and BRCA2 mutations lead to Differential Wnt Signaling in Ovarian Cancer Cells

Mira Kheil<sup>1</sup>, Ayesha Alvero<sup>1</sup>, Radhika Gogoi<sup>2</sup>, Noor Suleiman<sup>3</sup>, Lauren Larson<sup>1</sup>, Omar Kazziha<sup>1</sup>, Omar Effendi<sup>4</sup>, Mannat Bedi<sup>1</sup>, Seongho Kim<sup>2</sup>, Omar Fehmi<sup>5</sup>, Sudeshna Bandyopadhyay<sup>1</sup>, Gil Mor<sup>1</sup>, Robert Morris<sup>2</sup>, Rouba Ali-Fehmi<sup>1</sup>

<sup>1</sup>Wayne State University, Detroit, MI, <sup>2</sup>Karmanos Cancer Institute, Detroit, MI, <sup>3</sup>Wayne State University School of Medicine, Detroit, MI, <sup>4</sup>Michigan State University, East Lansing, MI, <sup>5</sup>University of Michigan, Ann Arbor, MI

**Disclosures:** Mira Kheil: None; Ayesha Alvero: None; Radhika Gogoi: None; Noor Suleiman: None; Lauren Larson: None; Omar Kazziha: None; Omar Effendi: None; Mannat Bedi: None; Seongho Kim: None; Omar Fehmi: None; Sudeshna Bandyopadhyay: None; Gil Mor: None; Robert Morris: None; Rouba Ali-Fehmi: None

**Background:** Mutations in the genes BRCA1 and BRCA2 increase the risk of developing ovarian cancer. However, improved survival has been observed among these patients, particularly among those with BRCA2 mutations. Our objective is to identify differentially regulated pathways that may confer the improved survival.

**Design:** RNA sequencing and Pathway Analysis were performed on ovarian tumors from BRCA1 mutant (n=15), BRCA2 mutant (n=16) and homologous recombination wild type (HRwt; n= 626) patients. Signaling pathways were validated *in vitro* and *in vivo* using the isogenic mouse ovarian cancer cell lines ID8 p53<sup>-/-</sup>, ID8 p53<sup>-/-</sup>BRCA1<sup>-/-</sup> and ID8 p53<sup>-/-</sup> BRCA2<sup>-/-</sup>.

**Results:** The Wnt/  $\beta$ -catenin pathway was one of the six differentially regulated pathways in BRCA2 patients compared to BRCA1 and HRwt (p=0.004), as determined by meta-analysis of transcriptome data. Eight Wnt inhibitors (NOTUM, SFRP5, RNF43, ZNRF3, DKK1, DKK4, NDK1 and AXIN2) were upregulated in patient tumors with BRCA2 mutation. In ID8 p53<sup>-/-</sup> cells treated *in vitro* with Wnt3A, canonical Wnt target genes (Enpp2, Tcf7, Tcf4, Fgf9, Fst, Klf5, Id2 and Pitx2) were also upregulated. These genes were not upregulated in the ID8 p53<sup>-/-</sup> BRCA1<sup>-/-</sup> cell line. Instead, Wnt3A treatment led to a significant increase in only Antxr1 in these cells. In ID8p53<sup>-/-</sup>BRCA2<sup>-/-</sup> cell line, Wnt3A did significantly alter any of tested genes. Immunohistochemistry staining for  $\beta$ -catenin, a downstream Wnt target, in untreated intra-peritoneal tumors revealed 15% positivity for cytoplasmic staining in ID8 p53<sup>-/-</sup> tumors, 3% positivity for membrane staining with in ID8 p53<sup>-/-</sup>BRCA1<sup>-/-</sup> tumors, and 33% positivity for membrane staining in ID8 p53<sup>-/-</sup> BRCA2<sup>-/-</sup> tumors.

**Conclusions:** Our findings indicate that specific loss of BRCA1 or BRCA2 show in ovarian cancer cells results in a differential response to Wnt signaling, which may be associated with difference in Wnt localization. This may contribute to the observed differences in the clinical outcome.

## 924 DNA Methylation Based Classification of Rare Mesenchymal Tumors of the Uterus Identifies Novel Molecular Classes

Felix Kommoß<sup>1</sup>, David Kolin<sup>2</sup>, Brooke Howitt<sup>3</sup>, Carlos Parra-Herran<sup>4</sup>, Marisa Nucci<sup>4</sup>, Brendan Dickson<sup>5</sup>, Jen-Chieh Lee<sup>6</sup>, Abbas Agaimy<sup>7</sup>, Andreas von Deimling<sup>8</sup>, Cheng-Han Lee<sup>9</sup>

<sup>1</sup>University of Heidelberg, Heidelberg, Germany, <sup>2</sup>Brigham and Women's Hospital, Boston, MA, <sup>3</sup>Stanford University, Stanford, CA, <sup>4</sup>Brigham and Women's Hospital, Harvard Medical School, Boston, MA, <sup>5</sup>Mount Sinai Health System, Toronto, Ontario, <sup>6</sup>Taipei City, Turkey, <sup>7</sup>Universitätsklinikum, Erlangen, Germany, <sup>8</sup>Heidelberg University Hospital, Heidelberg, Germany, <sup>9</sup>BC Cancer, Vancouver, BC

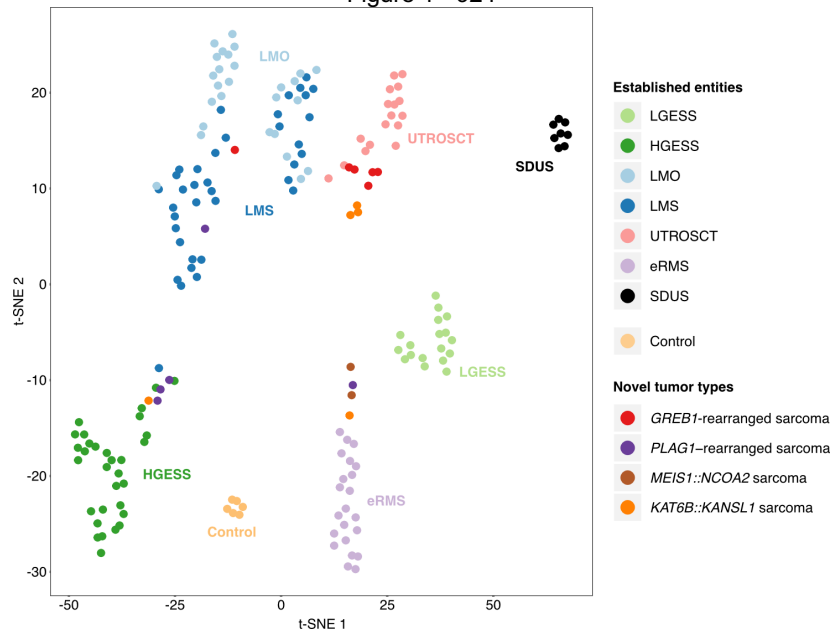
**Disclosures:** Felix Kommoß: None; David Kolin: None; Brooke Howitt: None; Carlos Parra-Herran: None; Marisa Nucci: None; Brendan Dickson: None; Jen-Chieh Lee: None; Abbas Agaimy: None; Andreas von Deimling: None; Cheng-Han Lee: None

**Background:** The last few years have witnessed the description of several "new" uterine sarcoma types, including rare tumors with novel gene-rearrangements. Here we analyze DNA methylation profiles in a cohort of uterine mesenchymal neoplasm with novel gene-rearrangements, in the context of established tumor types, to study their classification and gain insight into their biology.

**Design:** We collected a multicenter cohort including uterine mesenchymal tumors with *KAT6B::KANSL1* (n=5) and *MEIS1::NCOA2* (n=2) gene fusions, as well as *GREB1*- (n=6) and *PLAG1*-rearrangements (myxoid leiomysarcoma, n=5). Whole genome DNA-methylation analysis was performed using the Illumina Infinium MethylationEPIC 850k BeadChip kit. Data were analyzed by t-distributed stochastic neighbor embedding analysis (t-SNE).

**Results:** T-SNE analysis of array-based DNA methylation data together with a previously generated methylation data set including 8 samples of non-neoplastic muscle (control), 6 SMARCA4-deficient uterine sarcomas (SDUS), 18 low- (LGESS) and 31 high-grade endometrial stromal sarcomas (HGESS), 22 embryonal rhabdomyosarcomas (eRMS), 27 leiomyomas (LMO) and 37 leiomyosarcomas (LMS), as well as 15 uterine tumors resembling ovarian sex-cord tumors (UTROSCT) revealed multiple distinct methylation clusters (Figure 1). In detail, we identified a distinct cluster for UTROSCT (including two tumors with *ESR1::NCOA3* gene fusion), that clustered with *GREB1*-rearranged tumors. *KAT6B::KANSL1* tumors and *PLAG1*-rearranged tumors formed two distinct clusters near UTROSCT and HGESS, respectively, with few outliers distributed among other clusters. Both *MEIS1::NCOA2* tumors clustered near eRMS. Interestingly, we observed two distinct clusters of smooth muscle tumors, both of which included LMO and LMS.

Figure 1 - 924



**Conclusions:** Our study shows that *GREB1*-rearranged tumors closely resemble conventional UTROSCT based on DNA methylation analysis. Mesenchymal tumors with *KAT6B::KANSL1*, *MEIS1::NCOA2* and *PLAG1*-rearrangement may represent molecularly distinct tumor entities, however larger cohorts of these rare neoplasms will have to be analyzed to expand on our findings. Furthermore, our study identifies two novel DNA methylation clusters of uterine smooth muscle tumors, which warrants further investigation.

## 925 Integrated Clinicopathologic and Gene Expression Analysis to Profile Immune Prognostic Indicators in Uterine and Non-Uterine Leiomyosarcoma (LMS)

Dimitrios Korentzelos<sup>1</sup>, Ziyu Huang<sup>2</sup>, Hyun Jung Park<sup>2</sup>, Esther Elishaev<sup>3</sup>, Ivy John<sup>1</sup>, Lauren Skvarca<sup>1</sup>, Terri Jones<sup>1</sup>, Chengquan Zhao<sup>4</sup>, Rohit Bhargava<sup>4</sup>, Mirka Jones<sup>5</sup>, Sarah Taylor<sup>1</sup>, Anette Duensing<sup>3</sup>, Thing Rinda Soong<sup>5</sup>

<sup>1</sup>University of Pittsburgh Medical Center, Pittsburgh, PA, <sup>2</sup>UPMC Hillman Cancer Center, Pittsburgh, PA, <sup>3</sup>University of Pittsburgh School of Medicine, Pittsburgh, PA, <sup>4</sup>UPMC Magee-Womens Hospital, Pittsburgh, PA, <sup>5</sup>University of Pittsburgh, Pittsburgh, PA

**Disclosures:** Dimitrios Korentzelos: None; Ziyu Huang: None; Hyun Jung Park: None; Esther Elishaev: None; Ivy John: None; Lauren Skvarca: None; Terri Jones: None; Chengquan Zhao: None; Rohit Bhargava: None; Mirka Jones: None; Sarah Taylor: None; Anette Duensing: None; Thing Rinda Soong: None

**Background:** LMS presents in a wide range of anatomic locations. Little is known about the immune microenvironments and sensitivities to immune checkpoint (IC) inhibitors across tumor sites. We aimed to characterize and compare the immune landscapes in uterine LMS (uLMS) and non-uterine/soft tissue LMS (stLMS) to identify prognostic immune markers.

**Design:** Immunohistochemical expression of PD-L1, TIM-3, Gal-9, LAG-3, CTLA4, MHC-I, T cells and macrophages was evaluated by digital quantification in 41 uLMS and 37 stLMS. Cross-sectional analyses were performed with Fisher's exact tests and logistic regression. Log-rank tests and Cox proportional regression models with adjusted hazard ratios (aHRs) and 95% confidence intervals (CIs) were used to assess overall survival (OS) and recurrence-free survival (RFS). Sixty-three cases yielded sufficient RNA for whole exome sequencing to study expression profiles of 12,000 genes.

**Results:** Median age was 58 years. More stLMS presented at higher stage than uLMS at diagnosis, and more uLMS (49%) exhibited PD-L1+ expression compared with stLMS (26%)(Fig.1). Expression of PD-L1, TIM-3, Gal-9 was associated with high MHC-I expression, as well as elevated CD8+ T cells and macrophages (Fig.1). PD-L1 CPS+ status also correlated with increased FOXP3+ T regulatory cells. Median follow-up time was 37 months (range:1-246 months), with 41 deaths and 51 recurrences observed. Independent indicators for worse RFS included PD-L1 CPS≥5 (aHR:3.0; CI:1.1-8.1)(Fig.2A), high MHC-I expression (aHR:5.0; CI:1.9-13.2)(Fig.2B) and stage III/IV disease (aHR:3.1; CI:1.3-7.6) after adjusting for tumor site and confounders. PD-L1 CPS≥5 also predicted shorter OS (aHR:3.3; CI:1.1-10.4) after controlling for tumor features and adjuvant treatments. Upregulation of genes involved in IC-related functions and antigen processing was noted in LMS with PD-L1 CPS≥5 (Fig.2C). Differential expression of a subset of genes involved in DNA damage and repair (DDR) pathways was seen by different PD-L1 status (Fig.2D).

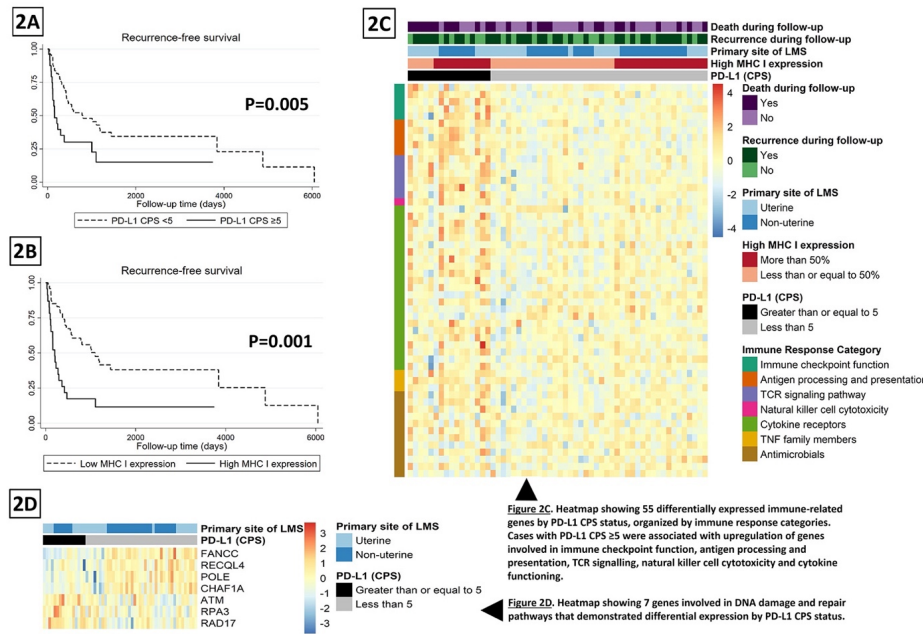
Figure 1 - 925

Table 1. Association between select immune marker expression and clinicopathologic features of LMS (N=78)																		
Tumor characteristics	Tumor primary site			MHC expression in tumor			*CD68+ macrophage density in tumor			*CD8+ TIL density in tumor			FOXP3+ T regulatory cell density in tumor					
	Uterine LMS n=41	Non-Uterine LMS n=37	P	Low n=54	High (strong and >50%) n=24	P	Low n=64	High >300 cells per mm <sup>2</sup> n=14	P	Low n=56	High >20 cells per mm <sup>2</sup> n=22	P	Low n=68	High <40 cells per mm <sup>2</sup> n=10	P			
PD-L1 CPS	<1	65	51	74	<b>0.04</b>		74	38	<b>0.002</b>	72	25	<b>0.002</b>	73	35	<b>0.001</b>	68	40	<b>0.08</b>
	Positive ( $\geq 1$ )	35	49	26			26	62		28	75		27	65		32	60	
PD-L1 CPS	<1	59	41	71	<b>0.01</b>		69	29	<b>0.001</b>	67	17	<b>0.001</b>	70	22	<b>&lt;0.001</b>	64	30	<b>0.04</b>
	Positive ( $\geq 1$ )	41	59	29			31	71		33	83		30	78		36	70	
TIM-3 CPS	<1	26	17	32	0.13		28	17	0.29	31	0	0.02	31	9	0.04	29	10	0.21
	Positive ( $\geq 1$ )	74	83	68			72	83		69	100		69	91		71	90	
TIM-3 CPS	<10	13	61	71	0.35		80	37	<0.001	16	0	0.14	77	39	0.001	15	0	0.19
	$\geq 10$	87	39	29			20	63		84	100		23	61		85	100	
Gal-9 CPS	<1	59	51	60	0.41		69	29	0.001	67	17	0.001	61	43	0.16	62	40	0.19
	$\geq 1$	41	49	40			31	71		33	83		39	57		38	60	
Gal-9 CPS	<5	38	77	84	0.34		91	58	0.001	44	8	0.02	86	65	0.04	41	20	0.21
	$\geq 5$	62	23	16			9	42		56	92		14	35		59	80	
LAG-3 in tumor	Low	37	32	42	0.34		42	26	0.2	39	25	0.35	49	5	<0.001	38	30	0.63
	High (>10 cells per mm <sup>2</sup> )	63	68	58			58	74		61	75		51	95		62	70	
CTLA-4 in tumor	Low	71	63	79	0.13		75	61	0.2	80	25	<0.001	75	62	0.28	74	50	0.12
	High (>50 cells per mm <sup>2</sup> )	29	37	21			25	39		20	75		25	38		26	50	
Tumor stage	I or II	46	72	22	<0.001		51	26	0.07	50	27	0.17	45	39	0.62	47	33	0.51
	III or IV	54	28	78			49	74		50	73		55	61		53	67	

CPS: Combined Positive Score; CTLA-4: Cytotoxic T-Lymphocyte Associated Protein 4; Gal-9: Galectin-9; LAG-3: Lymphocyte-activation protein 3; LMS: leiomyosarcoma; PD-L1: Programmed death-ligand 1; TILs: tumor-infiltrating lymphocytes; TIM3: T-cell immunoglobulin and mucin domain 3; TPS: Tumor Proportion Score

\*High CD3+ T cell density (>30 cells per mm<sup>2</sup>) and high CD163+ macrophage density (>400 cells/mm<sup>2</sup>) showed similar pattern of associations as seen with high CD8+ T cell density and high CD68+ macrophage density respectively (data not shown in table).

Figure 2 - 925



**Conclusions:** PD-L1 CPS $\geq 5$  was a poor prognostic indicator of LMS regardless of uterine or non-uterine tumor site. Our findings highlight differences of PD-L1 positivity in uLMS and sLMS with gene expression correlation. Differential expression of DDR genes was associated with PD-L1 status, supporting IC ligand expression and its possible interaction with the DDR pathways, suggesting a potential opportunity of combined DDR and IC targeting therapies for LMS to achieve greater treatment efficacy.

## 926 Classification of the Tumor Microenvironment as Novel Therapeutic Approaches in Ovarian Cancer

Caddie Laberiano<sup>1</sup>, Claudio Arrechedera<sup>1</sup>, Auriole Tamegnon<sup>1</sup>, Richard Hajek<sup>1</sup>, Joseph Celestino<sup>1</sup>, Ignacio Wistuba<sup>1</sup>, Sanghoon Lee<sup>1</sup>, Amir Jazaeri<sup>1</sup>, Edwin Parra<sup>1</sup>

<sup>1</sup>The University of Texas MD Anderson Cancer Center, Houston, TX

**Disclosures:** Caddie Laberiano: None; Claudio Arrechedera: None; Auriole Tamegnon: None; Richard Hajek: None; Joseph Celestino: None; Ignacio Wistuba: None; Sanghoon Lee: None; Amir Jazaeri: None; Edwin Parra: None

**Background:** Recent immune checkpoint blockade therapies such as PD-1/PD-L1 have shown a low response in patients with ovarian carcinomas. It is still unclear if these therapies' advantages are related to the histology characterization or their tumor microenvironment (TME). This study aims to stratify a cohort of ovarian cancer according to their TME based on the cytotoxic T-cells (CTLs) densities and PD-L1 expression by malignant cells (MCs) and correlate with pathologic characteristics in patients with ovarian carcinomas (OC).

# ABSTRACTS | GYNECOLOGIC AND OBSTETRIC PATHOLOGY

**Design:** The TME was analyzed in 53 OC tissue samples from patients with high-grade serous carcinoma (HGSC,n=39) and clear cell carcinoma(CCC,n=14) using two multiplex immunofluorescence (mIF) panels(Figure 1). The cell phenotype's densities were dichotomized in > than the median as positive expression and ≤ than the median as negative expression. CTLs CD3<sup>+</sup>CD8<sup>+</sup> and MCs PD-L1 expression were used to characterize four TMEs as adaptive immune resistance(Type I=CTL<sup>+</sup>PDL1<sup>+</sup>), immunological ignorance (Type II=CTL<sup>-</sup>PDL1<sup>-</sup>), intrinsic induction(Type III=CTL<sup>-</sup>PDL1<sup>+</sup>), and tolerance(Type IV=CTL<sup>+</sup>PDL1<sup>-</sup>)(Figure 2).

**Results:** Thirty-eight out of 53 cases were metastatic tumors and 15 primary tumors. Type II(45.28%)group was the predominant group in the patient cohort. HGSC cases were grouped mainly in Type II TME, and the CCC cases were mostly distributed in TME Type I and III. We identified that the T-cell antigen-experienced CD3<sup>+</sup>PD-1<sup>-</sup> had significantly higher densities(> median value as cutoff)in TME Type IV (median,25.2 cells/mm<sup>2</sup>,respectively)compared with the other three groups(median,10.5 cells/mm<sup>2</sup> P=0.0003)(Table 1).Similar, higher densities of CTLs PD-L1<sup>+</sup>(median,3.05 cells/mm<sup>2</sup>)and regulatory T-cells CD3<sup>+</sup>CD8<sup>-</sup>FOXP3<sup>+</sup>(33.35 cells/mm<sup>2</sup>)were observed in the TME Type IV than in the other groups (median,2.2 cells/mm<sup>2</sup> and 11.2 cells/mm<sup>2</sup>,P=0.004 and P<0.0001,respectively).Macrophages were significantly higher in the TME Type I (median,118 cells/mm<sup>2</sup>)when compared with the other groups(median,55 cells/mm<sup>2</sup>,P<0.0001).Higher densities of DC macrophages(median,5.4 cells/mm<sup>2</sup>) were observed in Type I and total granulocytic cells(median 2.5cells/mm<sup>2</sup>) were observed in TME Type III than in the other groups (median,1.5cells/mm<sup>2</sup> and 0 cells/mm<sup>2</sup>,respectively);no statistical significance was obtained.

## Types of tumor microenvironment by CTL (CD3+ CD8+) and PD-L1 (CK+PDL1+)\*

PHENOTYPES	Tumor microenvironment			
	Type I	Type II	Type III	Type IV
	CTLs+PDL1+	CTLs-PDL1-	CTLs-PDL1+	CTLs+PDL1-
	n=13	n=24	n=2	n=14
	Median	Median	Median	Median
	(cells/mm <sup>2</sup> )	(cells/mm <sup>2</sup> )	(cells/mm <sup>2</sup> )	(cells/mm <sup>2</sup> )
Cytotoxic T cells (CD3+CD8+)	49.80	3.90	5.25	95.70
T cells antigen-experienced (CD3+PD-1+)	15.50	2.20	5.50	25.20
Total lymphocytes PD-L1+ (CD3+PD-L1+)	0.00	0.00	0.00	0.00
Cytotoxic T cells PD-L1+ (CD3+CD8+PD-L1+)	1.70	0.00	2.65	3.05
Cytotoxic antigen-experienced T cells (CD3+CD8+PD-1+)	0.00	0.00	0.00	0.00
Macrophages (CD68+)	118.0	22.90	10.80	87.25
Regulatory T cells (CD3+FOXP3+CD8-)	18.20	4.20	0.30	33.35
DC macrophages (CD68+CD11b+)	5.36	1.47	0.00	1.60
Tumor associated macrophage type 2 (Arg1+CD68+CD11b+)	0.00	0.00	0.00	0.00
Total granulocytic (CD66b+CD11b+)	0.00	0.00	2.54	0.00
Myeloid derived suppressor cells (MDSC-monocytic) (CD11b+Arg1+CD14+CD33+)	0.00	0.00	0.00	0.00
Myeloid derived suppressor cells (MDSC-granulocytic) (CD11b+CD66b+CD33+)	0.00	0.00	0.00	0.00

\* Positive PDL1: > 1% in malignant cells

Figure 1 - 926

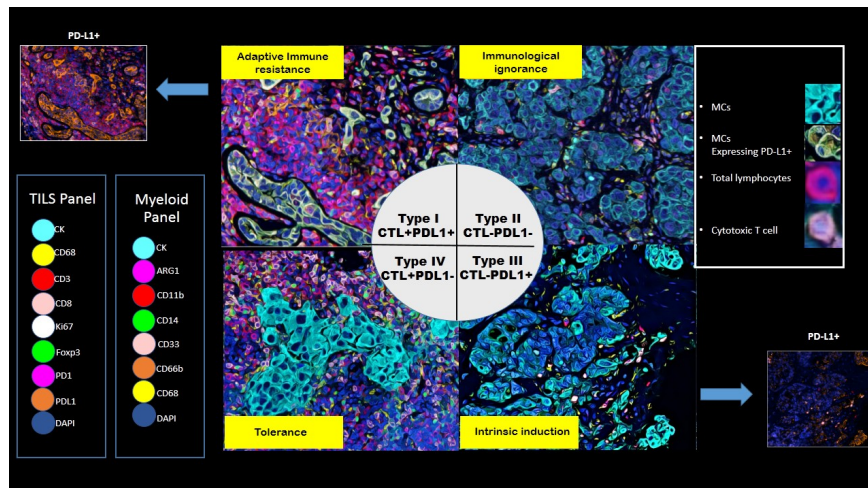
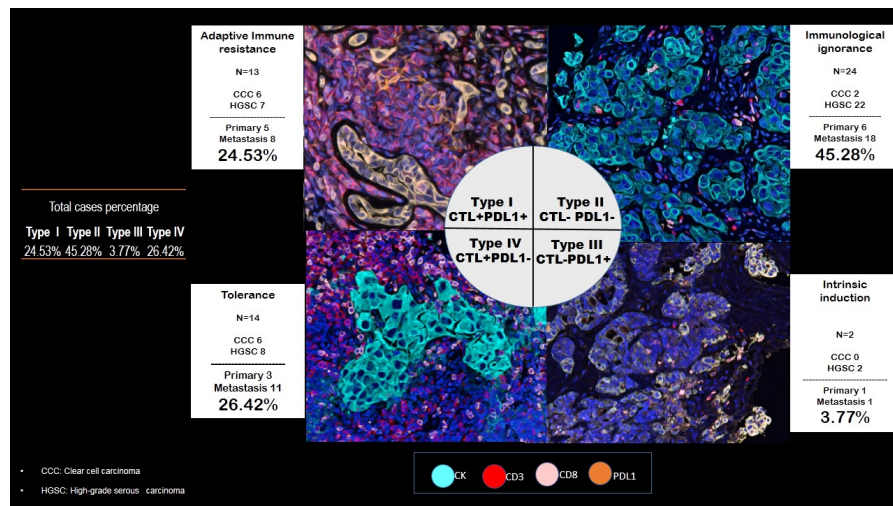


Figure 2 - 926



**Conclusions:** We found that HGSC was predominantly an immunological ignorance TME (CTL-PD-L1<sup>-</sup>) and probably will not benefit from anti-PD-L1 not only for the lack of this expression but also for the lack of low CT. This TME classification could drive a better approach to personalized immunotherapy in patients with OC.

## 927 Molecular Analysis of High-Grade Serous Carcinoma Simultaneously Involving the Endometrium and Adnexa are Clonal and Molecular Analysis May Help Determine Site of Origin

Nicholas Ladwig<sup>1</sup>, Karuna Garg<sup>2</sup>

<sup>1</sup>University of California, San Francisco, San Francisco, CA, <sup>2</sup>Cleveland Clinic, Cleveland, OH

**Disclosures:** Nicholas Ladwig: None; Karuna Garg: None

**Background:** Pelvic high-grade serous carcinoma (pHGSC) and uterine serous carcinoma (USC) show near-identical morphologic features and can be difficult to distinguish, although separation of these entities has implications for tumor staging, considerations for targeted therapy (i.e. HER2 for USC and homologous repair deficiency pathway for pHGSC), as well as for germline mutational testing for BCRA1/2 mutations. Patient age, tumor distribution, and WT1 staining patterns are traditionally used to help separate these entities but there can be significant overlap. We previously demonstrated that USC and pHGSC show distinct molecular profiles. USC harbor frequent alterations in PIK3CA, PPP2R1A, FBXW7, SPOP, PIK3R1, FGFR2, and HER2 compared to pHGSC (p-value < 0.01), and pHGSC showing exclusive or more frequent alterations in BRCA1 and BRCA2 and NF1 (p-value = 0.03). We now sought to use paired sequencing of HGSC involving both the endometrium and adnexa to determine the utility of the proposed genes above versus clinicopathologic variables / WT1 staining in assigning a primary site.

**Design:** Eight cases of HGSC involving both the endometrium and adnexa were identified (5 USC and 3 pHGSC), from which genomic DNA was purified from formalin-fixed, paraffin-embedded tumor tissue and capture based next-generation sequencing targeting 479 cancer genes was performed. Staining results for WT1 and HER2 (and HER2 FISH) were available for a subset of cases.

**Results:** All sites tested from each case showed molecular clonality. No cases showed molecular alterations discordant with the original primary site designation. Cases of USC harbored either USC-associated alterations only (3/5); both USC (x2) and pHGSC-associated (x1) alterations (1/5); or no USC or pHGSC-associated alterations (1/5). None of the pHGSC cases showed USC or pHGSC-associated alterations. USC showed negative or patchy WT1 staining, while all three pHGSC showed diffuse WT1 labeling.

Figure 1 - 927

Diagnosis	USC	USC	USC	USC	USC	p-HGSC	p-HGSC	p-HGSC
Age	67	67	72	64	63	75	66	54
FIGO Stage	IIIC	IVB	IVB	IVB	IVB	IIIA	IIIC	IIIC
Site Tumor Involved?	Endometrium   Ovary	Endometrium   Ovary	Endometrium   Ovary	Endometrium   Ovary   Omentum	Endometrium   Ovary	Endometrium   Fallopian Tube	Endometrium   Ovary	Endometrium   Ovary
Fallopian Tube Involved?	Yes (serosal)	None	Yes (mucosal)	No	Patchy	Yes (transmural)	Yes (serosa/muscularis)	Yes (obliterrated)
WT1 IHC	Patchy   Focal	N/A	N/A	Neg	Neg	Diffuse	Diffuse	Diffuse
HER2 IHC	N/A	N/A	2+	N/A	0+	N/A	N/A	N/A
HER2 FISH	N/A	N/A	Neg	N/A	Pos	N/A	N/A	N/A
TP53	p.S241A	p.S241A	p.C277F	p.C277F	p.213*	p.213*	p.1255del	p.1255del
PIK3CA						p.K111E	p.K111E	p.K111E
PPP2R2A	p.S256F	p.S256F			p.P179R	p.P179R		
FBXW7			p.Y545C	p.Y545C				
SPOP								
PIK3R1								
FIGFR2			p.253R	p.253R				
ERBB2 amp			Low Cellularity	Low Cellularity		Low Cellularity	Yes	No
BRCA1								
BRCA2								
NF1						Structural Variant	Structural Variant	Structural Variant
NOTCH1			p.N304fs	p.N304fs				
MGA								
MTC amp								
CCL20 amp								
TSHB amp						Yes	Yes	
YAP1 amp						Yes	Yes	
TERT amp						Yes	Yes	
FRS2 amp							No	Yes
FGR4 amp						Low Cellularity	Yes	
ERBB3 amp						Low Cellularity	Yes	
IGFBP3 amp						Low Cellularity	Yes	No

**Conclusions:** Molecular analysis of HGSC involving the endometrium and adnexa showed universal clonality; there was no evidence of synchronous primary tumors. Although not all cases showed specific molecular alterations associated with a particular primary site, there were no cases with alterations discordant with the assigned primary site. Our data also shows that USC often display patchy WT1 staining while pHGSC are typically diffusely WT1 positive.

## 928 Clinical Outcomes of Atypical Placental Site Nodule

Hansini Laharwani<sup>1</sup>, Ian Hagemann<sup>2</sup>

<sup>1</sup>Barnes-Jewish Hospital/Washington University, St. Louis, MO, <sup>2</sup>Washington University School of Medicine, St. Louis, MO

**Disclosures:** Hansini Laharwani: None; Ian Hagemann: None

**Background:** Placental site nodule is a trophoblastic lesion typically diagnosed in patients with a recent pregnancy presenting with persistent uterine bleeding or retained products of conception. When cytologic atypia or an elevated Ki-67 index is present, current diagnostic criteria recommend assigning a diagnosis of atypical placental site nodule (APSN). This entity presents a dilemma to treating gynecologists because there is little data on the outcome of APSN. Most patients receive curettage only and show uneventful follow up, but some patients have experienced recurrence of trophoblastic neoplasia or progression to malignancy. The aim of the study is to further document the clinical significance of APSN.

**Design:** The study received institutional review board approval. Cases receiving primary diagnosis at a single institution from 2011 to 2022 were identified. The initial natural language search retrieved all cases containing the term “placental site nodule”. Results were manually curated to retain only cases classified as “atypical” or in which such classification was seriously entertained. Glass slides were reviewed by two pathologists for confirmation. Required diagnostic features included large atypical trophoblastic cells, cohesive nests/cords, Ki-67 index, and/or necrosis.

**Results:** The search identified 20 cases (15 primary; 5 residual/recurrent) of APSN in 15 women. Clinical data, management and outcome are summarized in Table 1. Three patients had persistently elevated serum HCG at presentation or follow-up. Ki-67 was used in diagnostic workup for 18 cases and was approximately 10% for all cases but two. In these, the index was <10% but abundant necrosis was present. Ten patients underwent immediate repeat uterine sampling, including four who had hysterectomy. Residual disease was identified in 0/10. Two patients received adjuvant methotrexate. All patients had some form of subsequent follow-up sampling. Within a mean follow-up interval of 4.6 months (range 1–12 months), four patients (27%) experienced locally recurrent disease which was managed with D&C or hysterectomy. No patients had distant recurrence or died of disease.

Clinicopathologic parameter	Baseline findings in n=15 cases
Age (y)	Mean 37.8 (range 31–42)
Interval from prior pregnancy	
< 6 mo	2
≥6, <12 mo	2
>12 mo	9
Unknown	2
Presenting signs/symptoms	
Abnormal uterine bleeding	3
Polyp on clinical examination	2
Incidental	10
Urine hCG at presentation	
Positive	2
Negative	12
Not performed	1
Serum hCG at presentation	
Positive	3
Negative	5
Not performed	7
Initial sampling	
Biopsy	5
Curettage	6
Polypectomy	1
Other	3
Immediate management	
None	5
Dilation and curettage	4
Hysterectomy	4
Other*	2
Diagnosis on follow-up sampling	
No APSN	10
Persistent/residual APSN	4
Non-atypical PSN	1
Adjuvant therapy	
Methotrexate	2
None	0
Clinical outcome	
Alive, no recurrence	11
Alive with recurrence	4

\*One patient who initially had a cervical APSN underwent LEEP; one patient had a subsequent delivery with examination of a placenta and uterine curettage

**Conclusions:** A series of 15 patients with APSN showed occasional local recurrences, but no metastases or deaths. Conservative management may be acceptable in this disease.

## 929 Mammary-like Lesions of the Vulva: A Series of 31 Cases Including Benign Glandular Lesions, Fibroepithelial Tumors and Carcinomas

Natthawadee Laokulrath<sup>1</sup>, Robert Young<sup>2</sup>, Esther Oliva<sup>3</sup>, Melinda Lerwill<sup>3</sup>

<sup>1</sup>Faculty of Medicine Siriraj Hospital, Mahidol University, Thailand, <sup>2</sup>Harvard Medical School, Boston, MA, <sup>3</sup>Massachusetts General Hospital, Harvard Medical School, Boston, MA

**Disclosures:** Natthawadee Laokulrath: None; Robert Young: None; Esther Oliva: None; Melinda Lerwill: None

**Background:** Mammary-like lesions of the vulva (MLLV) are rare with only a limited number of cases reported in the literature. Herein, we describe a wide spectrum of MLLV, including benign glandular lesions, fibroepithelial tumors and carcinomas, some subtypes of which have not been previously reported.

**Design:** 31 MLLV were retrieved from the files of two large academic hospitals. Hidradenoma papilliferum and Paget disease were excluded. An average of 3 H&E slides (range 1 to 16) and available immunohistochemical stains were reviewed. Tumors were classified based on the 2019 WHO Classification of Breast Tumours.

**Results:** Patients ranged from 17 to 77 years and presented with a vulvar mass (n=11), cyst (n=6), or ulcer (n=1); in 1 case, the lesion was an incidental finding. Two patients had bilateral lesions, and two patients were pregnant. Benign glandular lesions included 6 nodular adenosis and 1 each of adenosis, galactocele, complex sclerosing lesion with collagenous spherulosis, nipple adenoma-like lesion, proliferative fibrocystic change, and periglandular stromal fibrosis. There were 11 fibroepithelial tumors including 6 fibroadenomas (1 with lactational change) and 5 phyllodes tumors (4 benign, 1 borderline). Two in-situ ductal

carcinomas, 1 arising in a recurrent fibroadenoma and 1 within a complex sclerosing lesion, were identified. There were 6 invasive ductal carcinomas, 5 of no special type and 1 with papillary features, and associated in-situ carcinoma was seen in 4 cases. Of the invasive carcinomas, 3 were ER/PR+HER2-, 1 ER/PR/HER2+, 1 ER/PR/HER2-, and 1 ER/PR+ with unknown HER2. Background mammary-type glands and/or lesions were present in 7/8 carcinoma cases. Follow-up was available for all carcinoma patients (range 36-108 months, mean 60 months; and 1 patient only recently diagnosed). 4 patients were alive and well at 7 to 9 years (including both in-situ cases), 2 were alive with disease at 1 and 60 months, and 1 died of other causes at 8 years. 1 patient died and with liver, brain and bone metastases at 3 years after chemoradiation.

**Conclusions:** We describe 31 MLLV, including several unique lesions such as galactocele, complex sclerosing lesion with collagenous spherulosis, nipple adenoma-like lesion, and carcinoma with papillary features that have not been previously reported to our knowledge. We also highlight the potentially aggressive behavior of invasive ductal carcinoma in this location, an uncommon progression only occasionally documented in the literature.

## 930 Artificial Intelligence-Guided Spatial Transcriptomics in High Grade Serous Carcinoma: Toward Image Analysis Based Precision Oncology

Anna Laury<sup>1</sup>, Omar Youssef<sup>1</sup>, Carpen Olli<sup>1</sup>

<sup>1</sup>University of Helsinki, Helsinki, Finland

**Disclosures:** Anna Laury: None; Omar Youssef: None; Carpen Olli: None

**Background:** H&E images of high-grade serous ovarian carcinoma (HGSC) may contain prognostic information currently detectable only by artificial intelligence (AI). We hypothesise that AI can identify regions with prognostic value, and that the biology of these regions can be revealed with spatial transcriptomics.

**Design:** The initial cohort included 55 stage III-IV patients who underwent standard treatment (debulking surgery and platinum-based therapy) but experienced distinct platinum-free intervals (PFI) (<6 vs >18 months). Previously, a deep learning neural network tool identified tumour regions most indicative of outcome within whole slide images (high confidence regions). Tissue microarrays were created containing both these high confidence (HC) tumor regions and background (BG) tumor regions from 16 patients (8 with a PFI <6 months; S-PFI, and 8 with a PFI >18 months; L-PFI). The HC and BG regions were probed with the nanoString GeoMX for FFPE system, using pankeratin as the marker for region of interest selection, and analysed using the GeoMX Digital Spatial Profiler.

**Results:** Analysis of the transcriptomics results reveal that 461 of the 10774 detected targets (4.2%) show significant ( $p = <0.05$ ) differential expression between the S-PFI and L-PFI in the HC regions. Of these, 295 (2.7%) also showed no significant differential expression within the BG tissue regions. Among these 295 are several targets of interest, including: JUNB ( $p=0.004$ ), ITGB8 ( $p=0.035$ ) and LPAR3 ( $p=0.040$ ). Interestingly, cytokeratin 7 ( $p=0.011$ ) expression was also significantly higher in S-PFI outcome group.

**Conclusions:** Artificial intelligence-based image-analysis (AI-IA) of diagnostic HGSC slides can identify morphologic patterns invisible to the human eye and guide selection of biologically meaningful regions. Transcriptomics reveal several transcripts separating S-PFI and L-PFI tumors, specifically within the HC regions identified by AI-IA. In conclusion, AI-IA together with spatial transcriptomics offers a promising toolkit to identify biological features associated with cancer behaviour, making AI-based diagnoses more interpretable and clinically relevant.

## 931 Borderline and Malignant Brenner Tumors: A Clinicopathologic Study of 43 Cases

Barrett Lawson<sup>1</sup>, Anais Malpica<sup>1</sup>

<sup>1</sup>The University of Texas MD Anderson Cancer Center, Houston, TX

**Disclosures:** Barrett Lawson: None; Anais Malpica: None

**Background:** Borderline (BBT) and malignant Brenner tumors (MBT) are rare, with limited clinicopathologic data, including immunohistochemical (IHC) and molecular characteristics. In this study, we present our experience with 43 of such cases.

**Design:** A retrospective search of our laboratory information system using the term "Brenner" was conducted. This search covered the time period between 1/1/1985 and 7/31/2022. All cases had been diagnosed by gynecologic pathologists at our institution. The following information was recorded: patient's (pt's) age, diagnosis, tumor (Tu) size, IHC and molecular findings, FIGO stage, treatment and follow-up (f/u).

**Results:** A total of 441 Brenner tumors were identified: MBT, 27 cases, and BBT, 16. Median age: pts with MBT, 62 yrs (34-80); pts with BBT, 70 yrs (38-81). Two MBT also had associated teratoma, and 1 had intraepithelial carcinoma (IEC). FIGO stage (18

cases): stage 1A (11), stage 1B (1), stage 1C (3), and stage 3 (3). Median Tu size was 17.5 cm (12-25 cm). Treatment known in 16 cases: 13 received adjuvant chemotherapy and 3 had surveillance only. On f/u, 2 died without disease, 1 alive with disease (AWD), 1 dead of disease, and 11 were alive with no evidence of disease (NED); median f/u 48 months (m) (1-291 m). Of 16 cases with data for recurrence, 4 had progression/recurrence (median: 1.5 yrs, 0.75 to 5.3 yrs). 1 case had molecular data, with a TP53 mutation. 12 cases had IHC (Table 1). One BBT had IEC, 1 with focal microinvasion (MI), and 2 with mucinous borderline tumors. FIGO stage (9 cases), all stage 1A. Median Tu size was 12.25 cm (5-32.5 cm). Treatment was known for 9 cases: 7 had BSO or TAH/BSO with peritoneum/omental sampling (of which 3 also had lymph node sampling), while 2 cases had only BSO or TAH/BSO; all of which had surveillance only. F/u (8 cases): 5 alive NED, 2 died without disease, and 1 AWD; median f/u 33 m (1-147 m). 1 of 8 cases had recurrence: a case with MI, 8 yrs after diagnosis, with metastatic disease to a cervical LN. No cases had molecular or IHC data.

Case #	CK7	CK20	CK 5/6	GATA3	P63	WT1	PAX8	ER	P53	Other
1	+	-	N/A	N/A	N/A	N/A	N/A	N/A	N/A	
2	+	N/A	+	N/A	N/A	N/A	N/A	N/A	N/A	
3	N/A	N/A	N/A	N/A	N/A	N/A	N/A	N/A	N/A	+ synaptophysin (rare); - CD56 and -chromogranin
4	+	+	N/A	+	+	N/A	-	-	N/A	
5	N/A	N/A	N/A	N/A	+	-	+	focal	N/A	
7	+	-	N/A	+	+	N/A	N/A	N/A	N/A	
8	+	N/A	+	+	+	N/A	N/A	N/A	N/A	
9	+	-	N/A	+	+	-	N/A	-	WT	
10	+	+	+	N/A	+	-	-	N/A	Diffuse	
11	+	N/A	N/A	+	+	N/A	-	-	N/A	
12	+	VF	N/A	focal	+	-	+	N/A	WT	
13	N/A	N/A	N/A	patchy	N/A	-	-	-	"extensive"	

+ = positive; - = negative; VF = very focal; WT = Wild-type; N/A = not performed

**Conclusions:** BBT and MBT are rare. All BBT were FIGO stage 1A, and a single case of recurrence had a focus of MI. MBT uncommonly present at high stage, while the majority of cases present at early stage and have a favorable outcome.

## 932 Clinical, Pathologic and Genomic Characterization of Rare Forms of Trophoblastic Disease: Placental Site Trophoblastic Tumor and Atypical Placental Site Nodule

Adam Lechner<sup>1</sup>, Neal Lindeman<sup>2</sup>, Carlos Parra-Herran<sup>2</sup>

<sup>1</sup>University of Missouri School of Medicine, Columbia, MO, <sup>2</sup>Brigham and Women's Hospital, Harvard Medical School, Boston, MA

**Disclosures:** Adam Lechner: None; Neal Lindeman: None; Carlos Parra-Herran: None

**Background:** LPCAT1-TERT fusions have been recently described in epithelioid trophoblastic tumor. Other non-molar trophoblastic lesions, including placental Site Trophoblastic Tumor (PSTT) and atypical placental site nodule (APSN), are still poorly understood from a molecular perspective. Our aim is to document the prevalence of genomic alterations in well-annotated cohorts of PSTTs and APSNs.

**Design:** Institutional specimens diagnosed as PSTT and APSN were retrieved, and diagnosis was confirmed by review of the available histologic material. Clinical and pathologic features were documented. Sequencing using a panel with 447-gene coverage was performed on formalin-fixed, paraffin-embedded tumoral tissue. Tumor mutational burden (TMB), single-nucleotide variants and copy number alterations were evaluated.

**Results:** Six patients with PSTT were included. Patient age ranged from 23 to 38 (median 33) years. All patients underwent simple hysterectomy. Tumor was confined to the uterus (FIGO stage I) in all cases. Myometrial invasion was 50% or greater in 5 of 6 cases. Follow-up information was available in 4 patients (median 71 months, range 12-156); all were alive with no evidence of disease. Sequencing was successful in 4 tumors. TMB ranged from 3 to 10.6 mutations/mb. Chromosomal gain of 17q21, involving ETV4, was identified in 2 cases; in one, this change was seen as part of broader copy number gain in 17q21, whereas the gain was focal in the second tumor. ZNF217 missense variants of uncertain significance (VUS) were identified in 2 cases. Other alterations included a missense MUTYH pathogenic variant and a RAD51D VUS, as well as GNA11 and PVRL4 amplification (each seen in one case). Of 20 APSNs, 4 with the largest size (range 2.5-7.5 cm) were selected for sequencing. Median patient age was 41 years (range 36-44). Three underwent hysterectomy, one curettage only. All had indolent outcome. TMB ranged from 2.3 to 6.1 mutations/mb. MGA VUS and 21q22.12 gain involving RUNX1 were identified in 2 cases each. One APSN had a BRCA1 pathogenic frameshift variant.

**Conclusions:** In this limited series, PSTT affects reproductive age women and, despite being often deeply myo-invasive, is confined to the uterus at time of presentation and followed by indolent outcome. PSTT and APSN are both characterized by a

relatively low mutational burden and scarce genomic alterations. The finding of *ETV4* copy gain and *ZNF217* mutations in PSTT, and *RUNX1* gain and *MGA* mutations in APSN, merits further study.

**933 Amount of Residual Disease Predicts Treatment outcome in Patients with Endometrioid Precancers after Progestin Therapy**

Yan Li<sup>1</sup>, Naijia Liu<sup>1</sup>, Hao Chen<sup>1</sup>, Elena Lucas<sup>1</sup>, Wenxin Zheng<sup>1</sup>

<sup>1</sup>UT Southwestern Medical Center, Dallas, TX

**Disclosures:** Yan Li: None; Naijia Liu: None; Hao Chen: None; Elena Lucas: None; Wenxin Zheng: None

**Background:** Conservative management with progestin is a treatment option for atypical hyperplasia or endometrioid intraepithelial neoplasia (AH/EIN). However, diagnosis of residual disease (RD) is often problematic because of the profound morphologic changes induced by progestin and lack of established diagnostic criteria. We have recently demonstrated that RD can be reliably identified by using biomarkers PTEN, PAX2, and β-catenin (PPB) in such setting. It is, however, currently unclear if the amount of RD in follow-up (F/U) samples has a predictive value for treatment outcome. The study aimed to address this question by quantifying the RD and the amount of RD changes in a cohort with series F/Us.

**Design:** 128 AH/EIN patients in the last 5 years were studied. A total of 452 F/U endometrial samples with each patient having at least 2 F/Us studied. The patients were divided into two outcome groups with successfully treated as responders and failure as non-responders. The criteria for the former were defined by no RD in the 4<sup>th</sup> or the last F/U identified in those measurable endometrial biopsies. RD diagnosis was based on morphologically none or poor responses after progestin therapy. Biomarkers PPB were applied when morphologic diagnosis was uncertain (partial responses), where RD was defined when aberrancy of any PPB marker was found (as previously described). The amount of RD was quantitated by using percentage against the total amount of evaluable endometria. Statistical analyses were performed by using SPSS software.

**Results:** The progestin resistant rate of this study was 22.6% with 29 non-responders and 99 responders. Among 99 responders, 44 patients had no RD in all F/Us and 53 patients showed RD decrease, while only 2 patients had an increased the amount of RD during F/Us. In contrast, all non-responders had RD with 14 decreases, 12 increases and 3 no changes during F/Us ( $p<0.0001$ ). We have noticed that the more RD amount in the first 2 F/Us was more associated with non-responders. Other selective data is listed in the following table.

	Responders	Non-Responders	p Values*
Frequency	99	29	
#RD occurrence in all F/Us (%)	87/351 (24.8)	94/101 (93)	<0.001
RD range (%) in all F/Us	0-50	0 - 90	<0.001
Mean range (%)	6.8	23.97	<0.001
20% or more RD in the 1 <sup>st</sup> F/U	22/89	20/27	<0.001
< 20% RD in the 1 <sup>st</sup> F/U	67/89	7/27	<0.001
>50% RD drop in subsequent F/Us	54/92	8/28	0.0052

Note: RD, residual diseases; F/U, follow up. \*The p values were calculated by comparisons between the responders and non-responders.

**Conclusions:** The amount of RD in progestin treated F/U endometrial samples predicts outcome. Failure of progestin therapy is associated with 20% or more RD in initial F/U biopsies, decrease less than 50% of RD amount or no significant changes in subsequent F/Us. In contrast, successful therapy typically shows less than 20% of RD in initial F/U and 50% or more drop the amount of RD in subsequent F/Us. It is important to document the amount of RD when evaluating F/U endometrial biopsies for patients with progestin therapy.

**934 Comprehensive Genomic Profiling of 29 “Multiple-Classifier” Endometrial Carcinomas**

Yimin Li<sup>1</sup>, Shaoxian Tang<sup>2</sup>, Qianlan Yao<sup>3</sup>, Rui Bi<sup>3</sup>, Xiaoyu Tu<sup>4</sup>, Xiaoyan Zhou<sup>3</sup>, Wentao Yang<sup>4</sup>

<sup>1</sup>Fudan University Shanghai Cancer Center, Fudan University Shanghai Medical College, Shanghai, China, <sup>2</sup>Shanghai, China, <sup>3</sup>Fudan University Shanghai Cancer Center, Shanghai Medical College, Fudan University, Shanghai, China, <sup>4</sup>Fudan University Shanghai Cancer Center, Shanghai, China

**Disclosures:** Yimin Li: None; Shaoxian Tang: None; Qianlan Yao: None; Rui Bi: None; Xiaoyu Tu: None; Xiaoyan Zhou: None; Wentao Yang: None

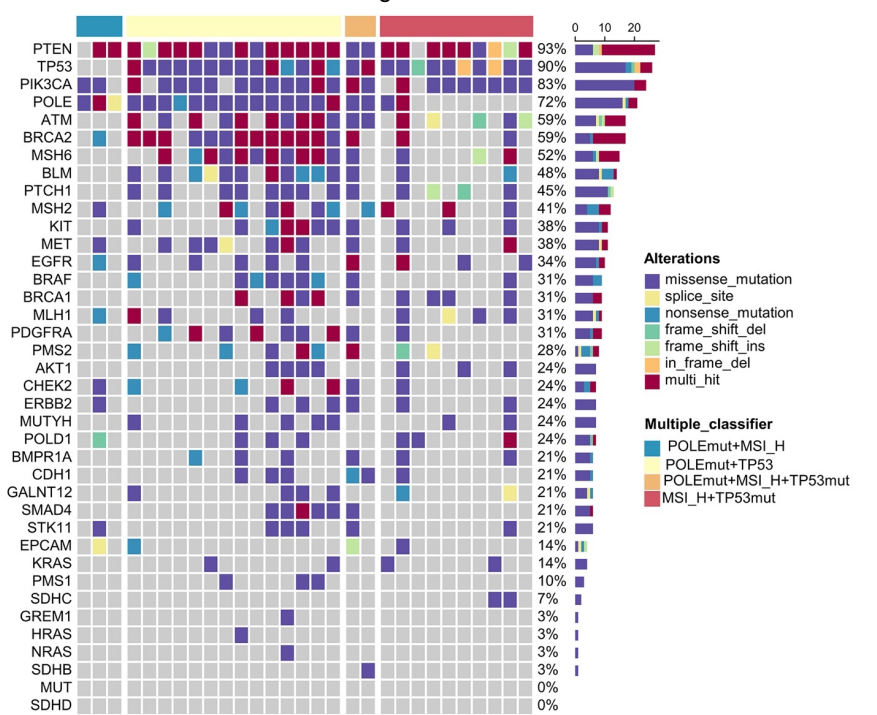
**Background:** According to the integrated multi-omics analyses of The Cancer Genome Atlas (TCGA), Uterine Corpus Endometrial Carcinoma (UCEC) can be divided into four subtypes including POLE/ultramutated, microsatellite instability-high/hypermutated, somatic copy-number alteration high/serous-like, and somatic copy-number alteration low. Besides single molecular classes

("single-classifier" ECs), there are some EC samples, with more than one molecular classifying feature ("multiple-classifier" ECs), of which the molecular genetic characteristics were unclear and deserved further investigations.

**Design:** From January 2019 to August 2022, Next-generation sequencing (NGS) analyses were performed in 269 Chinese EC patients' samples at Fudan University Shanghai Cancer Center using a 41-gene panel assay. On the basis of POLE mutations (POLEMut), microsatellite instability-high (MSI\_H), and TP53 mutations (TP53mut), these patients were divided into "single-classifier" ECs and "multiple-classifier" ECs. Mutations of "multiple-classifier" ECs were analyzed and then compared with "single-classifier" ECs. The mutation and clinical parameters of TCGA-UCEC patients were downloaded from public dataset. Then, we reclassified TCGA-UCEC patients according to the above "single or multiple-classifier" rule to compare the prognosis of different subtypes.

**Results:** Within the cohort of 269 Chinese patients with ECs, 29 patients were "multiple-classifier" (3 POLEMut+MSI\_H, 14 POLEMut+TP53mut, 2 POLEMut+MSI\_H+TP53mut, and 10 MSI\_H+TP53mut). In "multiple-classifier" ECs, the top ranked mutated genes were PTEN(93%), TP53(90%), and PIK3CA(83%). When compared with single POLEMut ECs, the "multiple-classifier" ECs with POLEMut underwent a higher frequency of TP53 mutations ( $p<0.05$ ). When compared with single MSI\_H ECs, the "multiple-classifier" ECs with MSI\_H underwent higher frequencies of TP53, EGFR, and AKT1 mutations ( $p<0.05$ ). When compared with single TP53mut ECs, a total of 28 genes with higher mutation frequencies were detected in the "multiple-classifier" ECs with TP53mut ( $p<0.05$ ). In terms of survival of UCEC patients, survival curves based on TCGA-UCEC dataset revealed that there was no statistic difference between POLEMut and "multiple-classifier" with POLEMut, nor statistic difference between MSI\_H and MSI+TP53.

Figure 1 - 934



**Conclusions:** Some ECs have the characteristics of "multiple-classifier", and further understanding of this will provide new insight into the diagnosis and treatment strategy of "multiple-classifier" EC patients.

## 935 Immunohistochemical Detection of the HPV L1 Major Capsid Protein, a Marker of Transient HPV Infections, in Cervical Dysplasia

Hava Liberman<sup>1</sup>, Ralf Hilfrich<sup>2</sup>, Qin Su<sup>1</sup>, Aril Yahyabeik<sup>1</sup>, Kelsea Cummings<sup>1</sup>, Raul Copaciu<sup>1</sup>

<sup>1</sup>Cell Marque, MilliporeSigma, Rocklin, CA, <sup>2</sup>Pirmasens, Germany

**Disclosures:** Hava Liberman: None; Ralf Hilfrich: None; Qin Su: None; Aril Yahyabeik: None; Kelsea Cummings: None; Raul Copaciu: None

**Background:** Human papillomavirus (HPV) is known to primarily infect human genital and oropharyngeal mucosa and persistent infections may lead to dysplasia and invasive carcinoma. The HPV L1 viral capsid protein is highly expressed during active viral

replication. In transient HPV infections, or those that regress, HPV DNA is episomal and there is active viral replication, while in lesions that progress to severe dysplasia and carcinoma, the viral genome is integrated into the human genome and there is no viral replication. Several studies have shown that immunohistochemistry for the HPV L1 protein, widely used within the European Union, labels cervical dysplasia that is transient in nature.<sup>1-4</sup> The aim of this study was to assess the performance of HPV L1 IHC in a control group and in a set of normal and dysplastic cervical tissues, to establish that the test performs similarly to the published literature.

**Design:** Immunohistochemistry for the HPV L1 protein was performed on 15 cervical biopsies and 25 cervical cytology cases with mild to moderate dysplasia (CIN 1 and 2) and verified HPV L1 protein expression and 15 negative cervical biopsies and 25 negative cervical cytology cases. The presence of HPV DNA was confirmed by PCR in all the positive cases. HPV L1 IHC was also evaluated in non-neoplastic cervix (3), CIN 1 (17), CIN 3 (39), and cervical squamous cell carcinoma (2). Strong nuclear staining in at least one cell was considered positive.

**Results:** For the positive control group, HPV L1 IHC was positive in 38/40 (95%) cases and for the negative group, 1/40 cases showed L1 expression in a single cell (2%). For the additional tissue samples, HPV L1 IHC was positive in 8/17 (47%) CIN 1 cases, 3/39 (8%) CIN 3 cases, and in no (0%) cervical squamous cell carcinoma and non-neoplastic cervix. This IHC test showed less background staining compared with the reference method.

Figure 1 - 935

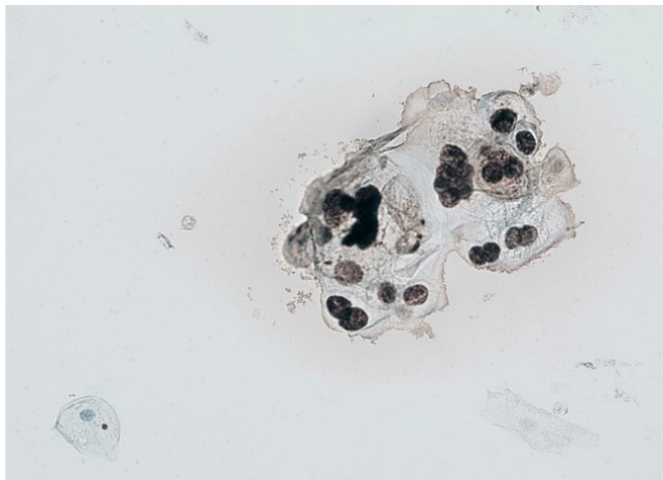
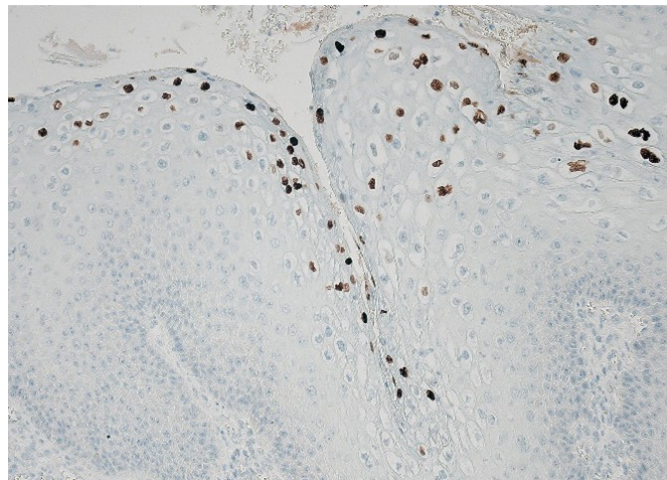


Figure 2 - 935



**Conclusions:** This study successfully validates the performance of HPV L1 IHC for identification of HPV L1 capsid protein in cervical dysplasia. In the control group, HPV L1 IHC showed a sensitivity of 95% and specificity of 98%. In the cervical tissue evaluation, HPV L1 IHC was frequently positive in CIN 1 lesions and only rarely positive in CIN 3 lesions, consistent with published literature.<sup>1-4</sup> These findings indicate that the HPV L1 antibody is a highly sensitive and specific marker for the HPV L1 capsid protein, which correlates with active viral replication and regression in cervical dysplasia.

## 936 Recurrent Activating ERBB2 V777L Point Mutation in Fusion-Negative, S100 and SOX10-Positive Uterine (Corpus and Cervix) Spindle Cell Neoplasms

Douglas Lin<sup>1</sup>, Richard Huang<sup>2</sup>, Jeffrey Ross<sup>3</sup>, Julia Elvin<sup>1</sup>, Erik Williams<sup>4</sup>

<sup>1</sup>Foundation Medicine, Inc., Cambridge, MA, <sup>2</sup>Foundation Medicine, Inc., Cary, NC, <sup>3</sup>SUNY Upstate Medical University, Syracuse, NY, <sup>4</sup>University of Miami, Miami, FL

**Disclosures:** Douglas Lin: Employee: Foundation Medicine, Inc.; Richard Huang: Employee: Foundation Medicine; Roche; Jeffrey Ross: Employee: Foundation Medicine; Foundation Medicine; Julia Elvin: Employee: Foundation Medicine; Erik Williams: Employee: Foundation Medicine, Inc.

**Background:** Uterine sarcomas resembling fibrosarcoma or malignant peripheral nerve sheath tumor (MPNST) is a group of tumors with predilection for the uterus and cervix that may harbor tyrosine kinase fusions (i.e. NTRK1/2/3, COL1A1-PDGFB, FGFR1 or RET). Within this group, distinguishing S100-positive uterine sarcomas resembling MPNST from spindle cell melanomas may be difficult. We sought to determine whether alterations in *ERBB2*, encoding a tyrosine kinase, may be a driver event in a subset of these tumors.

# ABSTRACTS | GYNECOLOGIC AND OBSTETRIC PATHOLOGY

**Design:** A retrospective search of a reference molecular laboratory (Foundation Medicine) was performed for *ERBB2*-mutated uterine and cervical sarcomas that had previously undergone hybrid capture-based comprehensive genomic profiling (CGP) during the course of clinical care. Clinicopathological and genomic data were centrally re-reviewed.

**Results:** We report recurrent activating *ERBB2* V777L point mutation in 7 uterine spindle cell neoplasms originally diagnosed as sarcomas (n=6) or malignant spindle cell tumor most consistent with MPNST (n=1). Tumors were primarily located in the cervix or in the uterine corpus with extensive cervical involvement extending into the vagina. Key pathological features included (1) a preponderance of spindle cells in a fascicular pattern, (2) irregular tumor borders with spindle cells infiltrating between muscle fibers of uterine or endocervical wall, (3) high-grade nuclear atypia, mitotic activity, and multifocal epithelioid morphology, (4) diffuse positivity for S100 and SOX10, (5) retained H3K27me3 expression and (6) negative expression of CD34, CD10 and caldesmon by immunohistochemistry. In addition to *ERRB2* V777L, 43% (3/7) of tumors harbored co-occurring *ERBB2* amplification, while 29% (2/7) had a co-occurring *ERRB3* point mutation, further enhancing *ERRB2*/HER2 pathway activation. Other recurrent molecular alterations included *CDKN2A* loss (86%, 6/7), inactivating mutations of *ATRX* (71%, 5/7), *TP53* (29%, 2/7), and all tumors were negative for *NTRK1/2/3*, *COL1A1-PDGFB*, *FGFR1*, *RET* fusions.

**Conclusions:** *ERBB2* V777L defines a subset of uterine spindle cell neoplasms that, in current practice, may best be tentatively classified as melanomas based on diffuse S100 and SOX10 positivity and retained H3K27me3 expression, although MPNSTs cannot be entirely excluded. Identification of *ERBB2*-mutated uterine spindle cell neoplasms may be of potential diagnostic significance in difficult-to-classify tumors and of therapeutic value with FDA-approved, anti-HER2 inhibitors.

## 937 Clinicopathological and Immune Characterization of Mismatch Repair Deficient Endocervical Adenocarcinoma

Lili Liu<sup>1</sup>, Rongzhen Luo<sup>2</sup>, Mu-Yan Cai<sup>2</sup>, Yingwen Wu<sup>2</sup>, Haoyu Liang<sup>2</sup>

<sup>1</sup>Koo Foundation Sun Yat-Sen Cancer Center, Guangzhou, China, <sup>2</sup>Sun Yat-sen University Cancer Center, Guangzhou, China

**Disclosures:** Lili Liu: None; Rongzhen Luo: None; Mu-Yan Cai: None; Yingwen Wu: None; Haoyu Liang: None

**Background:** Endocervical adenocarcinoma (ECA) is increasingly reported in young women and aggressive disease that lacks effective methods of targeted therapy. Since mismatch repair deficient (dMMR)/high microsatellite instable (MSI-H) are important biomarkers for predicting responses to immune checkpoint inhibitor (ICI) therapies, it is important to investigate the clinical, histopathological and immune microenvironment of dMMR ECAs.

**Design:** We assessed 701 ECAs on representative tissue microarray sections, gathered clinicopathologic information, review histological characteristics and performed immunohistochemical staining for MMR, programmed death ligand-1 (PD-L1) and tumor-infiltrating lymphocytes (TILs) markers.

**Results:** Of the 701 ECA samples, 27 (3.9%) had dMMR. Among them, loss of MMR protein expression was observed in 14/638 (2.2%) HPV-associated adenocarcinoma (HPVA) and 13/63 (23.6%) non-HPV-associated adenocarcinoma (NHPVA). In NHPVA cohort, dMMR status was observed in 8/27 (29.6%), 2/27 (7.40%), 3.7% (1/27) and 7.4% (2/27) patients with clear cell type, gastric-type, endometrioid type and unclassified type, respectively. Loss of MMR expression in tumors with pattern C was significantly higher than in those with pattern A and B in HPVA ( $P=0.03$ ). Moreover, dMMR ECAs association with histological types ( $P<0.001$ ), larger tumor size ( $P=0.009$ ), P16 negative ( $P<0.001$ ) and higher stromal TILs ( $P=0.031$ ) compared with pMMR ECAs. Among the morphologic variables evaluated, TILs and peritumoral lymphocytes are easily recognized in the dMMR ECAs. In addition, positive PD-L1 expression was seen in 369 of the 701 patients (52.6%) with an average combined positive score (CPS) of 15.3%. A relative high prevalence of PD-L1 expression was observed in dMMR ECAs (85.1% by CPS, 74.0% by immune cell score [ICS] and 37.0% by tumour proportion score [TPS]). dMMR ECAs had higher CD3+ TILs (557.2/mm<sup>2</sup> vs. 393.8/mm<sup>2</sup>), CD8+ TILs (678.2/mm<sup>2</sup> vs. 262.8/mm<sup>2</sup>) and CD68+ TILs (96.4/mm<sup>2</sup> vs. 49.1/mm<sup>2</sup>) phenotypes compared with the pMMR ECAs. PD-L1-positive expression was identified in 94.1% of TILs-high cases in the dMMR group, while only 67.8% of TILs-high cases were PD-L1-positive in the pMMR group.

**Conclusions:** The dMMR ECAs were found significantly more often in NHPVA, especially in patients with clear cell type. Compared with the pMMR ECAs, the dMMR ECAs was more likely to present with a TIL-high/PD-L1-positive status, which may contribute to the improved response to ICI therapies.

**938 β-catenin and PTEN as Predictive Biomarkers of Response to Progestin Therapy for Patients with Endometrioid Precancers**Naijia Liu<sup>1</sup>, Yan Wang<sup>1</sup>, Wanrun Lin<sup>1</sup>, Wenxin Zheng<sup>1</sup><sup>1</sup>UT Southwestern Medical Center, Dallas, TX,**Disclosures:** Naijia Liu: None; Yan Wang: None; Wanrun Lin: None; Wenxin Zheng: None**Background:** Biomarkers PTEN, PAX2, and β-catenin (PPB) have played a major role in the diagnosis of pre- and post-progestin treated atypical hyperplasia or endometrioid intraepithelial neoplasia (AH/EIN). However, their predictive significance remains undefined. We aimed to assess if aberrancy of PPB has a predictive value in response to progestin therapy.**Design:** 128 AH/EIN patients in the last 5 yrs were studied, covering a total of 452 follow-up (F/U) endometrial biopsies. Each patient had at least 2 and up to 4 F/Us in the cohort. Among initial and 4 F/Us, 351 samples were available for analyses. Patients had two outcome categories: responders and non-responders, which were defined by absence or presence of residual diseases (RD) in the 4<sup>th</sup> or the last F/U identified in those measurable samples. AH/EIN or RD was diagnosed if morphologically diagnosable. Biomarkers PPB were applied when ambiguous morphology encountered. RD was defined when aberrancy of any PPB marker was found (PMID: 32931681; 34545858). Statistical analyses were performed by using Fisher's exact test.**Results:** Among all 351 samples examined, the 3 PPB biomarkers showed the following results: 91 (26%) all negative, 140 (40%) 1 marker positive, 102 (29%) 2 markers positive, and 18 (5%) all positive. Compared to responders, the frequency of aberrant PPB at the initial AH/EIN diagnosis of non-responders had a significantly higher PTEN loss (75.86% vs 39.79%,  $p<0.01$ ), more β-catenin aberrancy (41.18% vs 33.93%,  $p<0.05$ ), but no significant differences for Pax2 (64.62% vs 66.33%,  $p=0.685$ ). This trend of aberrancy remained the same in F/U samples with PTEN (64.28% vs 26.27%,  $p<0.01$ ), β-catenin (60% vs 31.58%,  $p<0.001$ ), and Pax2 (64.28% vs 62.16%,  $p=0.703$ ). We also observed that the PPB marker expression changed from non-aberrancy to aberrant expression (Table 1).

Table 1. Biomarker changes during F/U in progestin-treated endometrial biopsies

Non-aberrancy at initial diagnosis ◊ aberrant in the F/Us	Responders	Non-Responders	p Values
PTEN	3/59	2/7	0.026
Pax2	3/33	3/12	>0.05
β-catenin	2/25	5/9	0.0025

Note:  $p$  values were obtained by using Fisher exact test.**Conclusions:** Significantly more aberrancy of PTEN and β-catenin in non-responders indicates that these two may be associated with poor outcome of progestin therapy, while Pax2 is not. Among the 3 PPB markers, newly emerged β-catenin aberrancy in any F/U biopsies may be indicative of progestin resistance. Studies with a larger sample size are needed to confirm the findings.**939 Immunohistochemical Expression of Lymphoid Enhancer-Binding Factor 1 in Endometrial Stromal Tumors**Haiyan Lu<sup>1</sup>, Wencheng Li<sup>1</sup>, Yanjun Hou<sup>2</sup><sup>1</sup>Wake Forest Baptist, Winston-Salem, NC, <sup>2</sup>Atrium Health, Winston Salem, NC**Disclosures:** Haiyan Lu: None; Wencheng Li: None; Yanjun Hou: None**Background:** Endometrial stromal tumor (EST) is rare uterine mesenchymal lesions, including endometrial stromal nodule (ESN) and low-grade endometrial stromal sarcoma (LGESS). Nuclear expression of β-catenin, an indication of activated Wnt/β-catenin signaling pathway, was described in over 60% of LGESS. β-catenin interacts with the T-cell factor/LEF family, specifically LEF-1, in the nucleus to form a transcription complex which regulates Wnt/β-catenin signaling pathway downstream mediators in cell cycle control and oncogenesis. In the present study, we evaluated the expression of LEF-1 in ESTs and compared the utility of β-catenin and LEF-1 immunostaining for the characterization of ESTs.**Design:** A pathology archive database search was performed for cases with a diagnosis of ESN and LGESS at our institution from 01/2002 to 08/2022. The corresponding clinicopathological features were collected. Immunohistochemistry for β-catenin and LEF-1 were performed on whole slide sections. Only nuclear staining pattern of β-catenin and LEF-1 were considered as positive. The degree of immunoreactivity for β-catenin and LEF-1 was evaluated semiquantitatively on the basis of staining intensity and the percentage of positive cells. For evaluating β-catenin, 30% of stained tumor cells was considered as positive.

**Results:** A total of 20 cases from 19 patients were identified, including 2 ESN and 18 LGESS. Among the 18 LGESS, 10 were primary from the uterus and 8 were metastases/recurrence. The average age was of 48.7 (ranges 22-77) years for LGESS. 90% (18/20) of the cases was positive for  $\beta$ -catenin. 80% (16/20) of cases was LEF-1 positive if any tumor nuclear staining was considered as positive. 70% (14/20) was LEF-1 positive if 30% was used as the cut-off value (Figure 1/Table 1). There is no significant difference of the performance of  $\beta$ -catenin and LEF-1 in primary or metastatic/recurrent settings ( $p=0.12$  and  $0.42$ , respectively). The staining pattern of LEF-1 in cellular leiomyoma and leiomyosarcoma is ongoing to evaluate its sensitivity and specificity for diagnosis of LGESS.

Figure 1 - 939

Table 1 Demographic, clinicopathological features and  $\beta$ -catenin / LEF-1 immunohistochemical results in 20 ESTs.

Case	Diagnosis	Site	Age	Stage	LVI	Mitosis/10 HPFs	Necrosis	$\beta$ -catenin %	$\beta$ -catenin intensity	LEF-1 %	LEF-1 intensity
1	ESN	P	52	N/A	-	1	-	50	1	0	0
2	ESN	P	79	N/A	-	1	-	95	3	99	3
3	LGEss	P	75	T1aN0	+	0	-	5	1	5	1
4	LGEss	P	47	T1aN0	-	1	+	90	2	85	2
5*	LGEss	P	52	T1aNx	-	0	-	70	2	40	2
6	LGEss	P	52	T1aNx	-	2	-	90	3	70	1
7	LGEss	P	40	T1aNx	+	2	-	99	3	90	3
8	LGEss	P	55	T1bN0	-	0	-	0	0	0	0
9	LGEss	P	47	T1bN0	-	2	-	100	3	40	1
10	LGEss	P	44	T1bN0	-	0	-	50	2	0	0
11	LGEss	P	22	T1bN0	+	5	-	70	2	60	2
12*	LGEss	P	40	T4N0M1	+	4	-	100	3	60	2
13	LGEss	M	53	N/A	+	2	+	95	3	60	2
14	LGEss	M	39	N/A	+	1	+	80	2	90	2
15	LGEss	M	26	N/A	-	4	-	90	3	50	1
16	LGEss	M	77	N/A	-	0	-	60	2	70	2
17	LGEss	M	66	N/A	+	4	+	100	3	0	0
18	LGEss	M	44	N/A	+	5	+	100	3	10	3
19	LGEss	M	44	N/A	-	13	-	95	3	95	3
20	LGEss	M	53	N/A	+	2	+	95	3	90	2

P: primary/uterus; M: metastasis/recurrence; N/A: not applicable

IHC intensity: 0= negative; 1=weak; 2= moderate; 3=strong

Case 5: NGS identified *JAZF1::SUZ12* fusion

Case 12: FISH analysis showed rearrangement of *JAZF1*

**Conclusions:** Our study showed high positivity of LEF-1 staining in LGESS in both primary and metastatic/recurrent settings.  $\beta$ -catenin has strong background cytoplasmic and membranous staining and can be challenging to interpret. In contrast, LEF-1 shows a clear nuclear staining pattern. In conjunction with  $\beta$ -catenin, LEF-1 can be a potential useful immunohistochemical marker for diagnosis of LGESS.

## 940 Prostatic Metaplasia of the Vaginal Epithelium in Female-To-Male Transgender Patients Occurs More Commonly in Younger Patients Irrespective of Hormonal Influences

Miranda Machacek<sup>1</sup>, Kristine Cornejo<sup>2</sup>, Jaclyn Watkins<sup>1</sup>, Esther Oliva<sup>1</sup>

<sup>1</sup>Massachusetts General Hospital, Harvard Medical School, Boston, MA, <sup>2</sup>Massachusetts General Hospital, Boston, MA

**Disclosures:** Miranda Machacek: None; Kristine Cornejo: None; Jaclyn Watkins: None; Esther Oliva: None

**Background:** Prostatic metaplasia of the vaginal epithelium is an established phenomenon in female-to-male (FtM) transgender patients on hormonal testosterone therapy. However, etiologic factors influencing the development of prostatic metaplasia (i.e., years or dose of hormonal therapy and estrogenic effects from increased body mass index (BMI)) are unknown. Additionally, it is unclear if premalignant or malignant transformation may occur. Assessing the natural course of prostatic metaplasia is thus important to understand potential health risks and need for screening for FtM patients on long-term hormonal therapy.

**Design:** We collected 41 vaginal excision specimens from 37 FtM patients from December 2019 to June 2022. The presence or absence of prostatic metaplasia was correlated to dose and duration of testosterone therapy as well as BMI, which were obtained from the electronic medical record. One to four H&E slides (mean=2.19) were examined per patient.

**Results:** Twenty-two patients had prostatic metaplasia (22/37=59%), while 15 did not (41%). The development of prostatic metaplasia in vaginal epithelium was not significantly associated with dose of testosterone (range = 25-420 mg/week, t-test,  $p=.55$ ,

Fig. 1A) or BMI (range=18.79-46,  $\chi^2=0.16$ ,  $p=.69$ , Fig. 1B). However, the length of time on testosterone therapy (range=2-33 years) was significantly different between those with (median=4) and without (median=11.5) prostatic metaplasia (*t*-test,  $p=.014$ , Fig. 2A). Interestingly, a shorter—rather than longer—duration of hormonal therapy was associated with the finding of prostatic metaplasia (Fig. 2A). When patients were stratified based on age (range = 19-61 years), those <50 years old were significantly more likely to have prostatic metaplasia compared to those >50 years old (Fisher's exact test,  $p=.042$ , Fig. 2B). Premalignant or malignant changes were not identified.

Figure 1 - 940

Fig. 1 – Dose of testosterone and BMI are not significantly different between patients with or without prostatic metaplasia.

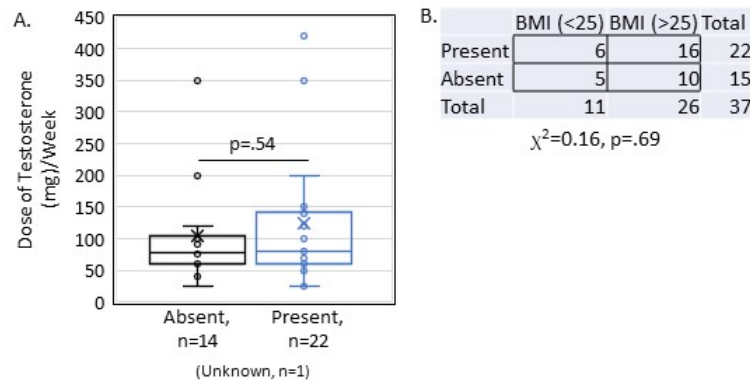
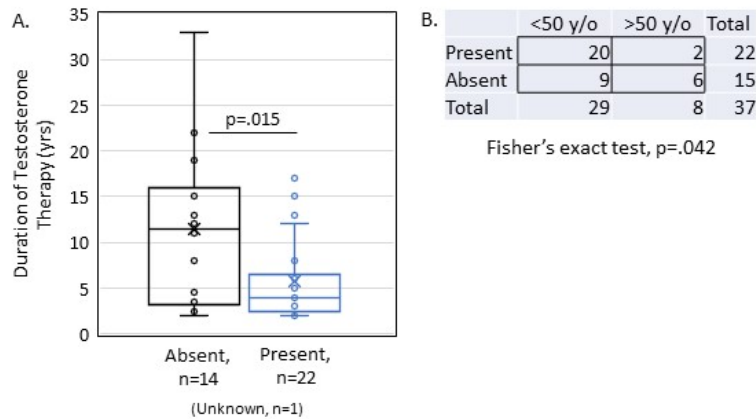


Figure 2 - 940

Fig. 2 – Duration of testosterone therapy and age are significantly different between patients with or without prostatic metaplasia.



**Conclusions:** At the time of surgery, younger individuals (<50 years) are more likely to have prostatic metaplasia than older individuals (>50 years) irrespective of dose of testosterone therapy or BMI, suggesting a different inherent response of the squamous epithelium to testosterone in younger individuals. Importantly, none of the patients developed premalignant or malignant changes, which suggests that long-term hormonal therapy can be a safe alternative for patients choosing not to undergo surgical intervention.

## 941 Somatic Tumor Sequencing and Microsatellite Instability Results in Mismatch Repair-Deficient Endometrial Carcinomas from Patients without Lynch Syndrome: Implications for Immunotherapeutic Biomarkers

Ngome Makia<sup>1</sup>, Kari Ring<sup>1</sup>, Anne Mills<sup>1</sup>

<sup>1</sup>University of Virginia, Charlottesville, VA

**Disclosures:** Ngome Makia: None; Kari Ring: None; Anne Mills: None

**Background:** Checkpoint inhibitors targeting the PD-1/PD-L1 axis are FDA-approved for patients with solid tumors showing mismatch repair deficiency (MMRd), including endometrial carcinomas. The College of American Pathologists recently released guidelines recommending MMR IHC as the first-line biomarker for these immunotherapies, though abnormalities detected on next-generation sequencing (NGS) or microsatellite instability (MSI) testing can also qualify patients. While most MMRd ECAs are attributable to either *MLH1* hypermethylation (*MLH1hm*) or Lynch syndrome (LS), somatic mutations are increasingly recognized contributors. It is important to understand how frequently non-LS-associated, non-*MLH1hm* ECAs with MMR IHC loss have somatic MMR pathogenic variants identified on NGS and/or are MSI-high in order to optimize immunotherapeutic biomarker selection in this population.

**Design:** Tumor NGS +/- MSI testing was performed on 18 ECAs with IHC loss of *MLH1*, *PMS2*, *MSH2*, or *MSH6* but negative MMR germline results, as well as negative *MLH1hm* where relevant (all *MLH1*/*PMS2*-deficient tumors).

**Results:** Average patient age was 60.5 (Range: 21-85). The majority (16/18) of tumors were endometrioid (FIGO 1: 12, FIGO 2: 2, FIGO 3: 3); the 2 remaining cases were dedifferentiated. Somatic tumor NGS was successful in 94% (17/18) and provided a molecular correlate for the IHC loss pattern in 94% (16/17) with available results. MSI testing was successful in 94% (15/16) and was MSI-H in 80% (12/15) and MSI-low in 20% (3/15). One case showed *MSH2*/*MSH6* IHC loss, but failed somatic NGS and MSI testing due to the paucity of tumor present. Another case showed loss of *MSH6* by IHC, but showed no tumoral pathogenic variants on somatic NGS analysis; MSI testing was MSI-low.

**Conclusions:** Somatic tumor NGS and MSI testing were successful in the majority of non-LS, non-*MLH1hm* ECAs with MMR deficiency by IHC, however each failed in one instance. While tumor NGS and MSI testing identified an expected MMR gene pathogenic variant and high-level MSI in most cases when successful, a subset were MSI-low and one showed no pathogenic variants on NGS. These occasional discrepant results underscore the fact that these tests are not entirely interchangeable as biomarkers of immunotherapeutic vulnerability, and that both MSI testing and tumor NGS may miss rare checkpoint inhibitor candidates based on IHC. This is particularly relevant as some institutions consider replacing MMR IHC entirely with molecular methods.

## 942 Targetable HER2 Mutations in Gynecologic Malignancies: Clinicopathological, Immunohistochemical and Molecular Correlations

Padmini Manrai<sup>1</sup>, Austin McHenry<sup>1</sup>, Pei Hui<sup>2</sup>, Natalia Buza<sup>3</sup>

<sup>1</sup>Yale University, New Haven, CT, <sup>2</sup>Yale University School of Medicine, New Haven, CT, <sup>3</sup>Yale School of Medicine, New Haven, CT

**Disclosures:** Padmini Manrai: None; Austin McHenry: None; Pei Hui: None; Natalia Buza: None

**Background:** HER2 (ErbB2) is a well-established therapeutic target not only in breast and gastric cancer, but also in endometrial carcinoma (EC). Current treatment eligibility requires HER2 overexpression by immunohistochemistry (IHC) and/or gene amplification. Recent evidence supports the efficacy of HER2-inhibitors against activating mutations in breast, lung, and other solid cancers. However, comprehensive studies on HER2 mutations in gynecologic tumors are lacking.

**Design:** Our institutional database was searched for HER2 mutations in gynecologic specimens. Clinicopathological information and Next Generation Sequencing (NGS) results were retrieved from medical records. HER2 IHC (Abcam EP3, 1:250) was performed on a representative slide of all tumors. The proposed scoring system for serous EC, requiring strong, complete or lateral/basolateral staining in >30% of tumor cells (3+ score) was used for IHC interpretation. The cBioportal database was queried for HER2-mutant gynecologic tumors and the OncoKB™ database to extract information about specific alterations.

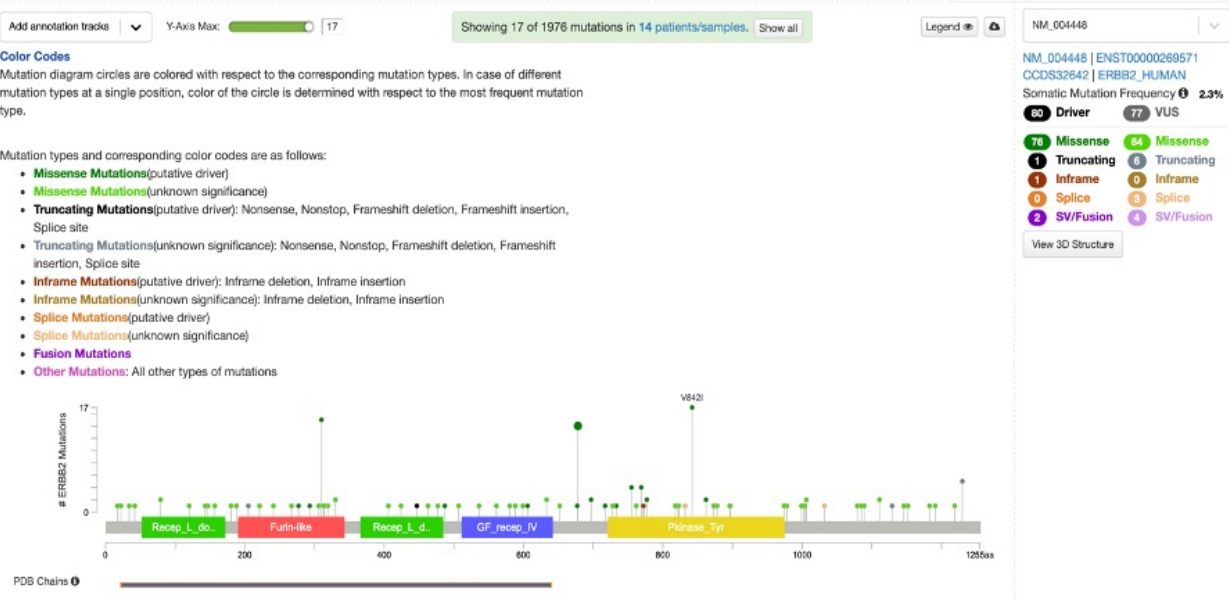
**Results:** We identified 12 gynecologic tumors with HER2 mutations: 10 (83%) endometrial (4 clear cell EC, 3 mixed EC, 1 endometrioid EC, 1 carcinosarcoma, and 1 low grade stromal sarcoma), 1 ovarian mucinous adenocarcinoma, and 1 HPV-associated endocervical adenocarcinoma. HER2 IHC was negative (0 or 1+) in 8 tumors (67%) and 2+ in 4 (33%). We identified 9 discrete HER2 mutations (Table 1). The most frequent was R678Q (n=5, 41.7%), 5 were in the active region of the tyrosine kinase domain (D769Y, V777L, L755S, T733I, and T862A), 2 in the extracellular domain (L313V and G152A), and 2 harbored HER2 rearrangements. No tumors had coexisting HER2 amplification. cBioportal revealed 155 of 4569 (3.4%) gynecologic tumors (114 endometrial, 24 ovarian, 17 cervical) with 83 discrete ERBB2 mutations (Figure 1). Of the 114 endometrial, 18 (16%) harbored T862A (c.2524G>A), 15 (13%) R678Q (c.2033G>A), and 5 (4%) L755S (c.2264T>C).

# ABSTRACTS | GYNECOLOGIC AND OBSTETRIC PATHOLOGY

Table 1. Gynecologic tumors with ERBB2 mutations and rearrangements (n = 12). Abbreviations: ECD, extracellular domain; JMD, Juxtamembrane domain; TKD, tyrosine kinase domain.

Pt	Diagnosis	HER2 IHC	ERBB2 Alteration	Protein Domain	Purported Oncogenic Activity	OncoKB™ Classification
1	Endometrial Endometrioid Adenocarcinoma	0	T733I	TKD	Weakly / non-transforming	Likely Oncogenic; Likely Gain of Function
2	Low Grade Endometrial Stromal Sarcoma	0	V777L	TKD	Constitutive kinase activity and oncogenic transformation	Oncogenic; Gain of Function
3	Endometrial Clear Cell Carcinoma	0	L755S	TKD	Weakly / non-transforming	Oncogenic; Gain of Function
			R678Q	JMD	Weakly / non-transforming	Oncogenic; Gain of Function
4	Mixed Endometrial Adenocarcinoma (Endometrioid and Clear Cell)	0	R678Q	JMD	Weakly / non-transforming	Oncogenic; Gain of Function
5	Ovarian Mucinous Adenocarcinoma	1+	R678Q	JMD	Weakly / non-transforming	Oncogenic; Gain of Function
6	Endocervical Adenocarcinoma	1+	D769Y	TKD	Constitutive kinase activity and oncogenic transformation	Oncogenic; Gain of Function
7	Mixed Endometrial Adenocarcinoma (Serous and Endometrioid)	1+	G152A	ECD	Post-translational modification (proximal) ubiquitination	N/A
			Rearrangement			N/A
8	Mixed Endometrial Adenocarcinoma (Endometrioid and Clear Cell)	1+	R678Q	JMD	Weakly / non-transforming	Oncogenic; Gain of Function
9	Carcinosarcoma	2+	L313V	ECD	N/A	Likely Neutral; Likely Loss of Function
10	Endometrial Clear Cell Carcinoma	2+	Rearrangement		N/A	N/A
11	Endometrial Clear Cell Carcinoma	2+	R678Q	JMD	Weakly / non-transforming	Oncogenic; Gain of Function
12	Endometrial Clear Cell Carcinoma	2+	T862A	TKD	Constitutive kinase activity and oncogenic transformation	Oncogenic; Gain of Function

Figure 1 - 942



**Conclusions:** HER2 mutations are most common in EC among gynecologic cancers, with R678Q most frequent in our cohort, and T862A in cBioportal. While no *HER2*-mutated tumors had a 3+ IHC score, increased *HER2* expression (2+) was seen in tumors with L313V, R678Q, and T862A mutations, and *HER2* rearrangement. Targeted therapy has already been applied in other tumor types with these *HER2* mutations; however, further studies are necessary to explore the prognostic and therapeutic implications of these findings in gynecologic cancers.

## 943 Utility of Beta-catenin Immunohistochemistry in Evaluating Squamous Morules in Endometrial Biopsy and Curettage Specimens

Padmini Manrai<sup>1</sup>, Ernest Hidalgo Cedeno<sup>2</sup>, Sarah Davidson<sup>3</sup>, Natalia Buza<sup>3</sup>, Pei Hui<sup>4</sup>, Tong Sun<sup>3</sup>

<sup>1</sup>Yale University, New Haven, CT, <sup>2</sup>Yale New Haven Hospital, Yale School of Medicine, New Haven, CT, <sup>3</sup>Yale School of Medicine, New Haven, CT, <sup>4</sup>Yale University School of Medicine, New Haven, CT

**Disclosures:** Padmini Manrai: None; Ernest Hidalgo Cedeno: None; Sarah Davidson: None; Natalia Buza: None; Pei Hui: None; Tong Sun: None

**Background:** Squamous morules can be seen in a variety of gynecologic lesions ranging from benign entities such as endometriosis and endometrial polyp to endometrial hyperplasia and endometrial endometrioid adenocarcinoma (EEC). Previous studies have established an association between squamous morules and EEC and a recent study showed *CTNNB1* (Beta-catenin) mutations in squamous morules associated with EEC. In this study we explore the utility of Beta-catenin immunohistochemistry (IHC), specifically aberrant nuclear Beta-catenin expression, as a surrogate for *CTNNB1* mutation, in predicting the behavior of squamous morules across the spectrum of various gynecologic lesions.

**Design:** A total of 38 women with diagnostic findings of squamous morules on endometrial biopsy/curettage were identified, with median follow-up of 22 months (Table 1). Patients were chosen such that a spectrum of benign and malignant entities were present in the cohort to include benign (endometriosis, polyp, etc.), simple hyperplasia without atypia (SH), progestin treated hyperplasia without residual disease (xSH), and complex atypical hyperplasia (CAH) or EEC. Beta-catenin immunostain was performed on a representative slide from each patient and aberrant staining was defined as strong nuclear and cytoplasmic staining.

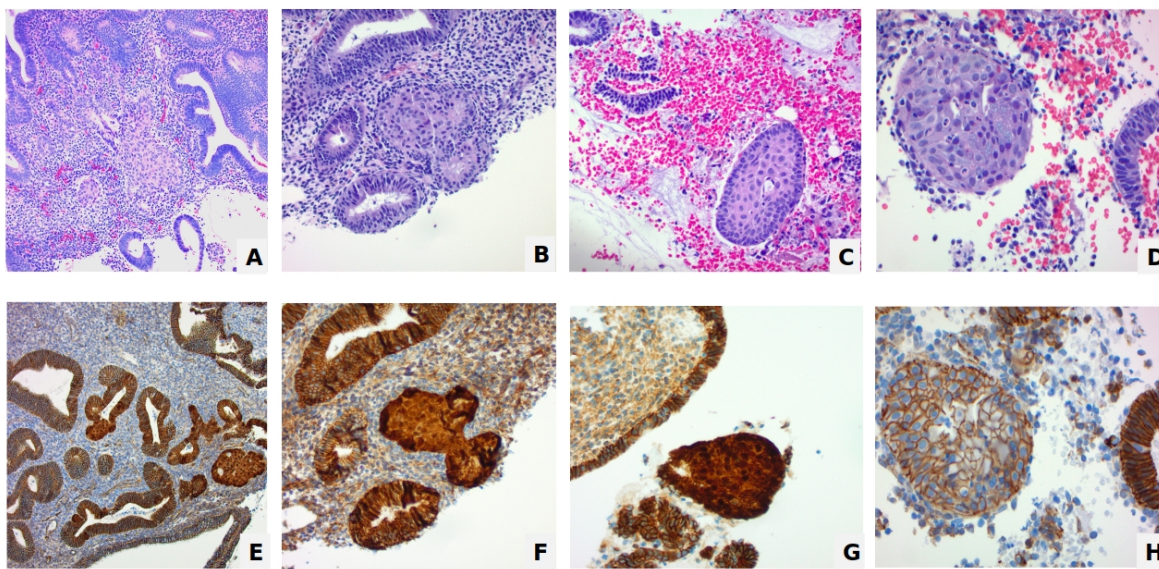
**Results:** Our cohort consisted of patients with biopsies reported as benign (n=12), SH (n=12), xSH (n=6), CAH/EEC (n=8). All squamous morules were focally distributed in the 12 benign biopsies. Diffuse distribution of squamous morules was seen in one biopsy with xSH and two cases of CAH/EEC. Aberrant Beta-catenin expression was observed in 8 (75%) of benign, 10 (83%) SH, 6 (100%) xSH and 8 (100%) CAH/EEC biopsies (Figure 1). Aberrant expression of Beta-catenin was more common in biopsies from patients with a diagnosis of CAH/EEC than benign or SH (100 % vs 75%, p = 0.02). 14 patients presenting with benign or SH (+/- treatment) on initial biopsy had either CAH or EEC at 22 month follow-up (4 benign, 6 SH, 4 xSH). All of these patients had aberrant Beta-catenin expression of squamous morules on initial biopsy (sensitivity = 100%; specificity = 37.5%).

Table 1. Summary of Beta-Catenin Expression in Endometrial Biopsies

	Benign findings	Simple hyperplasia without atypia	Treated hyperplasia	Complex atypical hyperplasia or endometrioid adenocarcinoma
<b>Median Age, (range) years</b>	52 (32-66)	43 (26-68)	47 (26-64)	46 (28-64)
<b>Distribution of squamous morules</b>				
Focal	12 (100%)	12 (100%)	5 (83%)	6 (75%)
Diffuse	0 (0%)	0 (0%)	1 (17%)	2 (25%)
<b>Aberrant Beta-catenin expression (%)</b>	8 (75%)	10 (83%)	6 (100%)	8 (100%)
<b>CAH or EEC at follow-up</b>	4 (33%)	6 (50%)	4 (66%)	n/a
<b>Aberrant Beta-catenin in prior biopsy with malignant follow-up</b>	4/4 (100%)	6/6 (100%)	4/4 (100%)	n/a

Figure 1 - 943

**Figure 1.** **Top row:** H&E sections from endometrial biopsies A) complex atypical hyperplasia B) simple hyperplasia without atypia C) squamous morule found in an otherwise benign biopsy D) squamous morule in endometriosis. **Bottom row:** E-G demonstrate aberrant Beta-catenin immunohistochemistry from cases A-C respectively. H demonstrates normal membranous Beta-catenin expression.



**Conclusions:** Our data show that aberrant Beta-catenin staining of squamous morules in benign endometrial biopsies is sensitive for CAH/EEC on subsequent sampling while normal (membranous) Beta-catenin is associated with benign lesions at follow-up. Larger prospective cohort validation is warranted to fully explore potential negative predictive value of Beta-catenin IHC.

## 944 KRAS Mutation in Endometrial Complex Mucinous Change Is Associated with Concurrent or Subsequent Development of Atypical Endometrial Hyperplasia and Endometrioid Carcinoma

Austin McHenry<sup>1</sup>, Natalia Buza<sup>2</sup>, Pei Hui<sup>3</sup>

<sup>1</sup>Yale University, New Haven, CT, <sup>2</sup>Yale School of Medicine, New Haven, CT, <sup>3</sup>Yale University School of Medicine, New Haven, CT

**Disclosures:** Austin McHenry: None; Natalia Buza: None; Pei Hui: None

**Background:** Endometrial Complex Mucinous Change (CMC) is a spectrum of mucinous epithelial alterations (epithelial stratification, intraglandular papillation to architecturally more complex proliferation without confluent growth, and simple mucinous change with cytological atypia). CMC may harbor KRAS mutations and is associated with subsequent or concurrent endometrial atypical hyperplasia (AH) or endometrioid adenocarcinoma (EC). We investigated clinicopathologic outcomes of KRAS mutation in CMC in a large prospective cohort.

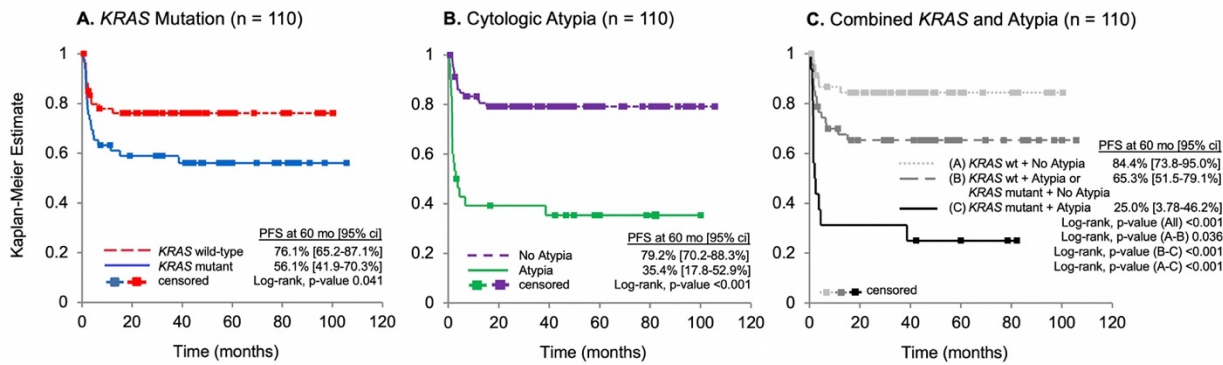
**Design:** Consecutive endometrial biopsy/curettage specimens of CMC were retrieved, excluding those with coexisting AH or EC. Cytological atypia, a component of the original diagnosis albeit not retrospectively reviewed, was defined by variably enlarged nuclei, hyperchromatic chromatin, and presence of prominent nucleoli. KRAS mutation analysis was performed by single strand conformation polymorphism and Sanger sequencing. Statistical analyses included student t-tests, Pearson chi-squared tests, and Kaplan-Meier statistic/Cox-Mantel Log-Rank tests ( $\alpha=0.05$ ). Progression-free survival (PFS) was measured from CMC diagnosis to the date of subsequent disease (AH or EC) or last known alive without progression.

**Results:** Among 110 CMC study cases (Table 1), KRAS mutation was found in 49 (45%) cases. Cytological atypia was seen in 33% (16/49) of KRAS mutants vs 23% (14/61) of cases without the mutation ( $p=0.26$ ). Subsequent disease (AH or EC) was seen in 43% (21/49) of cases with KRAS mutation vs 23% (14/61) of cases without the mutation ( $p=0.026$ ). Of 8 ECs, KRAS mutation was detected in 7 (87.5%) corresponding CMCS. When stratified by cytological atypia, progression occurred in 63% (19/30) with cytological atypia, compared to 20% (16/80) without ( $p<0.001$ ). Half (4/8) of CMC cases that progressed to EC had cytological atypia. KRAS mutation predicted adverse PFS (56% at 60 months) compared to wt KRAS (76%,  $p=0.041$ ; Fig A). The presence of cytological atypia also predicted worse PFS (35% at 60 months) compared to its absence (79%,  $p<0.001$ ; Fig B). The presence of both KRAS mutation and cytological atypia better stratified patients for worse PFS (25% at 60 months) compared to the absence of KRAS mutation with or without cytological atypia (75%,  $p<0.001$ ; Fig C).

**Table 1:** Clinicopathologic data of study cohort (n=110). Abbreviations: mo, months.

	All Patients n = 110	KRAS wild-type n = 61	KRAS mutant n = 49	P-value	No Atypical Cytology n = 80	Atypical Cytology n = 30	P-value
Age (range, mean)	33-85, 59	34-85, 60	33-79, 59	0.66	33-85, 60	37-79, 59	0.87
Postmenopausal	97 (88%)	53 (87%)	44 (90%)	0.64	69 (86%)	28 (93%)	0.31
Involving a Polyp	69 (63%)	39 (64%)	30 (61%)	0.77	53 (66%)	16 (53%)	0.21
Subsequent Hysterectomy	59 (53.5%)	24 (39%)	35 (71%)	0.0007	33 (41%)	26 (87%)	<0.001
Follow-Up [mo] (range, mean)	0.7-106, 46	0.7-100, 44	7.3-106, 54	0.0539	0.7-106, 48	3.2-100, 51	0.59
KRAS mutant					33 (41%)	16 (53%)	0.26
Atypical Cytology	30 (27%)	14 (23%)	16 (33%)	0.256			
Subsequent Disease Progression:							
All Forms	35 (32%)	14 (23%)	21 (43%)	0.0259	16 (20%)	19 (63%)	<0.001
Atypical Hyperplasia	27 (25%)	13 (21%)	14 (29%)	0.14	12 (15%)	15 (50%)	<0.001
Carcinoma	8 (7.2%)	1 (1.6%)	7 (14.3%)		4 (5%)	4 (13%)	
Time to Subsequent Disease in Months (range, mean):							
All Forms	0.47-37.9, 4.3	0.7-12.3, 3.1	0.47-37.9, 5.0	0.32	1.5-15, 4.8	0.5-37.9, 3.9	0.65
Atypical Hyperplasia	0.7-38.6, 4.6	0.7-12.3, 3.2	1.1-38.6, 5.9	0.34	1.5-15, 4.8	0.7-38.6, 4.4	0.88
Carcinoma	0.47-11.4, 3.6	2.4-2.4, 2.4	0.47-11.4, 3.8		1.9-11.4, 4.8	0.5-4.5, 2.4	0.39
Rate of Progression-Free Survival at 60 months [95% confidence interval, upper and lower]	66.8% [57.7-75.9%]	76.1% [65.2-87.1%]	56.1% [41.9-70.3%]	0.041	79.2% [70.2-88.3%]	35.4% [17.8-52.9%]	<0.001

Figure 1 - 944



**Conclusions:** Presence of KRAS mutation and/or cytological atypia is significantly associated with concurrent or subsequent development of AH or EC. KRAS mutation testing of CMC may offer an added value for disease prognostication.

#### 945 Molecular and Clinicopathologic Characterization of HER2-Overexpressed and HER2/neu-Amplified Squamous Cell Carcinoma of the Cervix

Rachelle Mendoza<sup>1</sup>, Anusha Vemuri<sup>1</sup>, Kristina Doytcheva<sup>1</sup>, Elmer Gabutan<sup>2</sup>, Raavi Gupta<sup>3</sup>, Natalie Briese<sup>1</sup>, Lisa Brannon<sup>1</sup>, Anum Shahid<sup>1</sup>, Kristin Petras<sup>4</sup>, Carrie Fitzpatrick<sup>1</sup>, Minhaz Ud-Dean<sup>5</sup>, Jeremy Segal<sup>1</sup>, Peng Wang<sup>6</sup>, Ricardo Lastra<sup>1</sup>

<sup>1</sup>University of Chicago, Chicago, IL, <sup>2</sup>SUNY Downstate Health Sciences University, Brooklyn, NY, <sup>3</sup>SUNY Downstate Medical Center, Brooklyn, NY, <sup>4</sup>University of Chicago, Chicago, IL, <sup>5</sup>University of Chicago Medical Center, Chicago, IL, <sup>6</sup>University of Chicago Medicine, Chicago, IL

**Disclosures:** Rachelle Mendoza: None; Anusha Vemuri: None; Kristina Doytcheva: None; Elmer Gabutan: None; Raavi Gupta: None; Natalie Briese: None; Lisa Brannon: None; Anum Shahid: None; Kristin Petras: None; Carrie Fitzpatrick: None; Minhaz Ud-Dean: None; Jeremy Segal: None; Peng Wang: None; Ricardo Lastra: None

**Background:** HER2/neu (HER2) amplification in cervical cancers ranges from 1-12% and has been associated with worse clinical prognosis. Pre-clinical studies have shown efficacy of various HER2 inhibitors in HER2-amplified cervical cancers.

Immunohistochemistry (IHC) for HER2 receptor has been a universally accepted surrogate test for HER2 amplification, however there is no standardized immunohistochemistry scoring system for cervical carcinomas. In this study, we investigated HER2

overexpression in cervical squamous cell carcinoma, and correlated it with *HER2* amplification by fluorescent in situ hybridization (FISH) and molecular methods.

**Design:** 72 cases of cervical squamous cell carcinoma were retrospectively reviewed and two representative tumor sections were retrieved and stained for *HER2*. *HER2* scoring was performed using the breast criteria, and cases with moderate (2+) to strong (3+) expression were analyzed for *HER2* amplification by FISH, followed by molecular analysis using a 168-gene next-generation sequencing (NGS) panel on *HER2*-amplified cases. DNA extraction, DNA quantification, library preparation and sequencing were performed as described (Kadri S. et al, 2017).

**Results:** The average age at diagnosis was 50 years (range 27-85), and most patients were African American (73.6%) and diagnosed at FIGO stage I (65.3%) (Table 1). 19 cases (26.4%) had 2+ *HER2* expression and 4 (5.5%) had 3+ expression. Three of 4 cases with 3+ expression had enough tumor for FISH and all 3 were amplified (Figure 1). Three cases with moderate expression showed *HER2* polysomy on FISH, and 12 did not show any amplification. Higher tumor grade and regional lymph node metastasis had significant correlation with both *HER2* overexpression ( $p=0.023$  and 0.010, respectively) and *HER2* FISH amplification ( $p=0.027$  and  $<0.001$ , respectively). Increased depth of invasion and higher tumor stage were associated with *HER2* amplification ( $p=0.047$  and 0.004, respectively). *HER2* amplification trended towards significance for survival. NGS of the *HER2*-amplified tumors showed amplification of *CD274*, *JAK2*, *BIRC3*, and *ERBB2* (equivocal), and *PIK3CA* missense mutation. All tested positive for HPV (two HPV 16, one HPV 18).

Table 1. Clinicopathologic features of patients with squamous cell carcinoma of the cervix based on *HER2* expression and *HER2* FISH amplification.

Categories	All N=72	HER2 expression by immunohistochemistry					<i>HER2/neu</i> amplification by FISH (N=18)					
		Negative N=29		1+ N=20		2+ N=19		3+ N=4		Not amplified N=12	Polysomy N=3	Amplified N=3
Age, years, median (range)	50 (27-85)	48 (27-75)	53.5 (36-85)	48 (30-65)	60 (31-67)	44.5 (30-61)	48 (35-65)	49 (31-67)				
Race, n(%)	African American 53 (73.6)	24 (82.8)	16 (80.0)	10 (52.6)	3 (75.0)	5 (41.7)	1 (33.3)	2 (66.7)				
	Caucasian 14 (19.4)	1 (3.4)	4 (20.0)	8 (42.1)	1 (25.0)	6 (50)	2 (66.7)	1 (33.3)				
	Other 5 (6.9)	4 (13.7)	0 (0)	1 (5.3)	0 (0)	1 (8.3)	0 (0.0)	0 (0.0)				
HPV test, n(%)	Unknown 27 (37.5)	9 (31.0)	9 (45.0)	7 (36.8)	2 (50.0)	6 (50.0)	1 (33.3)	2 (66.7)				
	Positive 45 (62.5)	20 (69.0)	11 (55.0)	12 (63.2)	2 (50.0)	6 (50.0)	2 (66.7)	1 (33.3)				
FIGO Stage, n(%)	I 47 (65.3)	18 (62.1)	12 (60.0)	14 (73.7)	3 (75.0)	10 (83.3)	2 (66.7)	2 (66.7)				
	II 11 (15.3)	3 (10.3)	4 (20.0)	3 (15.8)	1 (25.0)	2 (16.7)	0 (0.0)	1 (33.3)				
	III 7 (9.7)	5 (17.2)	2 (10.0)	0 (0.0)	0 (0.0)	0 (0.0)	0 (0.0)	0 (0.0)				
	IV 7 (9.7)	3 (10.3)	2 (10.0)	2 (10.5)	0 (0.0)	0 (0.0)	1 (33.3)	0 (0.0)				
Tumor size, greatest horizontal extent, cm (median, range)	2.15 (0.7-9.5)	1.5 (0.9-4.2)	2.4 (1.2-3.5)	2.0 (0.7-9.5)	4.1 (2.7-5.5)	2.0 (0.7-9.5)	n/a	4.1 (2.7-5.5)				
Tumor size, greatest depth, cm (median, range)	0.7 (0.3-2.7)	0.6 (0.6-1.2)	0.6 (0.3-1.4)	0.8 (0.5-2.5)	2.7 (2.7-2.7)	0.8 (0.5-2.5)	n/a	2.7 (2.7-2.7)				
Tumor grade, n(%)	Well 8 (11.1)	2 (6.9)	1 (5.0)	5 (26.3)	0 (0.0)	2 (16.7)	1 (33.3)	0 (0.0)				
	Moderate 28 (38.9)	9 (31.0)	9 (45.0)	10 (52.6)	0 (0.0)	7 (58.3)	2 (66.7)	0 (0.0)				
	Poor 36 (50.0)	18 (62.1)	10 (50.0)	4 (21.1)	4 (100.0)	3 (25.0)	0 (0.0)	3 (100.0)				
Recurrence, n(%)	No 49 (68.1)	18 (62.1)	14 (70.0)	14 (73.7)	2 (50.0)	10 (83.3)	2 (66.7)	2 (66.7)				
	Yes 18 (25.0)	8 (27.6)	5 (25.0)	4 (21.1)	1 (25.0)	1 (8.3)	1 (33.3)	1 (33.3)				
	Lost to follow up 6 (8.3)	3 (10.3)	1 (5.0)	1 (5.3)	1 (25.0)	1 (8.3)	0	0 (0.0)				
Status at follow-up, n(%)	Alive 51 (70.8)	20 (69.0)	15 (75.0)	14 (73.7)	2 (50.0)	10 (83.3)	2 (66.7)	2 (66.7)				
	Died of disease 13 (18.1)	6 (20.7)	2 (10.0)	4 (21.1)	1 (25.0)	1 (8.3)	1 (33.3)	1 (33.3)				
	Died of other cause 2 (2.8)	0 (0.0)	2 (10.0)	0 (0.0)	0 (0.0)	0 (0.0)	0 (0.0)	0 (0.0)				
	Lost to follow up 6 (8.3)	3 (10.3)	1 (5.0)	1 (5.3)	1 (25.0)	1 (8.3)	0 (0.0)	0 (0.0)				
Progression-free survival, months, median (range)	42.4 (0.4-60.0)	14.7 (1.0-60.0)	60.0 (3.6-60.0)	47.9 (0.43-60.0)	53.8 (47.6-60.0)	60.0 (3.5-60.0)	40.3 (0.43-60.0)	53.8 (47.6-60.0)				
Overall survival, median (range)	46.6 (0.4-60.0)	31.2 (1.0-60.0)	60 (3.6-60.0)	47.9 (0.43-60.0)	53.8 (47.6-60.0)	60.0 (3.5-60.0)	40.3 (0.43-60.0)	53.8 (47.6-60.0)				

Figure 1 - 945

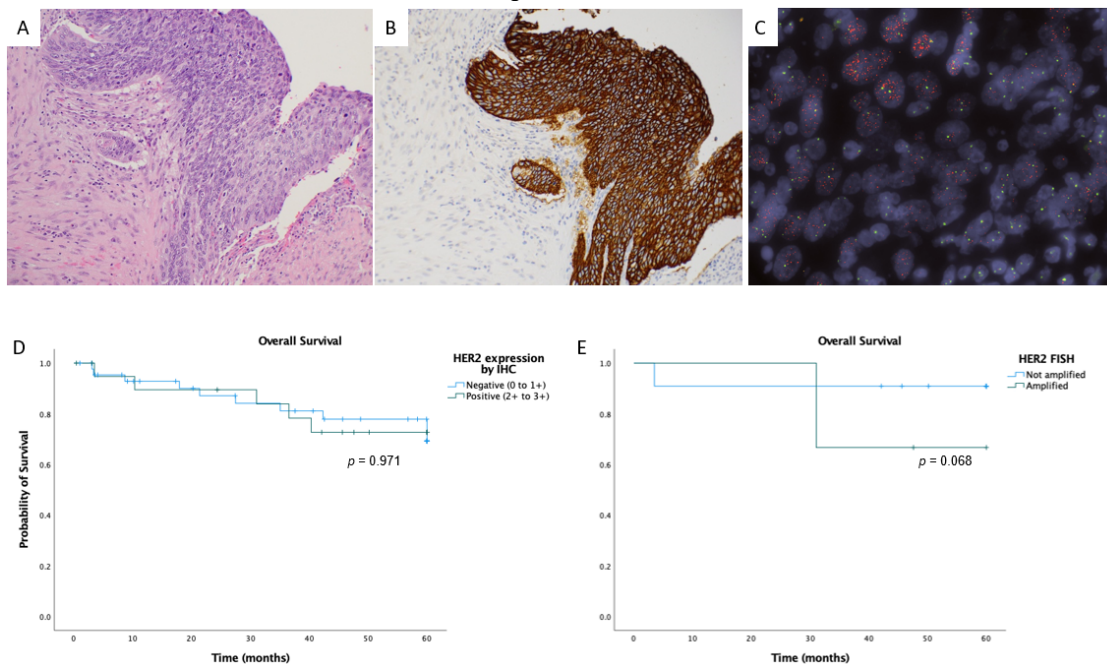


Figure 1. A-C: Cervical squamous cell carcinoma with HER2 overexpression. A: H&E morphology (200x); B: HER2 immunohistochemistry shows strong, circumferential membranous (3+) expression in almost 100% of tumor cells; C: Corresponding FISH showed HER2 amplification (red probe) in tumor cells. D: Kaplan-Meier curve showing overall survival of patients based on HER2 expression by IHC. E: Kaplan-Meier curve showing overall survival of patients based on HER2 amplification, demonstrating trend towards significance.

**Conclusions:** HER2 immunohistochemistry is a reliable predictive marker of HER2 gene amplification in squamous cell carcinoma of the cervix. HER2 overexpression and/or HER2 amplification are associated with poor prognostic factors, such as increased tumor grade, size, and depth of invasion, as well as nodal metastasis.

#### 946 Lymphovascular Space Invasion (LVSI) to Guide Adjuvant Treatment in Endometrial Carcinoma (EC) – Assessment with and without the Use of Vascular Markers

Charlotte Meyer<sup>1</sup>, Marcel Grube<sup>1</sup>, Karen Greif<sup>1</sup>, Teresa Praetorius<sup>1</sup>, Friedrich Kommooss<sup>2</sup>, C. Blake Gilks<sup>3</sup>, Annette Staebler<sup>1</sup>, Stefan Kommooss<sup>1</sup>, Naveena Singh<sup>4</sup>

<sup>1</sup>Tübingen University Hospital, Tübingen, Germany, <sup>2</sup>Institute of Pathology, Friedrichshafen, Friedrichshafen, Germany, <sup>3</sup>Vancouver General Hospital/University of British Columbia, Vancouver, BC, <sup>4</sup>Vancouver General Hospital, Vancouver, BC

**Disclosures:** Charlotte Meyer: None; Marcel Grube: None; Karen Greif: None; Teresa Praetorius: None; Friedrich Kommooss: None; C. Blake Gilks: None; Annette Staebler: None; Stefan Kommooss: None; Naveena Singh: None

**Background:** LVSI is known to be associated with an unfavourable outcome in EC. Recent studies have shown that distinguishing cases with "negative or focal" LVSI from cases with "substantial" LVSI is one of the strongest prognosticators of local as well as distant recurrence after primary therapy. Therefore, modern risk-assessment algorithms will have to include thorough LVSI quantification during routine histopathological workup. It was the aim of this study to investigate impact and interobserver variability of LVSI quantification in a consecutive series of EC in which LVSI had been reported to be positive after routine pathology assessment.

**Design:** EC patients (n=770) treated at the Tuebingen University Women's Hospital between 2003 and 2016 were identified. All cases in which LVSI had been reported as being "positive" after routine pathology assessment of hysterectomy specimens were independently reviewed by four experienced gynecopathologists according to current clinical practice (review of all tumor-containing H&E stained slides). A subset of cases was additionally submitted for D2-40 and CD31 immunohistochemistry (IHC). A final LVSI score was reached by majority vote of the expert panel.

**Results:** A total of 95 cases was available for this study. Interobserver variability after initial H&E scoring was high, with a total agreement reached in 47 of 95 (49.5%) cases. Additional IHC contributed to reaching total agreement. According to the final majority vote, LVSI was called substantial in 50/95 (53%) cases. In the latter subset of cases, 5-yr disease-specific survival (DSS) was 42%, in contrast to 74% in LVSI focal/negative cases. While established clinicopathological parameters were shown to be of

prognostic significance after univariate analyses, LVSI quantification was shown to be the only independent prognosticator after multivariate analyses in this cohort (HR 2.24; p=0.04).

**Conclusions:** The results of our study strongly support LVSI quantification in EC as a means to guide adjuvant treatment. IHC staining of vascular markers might help reduce interobserver variability in the assessment of LVSI. Further studies are warranted and may change future surgical pathology practice.

## 947 PLAG1-Rearranged Uterine Sarcomas Show a Wide Phenotypical Spectrum Encompassing but Not Limited to Myxoid Leiomyosarcoma-like Morphology and Frequently Exhibit Heterologous Differentiation: A Study of 8 Cases

Michael Michal<sup>1</sup>, John Schoolmeester<sup>2</sup>, Abbas Agaimy<sup>3</sup>, Gunhild Mechtersheimer<sup>4</sup>, Debra Bell<sup>5</sup>, Sounak Gupta<sup>5</sup>, Elaheh Mosaieby<sup>6</sup>, Kvetoslava Michalova<sup>1</sup>, Michal Michal<sup>1</sup>, Ondrej Ondic<sup>1</sup>

<sup>1</sup>Biopticka laborator s.r.o., Plzen, Czech Republic, <sup>2</sup>Mayo Clinic, FL, <sup>3</sup>Universitätsklinikum, Erlangen, Germany, <sup>4</sup>Institute of Pathology, Heidelberg University Hospital, <sup>5</sup>Mayo Clinic, Rochester, MN, <sup>6</sup>Charles University, Faculty of Medicine in Plzen, Plzen, Czech Republic

**Disclosures:** Michael Michal: None; John Schoolmeester: None; Abbas Agaimy: None; Gunhild Mechtersheimer: None; Debra Bell: None; Sounak Gupta: None; Elaheh Mosaieby: None; Kvetoslava Michalova: None; Michal Michal: None; Ondrej Ondic: None

**Background:** A recent molecular study of myxoid uterine leiomyosarcomas (M-LMS) reported that almost 1/3 of cases harbor *PLAG1* fusions. A single additional report described M-LMS with *PLAG1* fusion and osteosarcomatous and liposarcomatous (LPS) differentiation. Triggered by a case of *PLAG1*-rearranged uterine sarcoma (PLAG1-US) lacking convincing expression of smooth muscle markers (SMM), we decided to study a larger cohort of these tumors.

**Design:** Cases of PLAG1-US irrespective of their histology were collected from 4 different institutions and reviewed with a particular focus on their morphology and the presence of convincing smooth muscle immunophenotype (SMI) defined by the expression of at least 2 SMM.

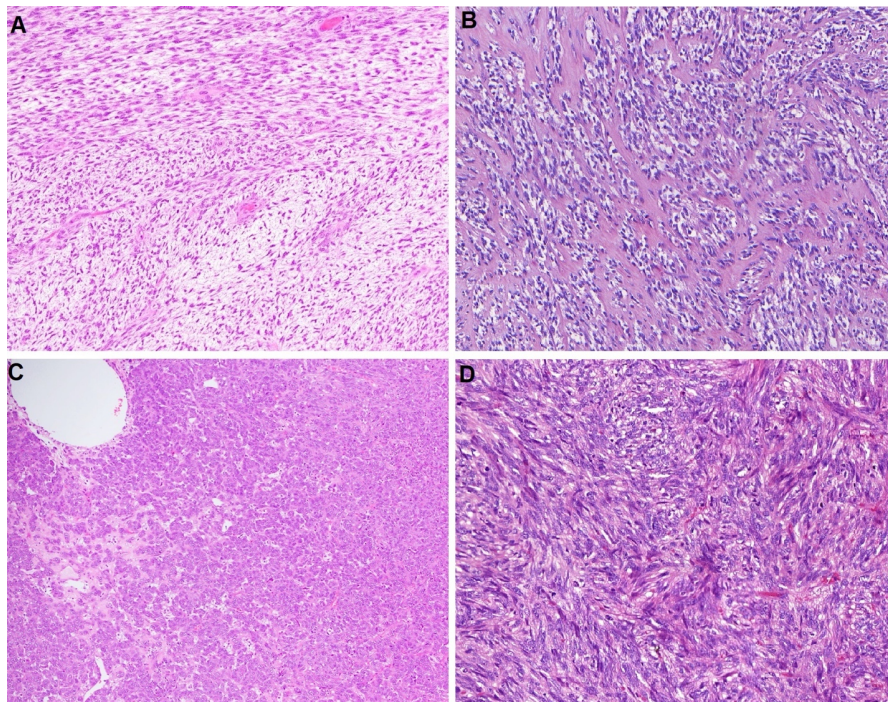
**Results:** Eight cases of PLAG1-US were collected; their features are summarized in Table. Patients ranged in age from 38-67 years (mean: 54.4). All tumors were centered to the uterine corpus and ranged in size from 6.5-32 cm (mean: 17.8). Most were treated by hysterectomy with salpingectomy/adnexitomy. All 4 cases with follow-up behaved aggressively (recurred/metastasized). Morphologically, the tumors showed a high intertumoral but also intratumoral heterogeneity which was also noted between primary lesions and recurrences/metastases. M-LMS-like morphology was present in only 2 of the primaries; cases 1 and 7 showed such areas in the metastases. Most tumors consisted of variably ovoid/spindled to epithelioid cells growing predominantly in solid sheets. In some cases, the stroma was prominently hyalinized or partially myxoid. High-grade myxoid LPS-like areas were present in the metastasis in case 7; case 8 showed myxoid LPS-like (both low and high-grade) and chondrosarcomatous (CHS) areas. Metastasis in case 1 also exhibited foci of ambiguous adipocytic differentiation (with focal S100 expression). Immunohistochemically, cases 1, 2, and 4 did not exhibit a convincing SMI. The metastasis in case 7 showed diffuse S100 protein expression while lacking SMI. All 6 different fusion partners detected were novel in this tumor type. In case 8, only PLAG1 FISH was performed. Tumor mutation burden was assessed in 2 cases, being high (12.3 mut/MB) in one case and low (4 mut/MB) in the other.

# ABSTRACTS | GYNECOLOGIC AND OBSTETRIC PATHOLOGY

Case Nr.	Age (yrs)	Size (cm)	Morphology	Desmin/ h-CD/SMA	Other IHC	Fusion partner and TMB	Treatment and outcome
1	57	13x12 x3	<b>Primary:</b> spindle cell tumor with stromal hyalinization; <b>Abdominal lesions:</b> Myxoid LMS-like + non-myxoid spindle cell sarcoma with ambiguous adipocytic differentiation	-/-/focal	<b>Positive:</b> PLAG1 and CD10 (both diffuse strong), S100 (focal/patchy); <b>Negative:</b> DDIT3, ALK, DOG1, CD117	<i>PUM1</i> ; High (12.3 mut/MB)	HE by morcellation + AE; 4x recurrence in pelvis + intraabdominal spread - resection + CHT
2	61	32	Myxoid LMS-like	-/-	<b>Negative:</b> ALK	<i>C15orf29</i> ; low (4 mut/MB)	HE, pelvic recurrence - resection
3	45	6.5	Epithelioid/spindled cells in solid sheets with focal myxoid change	+/-/++	<b>Positive:</b> ER, PR, WT1, Cyclin D1 (weak and patchy); <b>Negative:</b> HMB45, pankeratin, CD10, SF1, Melan-A, calretinin, BCOR, panTRK, ALK	<i>CD44</i>	HE + SE; F-U NA
4	57	20	Round/ovoid cells in solid sheets	+/-/-	<b>Positive:</b> ER, PR, CD34, Cyclin D1, CD10 (Patchy); <b>Negative:</b> CD117, ALK, BCOR, MyoD1, Myogenin, S100 protein	<i>CHCD7</i>	HE + AE; F-U NA
5	44	~14	Epithelioid LMS-like with stromal hyalinization	++/ND/+	<b>Positive:</b> CAM5.2, AE1/AE3 (patchy weak), CD10 (focal); <b>Negative:</b> S100, INSM1, SF1, Inhibin, Calretinin, myogenin, MYOD1	<i>MYOCD</i>	HE + SE, L OE; F-U NA
6	67	14.5	Spindle cell sarcoma	+++/+++/+++	<b>Positive:</b> ER (diffuse); PR (focal); <b>Negative:</b> CD10, CyclinD1, CD34, ALK, S100, pankeratin, MUC4, TFE3, panTRK	<i>FRMD6</i>	NA
7	66	18	<b>Primary:</b> epithelioid LMS-like; <b>Mets:</b> epithelioid LMS-like + myxoid LMS-like + high-grade myxoid LPS-like areas	<b>2017 mets:</b> +/-/++; <b>2022 mets:</b> neg/-/neg	<b>Positive:</b> S100 protein (diffuse strong); CD10 and CD34 (both focal); <b>Negative:</b> SOX-10; Melan A; HMB45; Cyclin D1; ER; PR; DOG1; CD117; STAT6; CD31; ERG	<i>PUM1</i>	HE + L-AE + adjuvant RT; pulmonary + abdominal mets - resection, CHT
8	38	23x 20x 12	<b>Primary:</b> Myxoid LMS-like + low and high-grade myxoid LPS-like + CHS	+/-/++	<b>Positive:</b> PLAG1 (diffuse), CD10 (patchy) <b>Negative:</b> S100 protein, SOX10 AE1/3, EMA	<i>PLAG1</i> FISH only	HE + AE; peritoneal spread - resection; lung + mediastinal mets - resection + CHT; died

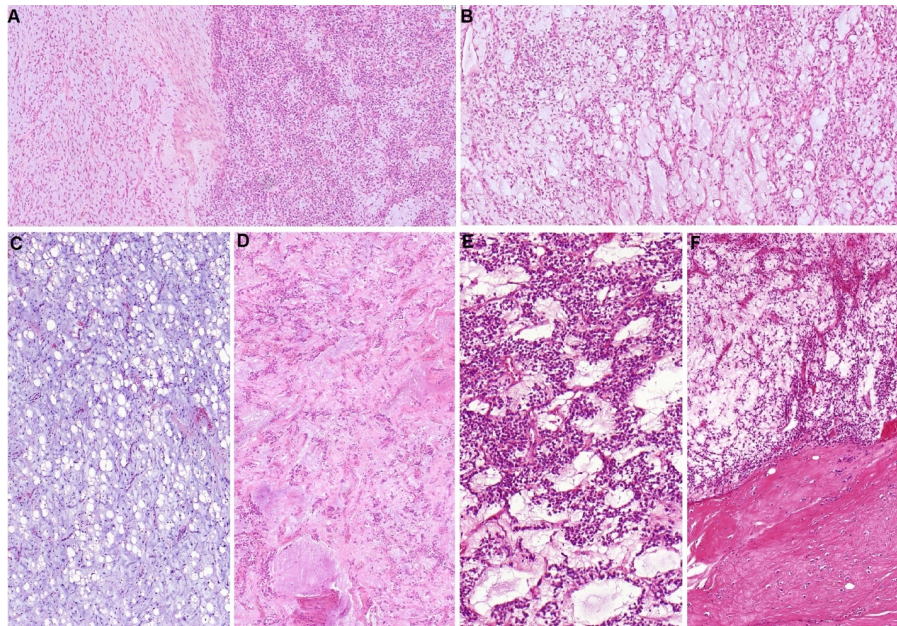
**LEGEND:** HE - hysterectomy; SE - salpingectomy; OE - oophorectomy; AE - adnexectomy; RT - radiotherapy; CHT - chemotherapy; F-U - follow-up; ND - not done; LPS - liposarcoma; LMS - leiomyosarcoma; CHS - chondrosarcoma; NA - not available; h-CD: heavy caldesmon; TMB - tumor mutational burden; **DEFINITION:** focal+ positivity in up to 5% of cells; +: positivity in 6-33% of cells; ++: positivity in 34-66% of cells; +++: positivity in 67-100% of cells

Figure 1 - 947



A.: Case 2 showed M-LMS-like morphology but completely lacked SMI. B: The primary tumor in case 1 showed spindle cell sarcoma pattern with stromal hyalinization. C: Case 5 with epithelioid LMS-like morphology. D: Case 6 had features of uncharacteristic spindle cell sarcoma.

Figure 2 - 947



A: Case 7 showing transition from myxoid LMS-like into high-grade myxoid LPS-like areas. B: High-grade myxoid LPS-like areas with visible adipocytic differentiation in case 7. C, D: Case 8 with areas somewhat resembling low-grade myxoid LPS. E: High-grade myxoid LPS-like areas in case 8. F: In some parts, this component showed transition into chondrosarcoma

**Conclusions:** PLAG1-US tend to present as large uterine masses and frequently behave aggressively. Their heterogeneous morphology encompasses a much broader spectrum than previously reported, and also includes heterologous CHS or adipocytic/LPS differentiation. Many cases lack convincing SMI or expression of SMM altogether.

## 948 Interobserver Agreement on the Interpretation of Programmed Death-ligand 1 (PD-L1) Combined Positive Score (CPS) among Gynecologic Pathologists

Anne Mills<sup>1</sup>, Jennifer Bennett<sup>2</sup>, Natalie Banet<sup>3</sup>, Debamita Kundu<sup>4</sup>, Jaclyn Watkins<sup>5</sup>, Andre Pinto<sup>6</sup>

<sup>1</sup>University of Virginia, Charlottesville, VA, <sup>2</sup>University of Chicago, Chicago, IL, <sup>3</sup>Cleveland Clinic, Cleveland, OH, <sup>4</sup>University of Virginia Health System, Charlottesville, VA, <sup>5</sup>Massachusetts General Hospital, Harvard Medical School, Boston, MA, <sup>6</sup>University of Miami Health System, Miami Beach, FL

**Disclosures:** Anne Mills: None; Jennifer Bennett: None; Natalie Banet: None; Debamita Kundu: None; Jaclyn Watkins: None; Andre Pinto: None

**Background:** The anti-PD-1 checkpoint inhibitor pembrolizumab is FDA-approved for the treatment of cervical carcinoma with a PD-L1 Combined Positive Score (CPS) of  $\geq 1$ . We aimed to evaluate PD-L1 expression in the most common histologic types of cervical carcinoma, and assess interobserver agreement in CPS to identify whether it may impact patient selection for immunotherapeutic candidacy.

**Design:** 29 cervical carcinomas (18 squamous cell carcinomas [SCC], 6 HPV-associated adenocarcinomas [HPVA], 3 adenosquamous carcinomas [ASC], 1 mixed squamous and small cell carcinoma, and 1 small cell carcinoma) represented on cervical biopsy/endocervical curettage (7), cone/LEEP (10), hysterectomy (11), and lung biopsy (1) were stained for PD-L1 (Dako 22C3). Glass slides corresponding to whole-tissue sections were interpreted by 5 subspecialty-trained gynecologic pathologists with experience reading PD-L1 immunohistochemistry. Expression was scored using the CPS and read out as positive ( $\geq 1$ ) or negative ( $< 1$ ); in positive cases, a final score was assigned (0-100).

**Results:** There was consensus agreement across all five pathologists for 90% (26/29) of cases (Light's Kappa interobserver agreement: 0.799). Of the 26 with consensus, 88% (23/26) were positive and 12% (3/26) were negative. 100% (16/16) of SCC with consensus were interpreted as positive, whereas tumors with glandular components (HPVA, ASC) were commonly consensus negative (33%, 3/9); this difference was significant ( $p=0.037$ ). Biopsy cases more often had a consensus negative read than LEEP/cones or resections, however this trend was not significant (29%, 2/7 versus 5%, 1/19,  $p=0.167$ ). The three cases with disagreement were comprised of two SCC and one small cell carcinoma. One case was called negative by three readers, while the other two were called negative by a single reader. Disagreements were attributable to low CPS versus negative reads (2 cases) and difficulty discerning glandular involvement from pushing invasion (1 case).

**Conclusions:** Experienced gynecologic pathologists show substantial interobserver agreement in the interpretation of PD-L1 CPS at the FDA-approved treatment threshold, with the majority of tumors interpreted as positive. Pure squamous histology was strongly associated with a consensus positive read, whereas a subset of tumors with glandular differentiation were negative by all readers. Disagreements occurred in tumors with low versus negative CPS values and in the setting of limited invasion.

## 949 Immunohistochemical Expression of HIK1083 in Ovarian Epithelial Malignant Tumors

Jelena Mirkovic<sup>1</sup>, Anna Plotkin<sup>2</sup>, Dina Bassiouny<sup>3</sup>, Fang-I Lu<sup>1</sup>, Bojana Djordjevic<sup>3</sup>, Sharon Nofech-Mozes<sup>3</sup>

<sup>1</sup>Sunnybrook Health Sciences Centre, University of Toronto, Toronto, ON, <sup>2</sup>University of Toronto, Toronto, ON, <sup>3</sup>Sunnybrook Health Sciences Centre, University of Toronto, Toronto, Ontario

**Disclosures:** Jelena Mirkovic: None; Anna Plotkin: None; Dina Bassiouny: None; Fang-I Lu: None; Bojana Djordjevic: None; Sharon Nofech-Mozes: None

**Background:** Immunohistochemistry expression of HIK1083, a component of pyloric-type mucin, has been used as a specific marker of gastric-type endocervical carcinoma in the context of gynecologic malignancies. HIK1083 immunohistochemical expression in primary ovarian epithelial malignant tumors was previously evaluated only in limited case series. Our aim was to comprehensively analyze HIK1083 immunohistochemical expression in a large cohort of ovarian epithelial malignant tumors. As a secondary objective, we examined HIK1083 expression in metastasis to the ovary from colonic and appendiceal primaries.

**Design:** Tissue microarrays consisting of two 2mm tissue cores of each of the ovarian epithelial malignant tumors including high grade serous (HGSC), low grade serous (LGSC), high grade endometrioid (HGEC), low-grade endometrioid (LGEC), clear cell (CCC), mucinous (MC) carcinomas, as well as appendiceal/colonic metastatic carcinomas secondarily involving the ovary were stained for HIK1083. Cytoplasmic staining intensity (weak, moderate, strong) and percentage of tumor cells staining was recorded. Any staining in  $\geq 1\%$  of cells was considered positive.

**Results:** A total of 699 primary ovarian epithelial malignant tumors including 434 HGSC, 34 LGSC, 55 HGEC, 43 LGEC, 89 CCC, 36 MC, and 8 carcinosarcoma and 91 metastatic carcinomas to the ovary (47 colonic and 44 appendiceal) were evaluated. Overall 3/699 (0.4%) of primary ovarian cases and none of the metastatic cases demonstrated HIK103 expression. There were only 3 positive cases, all in the primary mucinous carcinoma category (3 of 36, 8%). All three cases exhibited strong apical and focal cytoplasmic staining in 5, 40, and 70% of the cells, respectively. All three of these cases had tumor limited to the ovary (T1a

stage); two patients had hysterectomy demonstrating benign cervix and one patient had been followed for 9 years with no evidence of cervical cancer.

**Conclusions:** HIK1083 is rarely expressed in primary ovarian epithelial malignancies (only 0.4% of the overall cases, limited to mucinous carcinomas). However, 8% of primary mucinous carcinomas in our cohort showed HIK1083 expression. Therefore, even though HIK1083 expression is highly correlated with gastric-type cervical carcinoma in the literature, in the work up of carcinoma involving the ovary, our results show that it is not an unequivocal marker of metastatic carcinoma with gastric-type differentiation.

## 950 Clinico-pathologic Spectrum of Neuroendocrine Neoplasms of the Cervix with Special Emphasis on the Applicability of the Revised Classification System

Neha Mittal<sup>1</sup>, Santosh Menon<sup>1</sup>, Bharat Rekhi<sup>2</sup>, Kedar Deodhar<sup>1</sup>

<sup>1</sup>Tata Memorial Hospital, Mumbai, India, <sup>2</sup>Tata Memorial Centre, Mumbai, India

**Disclosures:** Neha Mittal: None; Santosh Menon: None; Bharat Rekhi: None; Kedar Deodhar: None

**Background:** The classification of the neuroendocrine neoplasms (NEN) has undergone a monumental change for ease of applicability and site-agnostic uniformity of terminology. Thus, the present classification, based on Pancreatic NEN, classifies NENs of cervix as neuroendocrine tumors (NET; G1,2 or 3), neuroendocrine carcinomas, NECs (Small cell neuroendocrine carcinoma, SCNEC and Large cell neuroendocrine carcinoma, LCNEC), and mixed neuroendocrine non-neuroendocrine carcinomas (MiNENs).

**Design:** A retrospective observational study with a detailed review of clinical and histological parameters of Cervix NEN cases diagnosed from Jan 2018 till date (55 months) was undertaken.

**Results:** A cohort of 40 women, mean age of 51.1years, were diagnosed with NET/NEC. Bleeding per vaginum was the most common symptom. On imaging, tumor size ranged from 2.5-13 cm (mean size: 6.15cm) with lower uterine segment, vaginal and parametrial involvement in 58.1%, 61.8%, and 81.25% respectively. On histopathology, 50% were SCNEC, 25% LCNEC, NET G3 in 5%(2/40), mixed carcinomas in 17.5% (7/40), and MiNEN in 2.5%(1/40) cases. Of the mixed carcinomas, 5 were mixed (not separate) adenocarcinoma and NEC, and 2 were mixed SCNEC and LCNEC. Lymphoepithelial histology was seen in 2 LCNEC, a hitherto unreported finding. Necrosis (90%) and mitoses>10/10hpf (100%)were frequent findings. On immunohistochemistry (IHC), all (100%) cases were positive for keratins, 92.1% for synaptophysin, 91.7% for INSM1, 80% for chromogranin, and 72.7% for p16. NKX2.2 was positive in both the cases tested. Ki-67 positivity ranged from 35-90% tumor cells. Only 15.1% were FIGO stage 1. Lymph node and distant metastases (DM) were seen in 65.2% and 60.9% cases; lung (57.1%) being the most common site. Trimodality therapy with curative intent was completed in 4, 2 of whom developed recurrences within 6 months of therapy completion.

Parameters	Results
<b>Age in years: Mean (Range)</b>	51.1 (30-86years)
<b>Menstrual status: n (%)</b> Perimenopausal Premenopausal Postmenopausal	8/40 (25%) 13/40 (32.5%) 19/40 (47.5%)
<b>Predominant Symptom: n (%)</b> Bleeding per vaginum Heavy periods White discharge	28/37 (75.7%) 2 (5.4%) 7/37 (18.9%)
<b>Site of tumor: n (%)</b> Cervix only LUS involvement Vaginal involvement Parametrial involvement Bladder and/or Rectal fat stranding	4/36 (11.1%) 18/31 (58.1%) 27/34 (79.4%) 26/32(81.25%) 6/30 (20%)
<b>Tumor size in cms: Mean (range)</b>	2.5-13 cm (mean: 6.15 cm)
<b>FIGO stage: n(%)</b> Stage I Stage II Stage III Stage IV	5 (15.1%) 6 (18.2%) 9 (27.3%) 13 (39.4%)
<b>Lymph node metastasis at presentation: n (%)</b> Present Absent	16/23 (65.2%) 7/23 (30.4%)
<b>Distant metastasis at presentation: n (%)</b>	14/23 (60.9%)
<b>Site of distant metastasis (DM)</b> Lung	8/14 (57.1%) 4/14 (28.6%)

# ABSTRACTS | GYNECOLOGIC AND OBSTETRIC PATHOLOGY

Liver	2/14 (14.3%)
Bone	4/14 (28.6%)
Non regional nodes	1/14 (7.14%)
Adrenal	
<b>Number of cases with &gt;1 site of DM</b>	42.9%
<b>Histology: n (%)</b>	20/40 (60%)
SCNEC	10/40 (12%)
LCNEC	7/40 (8%),
Mixed Carcinoma	5/7; LCNEC in 2 and SCNEC in 3 as the NEC component
Mixed carcinoma: Adenocarcinoma+NEC	2/7
Mixed carcinoma: SCNEC+LCNEC	2/40(5%), one pure and one mixed with SCNEC and LCNEC areas
NET, Gr 3	1/40(2.5%)
MINEN	
<b>Unusual Histology: n (%)</b>	2/40 (5%)
Bizarre giant cells	2/40 (5%)
Lymphoepithelial histology (both LCNEC)	2 (5%)
Rhabdoid histology	
<b>Necrosis: n (%)</b>	36/40 (90%)
Present	4/40 (10%)
Absent	
<b>Mitosis &gt;10/10HPF: n (%)</b>	40/40 (100%)
Present	0 (0%)
Absent	
<b>Immunohistochemistry:</b>	Positive: 32/32; EMA>AE1/AE3: 4/4 (100%)
Keratins	Positive: 35/38 (92.2%)
Synaptophysin	Negative: 3/38 (7.8%)
Chromogranin	Positive: 28/35 (18; diffuse, 10; focal)
INSM1	Negative: 7/35
P16	Positive: 12/13 (91.7%)
	Negative: 1/13 (8.3%)
	Positive: 13/22 (59.1%)
	Negative: 7/22 (31.8%)
	Equivocal: 2/22 (9.1%)
<b>Treatment: n (%)</b>	8/32 (25%)
Surgery	15/32 (46.9%)
NACT	14/32 (43.7%)
CTRT	5/32 (15.6%)
Brachytherapy	15/32 (46.9%)
Palliative therapy (upfront or for progression)	

**Conclusions:** NENs in cervix are uncommon; a vast majority comprising of NECs. NETs, though described are exceedingly rare, are almost always NET, G3 in type; either pure or mixed with NECs. Majority of the mixed carcinomas are characterized by an admixture of the various areas, thus defying the rules of classification as MINEN in the current classification system. A panel of immunohistochemical markers are required for diagnoses. LCNEC is frequently misdiagnosed due to variant histologies. Despite multimodality treatment, the outcomes are uniformly dismal, necessitating a larger, multicentric evaluation of NENs of the cervix.

## 951 Transcriptomic and Proteomic Characterization of Myxoid and Epithelioid Uterine Leiomyosarcoma Reveals Potential Diagnostic Biomarkers

Cara Monroe<sup>1</sup>, Raul Maia Falcao<sup>2</sup>, Georgia Kokaraki<sup>2</sup>, Tirzah Braz Petta<sup>2</sup>, Joseph Carlson<sup>2</sup>

<sup>1</sup>Keck Hospital of USC, LAC+USC Medical Center, Los Angeles, CA, <sup>2</sup>Keck School of Medicine of USC, Los Angeles, CA

**Disclosures:** Cara Monroe: None; Raul Maia Falcao: None; Georgia Kokaraki: None; Tirzah Braz Petta: None; Joseph Carlson: None

**Background:** Uterine leiomyosarcoma (ULMS) is a rare, aggressive tumor, comprising only 3% of uterine corpus malignancies. According to the current WHO classification, these tumors are further subdivided into epithelioid (eLMS), myxoid (mLMS) and spindle (sLMS) subtypes, based entirely on morphologic criteria. Due to their rarity, the molecular underpinnings of eLMS and mLMS are almost entirely unknown. The goal of this project was to identify molecular similarities and differences at the RNA and protein level, in order to identify potential biomarkers that could aid in diagnosis.

**Design:** Fresh frozen samples of normal myometrium (MM) and uLMS subtypes (31 MM, 17 sLMS, 3 eLMS, and 1 mLMS) underwent RNA sequencing and proteomic analysis. Expression values were calculated as Transcripts Per Million (TPM) using scater (R package). Differentially expressed genes (DEG) were analyzed with Qiagen Ingenuity Pathway Analysis (IPA) software. Proteomics analysis was performed using Proteome Discoverer and MSstatsTMT (R package).

**Results:** Transcriptomic analysis revealed a shared role for the *Kinetochore Metaphase Signaling* pathway, as well as upregulation of amphiregulin (AREG) in all uLMS subtypes. Amphiregulin (AREG) is an upstream regulator of the EGFR pathway overexpressed in advanced gynecological malignancies. Transcriptomic analysis further revealed that sLMS and eLMS were more similar to each other than mLMS. Furthermore, *NF Kappa Beta* presented as a common upregulated pathway for the sLMS and eLMS and *PI3*

# ABSTRACTS | GYNECOLOGIC AND OBSTETRIC PATHOLOGY

Kinase pathway was upregulated in the mLMS. Distinct, putative, diagnostic biomarkers were identified for each uLMS subtypes (p-values < 0.01). For eLMS, *S100A1* (log2FC: 12.0) and *HOXB13* (log2FC: 12.6); for sLMS, *ANKRD1*(log2FC: 11.2) and *PAX6* (log2FC: 11.3); and for mLMS, *SCUBE1* (log2FC: 8.2) and *IGFN1* (log2FC: 7.0) were identified. Proteomics analysis directly supports the *SCUBE1* RNA-seq mLMS findings.

**Conclusions:** These results are the first transcriptomic analysis of eLMS and mLMS, and serve to identify biomarkers between and within uLMS subtypes. AREG inhibitors have been studied for treatment of endometrial and ovarian malignancies, and may have a role in uLMS therapy, independent of subtype. The identification of candidate biomarkers may help with diagnosis of these tumors. Future studies will utilize these candidate biomarkers in development of immunohistochemical assays.

## 952 4-Gene Circulating Tumor Panel as a Potential Pre-operative Identification of Uterine Leiomyosarcoma

Manando Nakasaki<sup>1</sup>, Saleh Heneidi<sup>1</sup>, Jean Lopategui<sup>1</sup>, Bonnie Balzer<sup>1</sup>, Allan Silberman<sup>1</sup>

<sup>1</sup>Cedars-Sinai Medical Center, Los Angeles, CA

**Disclosures:** Manando Nakasaki: None; Saleh Heneidi: None; Jean Lopategui: None; Bonnie Balzer: None; Allan Silberman: None

**Background:** Uterine leiomyosarcoma (LMS) has a dismal prognosis and is nearly always unsuspected prior to resection for presumed leiomyoma (LM). Occult LMS is reported in 0.2% (1 in 500) women having surgery for fibroids. The major problem is that there is no reliable preoperative method to distinguish LMS from a LM or STUMP (smooth muscle tumor of uncertain malignant potential), and patient prognosis for LMS is even poorer if the tumor is transected, which occurs in procedures performed for LM. Our prior study demonstrated the feasibility of testing preoperative blood and identifying pathogenic variants of TP53 and matching those with LMS samples. TP53 alterations are reportedly associated with uterine LMS in 60-80% of cases, thus, the addition of a small set of genes would be required to increase sensitivity of testing while also increasing specificity by ruling out low level pathogenic TP53 due to other conditions such as clonal hematopoiesis of indeterminate potential.

**Design:** We previously evaluated TP53 circulating tumor DNA (ctDNA) by next-generation sequencing (NGS) in both plasma and formalin-fixed paraffin embedded tissue. We screened plasma for TP53 variants with pathologically confirmed LMS. FFPE samples were matched with plasma samples taken before surgery (when available). A retrospective analysis of LMS tissue was performed in our case list (n=13) and compared to LMS in COSMIC (n=254) and uterine LMS in TCGA (n=71) to identify a small panel that to potentially increase accurate detection of LMS by ctDNA.

**Results:** Most commonly co-mutated genes with TP53 are ATRX, RB1, and MED12, and while some cases overlap, these create three distinct subclasses or TP53-mutated LMS. When no TP53 was identified, ATRX and RB1 loss were the second and third most common alteration, respectively. The addition of ATRX, RB1, and MED12 would potentially increase the number of LMS detected by 20-40% and increase sensitivity to 80-90%. The detection of copy number loss would increase total cases by approximately 5-8%, although this can be technically demanding.

**Conclusions:** While detection of pathogenic TP53 variants by ctDNA is feasible, a panel including TP53, ATRX, RB1 and MED12 could potentially increase the sensitivity from 60-80% to over 90%. MED12 alterations are commonly identified in benign LM, but coupled with TP53, combinations of the 4 target genes would greatly reduce the potential for a TP53-associated low-level CHIP, which was a potential confounder for a single gene screening test.

## 953 Performance of HER2 DAKO HercepTest and Ventana 4B5 on Detecting HER2 Gene-Expression in Uterine Serous Carcinomas

Janira Navarro Sanchez<sup>1</sup>, Haley Tyburski<sup>2</sup>, Bradley Turner<sup>1</sup>, David Hicks<sup>1</sup>, Sharlin Varghese<sup>1</sup>, Xi Wang<sup>2</sup>, Hani Katerji<sup>1</sup>, Brian Finkelman<sup>1</sup>, Jack Chen<sup>2</sup>, Huina Zhang<sup>1</sup>

<sup>1</sup>University of Rochester Medical Center, Rochester, NY, <sup>2</sup>University of Rochester, Rochester, NY

**Disclosures:** Janira Navarro Sanchez: None; Haley Tyburski: None; Bradley Turner: None; David Hicks: None; Sharlin Varghese: None; Xi Wang: None; Hani Katerji: None; Brian Finkelman: None; Jack Chen: None; Huina Zhang: None

**Background:** Uterine serous carcinoma (USC) is an aggressive uterine carcinoma with few treatment options. Clinical trial results have demonstrated USC with HER2 overexpression/amplification may benefit from HER2-targeted therapy. However, there is no formal HER2 testing guidelines in USC. Few studies have evaluated USC HER2 gene amplification by in-situ hybridization (FISH), but they were limited to those cases with HER2 immunohistochemistry (IHC) 2+/3+. In this study, we compared the performance of two FDA-approved HER2 IHC stains, DAKO HercepTest and Ventana 4B5 clones and their correlation with Fluorescent ISH (FISH) for detection of HER2 gene amplification in USC.

# ABSTRACTS | GYNECOLOGIC AND OBSTETRIC PATHOLOGY

**Design:** Forty cases of USC were selected including 25 pure USC, 10 mixed tumors and 5 carcinosarcomas with a serous epithelial component. The cases were stained for DAKO HercepTest and Ventana 4B5 clones. HER2 IHC stained sections were interpreted based on the USC testing algorithm proposed by Buza et al., and the interpretation received consensus by 8 subspecialized breast and gynecological pathologists. HER2 FISH was performed in all cases by HER2 IQFISH pharmDx™ (DAKO) and were interpreted using 2018 HER2 testing guidelines in breast cancers.

**Results:** The correlation between IHC testing and FISH is illustrated in Table 1. All HER2 3+ positive cases with HercepTest and 4B5 were amplified by FISH. Interestingly, in HER2 IHC 0-1+ cases, 1 of 22 HER2 (5%) by HercepTest and 3 of 26 (11.5%) by 4B5 showed amplified FISH results. HER2 4B5 and HercepTest had great specificity (both 100%). The sensitivity for HercepTest and 4B5 were 64% and 40% by using the cut-off of IHC 3+, and 90% and 70% by using the cut-off IHC 2+. The overall agreement between HercepTest and 4B5 was moderate with weighted Kappa=0.418.

Correlation of FISH and IHC results								
FISH	HERCEPTTest				IHC			
	Negative 0	Negative 1+	Equivocal 2+	Positive 3+	Negative 0	Negative 1+	Equivocal 2+	Positive 3+
Non amplified	21(95%)	0(0%)	8 (73%)	0(0%)	12(100%)	11(79%)	7(70%)	0
Amplified	1 (5%)	0(0%)	3(27%)	7(100%)	0(0%)	3(21%)	3(30%)	4(100%)
Total=40	22	0	11	7	12	14	10	4

**Conclusions:** To our knowledge, this study is the first to compare the performance of the two most commonly-used HER2 IHC methods to HER2 gene amplification by FISH. Both HercepTest and 4B5 HER2 IHC had 100% specificity for detecting HER2 gene amplification in USC, while HercepTest has superior sensitivity. Therapeutic targeting of HER2 is among the most significant advancements in this disease in decades, specifically for patients with HER2 positive advanced stage and recurrent USC. Our findings contribute to the knowledge of HER2 testing methodologies in USC and may aid in developing guidelines for selecting suitable patients for HER2-targeted therapy in USC.

## 954 Genome-Wide DNA Methylation Identifies Distinct Subgroups of Vulvovaginal Mesenchymal Neoplasia

Alexander Neil<sup>1</sup>, Brooke Howitt<sup>2</sup>, Jingru Yu<sup>2</sup>, Jennifer Bennett<sup>3</sup>, Andre Pinto<sup>4</sup>, Charles Quick<sup>5</sup>, Grace Neville<sup>6</sup>, Marisa Nucci<sup>6</sup>, David Chapel<sup>7</sup>, Lucas Heilbroner<sup>8</sup>, Aihui Wang<sup>8</sup>, Yvette Ysabel Yao<sup>2</sup>, Lauren Ahmann<sup>2</sup>, Wei Gu<sup>2</sup>, Carlos Parra-Herran<sup>6</sup>

<sup>1</sup>Brigham and Women's Hospital, Boston, MA, <sup>2</sup>Stanford University, Stanford, CA, <sup>3</sup>University of Chicago, Chicago, IL, <sup>4</sup>University of Miami Health System, Miami Beach, FL, <sup>5</sup>University of Arkansas for Medical Sciences, Little Rock, AR, <sup>6</sup>Brigham and Women's Hospital, Harvard Medical School, Boston, MA, <sup>7</sup>Michigan Medicine, University of Michigan, Ann Arbor, MI, <sup>8</sup>Stanford Medicine/Stanford University, Stanford, CA

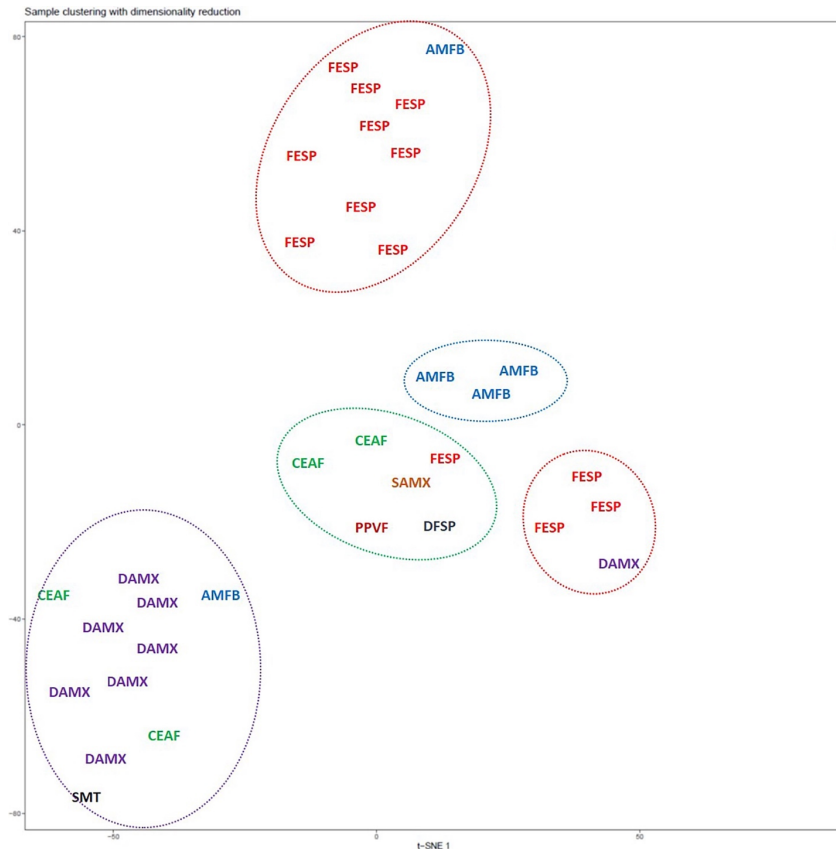
**Disclosures:** Alexander Neil: None; Brooke Howitt: None; Jingru Yu: None; Jennifer Bennett: None; Andre Pinto: None; Charles Quick: None; Grace Neville: None; Marisa Nucci: None; David Chapel: None; Lucas Heilbroner: None; Aihui Wang: None; Yvette Ysabel Yao: None; Lauren Ahmann: None; Wei Gu: None; Carlos Parra-Herran: None

**Background:** Genome-wide DNA methylation analysis has aided in the classification of neoplasms such as those of the central nervous system. In the uterus, it has been shown that benign and malignant mesenchymal tumors cluster in distinct methylation signatures. It is unknown whether the same applies to vulvovaginal mesenchymal neoplasms, a diverse group that includes indolent, locally aggressive, and malignant entities, which are often difficult to classify using conventional histomorphology and immunohistochemistry.

**Design:** Primary vulvar and vaginal mesenchymal lesions were collected from 4 institutions. DNA was extracted from archival formalin-fixed, paraffin embedded tissue, and analyzed using next generation sequencing of the methylome. Overall, there were 668,000 markers with more than 10X coverage across all samples. Unsupervised hierarchical clustering using t-distributed stochastic neighbor embedding (t-SNE) dimensionality reduction was performed on the top 1,000 markers with the highest median absolute deviation across beta values.

**Results:** Of 49 samples, copy number analysis was successful in 47. Methylation analysis was carried in the top 34 samples with coverage of CpG sites above 10. Based on rendered pathologic diagnoses, the methylation cohort included fibroepithelial stromal polyp (FESP, n=13), angiomyofibroblastoma (AMFB, n=5), cellular angiofibroma (CEAF, n=4), superficial angiomyxoma (SAMX, n=1), deep angiomyxoma (DAMX, n=8), prepubertal vulvar fibroma (PPVF, n=1), smooth muscle tumor (SMT, n=1) and dermatofibrosarcoma protuberans (DFSP, n=1). t-NSE analysis (Fig 1) revealed two major distinct clusters: one including most FESPs and a second including most DAMX, both with a few outliers including CEAF and AMFB. Most AMFB, however, grouped centrally in a separate cluster, close to a second FESP cluster (with one DAMX outlier) and a cluster with two CEAF as well as FESP, SAMX, PPVF and DFSP. Most cases had no detectable copy number changes, except 3/3 SMT (1p loss, among others) and 2/2 DFSP (17q gain).

Figure 1 - 954



**Conclusions:** Certain types of vulvovaginal mesenchymal neoplasia, including frequent lesions such as FESP and clinically relevant tumors like DAMX, have unique DNA methylation signatures compared to other primary lesions in this location. More infrequent lesions such as AMFB and CEAf also appear to have discrete methylation profiles. The presence of outliers in each methylation cluster may represent morphologic misclassification or molecular heterogeneity in these groups of lesions.

## 955 Placenta Accreta Spectrum Disorder: Review of Risk Factors, Pathology in Former Gestations and Associated Placental and Uterine Pathology in Hysterectomy

Grace Neville<sup>1</sup>, Carlos Parra-Herran<sup>1</sup>

<sup>1</sup>Brigham and Women's Hospital, Harvard Medical School, Boston, MA

**Disclosures:** Grace Neville: None; Carlos Parra-Herran: None

**Background:** Placenta accreta spectrum disorders (PAS) are increasing in incidence and are associated with significant maternal and fetal morbidity and mortality. They are typically seen in the setting of previous cesarean section (CS); however, not all cases have such antecedent. We report the associated placental and uterine pathology seen in a cohort of 62 gravid hysterectomy specimens with confirmed PAS.

**Design:** Cases of gravid hysterectomy for PAS at a single referral institution were reviewed. Demographic details, prior and metachronous pathology findings were documented.

**Results:** The cohort had a mean age of 36 (range 29–47) years and mean gestation at delivery of 35.3 (range 23.6–39.4) weeks. Prior history of CS was documented in 47 patients (76%). 34 patients had other forms of uterine instrumentation. Remarkably, 15 patients (24%) lacked history of prior CS; of these, 14 had other forms of uterine instrumentation. One patient had history of neither CS or uterine instrumentation. In 18 patients, 19 placentas from previous gestations were available. Among these, 8/18 (44%) had BPMF, disrupted parenchyma and/or RPOC in previous pregnancies (Table 1). Examination of the gravid hysterectomy specimen revealed leiomyomata in 9 cases (14%), adenomyosis in 6 (10%) and chronic endometritis in one (1.5%). Most placentas in the index (PAS) gestation were morphologically normal (n=30, 48.4%). However, a subset of patients had diverse placental lesions. Evidence of maternal vascular malperfusion included infarcts (n=11), retroplacental hemorrhage (n=6) and decidua arteriopathy (n=1).

Villitis of unknown etiology (n=3), chorioamnionitis (n=1), chorangiosis (n=2) and intervillous thrombi (n=16) were also seen.

Cord abnormalities including velamentous (n=1), membranous (n=1), vas previa (n=1) and a single umbilical artery were observed.

Table 1: Diagnoses rendered on previous surgical specimens and placentas from previous gestations:

	Number (%)	Associated Findings
RPOC post delivery	15 (24)	Chronic Endometritis (n=7)
RPOC post miscarriage	14 (22)	Molar Pregnancy (n=1)
Leiomyomata	6 (10)	With atypia (n=1)
Endometriosis	6 (10)	
Placenta:	19	
No specific pathologic change	10 (53)	Subsequent presentation with RPOC (n=2)
Basal Plate Myometrial Fibers	2 (11)	Subsequent presentation with RPOC (n=1)
Disrupted parenchyma	3 (16)	Subsequent presentation with RPOC (n=1)

**Conclusions:** In this large institutional cohort, previous CS is seen most patients with PAS. However, a quarter of patients lack such antecedent, and careful review of the clinical history is needed to identify other forms of uterine instrumentation that can lead to deficient decidua and PAS pathogenesis. Equally important is the review of pathology in placentas from former gestations, since 44% show findings alerting to the possibility of previous PAS, not only BPMF but also disrupted parenchyma and RPOC. The breath of pathologic conditions seen is reflective of the older and more medically complex cohort in which this condition typically occurs.

## 956 Polarization of Endothelial and Epithelial Cell States Predicts Recurrence in Endometrial Endometrioid Carcinoma

Corrine Nief<sup>1</sup>, Phoebe Hammer<sup>1</sup>, Aihui Wang<sup>1</sup>, Andrew Gentles<sup>1</sup>, Brooke Howitt<sup>2</sup>

<sup>1</sup>Stanford Medicine/Stanford University, Stanford, CA, <sup>2</sup>Stanford University, Stanford, CA

**Disclosures:** Corrine Nief: None; Phoebe Hammer: None; Aihui Wang: None; Andrew Gentles: None; Brooke Howitt: None

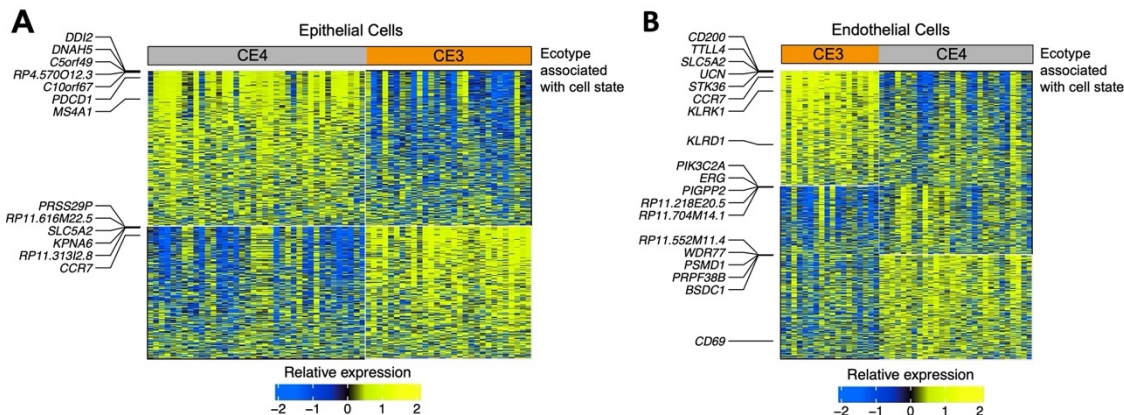
**Background:** Endometrial endometrioid carcinomas (EEC) are the 4th most common cancer in females and the most common gynecologic malignancy in developed countries. EEC has 5-year survival rate of 95%; however, there is a population of patients that have aggressive disease. Accurate prognostic markers for EEC could inform treatment of high-risk patients while reducing overtreatment of low-risk patients.

**Design:** The machine learning framework “EcoTyper” was used to identify patterns of cell state co-occurrences in 117 EECs to classify low- and high-risk EEC patients based on bulk RNA gene expression data. Targeted DNA (exonic regions of 648 genes) and whole transcriptomic RNA sequencing was performed on a cohort of EECs that recurred less than 5 years after resection (n=50) and EECs that did not recur (n=67) as a control group. The Cancer Genome Atlas (TCGA) molecular subgroups were established based on DNA sequencing. CIBERSORTx was used to deconvolve cell fractions from a previously validated carcinoma signature matrix. Cellular ecotypes (CEs) were identified from co-associated cell states with distinct expression profiles.

**Results:** All 117 samples were blinded to search for cell states present and significant CEs. Of the four CEs identified (CE1, CE2, CE3, CE4), only CE3 and CE4 demonstrated significantly different expression between the case and control group (Table 1). Samples 15% more abundant in CE3 than CE4 were designated as “CE3 high”, and vice versa. CE3 and CE4 were made of unique endothelial and epithelial cell states (Figure 1). CE3 was correlated with recurrence, abnormal CTNNB1 staining, and low grade. CE4 was correlated with no recurrence and high grade. There was no association with ecotype and age, race, ethnicity, LVSI status, or molecular subtype. The CE3 ecosystem has high levels of immunosuppressive genes (CCR7, CD200, EGFL8) with constituents from the NF-κB (FKBP4, RNF25), RAS (RAB31), and Hedgehog (STK36) pathways as well as several genes implicated in chemotherapy resistance (IFI16, SLC31A2, EIF3G). Conversely, the CE4 ecotype has high levels genes associated with tumor suppression (EAF2, NOL7, AL358852.1), apoptosis (APOPT1, BNIP3), PD1 pathway (PDCD1), and DNA repair mechanisms (ORC6, DDI2).

	Total	CE3 High	CE4 High	Neither	P value
Number of patients	117 (100%)	39 (33%)	48 (41%)	30 (26%)	
<b>Recurrence Status</b>					*p=0.028
Recurrence	51 (44%)	21 (54%)	13 (27%)	17 (57%)	
No Recurrence	66 (56%)	18 (46%)	35 (73%)	13 (43%)	
<b>Recurrence location</b>					*p=0.009
Locoregional	23 (20%)	6 (15%)	7 (15%)	10 (33%)	
Distant	15 (13%)	8 (21%)	2 (4%)	5 (17%)	
Vaginal cuff	13 (11%)	7 (18%)	4 (8%)	2 (7%)	
No Recurrence	66 (56%)	18 (46%)	35 (73%)	13 (43%)	
<b>TCGA Molecular Subtype</b>					p=0.486
MSI	35 (30%)	12 (31%)	17 (35%)	6 (20%)	
p53 abnormal	9 (8%)	3 (8%)	2 (4%)	4 (13%)	
POLE	2 (2%)	1 (3%)	1 (2%)	0 (0%)	
NSMP	71 (61%)	23 (59%)	28 (58%)	20 (67%)	
<b>NSMP Beta-Catenin Status</b>					*p=0.008
CTNNB1 normal	40 (56%)	7 (30%)	22 (79%)	11 (55%)	
CTNNB1 abnormal	31 (44%)	16 (70%)	6 (21%)	9 (45%)	
<b>Grade</b>					*p<0.001
Low (G1-G2)	102 (87%)	36 (92%)	42 (88%)	24 (80%)	
High (G3)	15 (13%)	3 (8%)	6 (13%)	6 (20%)	

Figure 1 - 956



**Conclusions:** We identified two ecotypes that correlate with EEC prognosis, with CE3 (endothelial cell immunosuppression, epithelial cell proliferation) correlating to recurrence, and CE4 (tumor suppressors, apoptotic genes, CA125, PD1) correlating to lower rates of recurrence.

## 957 Morphological Features are Neither Sensitive Nor Specific for the Diagnosis of Fumarate Hydratase Deficient Leiomyoma: A Clinicopathologic Study of 99 Uterine Leiomyomas with Atypical Nuclei

Na Niu<sup>1</sup>, Natalia Buza<sup>2</sup>, Pei Hui<sup>3</sup>, Tong Sun<sup>2</sup>

<sup>1</sup>Yale New Haven Hospital, New Haven, CT, <sup>2</sup>Yale School of Medicine, New Haven, CT, <sup>3</sup>Yale University School of Medicine, New Haven, CT

**Disclosures:** Na Niu: None; Natalia Buza: None; Pei Hui: None; Tong Sun: None

**Background:** Atypical nuclei can be seen in leiomyoma with bizarre nuclei (LBN), fumarate hydratase (FH) deficient leiomyoma, and leiomyosarcoma. Distinguishing between these entities is critical for clinical management. Though certain morphological features have been proposed for identifying FH deficient leiomyoma, including prominent eosinophilic nucleoli with perinucleolar halo, cytoplasmic eosinophilic inclusions, staghorn vessels, and alveolar type edema, the sensitivity, and specificity of these features have not been fully validated in large cohorts.

**Design:** Total 112 hysterectomy or myomectomy specimens from 99 women with diagnoses of “atypical leiomyoma”, “symplastic leiomyoma” or “leiomyoma with bizarre nuclei” from our institutional pathology archives during 2000 to 2021 were reviewed. Clinical history and a median of 56 months of clinical and pathological follow-up were obtained. FH immunohistochemistry was performed on selected sections in 60 cases with available tissue blocks. Comparing clinical and pathomorphological features were made between FH deficient leiomyoma and leiomyoma with bizarre nuclei.

**Results:** Two cases with increased mitotic figures (>5/10HFP) and/or ki-67 (>10%) were diagnosed as leiomyosarcoma during clinical follow-up and excluded from further analysis. A total of 24 leiomyomas (40%) demonstrated FH expression loss. Patients with FH deficient leiomyoma tended to be younger (mean age: 45 years vs. 50 years) and had larger tumors (mean size: 7.4 cm vs. 5.6 cm), although the difference was not statistically significant ( $p > 0.05$ ). FH deficient leiomyomas were also more likely to have diffuse, high-density bizarre cell distribution, nuclear pseudooinclusions, cytoplasmic eosinophilic inclusions, staghorn vessels, or alveolar type edema (Table 1). However, these previously reported features can also be seen in non-FH deficient leiomyomas, and none of them are sensitive or specific ( $p > 0.05$ )

**Table 1.** Summary of clinical, pathologic, and immunophenotypic features of leiomyoma with atypical nuclei

	Total Cohort (N = 99)	IHC confirmed FH deficient leiomyoma (N = 24)	Leiomyoma with Bizarre nuclei (N = 36)	P value
Age, mean (range), years	47 (26-85)	45 (26-80)	50 (31-76)	0.22
Surgical type				
Hysterectomy	65 (66%)	18 (75%)	25 (70%)	
Myomectomy	34 (34%)	6 (25%)	11 (30%)	
Size, mean (range), cm	6.2 (0.2-15)	7.4 (1.5-15)	5.6 (1-12)	0.46
Bizarre cell distribution, N (%)				0.23
Focal	27 (27%)	4 (17%)	10 (28%)	
Multifocal	40 (40%)	6 (25%)	13 (36%)	
Diffuse	32 (33%)	14 (58%)	13 (36%)	
Bizarre cell density, N (%)				
Low (<=30%)	50 (51%)	4 (16%)	14 (39%)	0.15
Intermediate (30-70%)	26 (26%)	10 (42%)	13 (36%)	
High (>=70%)	23 (23%)	10 (42%)	9 (25%)	
Mitotic count >=5/10HFP or Ki67 >10%	2	0	0	
Nuclear pseudooinclusion, N (%)				0.44
Absent	42 (42%)	10 (42%)	20 (53%)	
Present	57 (58%)	14 (58%)	18 (47%)	
Cytoplasmic eosinophilic inclusion, N (%)				0.30
Absent	65 (66%)	12 (50%)	23 (64%)	
Present	34 (34%)	12 (50%)	13 (36%)	
Staghorn vessels, N (%)				0.20
Absent	80 (81%)	16 (67%)	30 (83%)	
Present	19 (19%)	8 (33%)	6 (17%)	
Alveolar-type edema, N (%)				0.42
Absent	90 (91%)	20 (83%)	33 (92 %)	
Present	9 (9%)	4 (17%)	3 (8%)	
FH Immunostaining, N (%)				
Retained	36 (60%)	0 (0%)	36(100%)	
Loss	24 (40%)	24 (100%)	0 (0%)	

Figure 1 - 957

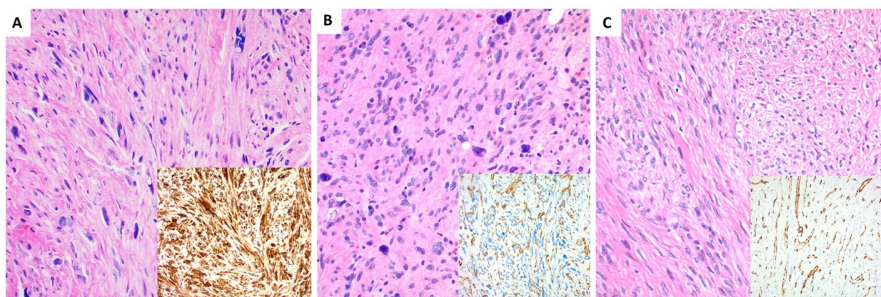


**Figure 1.** Leiomyoma with bizarre/atypical nuclei.

**A.** Cells characterized by bizarrely shaped, multilobulated, and multinucleated nuclei with nuclear pseudooinclusions. Insert shows retained FH expression.

**B.** Bizarre cells with focal perinucleolar halo. Insert shows loss of FH expression.

**C.** Bland cells without nuclear atypia. Insert shows loss of FH expression.

200x.

**Conclusions:** FH deficient leiomyoma is an important clue for identifying patients with hereditary leiomyomatosis and renal cell cancer (HLRCC) syndrome. Our data showed that FH-deficiency is relatively prevalent in leiomyomas with nuclei atypia. Reported morphologic features of FH deficient leiomyoma are neither sensitive nor specific. Younger age and larger leiomyomas are associated with a higher possibility of FH deficient leiomyomas, although the difference can be subtle. In routine practice, the threshold for performing FH IHC in leiomyomas with atypical nuclei should be low

## 958 STR Genotyping: A Precision Diagnostic Tool for Extrauterine Presentations of Epithelioid Trophoblastic Tumor and Its Somatic Carcinoma Mimics

Na Niu<sup>1</sup>, Natalia Buza<sup>2</sup>, Pei Hui<sup>3</sup>

<sup>1</sup>Yale New Haven Hospital, New Haven, CT, <sup>2</sup>Yale School of Medicine, New Haven, CT, <sup>3</sup>Yale University School of Medicine, New Haven, CT

**Disclosures:** Na Niu: None; Natalia Buza: None; Pei Hui: None

**Background:** Epithelioid trophoblastic tumor (ETT) is the rarest form of gestational trophoblastic neoplasms with histological presentations frequently simulating a somatic carcinoma. While ETT primarily arises from the uterus, cases have been documented to occur at extrauterine sites including the fallopian tube, ovary, and broad ligament in association with ectopic pregnancy, or as metastatic tumors to various organs. Moreover, somatic carcinomas may show trophoblastic differentiation histologically and immunohistochemically simulating ETT. Thus, a precise diagnosis of an extrauterine tumor with epithelioid trophoblastic cell differentiation of either gestational or somatic origin is highly relevant and crucial for patient management and prognosis.

**Design:** We present four challenging epithelioid tumors that had various initial interpretations with ETT as the main differential diagnosis. Immunohistochemistry and STR genotyping of tumor samples were performed.

**Results:** Patients' ages ranged from 38 to 65 years. All four cases presented as extrauterine lesions (Table 1) and showed overlapping histologic and immunohistochemical features between somatic carcinoma and ETT (Figures 1 and 2). Serum hCG elevation was documented in one patient (case #3, 1,800 mIU/ml). Surgical excision of the tumor was performed in two patients (#2 and #4), and core biopsy was performed in two cases (#3 and #4). Clinical and imaging studies were inconclusive in all four cases. One patient (case #3) received chemotherapy without response as a result of the initial diagnosis of ETT. STR genotyping was informative in all cases. Matching genetic profile with the patient's normal tissues was seen in two tumors (both initially considered as ETT), confirming that they were somatic carcinomas with trophoblastic differentiation (case #3 metastatic triple negative breast carcinoma and case #4 lung primary carcinoma). Another two cases, initially suspected as somatic carcinoma (case #1) and mixed trophoblastic tumor (case #2), demonstrated distinct paternal alleles (not present in the patient's normal tissues) at multiple STR loci in the tumor, confirming the diagnosis of ETT in both cases (Table 1).

Table 1. Clinical information

Case number	#1	#2	#3	#4
Patient age	61	38	65	57
Presenting symptoms	Vaginal bleeding, abdominal pain weight loss	N/A	Supraclavicular lymphadenopathy and liver nodules	Dyspnea
Reported PMH	Endometrial cancer, poorly differentiated	Uterine ETT involving lung, cervix and right ovary	Triple negative breast cancer, stage IV	N/A
Lesion site	Anterior abdominal wall, omentum, intestine	Left paravesical implant, perirectal implant	Multiple nodules in Liver	Multiple bilateral lung nodules, neck and mediastinal lymphadenopathy
Initial diagnosis at outside institution	Poorly differentiated carcinoma with squamoid features and extensive necrosis	Mixed gestational trophoblastic tumor	ETT	ETT
Treatment/procedure	Exploratory laparotomy, omentectomy	Hysterectomy, bilateral salpingectomy	First round chemotherapy for Trophoblastic tumor without response	Right lung core biopsy
Molecular genotyping	Distinct paternal alleles (not present in normal tissues)	Distinct paternal alleles (not present in normal tissues)	Matching alleles with the patient's normal tissues	Matching alleles with the patient's normal tissues
Final diagnosis	Metastatic ETT	Metastatic ETT	Somatic carcinoma with trophoblastic differentiation	Somatic carcinoma with trophoblastic differentiation

# ABSTRACTS | GYNECOLOGIC AND OBSTETRIC PATHOLOGY

**Abbreviation:** ETT, epithelioid trophoblast tumor; PMH, past medical history; N/A, not available.

Figure 1 - 958

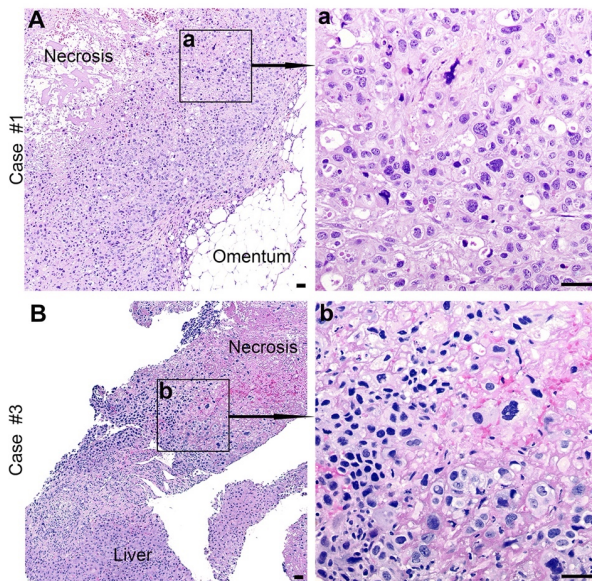


**Figure 1.** Histologic features

of Case #1 and Case #3:

Proliferation of atypical  
epithelioid tumor cells with  
abundant cytoplasm,  
presence of hyaline matrix,  
and geographic necrosis.

Bars, 100 µm.

Figure 2 - 958

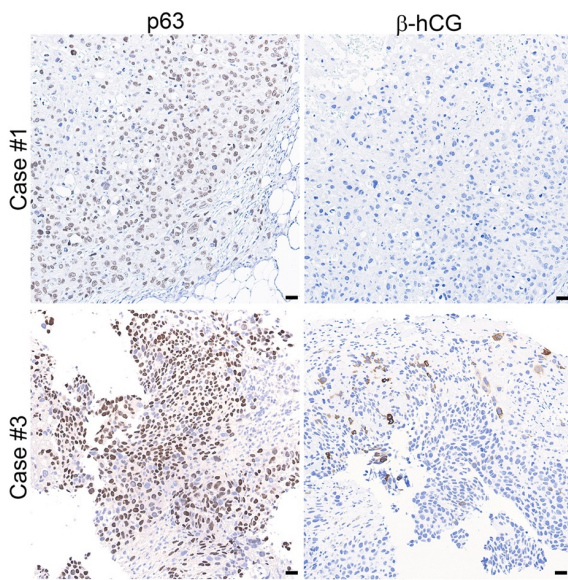


**Figure 2.** Representative IHC  
stains of cases #1 and #3.

Tumor cells are diffusely positive  
for p63 (both cases) with  
negative (case #1) or scattered  
positive cells (case #3) for  
β-hCG. Bars, 100 µm.

**Conclusions:** Diagnostic separation of ETT presenting at an extrauterine site from somatic carcinoma is frequently difficult at the histological and immunohistochemical levels. STR genotyping is a robust ancillary tool that precisely separates ETT from a somatic carcinoma with trophoblastic differentiation.

## 959 Identifying Opportunities for Improved Pathologic Diagnosis of Ovarian Cancer in West Africa

Ayodele Omotoso<sup>1</sup>, Sophia George<sup>2</sup>, Willy Chertman<sup>1</sup>, Alex Sanchez-Covarrubias<sup>3</sup>, Matthew Schlumbrecht<sup>4</sup>, Andre Pinto<sup>5</sup>

<sup>1</sup>University of Miami Health System, Miami, FL, <sup>2</sup>University of Miami Sylvester Comprehensive Cancer Center, Miami, FL,

<sup>3</sup>University of Miami Miller School of Medicine, Sylvester Cancer Center, Miami, FL, <sup>4</sup>University of Miami Miller School of Medicine, Miami, FL, <sup>5</sup>University of Miami Health System, Miami Beach, FL

**Disclosures:** Ayodele Omotoso: None; Sophia George: None; Willy Chertman: None; Alex Sanchez-Covarrubias: None; Matthew Schlumbrecht: None; Andre Pinto: None

**Background:** Ovarian cancer (OC) is the second most common gynecological malignancy among Nigerian women after cervical cancer. A precise histopathologic diagnosis can be extremely challenging in low resource countries where ancillary tools such as immunohistochemistry (IHC) and molecular techniques are not widely available. The massive exodus of specialists due to insecurity, poor infrastructure and low remuneration has further overstretched the few available anatomic pathologists. The objective of this initiative was to evaluate a large cohort of OC tumor from Nigeria to assess for tumor histology and estimated diagnostic accuracy, with the aim of identifying opportunities to improve OC diagnosis.

**Design:** FFPE tissue blocks of OC samples from 3 consecutive years (2017-2019) were obtained from 19 tertiary health institutions in the 6 geo-political regions of Nigeria. Whole-tissue sections were prepared and reviewed by two pathologists in the United States. Mislabeled, extremely poorly fixed tissue and repeated blocks were excluded from further processing. Selected IHC stains were performed on a subset of cases in which morphologic features were not diagnostic. Tumors were classified as having a "change in diagnosis" when there was any discrepancy regarding histologic subtype, site of origin (primary vs. metastasis) or biologic behavior (malignant to benign) between the original and revised diagnoses.

**Results:** 282 cases met the inclusion criteria, 90 of which (31.9%) required IHC for final diagnosis. For 231 cases (81.9%), the original pathologic diagnosis was made available. A change in diagnosis occurred in 104/231 (45%), mostly due to erroneous assignment of primary site (49/104, 47.1%), followed by incorrect histologic type (29/104, 27.8%), overdiagnosis of malignancy (16/104, 15.3%) and wrong line of differentiation (10/104, 9.6%). When accounting for the 163 reclassified primary malignant cases, most tumors were of epithelial origin (101/163 [61.9%], predominantly HGSC [65/101; 64.3%]). Tumors in the sex cord-stromal category were 41/163 (25.1%), followed by 21/163 (12.8%) germ cell malignancies.

**Conclusions:** OC in Nigerian women differs from the US population by demonstrating less incidence of HGSC and higher frequency of malignant sex cord-stromal tumors. The utilization of secondary histopathological review paired with ancillary studies from a subspecialized center can markedly improve diagnostic accuracy, with potential change in patient's management.

## 960 Uterine Leiomyosarcoma Arising in a Leiomyoma: A Clinicopathologic and Genomic Study of 11 Tumors

Zehra Ordulu<sup>1</sup>, Jennifer Bennett<sup>2</sup>, Kyle Devins<sup>3</sup>, Rishikesh Haridas<sup>4</sup>, Andrea Palicelli<sup>5</sup>, Esther Oliva<sup>6</sup>

<sup>1</sup>University of Florida, Gainesville, FL, <sup>2</sup>University of Chicago, Chicago, IL, <sup>3</sup>Massachusetts General Hospital, Boston, MA,

<sup>4</sup>University of Chicago Medicine, Chicago, IL, <sup>5</sup>Azienda Unità Sanitaria Locale - IRCCS di Reggio Emilia, Reggio Emilia, Italy, <sup>6</sup>Massachusetts General Hospital, Harvard Medical School, Boston, MA

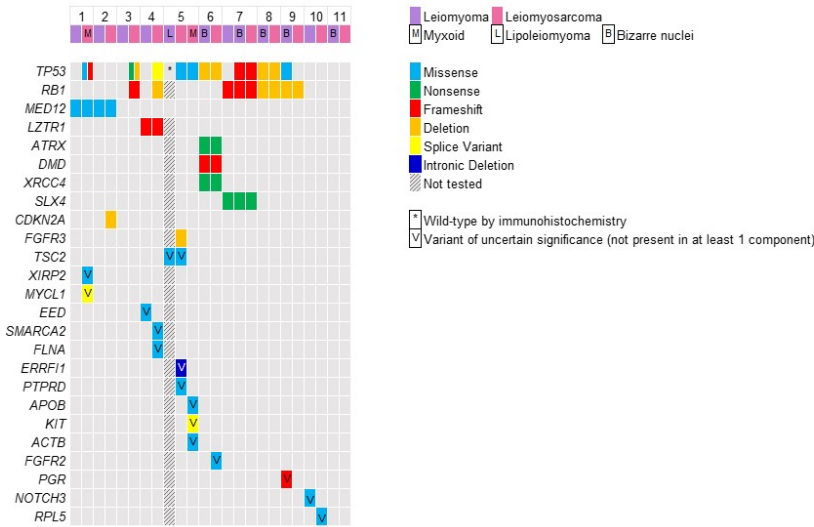
**Disclosures:** Zehra Ordulu: None; Jennifer Bennett: None; Kyle Devins: None; Rishikesh Haridas: None; Andrea Palicelli: None; Esther Oliva: None

**Background:** Uterine leiomyoma (LM) is the most common gynecologic tumor while its malignant counterpart, leiomyosarcoma (LMS) is rare. They typically harbor distinct molecular profiles, LM being characterized by *MED12*, *FH*, or *HMG2A*, and LMS by *TP53*, *RB1*, *ATRX*, and *PTEN* alterations as well as complex genomic architecture. Although rare LMS arising from LM have been reported, no comprehensive molecular study analyzing each component has been undertaken.

**Design:** We macrodissected LM and LMS components from 11 tumors and performed next-generation sequencing on a 1004-gene panel.

**Results:** Patients ranged from 38 to 79 (mean 55) years. Tumors ranged from 8.5 to 20 (mean 13) cm. Ten patients had stage I tumors and 1 stage III with peritoneal disease. Follow-up was available for 7; 3 alive and well, 3 dead of disease, and 1 dead from unrelated causes. The LM was conventional in 5, with bizarre nuclei (BN) in 4, both conventional and BN in 1, and a lipoleiomyoma in 1. Nine LMS were spindled, 1 myxoid, and 1 had both. None tested (n=6) showed *HMG2A* overexpression by immunohistochemistry. Cases 1-2 harbored *MED12* mutations in both components, with LMS acquiring *TP53* or *CDKN2A* alterations (Figure). Cases 3-5 lacked alterations in LM, but LMS harbored *TP53* mutations, with concurrent *RB1* in 2. In cases 6-9, near identical alterations in both LMBN and LMS were present, involving *TP53* (3 of 4) and *RB1* (3 of 3). Case 7 also had a conventional LM area that lacked the *TP53* mutation seen in the LMBN and LMS but shared the *RB1* and *SLX4* mutations. Cases 10-11 did not show significant gene level alterations in either component. Overall, *MED12* mutations were present in 2 conventional LMs and all 4 *TP53*-altered LMs had BN. Both alterations were shared with LMS, except case 9 where the LMS lacked the *TP53* mutation. Evaluation of chromosome arm level copy number alterations (CNA) in 10 tumors revealed 7 LMS (including cases 10-11) to have more CNAs than LM (5 conventional, 2 LMBN), were comparable in 2 LMS arising from LMBNs, while 1 LMS had more CNAs than the conventional LM but similar to the LMBN.

Figure 1 - 960



**Conclusions:** This is the first comprehensive genomic study showing shared clonal origin between LM and LMS, particularly in the setting of *MED12*-mutated LM and *TP53*-altered LMBN. Although it has been previously suggested that LMS represents an independent tumor both at clinical and genomic levels, there appears to be a subset of LM and LMS that are spatially and molecularly related.

## 961 Gastric-type Endocervical Adenocarcinoma Metastasized to the Ovary Frequently Simulating Primary Ovarian Mucinous Tumors; A Report of 15 Cases

Hyun Ju Park<sup>1</sup>, Uiree Jo<sup>1</sup>, Hyun-Soo Kim<sup>2</sup>, Kyu-Rae Kim<sup>3</sup>

<sup>1</sup>Asan Medical Center, University of Ulsan College of Medicine, Seoul, South Korea, <sup>2</sup>Samsung Medical Center, Sungkyunkwan University School of Medicine, Seoul, South Korea, <sup>3</sup>Asan Medical Center, South Korea

**Disclosures:** Hyun Ju Park: None; Uiree Jo: None; Hyun-Soo Kim: None; Kyu-Rae Kim: None

**Background:** Gastric-type endocervical adenocarcinoma (GAS) is well known for its aggressive clinical behavior and the absence of high-risk human papillomavirus (HPV), but gross and microscopic findings of ovarian metastasis from GAS has not been well described. We report 15 such cases to describe their gross and microscopic characteristics.

**Design:** We describe gross and microscopic characteristics of 15 GAS metastasized to the ovary.

**Results:** The ovarian tumors ranged from 1.5cm to 37cm in greatest dimension (average, 13.5cm). Nine cases involved unilateral ovary (6 right, and 3 left), and six were bilateral. Grossly, seven of 15 ovarian tumors formed unilocular or oligolocular cysts with thin septae with a smooth external surface, which resembled benign cystic lesions of the ovary. Four cases were mostly composed of solid and firm masses and the remaining four had cystic mass with thick septae and ragged ovarian surface adhesion. Microscopically, grossly benign-appearing masses were lined by single-layered mucinous epithelium, but with significant cytologic atypia at higher magnification, which resembled pancreatic adenocarcinoma metastasized to the ovary. Signet ring cells were identified in 6 cases, and papillary features in 8 cases.

**Conclusions:** It should be kept in mind that histologic features of metastatic GAS to the ovary share common features with metastatic carcinoma of pancreatic origin and often resembled primary benign or borderline mucinous neoplasms of the ovary, and it could commonly be misdiagnosed as such by radiologic findings.

## 962 High TIM-3 Expression is an Independent Predictor of Improved Post-Radiation Therapy (RT) Clinical Outcomes of Vulvar Squamous Cell Carcinoma (SCCA)

Pranav Patwardhan<sup>1</sup>, Baher Elgohari<sup>1</sup>, Lauren Skvarca<sup>1</sup>, Terri Jones<sup>1</sup>, Alison Garrett<sup>2</sup>, Emily O'Brien<sup>3</sup>, Emily MacArthur<sup>3</sup>, Esther Elishaev<sup>4</sup>, Chengquan Zhao<sup>2</sup>, Rohit Bhargava<sup>2</sup>, Mirka Jones<sup>5</sup>, John Vargo<sup>1</sup>, Thing Rinda Soong<sup>5</sup>

<sup>1</sup>University of Pittsburgh Medical Center, Pittsburgh, PA, <sup>2</sup>UPMC Magee-Womens Hospital, Pittsburgh, PA, <sup>3</sup>Magee-Womens Hospital, University of Pittsburgh Medical Center, Pittsburgh, PA, <sup>4</sup>University of Pittsburgh School of Medicine, Pittsburgh, PA, <sup>5</sup>University of Pittsburgh, Pittsburgh, PA

**Disclosures:** Pranav Patwardhan: None; Baher Elgohari: None; Lauren Skvarca: None; Terri Jones: None; Alison Garrett: None; Emily O'Brien: None; Emily MacArthur: None; Esther Elishaev: None; Chengquan Zhao: None; Rohit Bhargava: None; Mirka Jones: None; John Vargo: None; Thing Rinda Soong: None

**Background:** RT is a fundamental component of vulvar SCCA treatment. There has been growing appreciation on the potential of synchronizing RT and immune checkpoint (IC) inhibitors for greater treatment efficacy. We aimed to study the post-RT prognostic significance of IC molecules in vulvar SCCA, which has remained largely undefined.

**Design:** Immunohistochemical expression of TIM-3, PD-L1, Gal-9, MHC class I (MHCI), and extent of CD8+ tumor infiltrating lymphocytes (TILs) were evaluated in 90 vulvectomy specimens from patients who received RT. TIM-3, PD-L1 and Gal-9 expression was assessed via Tumor Proportion Score (TPS) and Combined Positive Score (CPS). Cross-sectional analyses were performed with Fisher's exact tests. Post-RT overall survival (OS) and recurrence-free survival (RFS) were examined via log-rank tests and Cox proportional regression models with adjusted hazard ratios (aHRs) and 95% confidence intervals (CIs).

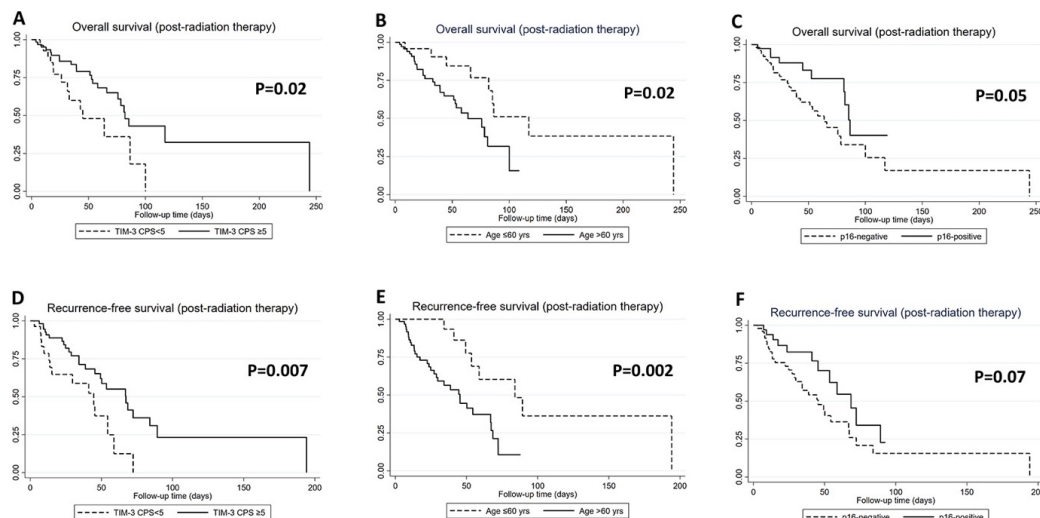
**Results:** Median age was 70 years. Over half were of FIGO stage 3 or 4 disease, with 43% being p16+ and 22% having lymph node metastases. TIM-3 TPS≥1, PDL-1 TPS≥1, and Gal-9 TPS≥1 status was seen in 65%, 52% and 52% of cases. TIM-3 CPS ≥5 was observed in 68% of tumors, and was significantly correlated with larger (>2 cm) tumor size, high expression of PD-L1, Gal-9 and MHCI, as well as extent of CD8+ TILs (Figure 1). No significant associations of PD-L1 or Gal-9 with characteristics other than MHCI expression or TIL density were seen. Most (62%) received RTs for adjuvant therapy, while others were treated for neoadjuvant (20%), definitive (12%), and palliative (6%) purposes. Median post-RT follow-up time was 26 months (range: 4-130 months). TIM-3 CPS ≥5 and ages≤60 years were correlated with improved post-RT OS and RFS, while p16+ status showed borderline associations (Figure 2). Only TIM-3 CPS≥5 independently predicted better post-RT OS after confounding adjustment. Statistically significant predictors for improved post-RT RFS included TIM-3 CPS ≥5 (aHR: 0.2; CI:0.1-0.5) and receipt of chemotherapy (aHR: 0.2; CI:0.1-0.7); while FIGO stage ≥3 (aHR: 3.0; CI:1.2-7.4) and age>60 years (aHR: 3.3; CI:1.2-9.0) predicted worse post-RT RFS after controlling for other tumor features.

Figure 1 - 962

Tumor characteristics		TIM-3 CPS*		P	
	n=90 column %	Low (<5) n=28	High (≥5) n=62		
PD-L1 CPS	<10 ≥10	58 42	89 11	45 55	<0.001
Gal-9 CPS	<10 ≥10	58 42	89 11	44 56	<0.001
CD8+ T cell density	Low High	33 57	46 54	21 79	0.021
MHCI expression of tumor cells	Low High (strong and greater than 50%)	46 54	54 46	30 70	0.03
p16	Negative Positive	57 43	53 47	64 36	0.31
p53	Wild-type Aberrant	46 54	49 51	39 61	0.37
Tumor size	≤2 cm >2 cm	21 79	28 72	9 91	0.03
Lymphovascular invasion	No Yes	72 28	70 30	76 24	0.67
Tumor stage	<3 ≥3	27 63	33 67	24 76	0.36
Positive lymph node metastasis	No Yes	48 52	50 50	47 53	0.78
Multiple recurrence episodes post-radiation therapy	No Yes	66 24	70 30	79 21	0.37

\*TIM-3 TPS≥5 shows similar statistically significant associations with higher PD-L1 TPS, Gal-9 TPS, MHCI expression and CD+ T cell density (data not shown in table).

Figure 2 - 962



**Conclusions:** TIM-3 CPS≥5 is an independent indicator of improved post-RT prognosis and is expressed by a significant proportion of vulvar SCCA. The findings warrant further assessment of TIM-3 as an alternative IC therapeutic target in combination with RT in patients who attain only partial response to RT.

### 963 Human Papillomavirus (HPV)-associated and HPV-independent Vulvar Squamous Cell Carcinomas Show Highly Similar Somatic Mutation Profile

Natalia Rakislova<sup>1</sup>, Nuria Carreras Dieguez<sup>1</sup>, Carla Sanchez<sup>2</sup>, Lorena Marimon<sup>2</sup>, Jaume Ordi<sup>3</sup>

<sup>1</sup>Hospital Clinic, Barcelona, Spain, <sup>2</sup>ISGlobal, Barcelona, Spain, <sup>3</sup>University of Barcelona, Barcelona, Spain

**Disclosures:** Natalia Rakislova: None; Nuria Carreras Dieguez: None; Carla Sanchez: None; Lorena Marimon: None; Jaume Ordi: None

**Background:** Vulvar squamous cell carcinoma (VSCC) is a rare cancer. Two different pathways have been described for this cancer, one associated with human papillomavirus (HPV), and the other independent of HPV. Genomic landscape of VSCC remains poorly explored.

**Design:** 64 VSCC with matched normal tissue underwent whole exome sequencing on an Illumina HiSeq6000. HPV testing and p16 immunohistochemistry were performed. Tumors with positive p16 and/or positivity for high-risk HPV were classified as HPV-associated.

**Results:** 12 VSCC (18.8%) were classified as HPV-associated and 52 (81.2%) as HPV-independent. HPV-associated VSCC showed predominantly *TTN* mutations (11/12; 92%), followed by *OBSCN* and *MUC16* (8/12 each; 67%), *DCHS1*, *DNAH11*, *DNHD1*, *HMCN1*, *MDN1*, *RYR1* and *UBR4* (6/12 each; 50%). HPV-independent VSCC showed frequently *TP53* mutations (39/52; 75%), followed by *TTN* (32/52; 62%), *OBSCN* (28/52; 54%), *PLEC* (25/52; 48%), *FAT1* and *MUC16* (22/52 each; 42%), *HSPG2* (19; 37%), *MACF1* (18; 35%), *HECTD4* and *RYR1* (17 each; 33%). Only *TP53* mutations correlated strongly with HPV-negative status ( $p=0.015$ ). The same top-10 pathways were identified in HPV-associated and -independent VSCC but in different proportions (Figure 1 and 2, respectively). HPV-associated VSCC showed enrichment for RTK-RAS pathway (12; 100%), followed by WNT and NOTCH (10 each; 83%), Hippo and PI3K pathway (9 each; 75%). HPV-independent VSCC showed involvement of NOTCH pathway (43; 83%), TP53 and Hippo (42 each; 81%), RTK-RAS and WNT (38 each; 73%). Mutational signatures were present in 61 out of 64 VSCC (95%). Two different patterns of mutations were inferred. Both patterns were enriched in C>T. The pattern 1 also showed an enrichment of C>A and C>G, and was more frequently associated with oncogenic activity of AID/APOBEC. The pattern 2 was related to defective DNA mismatch repair and microsatellite instability. The pattern 1 was identified in 49% of tumors (30/61), and pattern 2 in the remaining 51% (31/61). No association between the patterns and HPV status was identified ( $p=0.74$  for each pattern).

Figure 1 - 963

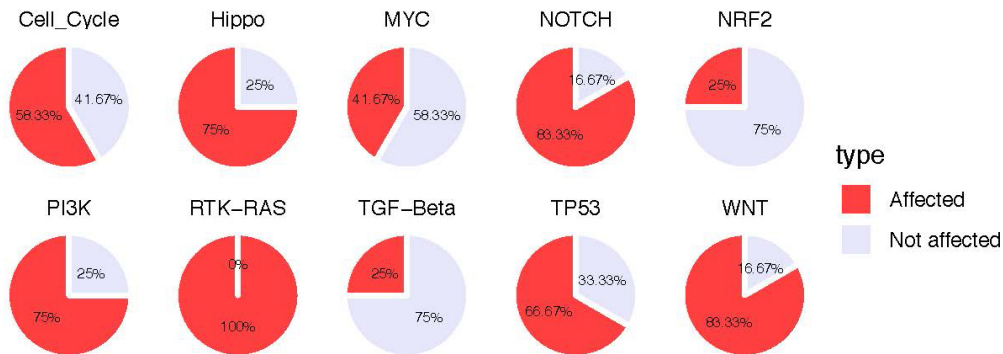
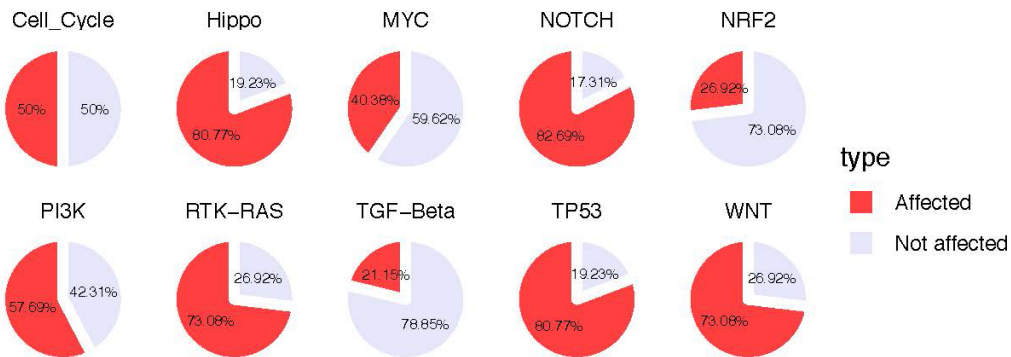


Figure 2 - 963



**Conclusions:** HPV-associated and HPV-independent VSCC are similar in the somatic mutation landscape, with the same top-10 pathways involved in different degrees. Only *TP53* mutations strongly correlated with HPV-independent status. At least half of the VSCC develop in association with defective DNA mismatch repair and microsatellite instability and other half in presence of AID/APOBEC oncogenic activity.

#### 964 Differences in Placental Pathologic Features by Trimester of Infection with SARS-CoV-2

Payu Raval<sup>1</sup>, Sunitha Suresh<sup>2</sup>, Alexa Freedman<sup>2</sup>, Linda Ernst<sup>1</sup>

<sup>1</sup>University of Chicago NorthShore, Evanston, IL, <sup>2</sup>NorthShore University HealthSystem, Evanston, IL

**Disclosures:** Payu Raval: None; Sunitha Suresh: None; Alexa Freedman: None; Linda Ernst: None

**Background:** SARS-CoV-2 (SV2) infection is associated with maternal illness and adverse perinatal outcomes, including stillbirth and preterm birth. Placental pathologies such as increased perivillous fibrin deposition, fibrin thrombi, villitis, villous infarct, and chorangiosis have been described in infected mothers. However, a meta-analysis failed to show a significant association between SV2 infection and placental pathology. This study aims to describe placental histological findings following SV2 infection in pregnancy and examine the association between the trimester (TRI) of infection and placental pathology.

**Design:** In this retrospective study, we included 314 pregnant women  $\geq$  18 years old who tested positive for SV2 during their pregnancy, delivered after  $\geq$  14 weeks of gestation, and had their placenta sent for pathology examination. Cases were classified into first (1st), second (2nd), and third (3rd) TRI cohorts based on the gestational age at the time of infection. The 3rd TRI cohort was divided into infection  $\leq$  10 days and  $>$ 10 days before delivery. Pathology reports were reviewed to collect placental findings. Placental lesions were categorized into acute inflammation (AI), chronic inflammation (CI), maternal vascular malperfusion (MVM), fetal vascular malperfusion (FVM), and other significant pathology. AI, CI, MVM, and FVM were divided into none, low grade (LG), and high-grade (HG). Chi-square or Fisher's exact tests were used to compare the prevalence of placental pathology by TRI of infection.

**Results:** Among those who tested positive  $<$ 37 weeks (at risk of preterm birth), 31.9% delivered preterm. There was no difference by TRI of infection (1st TRI: 32.5%; 2nd TRI: 28.4%; 3rd TRI: 34.5%; p-value=0.72). The prevalence of AI, CI, FVM, and MVM also did not differ by TRI of SV2 infection (see table). However, the prevalence of HG inflammatory and/or HG vascular placental pathology was most common in 1st TRI (27/40, 67.5%), followed by 2nd TRI (37/67, 55.2%), and 3rd TRI infection (82/207, 39.6%,

p<0.01). In the 3rd TRI cohort, SV2 infection ≤ 10 days before delivery was associated with a higher prevalence of FVM compared to infection more remote from delivery (46/134, 34.3% vs. 14/73, 19.2%; p<0.02).

Placental pathology		COVID infection First trimester (n=40)	COVID infection Second trimester (n=67)	COVID infection Third trimester (n=207)	p-value
<b>Placental Inflammation- Acute inflammation (AI)</b>					
Present	Total	24 (60.0)	44 (65.7)	123 (59.4)	0.66
	Low grade	17 (42.5)	31 (46.3)	93 (44.9)	
	High grade	7 (17.5)	13 (19.4)	30 (14.5)	
Not present		16 (40.0)	23 (34.3)	84 (40.6)	0.84
<b>Placental Inflammation- Chronic inflammation (CI)</b>					
Present	Total	25 (62.5)	35 (52.2)	116 (56.0)	0.59
	Low grade	14 (35.0)	18 (26.9)	78 (37.7)	
	High grade	11 (27.5)	17 (25.4)	38 (18.4)	
Not present		15 (37.5)	32 (47.8)	91 (44.0)	0.36
<b>Placental Vascular Pathology- Fetal Vascular Malperfusion (FVM)</b>					
Present	Total	15 (37.5)	21 (31.3)	60 (29.0)	0.56
	Low Grade	10 (25.0)	12 (17.9)	46 (22.2)	
	High Grade	5 (12.5)	9 (13.4)	14 (6.8)	
Not present		25 (62.5)	46 (68.7)	147 (71.0)	0.38
<b>Placental Vascular Pathology- Maternal Vascular Malperfusion (MVM)</b>					
Present	Total	16 (40.0)	22 (32.8)	56 (27.0)	0.22
	Low Grade	7 (17.5)	13 (19.4)	39 (18.8)	
	High Grade	9 (22.5)	9 (13.4)	17 (8.2)	
Not present		24 (60.0)	45 (67.2)	151 (73.0)	0.11
<b>Other/ Combined Placental Pathology</b>					
Villous chorangiosis		2 (5.0)	3 (4.5)	20 (9.7)	0.34
Increased peri villous fibrin deposition		3 (7.5)	3 (4.5)	20 (9.7)	0.4
Any AI OR CI		34 (85.0)	56 (83.6)	172 (83.1)	0.96
Any high-grade AI OR CI		17 (42.5)	28 (41.8)	61 (29.5)	0.08
Any CI AND MVM		9 (22.5)	14 (20.9)	34 (16.4)	0.53
Any high grade inflammatory or vascular pathology		27 (67.5)	37 (55.2)	82 (39.6)	<0.01

**Conclusions:** In our sample, the prevalence of preterm birth was elevated among those with SARS-CoV-2 infection <37 weeks gestation. In addition, 1st or 2nd TRI infection was associated with a higher prevalence of HG inflammatory and/or vascular placental pathology than 3rd TRI infection.

## 965 Potential New Placental Pathology Associated with Maternal SARS-CoV-2 Infection

Lauren Ray<sup>1</sup>, Jana Ritter<sup>2</sup>, Luciana Flannery<sup>2</sup>, Marlene DeLeon Carnes<sup>2</sup>, Lawrence Zukerberg<sup>1</sup>, Drucilla Roberts<sup>1</sup>, Lindsey Estetter<sup>2</sup>

<sup>1</sup>Massachusetts General Hospital, Boston, MA, <sup>2</sup>Centers for Disease Control and Prevention, Atlanta, GA

**Disclosures:** Lauren Ray: None; Jana Ritter: None; Luciana Flannery: None; Marlene DeLeon Carnes: None; Lawrence Zukerberg: None; Drucilla Roberts: None; Lindsey Estetter: None

**Background:** Acute SARS-CoV-2 placentitis is the triad of chronic histiocytic intervilllositis, massive perivillous fibrin deposition, and trophoblast necrosis. Recovered COVID-19 infections show placental pathologic sequelae including maternal, and probably fetal, vascular malperfusion. As the understanding of SARS-CoV-2 placental pathology continues to evolve, we present a new pathology seen in two placentas with maternal infections during the Omicron wave.

**Design:** Two cases of atypical placentitis in the setting of recovered maternal SARS-CoV-2 infection were reviewed at Massachusetts General Hospital (MGH) in June and July 2022. Given the gross and histopathologic findings, we performed special stains for bacteria, fungi, AFB, and spirochetes as well as RNA in-situ hybridization for SARS-CoV-2. In addition, immunohistochemistry was performed for CMV and spirochetes, and a representative formalin fixed paraffin embedded block was sent from each case to the Infectious Diseases Pathology Branch of the CDC for more complete studies (Table 1).

**Results:** Clinical histories were provided by the referring pathologists (Table 1). The timing of positive maternal SARS-CoV-2 testing was remote from delivery and both tested negative at delivery. Both neonates were liveborn, not tested for SARS-CoV-2, and remain healthy. Placental pathology for each case showed multifocal "abscess"-like lesions with negative infectious workups,

# ABSTRACTS | GYNECOLOGIC AND OBSTETRIC PATHOLOGY

including for SARS-CoV-2 (Table 1, Figure 1). The only documented infectious association for each patient, after evaluating history and an exhaustive infectious work up (Table 1), is the antepartum SARS-CoV-2 infection.

Table 1: Clinical histories provided by referring pathologists. Infectious work up with pan-negative results.

	Case 1	Case 2
<b>Maternal characteristics</b>		
Maternal age (years)	25	28
Gestational age corresponding to:		
Positive maternal SARS-CoV-2 test (trimester)	Second	First
Time of delivery (in weeks)	38 & 5/7	38 & 2/7
COVID-19 vaccination status	Unvaccinated	Unvaccinated
Severity of SARS-CoV-2 symptoms	Outpatient treatment	Outpatient treatment
Blood type	O positive	A positive
Parity	G3P2012	G3P2012
Maternal comorbidities	Hypertension, GERD <sup>a</sup>	Depression, anxiety
State of residence	New Hampshire	Massachusetts
Mode of delivery	Vaginal, induced	Vaginal, induced
Pregnancy complications	Chronic hypertension	GBS+ (penicillin treated)
<b>Infant characteristics</b>		
Apgar scores (1 and 5 minutes)	9, 9	8, 9
Birthweight (g)	3770	2510
Small for gestational age (SGA)	No	Yes
Infant gender	Male	Female
Infant SARS-CoV-2 test	Not performed	Not performed
Infant health at discharge	No concerns	No concerns
<b>Placental features</b>		
Placental weight (g)	585 <sup>b</sup>	345
Percentile for gestational age	~75-90th	< 10th
Percent of lesion involvement	> 50%	> 50%
Other placental findings	Accessory lobe Eccentric cord insertion Fetal vascular malperfusion Chronic chorioamnionitis Infarcts (30%)	Eccentric cord insertion Plasma cell deciduitis
<b>Indication for pathological evaluation</b>		
<b>Placental studies</b>		
RNA in situ hybridization		
SARS-CoV-2	Negative	Negative
Immunohistochemical stains		
Cytomegalovirus (CMV)	Negative	Negative
Spirochete	Negative	Negative
Polybacterial <sup>d</sup>	Negative	Negative
Listeria <sup>d</sup>	Negative	Negative
Chlamydia <sup>d</sup>	Negative	Negative
E. coli <sup>d</sup>	Negative	Negative
Group B Streptococcus (GBS) <sup>d</sup>	Negative	Negative
SARS-CoV-2 <sup>d</sup>	Negative	Negative
Select gram-negative bacteria <sup>d</sup>	Negative	Negative
Staphylococcus spp. (case 1) <sup>d</sup>	Negative	Negative
Streptococcus spp. <sup>d</sup>	Negative	Negative
Special stain		
Lillie-Twort gram <sup>d</sup>	Negative	Negative
Grocott methenamine silver (GMS)	Negative	Negative
Brown-Hopps	Negative	Negative
Acid-fast bacillus (AFB)	Negative	Negative
<b>Polymerase chain reaction</b>		
SARS-CoV-2 <sup>d</sup>	Negative	Negative
Gram-positive & gram-negative 16S rRNA <sup>d</sup>	Negative	Negative

<sup>a</sup> Gastroesophageal reflux disease

<sup>b</sup> Post-fixation weight

<sup>c</sup> Intrauterine growth restriction

<sup>d</sup> Performed by Centers for Disease Control and Prevention

Figure 1 - 965

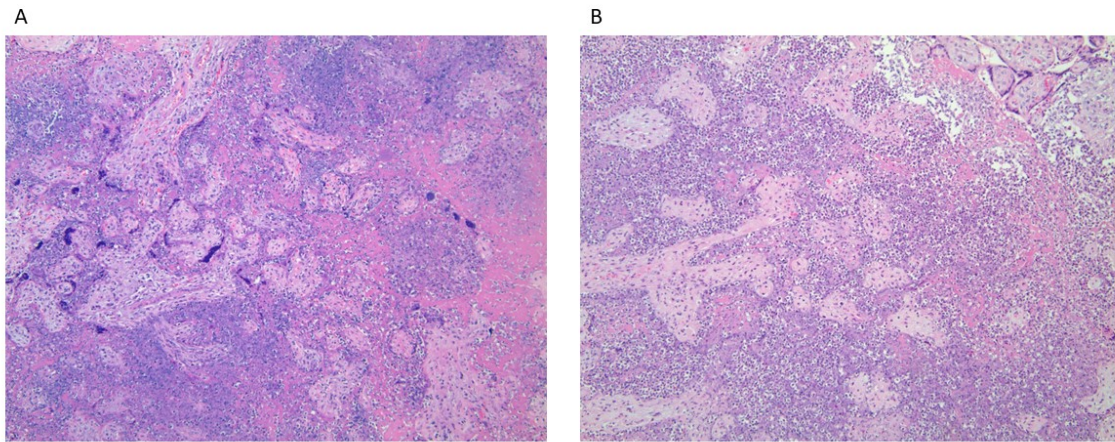


Figure 1: "Abscess"-like lesions in case 1 (A) and case 2 (B), showing acute intervillitis with acute villitis and moderate perivillous fibrin deposition. Villous necrosis was present. 10X original.

**Conclusions:** We describe two placentas with unique and striking pathology associated with recovered gestational SARS-CoV-2 infection. At this time, there are no apparent adverse neonatal outcomes. The absence of any positive result from the vast array of infectious studies performed (including SARS-CoV-2 RNA-ISH and IHC) suggest the cause of these abscess-like placental lesions may not be infectious. As this pathology is otherwise rare, and the two cases had only maternal SARS-CoV-2 infection in common, we propose this pathology to be related to COVID-19 but not caused by direct placental SARS-CoV-2 infection.

#### **966 Trichorhinophalangeal Syndrome Type 1 (TRPS1) Immunohistochemical Expression in Carcinomas of Müllerian Origin**

Felipe Ruiz Casas<sup>1</sup>, Youley Tjendra<sup>2</sup>, Nicolas Millan<sup>3</sup>, Carmen Gomez-Fernandez<sup>4</sup>, Andre Pinto<sup>2</sup>

<sup>1</sup>University of Miami Miller School of Medicine/Jackson Health System, Miami, FL, <sup>2</sup>University of Miami Health System, Miami, FL, <sup>3</sup>Jackson Memorial Hospital/ University of Miami Hospital, Miami, FL, <sup>4</sup>University of Miami Miller School of Medicine, Miami, FL

**Disclosures:** Felipe Ruiz Casas: None; Youley Tjendra: None; Nicolas Millan: None; Carmen Gomez-Fernandez: None; Andre Pinto: None

**Background:** Trichorhinophalangeal syndrome type 1 (TRPS1) is a new sensitive and reportedly specific marker for carcinomas of breast origin, including triple negative tumors. We have observed in our practice a subset of cases of non-mammary carcinomas that stained positive for TRPS1, with higher frequency in cytology effusion samples with gynecologic malignancies. The goal of this study was to evaluate the expression of TRPS1 in a large cohort of Müllerian carcinomas.

**Design:** 105 cases of formalin-fixed, paraffin embedded (FFPE) gynecologic tumors were retrospectively retrieved from our surgical pathology archives. Cases corresponded to tumors of tubo-ovarian (17 HGSC, 3 LGSC, 2 clear cell, 8 endometrioid), endometrial (25 endometrioid [16 low-grade, 9 high-grade], 8 serous, 6 clear cell, 12 carcinosarcoma, 1 dedifferentiated, 1 mesonephric-like), cervical (6 SCC, 11 HPVA, 2 gastric-type) and vulvar (3 SCC) origins. Whole tissue sections were stained by TRPS1 IHC and slides were assessed for positivity ( $\geq 5\%$  of nuclear labeling), distribution (focal: 5-49%, diffuse: 50-100%) and intensity (1+, 2+, 3+). Positive and negative controls were appropriately used.

**Results:** Positive staining was observed in 54/ 105 (51.4%) tumors. Most tumors demonstrated diffuse labeling (64.8%), while focal in (35.2%). Among positive cases, immunoreactivity was mostly 1+ (57.4%), followed by 2+ (33.3%) and 3+ (9.2%). Tumors with high percentage of positive cases consisted of tubo-ovarian origin (70%), followed by endometrial origin (58.4%). All LGSC, cervical adenocarcinomas and vulvar carcinomas were negative.

See Table 1.

**Table 1. TRPS1 Expression in Carcinomas of Müllerian Origin by site and tumor type**

	POSITIVE	DISTRIBUTION		INTENSITY		
		Diffuse	Focal	1+	2+	3+
<b>VULVA</b>						
SCC	0/3	n/a	n/a	n/a	n/a	n/a
<b>CERVIX</b>						
SCC	2/6	0	100%	100%	0	0
HPVA	0/11	n/a	n/a	n/a	n/a	n/a
Gastric-type CA	0/2	n/a	n/a	n/a	n/a	n/a
<b>ENDOMETRIUM</b>						
Endometrioid (low grade)	8/16	75%	25%	87.5%	12.5%	0
Endometrioid (high grade)	8/9	87.5%	12.5%	12.5%	62.5%	25%
USC	5/8	60%	40%	60%	40%	0
Carcinosarcoma	8/12	75%	25%	37.5%	50%	12.5%
Dedifferentiated CA	1/1	0	100%	100%	0	0
CCC	1/6	0	100%	100%	0	0
MLA	0/1	n/a	n/a	n/a	n/a	n/a
<b>TUBO-OVARIAN</b>						
HGSC	12/17	58.4%	41.6%	50%	33.3%	16.6%
LGSC	0/3	n/a	n/a	n/a	n/a	n/a
Endometrioid	7/8	85.8%	14.2%	71.5%	28.5%	0
CCC	2/2	0	100%	100%	0	0

**Abbreviations:** SCC: squamous cell carcinoma; HPVA: HPV associated adenocarcinoma, USC: uterine serous carcinoma, CCC: clear cell carcinoma, MLA: mesonephric-like adenocarcinoma, HGSC: high grade serous carcinoma, LGSC: low grade serous carcinoma

Figure 1 - 966

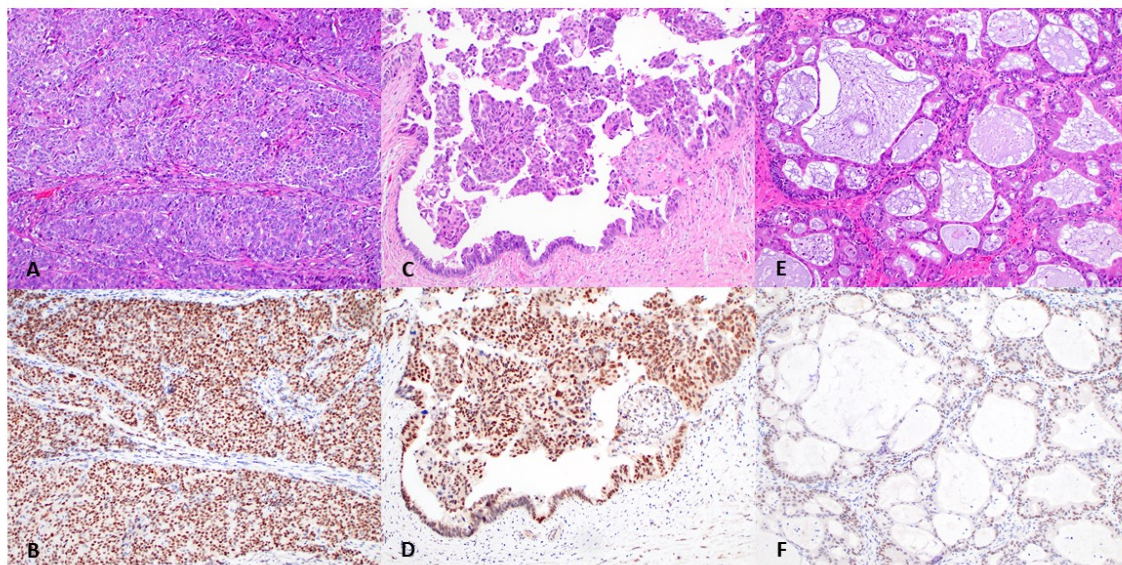


Figure 1. Endometrial endometrioid carcinoma (A; hematoxylin and eosin (H&E), 100x) with diffuse and strong TRPS1 staining intensity (3+) (B). Tubo-ovarian high-grade serous carcinoma (C; H&E, 100x) with focal and strong TRPS1 staining intensity (3+) (D). Ovarian endometrioid adenocarcinoma (E; H&E, 100x) with diffuse and moderate TRPS1 staining intensity (2+) (F).

**Conclusions:** Our results indicate that a significant subset (approximately half) of Müllerian carcinomas can be positive for TRPS1, in particular endometrial and tubo-ovarian malignancies. These findings should be considered when evaluating carcinomas of unknown origin, to avoid misclassification of the primary site.

## 967 Does the Presence of Plasma Cells in Infertility Evaluation Endometrial Biopsies Influence Clinical Fertility Outcomes?

Jason Scapa<sup>1</sup>, Sean Lau<sup>2</sup>

<sup>1</sup>Kaiser Permanente Medical Center, Anaheim, Anaheim, CA, <sup>2</sup>Kaiser Permanente (SCPMG), Anaheim, CA

**Disclosures:** Jason Scapa: None; Sean Lau: None

**Background:** Chronic endometritis and the presence of plasma cells (PCs) on endometrial biopsy (EMB) has been implicated as a cause of poor reproductive outcomes. Criteria for the histopathologic diagnosis of chronic endometritis is not well defined. In the context of infertile patients, there is variability on how many PCs are considered clinically significant to constitute treatment with antibiotics.

**Design:** Retrospective review of all EMBs in patients presenting for infertility evaluation at our institution accessioned from February to September 2021 was performed. Endometrial histomorphology and presence of PCs on hematoxylin and eosin (H&E) stain slides and immunohistochemical stains for CD138 and MUM1 were assessed. Findings were correlated with clinical and treatment parameters, with clinical outcome follow-up data being available for at least one year after biopsy for all patients.

**Results:** There were 93 EMBs from 86 unique patients presenting for infertility workup during the study period. Of the initial EMB cases, 47 (55%) showed the presence of at least one immunohistochemically confirmed PC per mm<sup>2</sup>, while 39 (45%) showed no PCs. Only 7 of the 47 cases (15%) with immunohistochemically confirmed PCs had the PCs readily identified on H&E stained material. 23 patients (49%) who had PCs on the initial biopsy had a viable pregnancy at time of follow-up versus 12 patients (30%) with no PCs on their initial biopsy having a subsequent pregnancy. 17 of the patients with at least one PC per mm<sup>2</sup> received antibiotic treatment with 8 (47%) having a pregnancy at follow-up. This is compared to 15 of the 30 patients (50%) with PCs on biopsy but not receiving antibiotics having a pregnancy at follow-up. In the 27 cases with greater than five immunohistochemically confirmed PCs per mm<sup>2</sup>, 5 of the 13 patients (38%) who received antibiotics had a viable pregnancy at follow-up contrasted with 7 of 14 (50%) in those not receiving antibiotics. Six patients had a "test of cure" follow-up biopsy for PCs after receiving antibiotics. Three of these patients (50%) had no PCs on repeat biopsy.

**Conclusions:** In our practice setting, many patients with PCs on their EMB for infertility evaluation, even those who do not receive subsequent antibiotics, were able to have a viable pregnancy at follow-up. Thus, the clinical significance of PC counts and routine utilization of CD138 and MUM1 immunohistochemistry to facilitate identification of PCs in EMBs performed for the assessment of female infertility is controversial.

## 968 Conventional Versus Alternative (FIGO) Methods for Depth of Invasion and Tumor Size Estimation in Vulvar Squamous Cell Carcinoma: Outcome-Based Validation Underscoring the Potential for Under-Staging

Aarti Sharma<sup>1</sup>, Nicolas Wyvekens<sup>2</sup>, David Chapel<sup>3</sup>, Marisa Nucci<sup>2</sup>, Carlos Parra-Herran<sup>2</sup>

<sup>1</sup>Hospital for Special Surgery, Boston, MA, <sup>2</sup>Brigham and Women's Hospital, Harvard Medical School, Boston, MA,

<sup>3</sup>Michigan Medicine, University of Michigan, Ann Arbor, MI

**Disclosures:** Aarti Sharma: None; Nicolas Wyvekens: None; David Chapel: None; Marisa Nucci: None; Carlos Parra-Herran: None

**Background:** Current staging of vulvar squamous cell carcinoma (VS) is complicated by shifting definitions. The 2021 FIGO staging changed the landmark for depth of invasion (DOI) measurement from the most superficial papillary plate (DOIp) to the closest rete peg (DOIr) (Fig 1). This shift was based on cohorts that showed no compromise in survival when reclassifying from stage IB to IA based on DOIr. Moreover, per AJCC staging, tumor size measurement should incorporate *in situ* disease (GS, conventional), and not solely the span of invasive disease (IS). Herein, we aim to evaluate the performance of these diverse metrics with respect to patient outcomes.

**Design:** Primary resections for VS were identified retrospectively. DOIr, DOIp, GS and IS metrics were obtained after evaluation of all tumor-containing slides. Clinicopathologic data was collected from the chart. Primary endpoints were recurrence-free survival (RFS) and lymph node involvement (LNI) at time of resection.

**Results:** A total of 79 cases were identified. Of these, 4 (5%) patients were staged IA per convention and 75 (95%) IB. Significant disparities were observed between average IS (13mm) and average GS (17mm, p\*<0.006) and between average DOIr (4.5mm) and average DOIp (5.2mm, p\*<0.0005) on paired t-tests. Clinicopathologic features are summarized in Table 1. Overall, 17 (22%) patients recurred after a median of 33 months. Fig 2 illustrates RFS for patients staged using conventional DOIp and alternative DOIr. While 100% of patients staged as IA by conventional DOIp measurement remain disease-free after resection, 3/12 (25%) that were 'downstaged' by DOIr measurement recurred after an average of 47 months. Of the 'downstaged' 11 with follow-up, 8 are alive without disease, 1 is alive with disease, and 2 are deceased of unknown causes. Of the 65 patients who underwent groin dissection, 13 (20%) showed LNI (all of which were stage IB regardless of measurement used). Logistic regression demonstrated all of DOIp (p\*=0.03), DOIr (p\*=0.02), and GS (p\*=0.049) to be significantly associated with LNI.

N (total patients)	79
Age (years)	64 (range 38-103)
Gross/clinical tumor size (mm)	28 ± 13
DOI (papillary plate, mm)	5.2 ± 4.5
DOI (rete peg, mm)	4.5 ± 4.6
GS ( <i>in situ</i> + invasive tumor, mm)	17 ± 10.2
IS (invasive tumor only, mm)	13 ± 10.1
Lymphovascular invasion	10/79 (13%)
Perineural invasion	5/79 (6%)
Lymph node metastasis at presentation	13/65 (20%)
Precursor lesion	
Usual (HPV-associated) VIN*	40/79 (51%)
Differentiated (HPV-independent) VIN*	20/79 (25%)
No specific precursor	19/79 (24%)
Margin status	
Negative	67/79 (85%)
Involved by precursor lesion	11/79 (14%)
Involved by invasive carcinoma	1/79 (1%)
Local recurrence	17/79 (22%)
Median time to recurrence (months)	33 (range 6-89)
Pathologic Stage by Method of Measurement	
IA	IA
Conventional (DOI <sub>p</sub> and GS)	4/79 (5%)
Alternative (DOI <sub>r</sub> and IS)	4/79 (5%)
IB	IB
Conventional (DOI <sub>p</sub> and GS)	75/79 (95%)
Alternative (DOI <sub>r</sub> and IS)	75/79 (95%)
Alternative (DOI <sub>r</sub> and GS)	63/79 (80%)
Alternative (DOI <sub>r</sub> and IS)	63/79 (80%)
Patients 'Downstaged' from IB to IA per DOI <sub>r</sub>	12/79 (15%)
Downstaged patients who recurred locally	3/12 (25%)
Precursor lesion for recurrent, downstaged patients	
HPV-associated	1/3 (33%)
HPV-independent	1/3 (33%)
No specific precursor	1/3 (33%)
<b>Table 1:</b> Clinicopathologic features of the cohort of early-stage vulvar squamous cell carcinomas	
*VIN=Vulvar Intraepithelial Neoplasia	
(Measurements are Average ± Standard Deviation unless otherwise specified)	

Figure 1 - 968

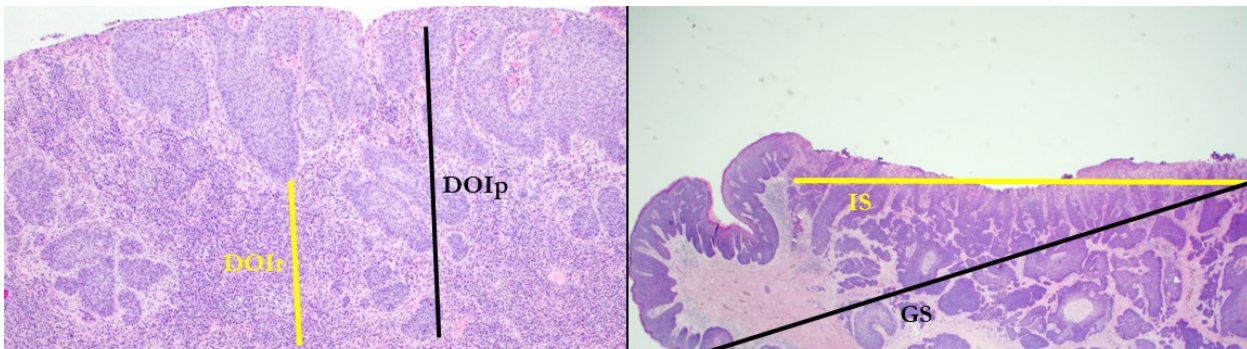
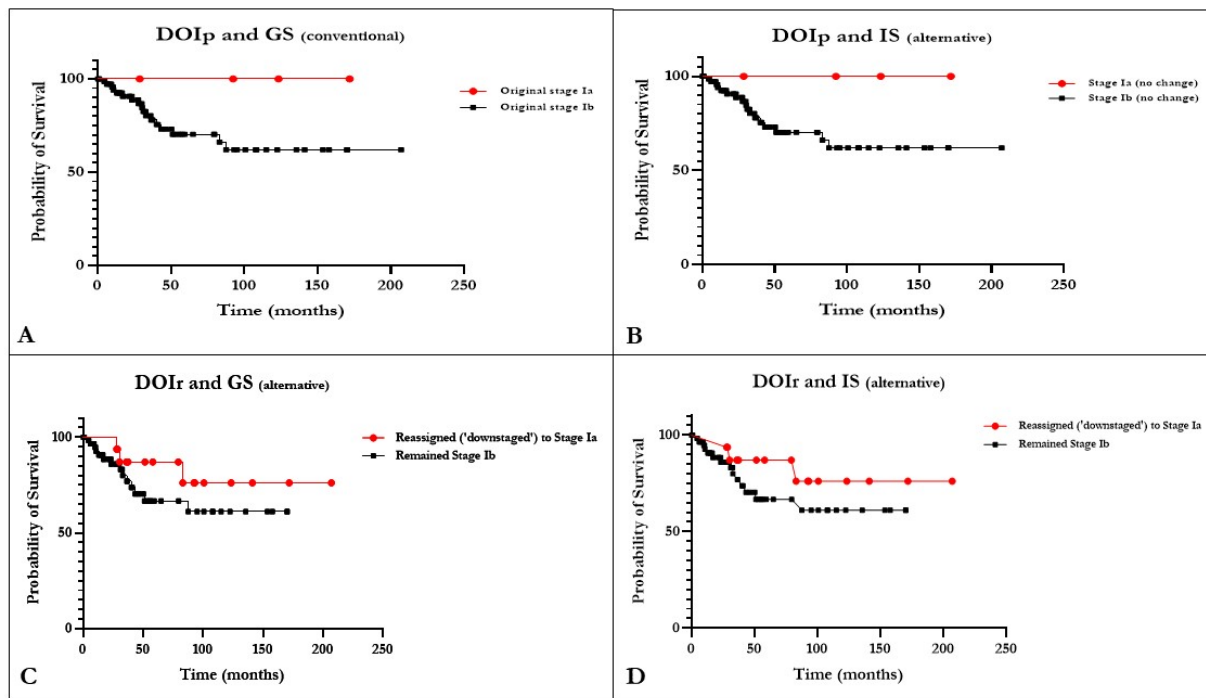


Figure 1A. Methods of depth of invasion (DOI) measurement. The black line is a measurement taken from the most superficial dermal papillary plate to the deepest point of invasion (DOI<sub>p</sub>, conventional). The yellow line is a measurement from the nearest *in situ* rete peg to the deepest point of invasion (DOI<sub>r</sub>, FIGO 2021, alternative).

Figure 1B. Methods of tumor size measurement. The black line illustrates the extent of both the *in situ* component – high-grade usual-type squamous intraepithelial lesion – along with the invasive component (GS, conventional, AJCC). The yellow line illustrates the extent of the invasive component only (IS, alternative).

Figure 2 - 968



**Figure 2.** Kaplan-Meier curves for recurrence-free survival (RFS) compared across conventional and alternative staging methods. **A.** RFS using conventional methods of measurement (DOI<sub>p</sub> and GS). Original stage Ia patients show 100% RFS with a clear departure from the RFS of original stage Ib patients. **B.** Use of DOI<sub>p</sub> and IS (alternative) did not change the stage of any patient. **C.** Use of DOI<sub>r</sub> (alternative) and GS resulting in 12 patients downstaged from Ib to Ia. A subsequent reapproximation of RFS curves is observed with this modification. A similar trend is observed in panel **D**, where both alternative methods (DOI<sub>r</sub> and IS) are used towards stage.

**Conclusions:** In contrast to prior studies, we document adverse events in patients downstaged from IB to IA using the new FIGO DOI method, a finding that merits study in large-scale, cross-institutional cohorts. Meanwhile, reporting DOI<sub>p</sub> is prudent for clinical management. While estimations of tumor size vary from AJCC recommendations (GS) when only the invasive span is measured (IS), their impact on outcome appears superseded by the DOI metric.

## 969 Vascular Neoplasms of the Distal Female Genital Tract: A Clinicopathologic Analysis of 48 Cases Illustrating Their Unusual and Diverse Presentations

Aarti Sharma<sup>1</sup>, Nicolas Wyvekens<sup>2</sup>, Carlos Parra-Herran<sup>2</sup>, Christopher Fletcher<sup>3</sup>, Marisa Nucci<sup>2</sup>

<sup>1</sup>Hospital for Special Surgery, Boston, MA, <sup>2</sup>Brigham and Women's Hospital, Harvard Medical School, Boston, MA, <sup>3</sup>Brigham and Women's Hospital, Boston, MA

**Disclosures:** Aarti Sharma: None; Nicolas Wyvekens: None; Carlos Parra-Herran: None; Christopher Fletcher: None; Marisa Nucci: None

**Background:** Scarce literature exists regarding the spectrum of vascular neoplasms of the vulvovaginal area. Herein, we describe the clinicopathologic features of a cohort of endothelial and myopericytic neoplasms of the vulva and vagina.

**Design:** Benign, intermediate, and malignant vascular proliferations were identified retrospectively from in-house and consultation files at our institution. Clinicopathologic data was obtained from review of the chart and available histologic material.

**Results:** A total of 49 cases were identified (Table 1). Lobular capillary hemangioma (LCH, n=35) presented with a symptomatic bleeding nodule, and - in contrast to extragenital sites - infrequently in association with ulceration (10/33, 30%), prior chemoradiation (1/35, 3%), or pregnancy (1/35, 3%). Myopericytic neoplasms encompassed myofibroma (MF, n=1), myopericytoma (MP, n=2), and glomus tumor (GT, n=1). These showed a spectrum of fasciculated spindle (MP, MF) to epithelioid cells (GT) with interspersed branching vasculature. All were positive for SMA (Fig 1). Kaposi sarcoma (KS, n=2) were of the enigmatic 'sporadic' form in elderly non-HIV females. KS and kaposiform hemangioendothelioma (KHE, n=1) both showed compressed vascular spaces resembling spindled fascicles, with up to moderate atypia and average mitoses 8/10 high-power fields. The single KHE presented at an older (rather than pediatric) age and was negative for HHV-8 by IHC; both KS were positive.

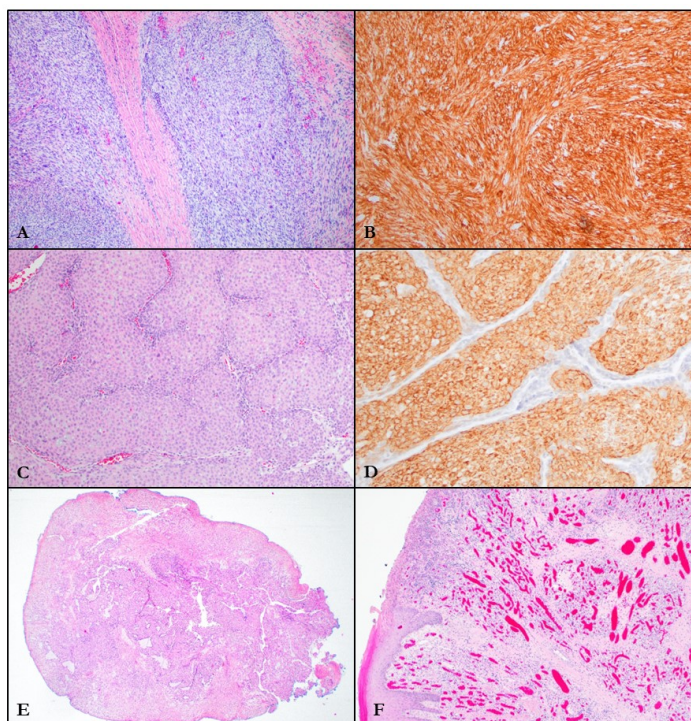
The single pseudomyogenic hemangioendothelioma in an elderly female (rather than young male) showed bundles of myoid-appearing cells in the superficial dermis with positivity for FOSB and AE1/3. Epithelioid hemangioendothelioma (EHE, n=4) had infiltrative borders, nests to cords of atypical epithelioid cells in variably well-developed chondromyxoid matrix (2/4, 50%) and CAMTA1 positivity (3/3, 100%). Epithelioid angiosarcoma (n=1) presented at the remarkably young age of 14 years and showed nodules of frankly anaplastic EMA and CD31-positive cells infiltrating through the deep dermis and subcutis (Fig 2).

	Lobular Capillary Hemangioma	Glomus Tumor	Myopericytoma	Kaposi Sarcoma	Epithelioid Hemangioendothelioma	Angiosarcoma
<b>N</b>	35	1	2	2	4	1
<b>Age (years <math>\pm</math> SD)</b>	49 $\pm$ 18	62	35 $\pm$ 0.7	72 $\pm$ 6	41 $\pm$ 25	14
<b>Site</b>						
Vulva/Pennum	27/35 (77%)	1/1 (100%)	2/2 (100%)	1/2 (59%)	1/4 (25%)	1/1 (100%)
Vagina	3/35 (9%)	0	0	0	0	0
Inguinal	5/35 (14%)	0	0	1/2 (50%)	3/4 (75%)	0
<b>Recurrence</b>	1/35 (3%)	NA	NA	0/1 (0%)	1/3 (33%)	NA
Time to recurrence/metastasis	Vulva, 10 years	NA	NA	NA	Lung, 6 months	NA
<b>Immunohistochemistry</b>						
EMA/Any cytokeratin	--	0/1 (0%)	--	--	1/4 (25%)	1/1 (100%)
ERG	--	--	--	1/1 (100%)	1/1 (100%)	--
CD31	--	--	--	--	1/3 (33%)	1/1 (100%)
CD34	--	--	--	--	4/4 (100%)	0/1 (0%)
SMA	--	1/1 (100%)	2/2 (100%)	--	3/3 (100%)	--
CAMTA1	--	--	--	--	3/3 (100%)	--
HHV-8	--	--	--	2/2 (100%)	--	--

**Table 1.** Clinicopathologic and immunohistochemical features of the cohort of vulvovaginal neoplasms.

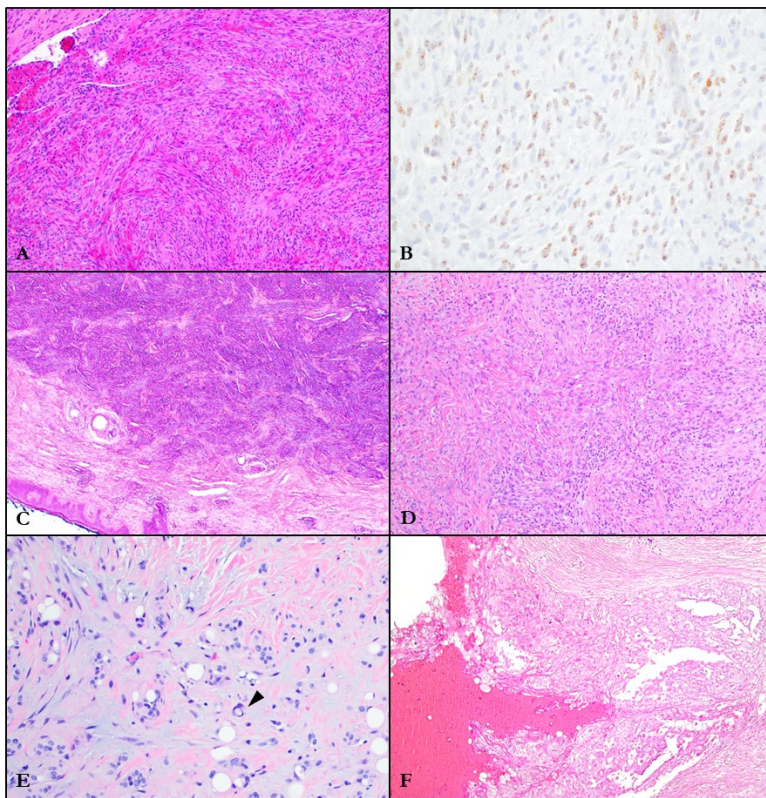
NA = not applicable, SD = standard deviation

Figure 1 - 969



**Figure 1.** A-B. *Vulvar Myofibroma*. A. Hypercellular, mitotically active fascicles of myoid spindle cells. B. Diffuse SMA positivity. C-D. *Vulvar Glomus Tumor*. C. Squamoid-appearing round cells configured around compressed branching capillaries. D. Strong SMA positivity (negative in intervening endothelium). E. *Vulvar Myopericytoma*. Spindle cells arranged around striking branching vasculature. F. *Vulvar Lobular Capillary Hemangioma*. Lobular capillary clusters ulcerating into overlying squamous mucosa, clinically mimicking malignancy.

Figure 2 - 969



**Figure 2.** A-B. *Vulvar Kaposi Sarcoma*. A. Nodular syncytial proliferation of bland endothelial cells with extravasated erythrocytes. B. Positive HHV-8 immunostain. C. *Vulvar Kaposiform Hemangiendothelioma*. Hypercellular dermal neoplasm with spindle cell fascicles and peripheral capillary proliferation. D. *Vulvar Pseudomalignant Hemangiendothelioma*. Myoid-appearing cells with deep eosinophilic cytoplasm amidst mixed inflammation. E. *Vulvar Epithelioid Hemangiendothelioma*. Epithelioid cells in a chondromyxoid stroma without discernable vessel formation. An intracytoplasmic vacuole is shown (arrowhead). F. *Vulvar Epithelioid Angiosarcoma*. Overtly pleomorphic cells with endothelial bridging and multilayering between anastomotic vascular spaces.

**Conclusions:** This series of 48 cases is the largest to characterize these rare vulvovaginal vascular tumors. While many morphologic features of vascular lesions at this site overlap with those of extragenital soft tissues, pathologists must be aware that these tumors may occur in the vulvovaginal area and display unconventional clinical profiles. As such, a broad differential for epithelioid and spindle cell neoplasms at this site is prudent.

## 970 Vulvovaginal Vascular Malformations: A Clinicopathologic Analysis of 90 Cases Illustrating Their Diverse Morphologic Spectrum and Limited Risk of Recurrence

Aarti Sharma<sup>1</sup>, Nicolas Wyvekens<sup>2</sup>, Carlos Parra-Herran<sup>2</sup>, Christopher Fletcher<sup>3</sup>, Marisa Nucci<sup>2</sup>

<sup>1</sup>Hospital for Special Surgery, Boston, MA, <sup>2</sup>Brigham and Women's Hospital, Harvard Medical School, Boston, MA, <sup>3</sup>Brigham and Women's Hospital, Boston, MA

**Disclosures:** Aarti Sharma: None; Nicolas Wyvekens: None; Carlos Parra-Herran: None; Christopher Fletcher: None; Marisa Nucci: None

**Background:** Routine clinical surveillance of vulvovaginal tissues for squamous dysplasia can reveal tumefactive but non-neoplastic vascular lesions that may be misconstrued as malignancy. Herein, we characterize a cohort of vascular malformations of the vulva and vagina to better understand their morphologic spectrum and risk of recurrence.

**Design:** Vulvovaginal vascular malformations were identified retrospectively from in-house and consultation files at our institution. Clinicopathologic data was obtained from chart and slide review.

**Results:** 90 cases from 85 patients were collected, including angiokeratoma (AK, n=53), lymphangioma circumscriptum (LC, n=8), hemangioma (HM, n=15), lymphangioma (LM, n=3), and 'venous' lake (VL, n=11). Mean patient age was 50 (range 22-85 years), with 80 cases in the vulva and 10 in the vagina (Table 1). None manifested syndromic stigmata, save for 2 LC patients with hidradenitis suppurativa. AK and LC showed epidermal interruption by ectatic, thrombosed superficial dermal capillaries and lymphatics. 5/56 (9%) were associated with prior pelvic radiation, 4/56 (7%) were incidentally discovered during pregnancy, and

8/56 (14%) recurred after 0.4-13 years. In contrast, VL consisted of a single ectatic, thrombosed superficial dermal vessel lacking an epidermal response, with peripheral fibroblastic stromal reaction (Fig 1). None recurred or were associated with prior radiation or pregnancy. While criteria for distinction between benign vascular 'neoplasm' and 'malformation' are not well-established in otherwise nonspecific vascular proliferations, LM and HM were considered best classified as the latter, due to morphologic features including poorly defined, haphazardly arranged vascular channels in the deeper dermis with variable investment of medial smooth muscle and degrees of ectasia (Fig 2). These presented as large masses (up to 9.5 cm); 3/16 recurred after 1-23 years, and 1/16 (6%) was associated with fatal Kasabach-Merritt phenomenon. Notably, features suggestive of endothelial malignancy (nuclear atypia, hobnailing, mitoses, bridging, multilayering), when present, were limited and interpreted as reactive within the clinicopathologic context.

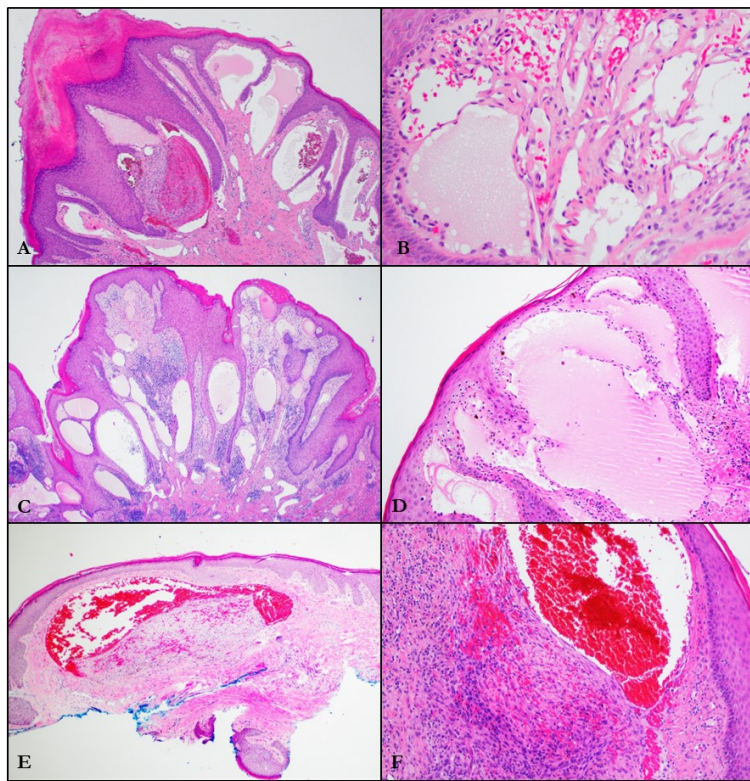
	Angiokeratoma	Lymphangioma Circumscriptum	Venous Lake	Hemangioma	Lymphangioma
<b>N</b>	53	8	11	15	3
<b>Age (years ± SD)</b>	52 ± 14	45 ± 11	46 ± 13	54 ± 14	45 ± 11
<b>Site</b>					
Vulva	53/53 (100%)	6/8 (75%)	8/8 (100%)	7/15 (47%)	2/3 (67%)
Vagina	0%	2/8 (25%)	0%	8/15 (53%)	0%
<b>Clinical</b>					
Prior chemoradiation	4/49 (8%)	1/7 (14%)	0%	0%	0%
Prerogestational	6/49 (2%)	0%	0%	0%	0%
Symptomatic	10/49 (20%)	1/7 (14%)	1/10 (10%)	0%	1/2 (50%)
Incidental during routine or surveillance checkup	13/39 (33%)	1/6 (17%)	8/10 (80%)	8/15 (53%)	0%
Vascular lesion suspected clinically	18/49 (37%)	1/7 (14%)	6/11	3/15 (20%)	0%
<b>Recurrence</b>	7/49 (14%)	1/7 (14%)	0%	3/15 (20%)	0%
Time to recurrence (years)	0.4-13	5	NA	1-23	NA
<b>Gross description</b>	Variable	Tan-white blister	Brown macule	Thrombosed ectatic channels	Variable
<b>Vascular caliber</b>					
Capillary	All	All	8/9 (89%)	3/15 (20%)	0
Variable medial smooth muscle	0	0	1/9 (11%)	4/15 (27%)	3/3 (100%)
Combination	NA	NA	0	8/15 (53%)	0
<b>Epidermal changes*</b>	45/53 (85%)	8/8 (100%)	4/11 (36%)	7/15 (47%)	NA
Thrombosis	26/53 (49%)	4/8 (50%)	6/11 (55%)	4/15 (27%)	1/3 (33%)
Stromal hyalinization	31/48 (65%)	6/7 (86%)	8/11 (73%)	8/15 (53%)	1/2 (50%)
Mitoses/10 HPF	0	0	0	0	0
Hobnail endothelium	25/53 (47%)	5/8 (63%)	3/11 (27%)	0	0

**Table 1.** Clinicopathologic features of the cohort of vulvovaginal malformations

\*Any of commensurate peripheral rete elongation, acanthosis, marked hyperkeratosis.

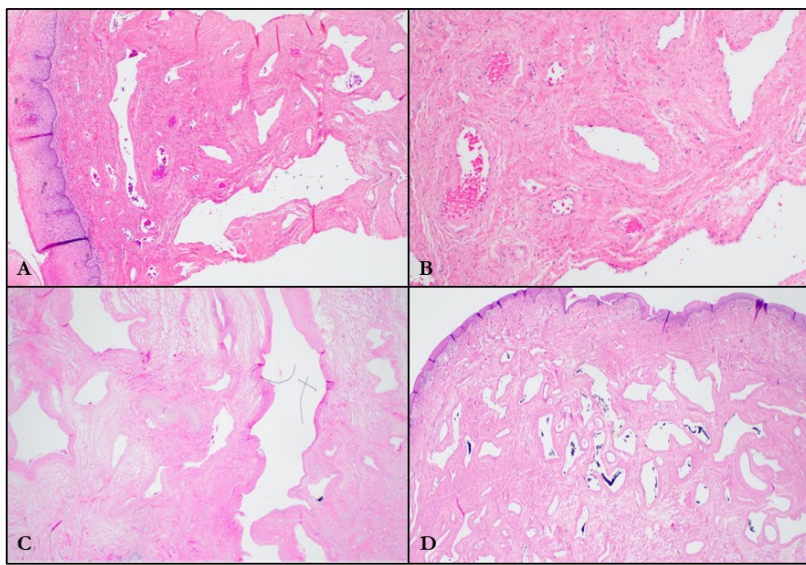
NA = not applicable, HPF = High-power fields, SD = standard deviation

Figure 1 - 970



**Figure 1.** **A-B.** *Vulvar Angiokeratoma*. A. Dermal capillaries herniating into a hyperplastic, verrucoid epidermis, mimicking squamous neoplasia. B. Interanastomosing sinusoids with focal hobnail endothelial cells. **C-D.** *Vulvar Lymphangioma Circumscriptum*. C. Dilated superficial lymphatics and accompanying squamous hyperplasia. D. Ectatic lymphatics filled with proteinaceous serum. **E-F.** *Vulvar Venous Lake*. E. Single ectatic, thrombosed dermal vessel without epidermal change. F. Adjacent fibroblastic stromal response.

Figure 2 - 970



**Figure 2.** **A-B.** *Vulvar Hemangioma/malformation*. A. Dilated irregular blood-filled vessels in the superficial and deep dermis. B. Nonspecific admixture of vascular channels of variable caliber with attenuated endothelium. **C-D.** *Vulvar Lymphangioma/malformation*. C. Haphazard arrangement of ectatic, thick-walled lymphatic channels. D. Ramifying meshwork of meandering vessels in the deep dermis without epidermal change.

**Conclusions:** This series of 92 cases is the largest to date characterizing non-neoplastic mass-forming vascular lesions of the vulvovaginal region. Recognition of clinical and morphologic hallmarks should aid in accurate diagnosis to limit overtreatment and stratify risk of recurrence.

## 971 PD-L1, IDO, and CD8 Expression in High-Grade Ovarian Carcinomas Treated with Checkpoint Inhibition: Current Barriers to Immunotherapeutic Response and Future Opportunities for Multimodal Therapy

Nancy Shen<sup>1</sup>, Laurie Griesinger<sup>2</sup>, Akua Nyarko-Odoom<sup>1</sup>, Santos Acosta Martinez<sup>1</sup>, Kari Ring<sup>1</sup>, Anne Mills<sup>1</sup>

<sup>1</sup>University of Virginia, Charlottesville, VA, <sup>2</sup>South Bend Medical Foundation, South Bend, IN

**Disclosures:** Nancy Shen: None; Laurie Griesinger: None; Akua Nyarko-Odoom: None; Santos Acosta Martinez: None; Kari Ring: None; Anne Mills: None

**Background:** PD-1/PD-L1-based checkpoint inhibitor therapy has been utilized successfully in many solid tumors, including some gynecologic cancers. Responses in ovarian carcinoma, however, have been limited even in the context of PD-L1 expression. Indoleamine dioxygenase 2,3 (IDO) is a targetable immunosuppressive enzyme which may contribute to immunotherapeutic resistance, but which has not been studied in ovarian carcinomas treated with checkpoint inhibition. Moreover, the relationship between overall cytotoxic T cell infiltration and immunotherapeutic response has not been well investigated in this setting.

**Design:** PD-L1, IDO, and CD8 immunostaining was performed on pre-treatment whole tissue sections from 30 high-grade ovarian carcinoma patients, including 17 who received immunotherapy in the setting of platinum-resistant recurrence. PD-L1 and IDO were each given a Combined Positive Score (CPS), with a score of greater than 1 considered positive. CD8-positive tumor-associated lymphocytes were manually enumerated and averaged across 10 high-power fields (HPF). In patients who received immunotherapy, drug response was assessed using RECIST criteria and final response status at the time of last follow-up was recorded.

**Results:** The tumors consisted of high-grade serous carcinomas (24), carcinosarcomas (2), clear cell carcinomas (2), small cell hypercalcemic-type carcinoma (1), and endometrioid carcinoma (1). PD-L1 and IDO were positive in 87% (26/30, CPS range 1-100) and 77% (23/30, CPS Range 1-60) of tumors, respectively, with 81% (21/26) of PD-L1-positive cases co-expressing IDO. Tumors showed an average of 10 CD8-positive cytotoxic T cells per HPF (range: 1-58); 67% (20/30) had  $\geq 10$  HPF, and there was no significant relationship between CD8 counts and IDO or PD-L1 expression. Only one of 17 patients who received immunotherapy in the setting of a platinum-resistant recurrence showed a partial response to the addition of immunotherapy; no tumors showed a complete response, and all 17 ultimately died of disease.

**Conclusions:** The majority of high-grade ovarian carcinomas show IDO and PD-L1 co-expression with low (greater than 10 per HPF) levels of CD8-positive cytotoxic T cell infiltration. Multimodal immunotherapeutic approaches that target IDO and enhance tumor lymphocytic recognition (such as radiotherapy or focused ultrasound treatment) may be of value in improving checkpoint inhibitor responses in this patient population.

## 972 Fumarate-Hydratase Deficient Leiomyoma of the Uterine Corpus: Comparative Morphologic Analysis of Protein-Deficient Tumors with and Without Pathogenic (Germline) FH Gene Mutations and Description of an Institutional Experience

Wangpan Shi<sup>1</sup>, Yu Liu<sup>1</sup>, Omonigho Aisagbonhi<sup>2</sup>, Andres Roma<sup>2</sup>, Farnaz Hasteh<sup>2</sup>, Somaye Zare<sup>2</sup>, Oluwole Fadare<sup>1</sup>

<sup>1</sup>UC San Diego School of Medicine, La Jolla, CA, <sup>2</sup>University of California, San Diego, La Jolla, CA

**Disclosures:** Wangpan Shi: None; Yu Liu: None; Omonigho Aisagbonhi: None; Andres Roma: None; Farnaz Hasteh: None; Somaye Zare: None; Oluwole Fadare: None

**Background:** Deficiency of fumarate hydratase (FH) protein expression in uterine corpus leiomyomas (uLM) may be attributable to either germline or somatic/epigenetic mutations of the *FH* gene, the former being definitional for the Hereditary leiomyomatosis and renal cell cancer (HLRCC) syndrome. We present our experience with FH-deficient (FH-d) leiomyomas, encompassing a period during which morphologic indicators that may suggest FH deficiency have become more widely applied in our group, and immunohistochemical analyses for FH expression in such tumors have become routine.

**Design:** Reports for all uLM diagnosed during a 5 year period were reviewed. Cases had been designated for FH immunohistochemistry (IHC) testing based on the presence therein of one or more morphologic features suggestive of FH deficiency ("FH-like features": table 1), in accordance with published literature. For patients that had consented to *FH* germline testing subsequent to their pathologic diagnoses, the resultant reports were reviewed. Morphologic and other clinicopathologic features were compared between cases with and without pathogenic mutations in the *FH* gene.

**Results:** From 2418 uLM that were diagnosed during the study period, 37 (1.5%) had been classified as displaying at least one "FH-like" morphological feature, and 29 (1.19%) had been classified as displaying such morphologic feature(s) and tested for FH expression by IHC. Compared to a control group of 370 uLM cases that were devoid of FH-like features, the 29 patients whose tumors showed FH like morphology were significantly younger (42 vs 47.86 years, p=0.009) and had substantially larger tumors

(means 11.06 cm vs 6.37 cm, p<0.01). 14 (48.27%) of the 29 cases showed FH protein deficiency by IHC (FH-d). 12 of these 14 patients elected to undergo germline testing; pathogenic *FH* mutations were present in 8 (66.67%) and were absent in 4 (33.33%). A comparison of morphologic features between the latter 2 groups is shown in table 1.

Table 1: Comparison of Fumarate Hydratase-Deficient uLM with and without pathogenic FH mutations

	Pathogenic mutations present	Pathogenic mutations absent	P-value
<b>Number of cases</b>	8 (67%)	4 (33%)	
<b>Mean patient age</b>	36.00±5.48	45.75±18.43	0.372
<b>Mean tumor greatest dimension (cm)</b>	14.58±11.23	8.90±4.08	0.36
<b>Primary FH-like features</b>			
<i>Staghorn vasculature</i>			0.515
present	6 (75%)	4 (100%)	
absent	2 (25%)	0 (0%)	
<i>Alveolar-type edema</i>			0.018*
present	8 (100%)	1 (25%)	
absent	0 (0%)	3 (75%)	
<i>Bizarre nuclei</i>			0.091
present	8 (100%)	2 (50%)	
absent	0 (0%)	2 (50%)	
<i>Chain-like tumor nuclei</i>			1
present	7 (88%)	3 (75%)	
absent	1 (12%)	1 (25%)	
<i>Hyaline globules</i>			0.061
present	6 (75%)	0 (0%)	
absent	2 (25%)	4 (100%)	
<i>Prominent eosinophilic or fibrillary cytoplasm</i>			0.018*
present	8 (100%)	1 (25%)	
absent	0 (0%)	3 (75%)	
<i>Prominent nucleoli and perinucleolar halo</i>			0.33
present	8 (100%)	3 (75%)	
absent	0 (0%)	1 (25%)	
<b>Mean number of FH-like morphologic features identified</b>	6.25±7.07	3.5±1.00	<0.001*
<b>Other potentially relevant features</b>			
<i>Necrosis</i>			0.491
present	0 (0%)	0 (0%)	
absent	8 (100%)	4 (100%)	
<i>Hypercellularity</i>			1
present	7 (88%)	4 (100%)	
absent	1 (12%)	0 (0%)	
<i>Leiomyomatosis-like morphology</i>	absent in all	absent in all	

**Conclusions:** Our findings affirm that FH-d uLM with germline *FH* mutations are not morphologically distinguishable from FH-d uLM with somatic *FH* mutations. Although the former more frequently show alveolar-type edema and prominent eosinophilic/fibrillary cytoplasm, no single morphologic feature, or combination of features, was found to be completely specific in making this distinction. Morphology and FH IHC based screening of uLM does facilitate the identification of a very minute subset of patients that harbor germline *FH* mutations.

## 973 High TRPS1 Expression Predicts Distant Recurrence of Early-Stage Endometrioid Adenocarcinoma (EMACA)

Lauren Skvarca<sup>1</sup>, Aisha Kousar<sup>2</sup>, Rayan Rammal<sup>1</sup>, Alison Garrett<sup>2</sup>, Christine McGough<sup>2</sup>, Esther Elishaev<sup>3</sup>, Chengquan Zhao<sup>2</sup>, Mirka Jones<sup>4</sup>, Rohit Bhargava<sup>2</sup>, Jamie Lesnock<sup>2</sup>, Thing Rinda Soong<sup>4</sup>

<sup>1</sup>University of Pittsburgh Medical Center, Pittsburgh, PA, <sup>2</sup>Magee-Womens Hospital, University of Pittsburgh Medical Center, Pittsburgh, PA, <sup>3</sup>University of Pittsburgh School of Medicine, Pittsburgh, PA, <sup>4</sup>University of Pittsburgh, Pittsburgh, PA

**Disclosures:** Lauren Skvarca: None; Aisha Kousar: None; Rayan Rammal: None; Alison Garrett: None; Christine McGough: None; Esther Elishaev: None; Chengquan Zhao: None; Mirka Jones: None; Rohit Bhargava: None; Jamie Lesnock: None; Thing Rinda Soong: None

**Background:** Early-stage EMACA generally carries a favorable prognosis but recurrences have been seen in a subset of cases. *TRPS1* was suggested as a candidate driver gene in EMACA and has been shown to have varying prognostic implications in breast and non-breast cancers. We evaluated the impact of *TRPS1* protein expression on the prognosis of low-stage (FIGO I) EMACA focusing on grade 3 (G3) endometrioid adenocarcinoma.

**Design:** TRPS1 immunohistochemical expression was examined in 184 hysterectomy specimens with FIGO stage I EMACA showing unequivocal G3 endometrioid histology. Cross-sectional analyses were tested with Fisher's exact tests. Log-rank tests and Cox proportional regression models with adjusted hazard ratios (aHRs) and 95% confidence intervals (CIs) were used to examine disease-specific survival (DSS) and recurrence-free survival (RFS).

**Results:** Median age was 65 years. Over 50% were FIGO IA disease, with 29% showing aberrant p53 expression. Two patients had isolated tumor cells in lymph nodes at the time of surgery. Most (78%) received adjuvant radiation therapy (RT), and 29% received chemotherapy. A subset (8%) harbored strong TRPS1 expression in more than 75% of tumor cells (TRPS1-high) (Fig. 1A-D). No statistically significant correlation was detected between TRPS1-high and other clinicopathologic features (Fig. 2). Median follow-up time was 35 months (up to 134 months). Deaths were reported in 33 women with 20 due to EMACA. Recurrences were seen in 30 women (distant: 22; local: 7; regional: 1). TRPS1-high was an independent poor distant RFS predictor (aHR: 4.4; CI: 1.4-14.1) after confounding adjustment (Fig. 1E). TRPS1-high and p53-aberrant status were associated with worse 3-year RFS (Fig. 1F-G) but only abnormal p53 expression was an independent predictor (aHR: 1.6; CI: 1.1-2.5). RT predicted better 3 year-RFS (Fig. 1H), improved long-term RFS (aHR: 0.4; CI: 0.1-0.9), and longer DSS (aHR: 0.1; CI: 0.04-0.5) in a multivariable model. No significant association was seen between TRPS1 expression, adjuvant chemotherapy, or other pathologic features with DSS or long-term RFS.

Figure 1 - 973

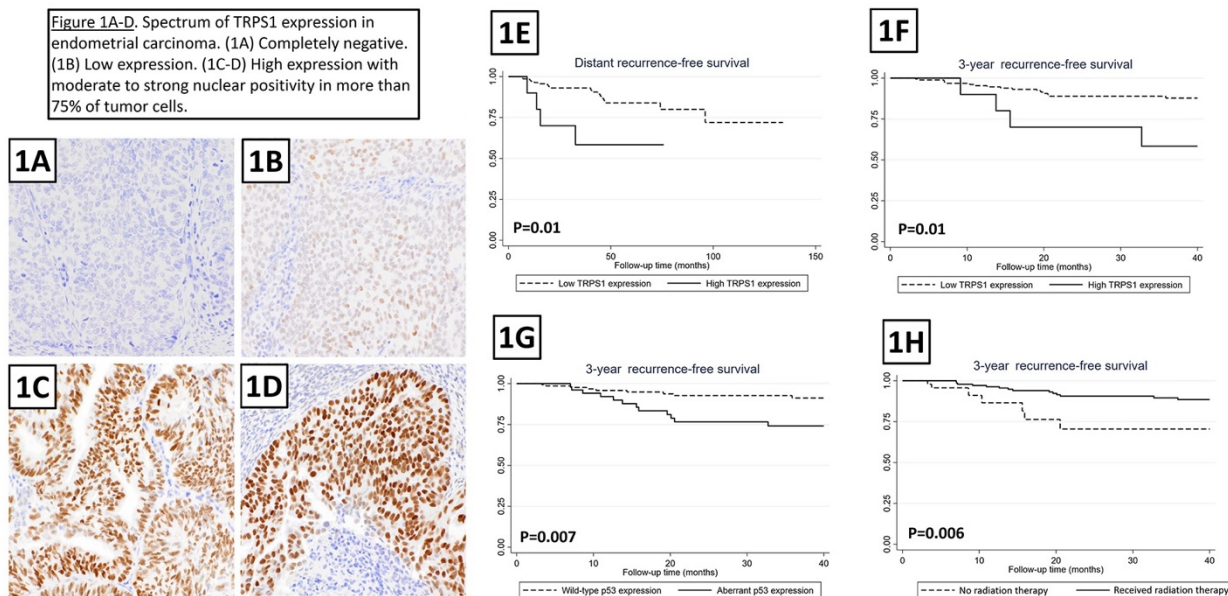


Figure 2 - 973

Tumor characteristics		TRPS1 expression		P
	n=184 column % <sup>b</sup>	Negative/low n=170	High <sup>a</sup> n=14 column % <sup>b</sup>	
Age (years)	<55	16	16	0.84
	55-70	53	53	
	>70	31	31	
Tumor size	≤4 cm	46	46	0.76
	>4 cm	54	54	
P53 status of tumor	Wild-type	71	72	0.17
	Aberrant	29	28	
Lymphovascular invasion	No	53	54	0.43
	Yes	47	46	
Tumor stage	IA	58	58	0.94
	IB	42	42	
Mismatch repair protein status	Preserved	38	47	0.55
	Deficient <sup>c</sup>	47	38	
Received chemotherapy	No	71	72	0.65
	Less than 6 cycles	11	11	
	6 cycles	18	17	
Received radiation therapy	No	22	20	0.11
	Yes	78	80	
Body mass index (kg/m <sup>2</sup> )	<25	16	15	0.24
	25-40	60	61	
	>40	24	24	
Presence of chronic comorbidities <sup>d</sup>	No	35	34	0.81
	Yes	65	66	

<sup>a</sup> High expression of TRPS1 was defined as moderate to strong expression in more than 75% of tumor cells.  
<sup>b</sup> Column percentages may not add up to 100% due to missing data.  
<sup>c</sup> Loss of expression in at least 1 mismatch repair protein on immunohistochemical studies.  
<sup>d</sup> Chronic comorbidities included cardiovascular disease, coronary artery disease, hypertension, chronic kidney disease, diabetes mellitus.

**Conclusions:** TRPS1-high status was present in a non-trivial subset of early-stage G3 endometrioid EMACA and independently predicted distant RFS in patients after controlling for adjuvant therapy exposure and dosage as well as other clinicopathologic features. Findings warrant further molecular studies to examine the potential role of TRPS1 in modulating tumor biology and treatment responsiveness in early EMACA.

#### 974 Chromosome 12 Abnormalities in Ovarian Germ Cell Tumors

Xiaojie Sun<sup>1</sup>, Yan Liu<sup>2</sup>, Congrong Liu<sup>3</sup>

<sup>1</sup>Peking University Health Science Center, Beijing, China, <sup>2</sup>School of Basic Medical Sciences, Third Hospital, Peking University Health Science Center, Beijing, China <sup>3</sup>Peking University Third Hospital, Beijing, China

**Disclosures:** Xiaojie Sun: None; Yan Liu: None; Congrong Liu: None

**Background:** Ovarian germ cell tumors (OGCTs) are heterogeneous neoplasms. OGCTs derive from primordial germ cells deviating from normal developmental path or primary oocytes that have escaped meiotic arrest. Rare mutation had been observed in OGCTs, while a high percentage of OGCTs are characterized by the appearance of isochromosome 12p [i(12p)] or 12p gain. Chromosome 12 abnormalities are genetic hallmarks in testicular germ cell tumors (TGCTs) of adolescents and adults. Little is known about these genetic changes in OGCTs.

**Design:** Here we performed fluorescence in-situ hybridization (FISH), using KRAS/CEN12 dual color probe DNA set of chromosome12, to interrogate the overrepresentation of 12p sequence of paraffin slides of 132 OGCTs, including 32dysgerminomas, 31 immature teratomas, 51yolksac tumors, 13ovarian carcinoids and 5 somatic-type tumors arising from dermoid cyst. To compare with ovarian carcinoid, 16 gastroenteropancreatic neuroendocrine neoplasms (NENs)were also subjected to FISH.

**Results:** All the dysgerminomas had abnormal 12 chromosome signal using KRAS/CEN12 dual color probe (Figure 1, Table 1). i12p was found in 78% of dysgerminomas (25/32) and was significantly higher than that of other OGCTs ( $P<0.01$ ). Other 7 dysgerminomas had KRAS amplification (3 cases) or 12 polysomy (4 cases). In primitive OGCTs, immature teratomas has significantly lower frequency (6/31, 19%) of i12p than dysgerminomas (25/32, 78%) and yolk sac tumors (25/51, 49%) ( $P<0.01$ ), indicating their different initiating cells and pathogenic mechanisms. Notably, i12p was found in 49% of ovarian carcinoids (6/13), while no NENs had i12p. Furthermore, the proportions of 12p gain (KRAS amplification) of each OGCT histological subtype were

similar (38-50%), as well as close to NENs (50%), indicating the *KRAS* amplification was a late and common molecular event in OGCTs.

Table 1. FISH results of KRAS/CEN12 dual color probe for chromosome 12p analysis

<b>Histological class</b>	<b>Total</b>	<b>12p abnormality</b>			<b>12 polysomy without 12p abnormal</b>	<b>12p intact</b>	<b>i12p (%)</b>	<b>KRAS Amplification (%)</b>	<b>12p abnormality (%)</b>
		<b>i12p only</b>	<b>KRAS Amplification</b>	<b>i12p+KRAS Amplification</b>					
Dysgerminoma	32	12	3	13	4	0	78%	50%	87.50%
Yolk sac tumor	51	14	10	11	12	4	49%	41%	68%
Immature teratoma	31	4	10	2		15	19%	38%	51%
Somatic-type tumors arising from dermoid cyst	5	0	1	1	1	2	20%	40%	40%
Ovarian carcinoid	13	3	3	3	0	4	46%	46%	69%
Gastroenteropancreatic neuroendocrine neoplasms	16	0	8	0	0	8	0	50%	50%

Figure 1 - 974

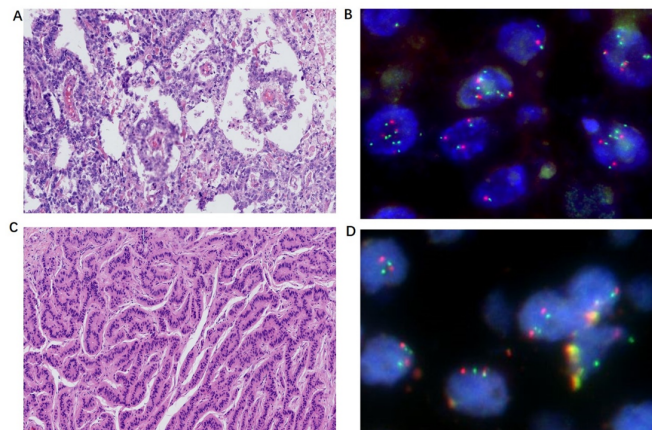


**Figure 1** (A) Ovarian yolk sac tumor. (B) 12p gain/KRAS amplification: Fluorescence in situ hybridization showed two signals for the chromosome 12 centromeric probe (red) and multiple signals for 12p *KRAS* probe (green). (C) Ovarian carcinoid. (D) i12p: Fluorescence in situ hybridization showed two signals for the chromosome 12 centromeric probe (red) and three signals for 12p (green), two of which were in close proximity to one centromeric signal, with an aggregation pattern.

**Conclusions:** Our findings suggest that among the primitive OGCTs, immature teratomas have more stable genome than dysgerminomas and yolk sac tumors, indicating a divergent histogenesis pathway. Furthermore, i12p was firstly reported in ovarian carcinoids with a similar frequency of yolk sac tumor. Different from NENs, ovarian carcinoids have the same molecular genetic characteristics as germ cell tumors. The i12p was a more specific molecular event than *KRAS* amplification for OGCTs. Additionally, rare mutations were reported in OGCTs, *KRAS* amplification rather than mutation may contribute to the tumor progression.

## 975 A Study into Micro-RNA Expression in Endometrial Carcinomas in an Asian Population

Gideon Tan<sup>1</sup>, Susan Swee-Shan Hue<sup>2</sup>, Elsie Cheruba<sup>3</sup>, Yu Jin<sup>3</sup>, Ling-Wen Ding<sup>2</sup>, Sai Mun Leong<sup>2</sup>, He Cheng<sup>3</sup>, Diana Lim<sup>1</sup>  
<sup>1</sup>National University Hospital, Singapore, Singapore, <sup>2</sup>National University of Singapore, Singapore, Singapore, <sup>3</sup>MIRXES, Singapore, Singapore

**Disclosures:** Gideon Tan: None; Susan Swee-Shan Hue: None; Elsie Cheruba: None; Yu Jin: None; Ling-Wen Ding: None; Sai Mun Leong: None; He Cheng: None; Diana Lim: None

**Background:** MicroRNAs (miRNAs) are small, non-coding RNA molecules which function in RNA silencing and post-transcriptional regulation of gene expression. We analyzed the expression of miRNAs in endometrial carcinomas, measuring their expression

between histological subtypes, molecular subtypes, in tumours with CTNNB1 mutations, and also correlated their expression with various prognostic factors.

**Design:** 119 formalin-fixed paraffin-embedded tissue samples from patients diagnosed with endometrial cancer between 2008 and 2018 were recruited. Tumours were subdivided into histological and molecular subtypes as defined by The Cancer Genome Atlas, and prognostic data was obtained from the pathology reports. The expression levels of 352 miRNAs were quantified using the panormaR panel.

**Results:** We identified differential expression of miRNAs between histological subtypes. For each miRNA, student's t-test was performed between cases of one subtype, versus the other subtypes. Permutated p-values were obtained by shuffling the case and control labels and repeating the t-test 1000 times. Mir-449a, mir-449b-5p, and mir-449c-5p were the top three miRNAs showing increased expression in both endometrioid and de-differentiated carcinomas, but were not significantly increased in serous and clear cell carcinomas (permutated p-values <0.05). The miRNAs with the most increased expression in serous and clear cell carcinomas were miR-9-3p and miR-375 respectively (permutated p-values <0.05). We also identified 62 differentially expressed miRNAs amongst molecular subtypes. Using sequential forward selection, we built subtype classification models for some molecular subtypes of endometrial cancer, comprising 5 miRNAs for MMR-deficient tumours, 10 miRNAs for p53 mutated tumours, and 3 miRNAs for CTNNB1 mutated tumours, with area under curves of 0.75, 0.85, and 0.78 respectively. Correlating miRNAs with histological prognostic factors, we identified miRNAs which showed differential expression with the presence of lymphovascular invasion, lymph node metastasis, myometrial invasion, and cervical invasion.

**Conclusions:** We have identified microRNAs that show differential expression between histological, molecular, and prognostic variables in endometrial carcinoma. These findings may potentially aid in the development of diagnostic and prognostic tools.

## 976 AKT1 Mutation Is Associated with a High Rate of Lung Metastasis in Endometrial Carcinomas “No Specific Molecular Profile” (NSMP/p53wt) Type

Basile Tessier-Cloutier<sup>1</sup>, Clarissa Lam<sup>2</sup>, Robert Soslow<sup>3</sup>, Amir Momeni Boroujeni<sup>2</sup>

<sup>1</sup>McGill University Health Centre, Montreal, QC, <sup>2</sup>Memorial Sloan Kettering Cancer Center, New York, NY, <sup>3</sup>Memorial Sloan Kettering Cancer Center/Weill Medical College of Cornell University, New York, NY

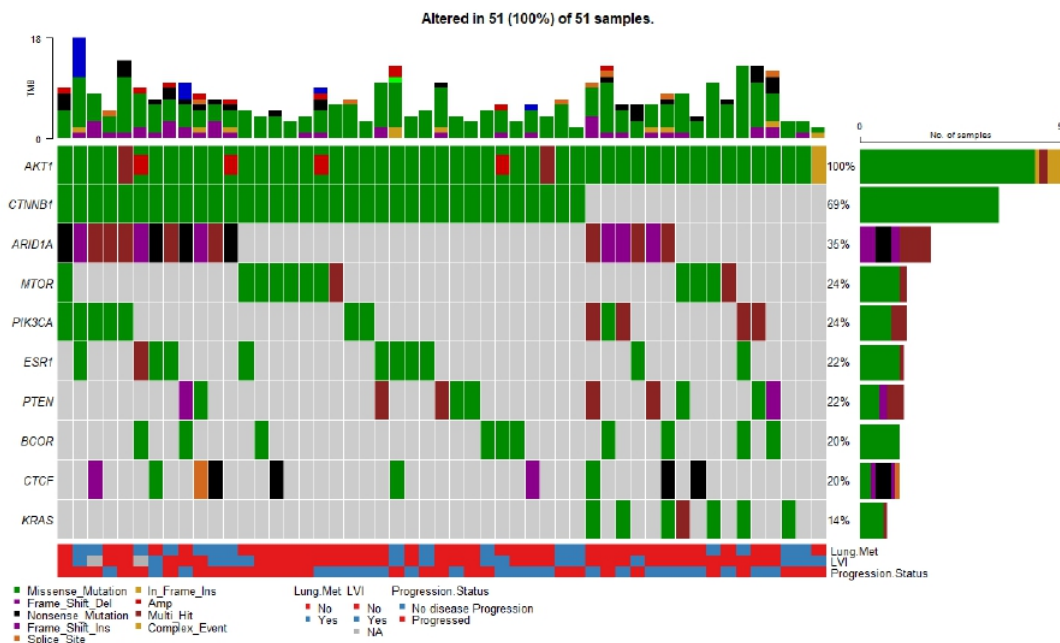
**Disclosures:** Basile Tessier-Cloutier: None; Clarissa Lam: None; Robert Soslow: None; Amir Momeni Boroujeni: None

**Background:** Within the endometrial carcinoma (EC) molecular classification the NSMP/p53wt group is defined by the exclusion of *POLE* mutation, mismatch repair (MMR) protein loss and aberrant p53 protein expression. Unlike the other three molecular groups, NSMP/p53wt EC show a wide range of clinical outcome profiles from indolent to “serous-like”. As we lean further into the molecular classification for the diagnosis of EC, the NSMP/p53wt group should be better characterized clinically and molecularly. We set to study clinicopathological features of NSMP/p53wt EC with *AKT1* mutations.

**Design:** We searched a clinically annotated cohort for EC previously characterized by a targeted sequencing panel. We included EC NSMP/p53wt type with pathogenic mutations in *AKT1*. Morphological review was performed for each case. Finally, a statistical analysis was performed to correlate both molecular and clinicopathological features.

**Results:** We identified 51 cases with pathogenic *AKT1* mutation. The median age was 63-year-old with most tumors being low stage (90%) and low FIGO grade (94%). Sixteen cases (31%) developed lung metastasis, of which 10 (63%) had associated lymphovascular invasion (LVI) within the hysterectomy specimen ( $p<0.0001$ ). Fraction of genome altered (FGA) and advanced FIGO stage were also correlated with lung metastases ( $p=0.008$  and 0.012 respectively). Disease progression was associated with LVI ( $p=0.005$ ), desmoplastic reaction ( $p=0.005$ ), FGA (0.017) and depth of invasion ( $p=0.024$ ). The co-existence of *PTEN* and *AKT1* mutations were seen in 11 patients (22%), none of which died, and was associated with a higher rate of disease-free status compared to *PTEN* wild-type cases (82% vs. 40%,  $p=0.044$ ). The other mutations co-occurring with *AKT1* included *CTNNB1* (69%), *ARID1A* (35%), *MTOR* (24%), *PIK3CA* (24%) and *KRAS* (14%). Forty-nine showed an endometrioid morphology (four showing mesonephric features), while the other two cases were diagnosed as mesonephric-like carcinosarcoma and high-grade endometrial carcinoma.

Figure 1 - 976



**Conclusions:** *AKT1* mutations in EC NSMP/p53wt type was associated with high rate of lung metastasis along with other poor prognostic factors. Interestingly the clinicopathological features were worst when the *AKT1* mutation accompanied a wild-type *PTEN*. Most had a conventional endometrioid appearance although rare cases showed mesonephric features. Our data support that NSMP/p53wt EC will benefit from clinically relevant molecular stratification to help guide management in these patients.

## 977 Dedifferentiated Ovarian Carcinoma: An Aggressive Type of Ovarian Carcinoma Characterized by Frequent Loss of Core SWI/SNF Complex Protein

Basile Tessier-Cloutier<sup>1</sup>, Felix Kommoß<sup>2</sup>, Jennifer Pors<sup>3</sup>, Colin Stewart<sup>4</sup>, W. Glenn McCluggage<sup>5</sup>, William Foulkes<sup>6</sup>, Andreas von Deimling<sup>7</sup>, Martin Koebel<sup>8</sup>, Cheng-Han Lee<sup>9</sup>

<sup>1</sup>McGill University Health Centre, Montreal, QC, <sup>2</sup>University of Heidelberg, Heidelberg, Germany, <sup>3</sup>BC Cancer, Stanford, CA, <sup>4</sup>King Edward Memorial Hospital, Subiaco, Australia, <sup>5</sup>The Royal Hospitals/Queen's University of Belfast, Belfast, United Kingdom, <sup>6</sup>McGill University, Montreal, QC, <sup>7</sup>Heidelberg University Hospital, Heidelberg, Germany, <sup>8</sup>Alberta Precision Laboratories, University of Calgary, Calgary, AB, <sup>9</sup>BC Cancer, Vancouver, BC

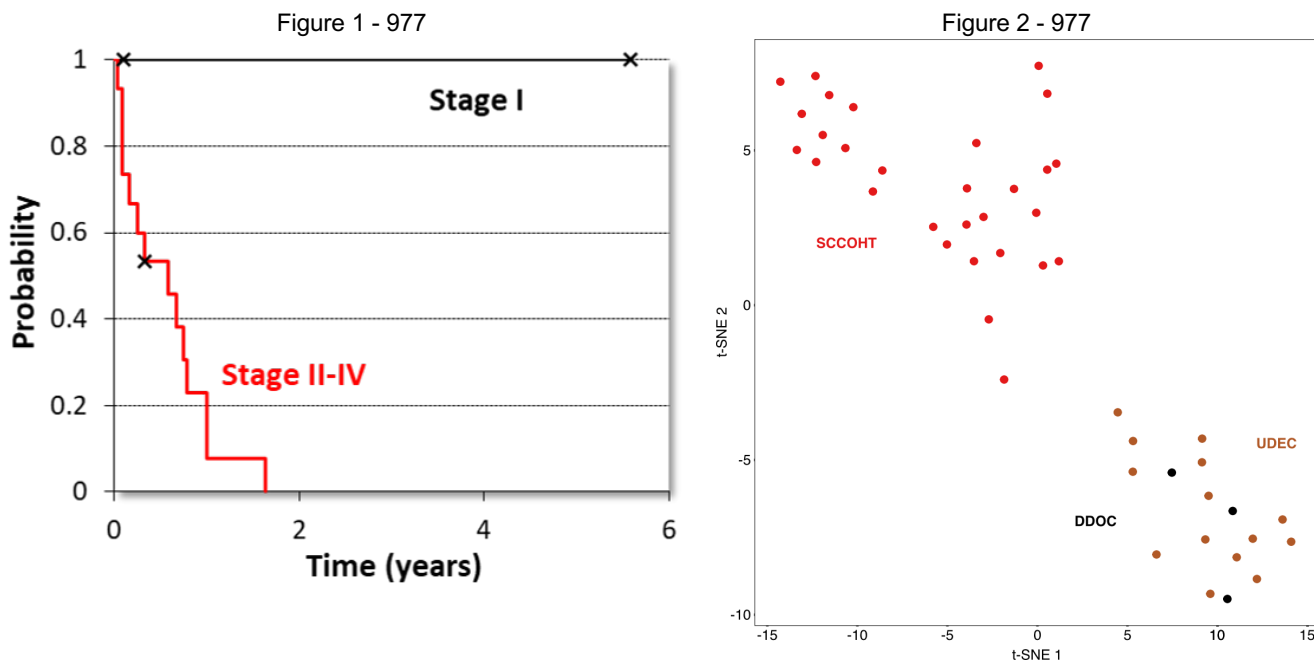
**Disclosures:** Basile Tessier-Cloutier: None; Felix Kommoß: None; Jennifer Pors: None; Colin Stewart: None; W. Glenn McCluggage: None; William Foulkes: None; Andreas von Deimling: None; Martin Koebel: None; Cheng-Han Lee: None

**Background:** Dedifferentiated ovarian carcinomas (DDOC), similar to their more common uterine corpus counterparts, are defined by the presence of an undifferentiated carcinoma component lacking evidence of specific line of differentiation and a differentiated component (typically a low-grade endometrioid carcinoma). In this study, we evaluated the expression of core SWIitch/Sucrose Non-Fermentable (SWI/SNF) complex proteins and mismatch repair (MMR) proteins on a series of DDOC and compared their global methylation profile to that of other core SWI/SNF-deficient gynecologic tract tumors, namely small cell carcinoma of ovary hypercalcemic type (SCCOHT) and undifferentiated endometrial carcinoma (UDEC).

**Design:** We collected a multi-institutional cohort of 17 DDOC and performed immunohistochemistry for ARID1A, ARID1B, SMARCA4, SMARCB1, p53, MLH1, PMS2, MSH2 and MSH6 on whole tissue sections. Whole genome DNA-methylation analysis was performed using the Illumina Infinium MethylationEPIC 850k BeadChip kit on 3 DDOC with comparison made to a previously reported cohort of SCCOHT (all SMARCA4-inactivated) and UDEC. Data were analyzed by t-distributed stochastic neighbor embedding analysis (t-SNE).

**Results:** The 17 patients with DDOC ranged from 32 to 71 years old (average of 53). Two presented with FIGO stage IA disease, while the remaining showed extra-ovarian tumor involvement (7 stage II, 4 stage III and 4 stage IV). With the exception of the 2 with stage IA disease, all patients died from their disease with a median survival of 4 months (Figure 1). The differentiated component

was endometrioid in type in all cases and all cases showed wild-type p53 expression in both the differentiated and undifferentiated components. By immunohistochemistry, 14 of 15 cases with interpretable results showed loss of expression of core SWI/SNF complex proteins, with 9 showing co-loss of ARID1A and ARID1B and 5 showing loss of SMARCA4 confined to the undifferentiated component. 3 of 17 cases were MMR-deficient (all ARID1A and ARID1B co-inactivated). t-SNE analysis of the DNA methylation profiles of 3 cases of DDOC (1 SMARCA4-deficient and 2 ARID1A/ARID1B co-deficient) showed clustering with UDEC that was distinct from SCCOHT (Figure 2).



**Conclusions:** Our results show that DDOC is a highly aggressive and molecularly unique type of ovarian carcinoma characterized by frequent inactivation of core SWI/SNF complex proteins. It displays a methylation profile that overlaps with UDEC but is distinct from SCCOHT.

### 978 Identification of Relevant Genomic Signatures and Potential Targets in Gynecologic Malignancies by Whole Genome and Transcriptomic Profiling

Jiangling Tu<sup>1</sup>, Majd Al Assaad<sup>2</sup>, Kevin Hadi<sup>3</sup>, Aditya Deshpande<sup>3</sup>, Ahmed Elsaeed<sup>4</sup>, Jyothi Manohar<sup>4</sup>, Michael Sigouros<sup>4</sup>, Andrea Sboner<sup>4</sup>, Juan Medina-Martínez<sup>3</sup>, Olivier Elemento<sup>4</sup>, Juan Miguel Mosquera<sup>4</sup>

<sup>1</sup>Weill Cornell Medical College, New York, NY, <sup>2</sup>New York-Presbyterian/Weill Cornell Medicine, New York, NY, <sup>3</sup>New York, NY, <sup>4</sup>Weill Cornell Medicine, New York, NY

**Disclosures:** Jiangling Tu: None; Majd Al Assaad: None; Kevin Hadi: Employee: Isabl, Inc.; Aditya Deshpande: Employee: Isabl Inc; Ahmed Elsaeed: None; Jyothi Manohar: None; Michael Sigouros: None; Andrea Sboner: None; Juan Medina-Martínez: Employee: Isabl Inc.; Olivier Elemento: None; Juan Miguel Mosquera: None

**Background:** Gynecologic malignancies are the leading causes of death for women in the United States, and they are fifth and sixth for ovarian cancer (OC) and endometrial cancer (EC), respectively. Nearly 75% of OC patients achieve clinical remission following surgery and chemotherapy, but most tumors recur within 24 months. We employed cutting-edge whole genome sequencing (WGS) analysis to study a group of gynecologic malignancies to further elucidate their molecular underpinnings and formulate a novel approach to detect potential targets.

**Design:** WGS was performed on 80 tumor/normal pairs from 74 female patients with different gynecological malignancies (Table 1), age range 17-91 years old. We employed the Isabl GxT analytic platform and manually curated single base substitution (SBS) molecular signatures and structural variants (SV) that involved tumor suppressor genes and oncogenes. Clinico-pathologic and molecular findings were correlated.

**Results:** Most cases (90%) had >20% tumor purity. In addition to known genomic alterations in gynecological malignancies, uncommon oncogenic mutations were detected in endometrial cancer, e.g., FGFR2, AKT1, TSC1 and CDK12, and in high-grade serous carcinoma of ovary/fallopian tube (PM1852), e.g., TSC2 and RAD51B. Pathogenic/likely pathogenic germline events included BRCA1, BRCA2, ATM, and FANCL. In addition, genomic signatures associated with homologous recombination

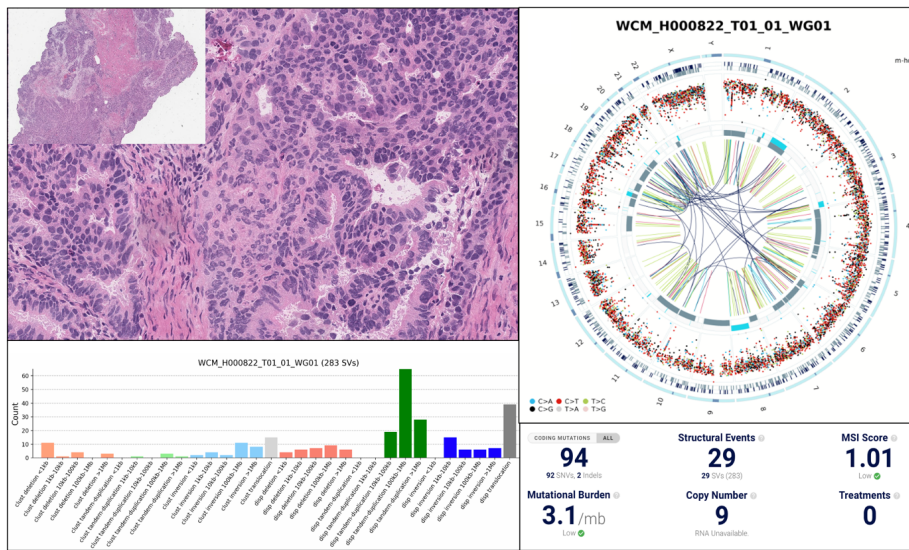
# ABSTRACTS | GYNECOLOGIC AND OBSTETRIC PATHOLOGY

deficiency (HRD) were detected in 15% of cases, CDK12-type genomic instability in 18% (Figure 1), and mismatch repair deficiency (MMR) in 21% (Table 1 and Figure 2). Remarkably, our genomic signature-based approach and manual data curation nominated potential targets in 12 cases that did not have treatment options per OncoKB.

	Tumor Type	Site	N	High-TMB cases	Biomarkers	Treatment	Select Molecular signature/phenotype	
	UEC	Uterus	27	15	PTEN, MSI-H, KRAS, PIK3CA, ATM, ARID1A, FGFR2, NF1, PTCH1, CDK12	AZD8186, Trametinib, Alpelisib, Olaparib, PLX2853, Evdafitinib, Sonidegib, Cemiplimab	HRD (n=1) MMR (n=11) CDK12/CCNE1 amp (n=3)	
	USC	Uterus	7	0	ERBB2, PIK3CA, KRAS, CHEK2, SMARCB1	Pembrolizumab, Alpelisib, Trametinib, Olaparib, Tazemetostat	HRD (n=1) CDK12/CCNE1 amp (n=7)	
	LGSO	Ovary	2	0	CDKN2A	Abemaciclip	MMR (n=2)	
	HGSOF	Ovary and Tube	13	1	BRCA1, BRCA2, ARID1A, ERBB2, TSC2, ERCC2, CDKN2A, NF1,	Olaparib, Niraparib, PLX2853, Pembrolizumab, Everolimus, Cisplatin, Abemaciclip, Trametinib	HRD (n=7) CDK12/CCNE1 amp (n=2)	
	ECOV	Ovary	7	0	PIK3CA, KRAS, CDKN2A, PTEN, ARID1A, BRCA2	Alpelisib, Trametinib, Abemaciclip, AZD8186, PLX2853, Olaparib	MMR (n=1)	
	MMMT	Uterus and Adnexa	9	2	PIK3CA, PTEN, ERBB2, KRAS, ARID1A, RET,	Alpelisib, AZD8186, Pembrolizumab, Trametinib, PLX2853, Pralsetinib	HRD (n=2) MMR (n=2)	
	ESS	Uterus	3	0	None	None	—	
	SQCX	Cervix	2	0	None	None	—	
	Others	Ovary and uterus	4	1	PTEN, PIK3CA, ERBB2, KRAS	AZD8186, Alpelisib, Pembrolizumab, Trametinib	CDK12/CCNE1 amp (n=1)	

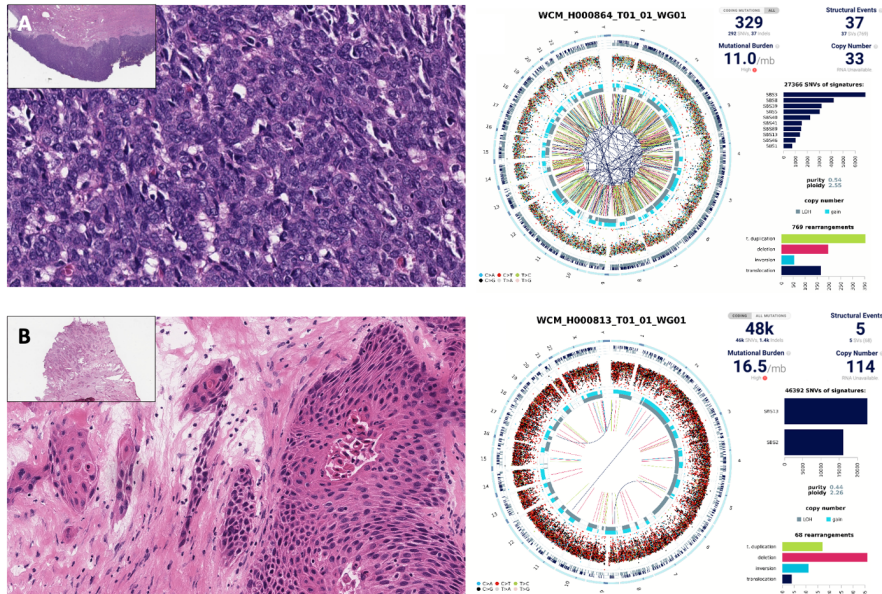
**Table 1. Biomarkers of various gynecologic malignancies detected by WGS analysis.** A total of 80 tumor/normal pairs from 74 female patients were studied. TMB density ranged from 0.7 to 695 mutations/Mb. Most of the high TMB (>10) tumors were clustered in endometrial carcinoma. TMB: Tumor Mutational Burden; UEC: Uterine endometrioid carcinoma; USC= Uterine Serous carcinoma including mixed endometrioid and serous carcinoma; LGSO= Low grade serous carcinoma of ovary; HGSOF=High grade serous carcinoma of ovary and Fallopian tube; ECOV=Endometrioid carcinoma of ovary; MMMT=Carcinosarcoma of uterus and adnexa; ESS=Endometrial stromal sarcoma; SQCX=Squamous cell carcinoma of cervix; Others=Ovary: Mucinous borderline tumor, Squamous carcinoma from teratoma, Clear cell carcinoma (CCC) of uterus and ovary

Figure 1 - 978



**Figure 1.** Whole genome sequencing analysis detects potentially relevant molecular signatures. Uterine mixed serous-endometrioid carcinoma without drivers or known targets per OncoKB. WGS elucidated CDK12-type genomic instability with a complex structural variant impacting *CDK12*, and an excess of large tandem duplications.

Figure 2 - 978



**Figure 2.** Detection of relevant molecular alterations by whole genome sequencing. A. Uterine endometrioid carcinoma with high-confidence *BRCA1*-like HRD, that harbored *TP53* hotspot, *RB1* mutation, *RAD51B* deletion, and a structural variant impacting *PTEN*. B. Squamous cell carcinoma arising in ovarian teratoma, an APOBEC hypermutator case that also harbored *PTEN* and *PIK3CA* hotspots.

**Conclusions:** WGS of gynecologic malignancies empowered by state-of-the-art analysis elucidates molecular signatures associated with high-confidence HRD, CDK12-type genomic instability and MMR, and uncommon oncogenic mutations. In the context of driver-negative gynecological cancers, these findings warrant further investigation.

## 979 Challenges in Histologic Evaluation of Ovarian Mucinous Neoplasms: A Multi-Institutional Interobserver Study

Gulisa Turashvili<sup>1</sup>, Oluwole Fadare<sup>2</sup>, David Gutman<sup>1</sup>, Brooke Howitt<sup>3</sup>, Brooke Liang<sup>4</sup>, Rajmohan Murali<sup>5</sup>, Marina Mosunjac<sup>1</sup>, Vinita Parkash<sup>6</sup>, Maryam Shahi<sup>7</sup>, Charles Quick<sup>8</sup>, Krisztina Hanley<sup>1</sup>

<sup>1</sup>Emory University, Atlanta, GA, <sup>2</sup>UC San Diego School of Medicine, La Jolla, CA, <sup>3</sup>Stanford University, Stanford, CA, <sup>4</sup>Stanford Health Care, Stanford, CA, <sup>5</sup>Memorial Sloan Kettering Cancer Center, New York, NY, <sup>6</sup>Yale School of Medicine, Yale School of Public Health, New Haven, CT, <sup>7</sup>Mayo Clinic, Rochester, MN, <sup>8</sup>University of Arkansas for Medical Sciences, Little Rock, AR

**Disclosures:** Gulisa Turashvili: None; Oluwole Fadare: None; David Gutman: None; Brooke Howitt: None; Brooke Liang: None; Rajmohan Murali: None; Marina Mosunjac: None; Vinita Parkash: None; Maryam Shahi: None; Charles Quick: None; Krisztina Hanley: None

**Background:** Accurate classification of ovarian mucinous neoplasms (OMNs) is crucial for optimal clinical management. Mucinous borderline tumors (MBT) are architecturally complex non-invasive neoplasms with gastrointestinal differentiation. MBTs may display foci of intraepithelial carcinoma (IEC) or mucinous carcinoma (MC), consisting of expansile and/or infiltrative growth patterns. Histologic criteria for IEC and expansile MC are not well-defined and appear subjective. To date there have been no reproducibility studies addressing this diagnostic challenge. We aimed to assess interobserver agreement for diagnosing OMNs.

**Design:** Archival microscopic slides from OMNs diagnosed as MBT, MBT with IEC and MC were digitized. Whole slide images were uploaded to an online digital slide archive and reviewed by 8 subspecialized gynecologic pathologists. Interobserver agreement was assessed using Fleiss' kappa in SPSS 28.0.1.0.

**Results:** A total of 109 OMNs were included in the study. The median number of slides reviewed was 3 (range 1-4). Fleiss' kappa showed that interobserver agreement was moderate for infiltrative MC ( $\kappa=0.405$ , 95% CI, 0.370-0.441,  $p<0.0005$ ) and MBT ( $\kappa=0.402$ , 95% CI, 0.366-0.437,  $p<0.0005$ ), and only fair for expansile MC ( $\kappa=0.366$ , 95% CI, 0.331-0.402,  $p<0.0005$ ) and IEC ( $\kappa=0.217$ , 95% CI, 0.181-0.252,  $p<0.0005$ ). Comparison of the diagnoses rendered by the 8 observers with the original diagnoses demonstrated fair agreement ( $\kappa=0.336$ , 95% CI, 0.318-0.355,  $p<0.0005$ ). Overall agreement among the 8 observers was fair ( $\kappa=0.335$ , 95% CI, 0.313-0.356,  $p<0.0005$ ), and a subset of OMNs were categorized by some observers as mucinous cystadenoma (MCA) not meeting criteria for MBTs. Comparison of individual kappa values indicated that observers were in better (moderate) agreement when categorizing OMNs as MBT vs other ( $\kappa=0.402$ , 95% CI, 0.366-0.437,  $p<0.0005$ ), but far less agreement over other categories (fair for expansile MC with or without IEC, infiltrative MC and MCA, poor for IEC in MBT;  $\kappa=0.345$ , 0.309-0.381;  $\kappa=0.330$ , 0.294-0.366;  $\kappa=0.334$ , 0.298-0.369;  $\kappa=0.179$ , 0.144-0.215, respectively; all 95% CI,  $p<0.0005$ ).

**Conclusions:** This multi-institutional interobserver study addresses the diagnostic challenges of OMNs. Overall agreement among subspecialized gynecologic pathologists is only fair and ranges from poor to moderate for different categories of OMNs. The study suggests that recalibration of the diagnostic criteria for IEC, expansile and infiltrative MC is needed to ensure accurate classification of OMNs.

## 980 Black Women Have Both Higher Rate of Leiomyosarcoma and More Aggressive Disease, and MED12 Mutations are Characteristic in Black/African American Women Potentially Defining a Subset of Leiomyoma-Derived Leiomyosarcomas Associated in Black Women

Asad Ullah<sup>1</sup>, Jaffar Khan<sup>2</sup>, Abdul Qahar Khan Yasinzai<sup>3</sup>, Elias Makhoul<sup>4</sup>, Kalyani Ballur<sup>5</sup>, Matthew Gayhart<sup>4</sup>, Eric Vail<sup>4</sup>, Saleh Heneidi<sup>4</sup>

<sup>1</sup>Vanderbilt University, Nashville, TN <sup>2</sup>Indiana University, Pathology & Laboratory Medicine, Indianapolis, IN, <sup>3</sup>Quetta, Pakistan, <sup>4</sup>Cedars-Sinai Medical Center, Los Angeles, CA, <sup>5</sup>Augusta University-Medical College of Georgia, Augusta, GA

**Disclosures:** Asad Ullah: None; Jaffar Khan: None; Abdul Qahar Khan Yasinzai: None; Elias Makhoul: None; Kalyani Ballur: None; Matthew Gayhart: None; Eric Vail: None; Saleh Heneidi: None

**Background:** Ascertaining if a subset leiomyomas (LM) can differentiate to become leiomyosarcomas (LMS) has been an area of interest and contention. Mediator complex subunit 12, encoded by MED12, has hotspot loss-of-function alterations in both intronic and exonic regions 1 and 2 that are identified in approximately 80-90% of LM and 15-20% of LMS, as well as a majority of both fibroadenomas and phyllodes tumors.

**Design:** The Surveillance, Epidemiology and End Results (SEER) database was explored for uterine LMS regarding race and OS. Leiomyosarcomas from The Cancer Genome Atlas (TCGA) database were explored to see most altered genes, with possible co-alterations and overall survival assessment. MED12 or PTEN was assessed in all uterine cancers in the TCGA database and compared by overall survival (OS) and race. To assess for racial associations, MED12 mRNA expression analysis was reviewed in uterine cancers in TCGA data accessed through The Human Protein Atlas.

**Results:** In uterine cancers overall, MED12-altered tumors (n=222) had a significantly worse overall survival than MED12 wild-type (WT) (N=996) ( $p=0.05$ ). Notably, MED12 alterations were most enriched in Black or African American (B/AA) women ( $q<10-10$ ). Expression data (mRNA and IHC) indicated MED12 was not prognostic in women with uterine cancers overall (n=1063 and  $p=0.18$ ). However, when MED12 expression results were separated by race, B/AA women made up 19.5% of highest expression tumors (top 5%) and 41.4% in tumors with lowest expression (bottom 5%) ( $p=0.02$ ). 5104 cases of LMS of the uterus were identified in the SEER database. Black women in the US were overrepresented with 1035 (20.3%) cases, while making up only 12-14% of the US population. Black women had the worst OS, this a median OS in White was 21.96 months (mo) vs Black 14.98 (mo).

**Conclusions:** In B/AA women with uterine LMS have significantly worse OS than other races, and suffer significantly more burden of disease, relative to population percentage. MED12 is altered in a subset of LMS, and in uterine cancers MED12-altered cancers are significantly more aggressive and significantly more enriched in B/AA women ( $p/q\text{-value}<10^{-10}$ ). Discrepancies in studies linking LM to LMS may be due to the subset of MED12-altered LMS being enriched in historically underrepresented and understudied populations. Future studies of MED12 in LMS must include underrepresented population to accurately reflect the role of MED12 in LMS.

## 981 GATA3 Expression in HPV-Associated and HPV-Independent Vulvar Squamous Cell Carcinomas: Patterns of Expression and Prognostic Significance

Elmira Vaziri Fard<sup>1</sup>, Somaye Zare<sup>2</sup>, Oluwole Fadare<sup>3</sup>

<sup>1</sup>UC San Diego Health, San Diego, CA, <sup>2</sup>University of California, San Diego, La Jolla, CA, <sup>3</sup>UC San Diego School of Medicine, La Jolla, CA

**Disclosures:** Elmira Vaziri Fard: None; Somaye Zare: None; Oluwole Fadare: None

**Background:** GATA3 expression has recently been reported to be a prognostic factor in esophageal squamous cell carcinoma (SCC) and urothelial carcinoma. Herein, we assess the prognostic significance and patterns of GATA3 expression in a cohort of vulvar SCC.

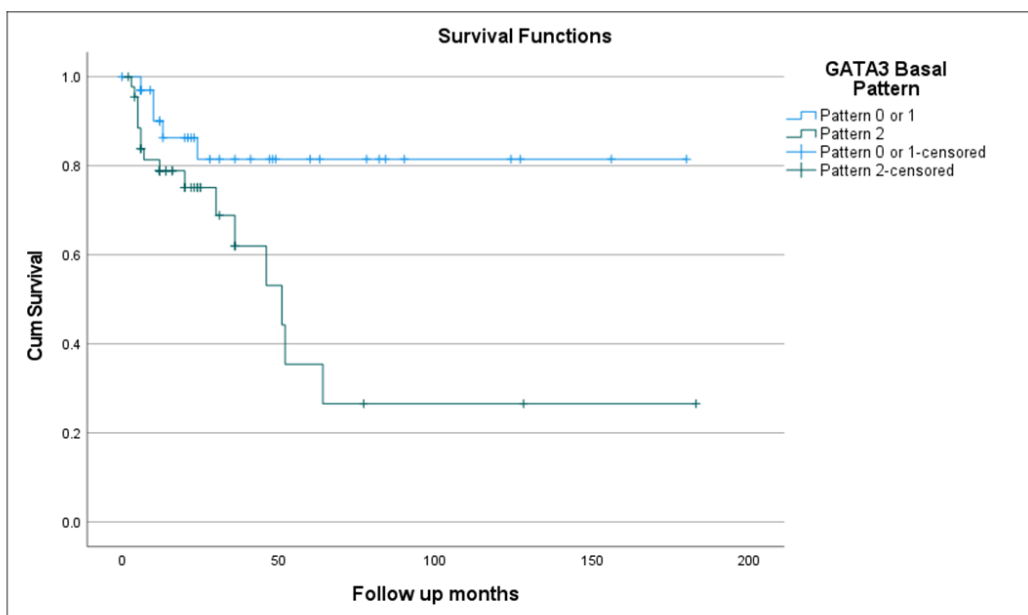
**Design:** 86 cases of vulvar SCC diagnosed at a single institution constituted our study cohort. Immunohistochemical studies for GATA3, p16 and p53 were performed on each case. p16 (block vs non-block) and p53 (mutation pattern vs wild type pattern) were scored by standard criteria. Given that the observed GATA3 expression pattern in normal vulva was strong basal staining with uniform upward extension until at least the mid epidermal layers, SCCs were scored using the tri-pattern criteria of Goyal et al [PMID: 29434343]: Pattern 0 (no loss of basal staining in nests), Pattern 1 (25-75% basal staining) and Pattern 2 (<25% basal staining). p16 status was used to classify the cohort into HPV associated (HPVA) if p16 block positive, or HPV independent (HPVI) if p16 block negative. We investigated any potential relationships between GATA3 expression and p53 status, p16/HPV status, stage and patient outcomes.

**Results:** The mean patient age for the entire cohort was 65.9 years (range 29-94). 52 (60.5%) cases were HPVA, and 34 (39.5%) were HPVI. 30 (34.9%) cases showed a p53 mutation pattern and 55 (64%) a p53 wild-type pattern. GATA3 expression patterns in relation to p53 mutation and p16 status are summarized in Table 1. Clear differences in GATA3 expression frequencies were discernible between p53 mutated versus p53 wild-type tumors as well as between HPVA and HPVI tumors ( $p<.001$ ). The cases that showed significant loss of GATA3 expression (Pattern 2, <25% basal staining) had significantly worse overall and disease-free survival in comparison to cases with Pattern 0 or 1 staining (>25% retained basal expression), ( $p=0.011$  and  $0.024$  respectively, see Figure 1). However, the significance of this finding was not independent of stage and p53 status on multivariate analysis (MVA). Within the p53 wild-type subset of the whole study cohort, however, Pattern 2 expression of GATA3 was associated with significantly worse overall survival (OS;  $p=0.002$ ), independent of stage and p16 expression ( $p=0.009$ , HR:8.2) on MVA.

Table 1-GATA3 expression patterns in HPVA and HPVI subgroups.

p53/p16 status	GATA3 Expression Patterns			
	Pattern 0	Pattern 1	Pattern 2	Total
<b>p53 status</b>	0	5	25	30
<i>Mutation pattern</i>	17	15	23	55
<i>Wild-type</i>	17	20	48	85
<b>Total</b>				
<b>p16 status</b>	16	15	21	52
<i>Block type</i>	1	5	28	34
<i>Non-block type</i>	17	20	49	86
<b>Total</b>				

Figure 1 - 981

**Figure 1- Kaplan-Meier Curve for Overall Survival According to GATA3 Expression Pattern.**

**Conclusions:** In our study, basal loss of GATA3 was seen in both HPVA and HPVI vulvar SCCs but was significantly more common in HPVI SCCs. Loss or substantial diminution of GATA3 expression (Pattern 2) is a negative prognostic factor in vulvar SCCs, but *only* in the p53 wild type subset, where its negative prognostic significance appears to be independent of p16 status and stage.

## 982 Molecular Landscape and Clinical Behavior of Stage I p53-Abnormal Low-Grade Endometrioid Endometrial Carcinomas

Lisa Vermij<sup>1</sup>, Amy Jamieson<sup>2</sup>, Joseph Carlson<sup>3</sup>, Brooke Howitt<sup>4</sup>, Philip Ip<sup>5</sup>, Sigurd Lax<sup>6</sup>, W. Glenn McCluggage<sup>7</sup>, Naveena Singh<sup>8</sup>, Jessica McAlpine<sup>9</sup>, Remi Nout<sup>10</sup>, Carien Creutzberg<sup>1</sup>, Nanda Horeweg<sup>1</sup>, Tjalling Bosse<sup>1</sup>, C. Blake Gilks<sup>11</sup>

<sup>1</sup>Leiden University Medical Center, Leiden, Netherlands, <sup>2</sup>The University of British Columbia, Vancouver, BC, <sup>3</sup>Keck School of Medicine of USC, Los Angeles, CA, <sup>4</sup>Stanford University, Stanford, CA, <sup>5</sup>Queen Mary Hospital, The University of Hong Kong, Hong Kong, Hong Kong, <sup>6</sup>Hospital Graz II, Graz, Austria, <sup>7</sup>The Royal Hospitals/Queen's University of Belfast, Birmingham, United Kingdom, <sup>8</sup>Vancouver General Hospital, Vancouver, BC, <sup>9</sup>The University of British Columbia, BC Cancer Agency, Vancouver, British Columbia, <sup>10</sup>Erasmus University Medical Center, Rotterdam, Netherlands, <sup>11</sup>Vancouver General Hospital/University of British Columbia, Vancouver, BC

**Disclosures:** Lisa Vermij: None; Amy Jamieson: None; Joseph Carlson: None; Brooke Howitt: None; Philip Ip: None; Sigurd Lax: None; W. Glenn McCluggage: None; Naveena Singh: None; Jessica McAlpine: None; Remi Nout: None; Carien Creutzberg: None; Nanda Horeweg: None; Tjalling Bosse: None; C. Blake Gilks: None

**Background:** The clinical significance of applying the TCGA molecular classification in stage I low-grade endometrioid carcinoma (EEC) is under debate as these patients generally have an excellent clinical outcome. However, a small subset of stage I low-grade EEC are p53-abnormal (p53abn) and may have a poor prognosis, although their existence is questioned. Here, we aimed to pathologically review and characterize stage I low-grade p53abn EEC previously identified in our databases.

**Design:** Tumor material from the PORTEC-1 and -2 trials (n=881) and retrospectively collected Canadian historic cohorts (n=2506) was available for analysis. All patients with previously reported stage I p53abn EEC were selected; none of these exhibited pathogenic POLE mutations or mismatch repair-deficiency. Abnormal p53 status was confirmed by p53 immunohistochemistry (IHC) and TP53 mutation analysis. Review of histotype and FIGO grading was performed by six expert gynecological pathologists, blinded to the molecular subgroup and study aim, using one H&E-stained section per case. Low-grade NSMP EEC (n=10) and p53abn serous carcinomas (n=13) were included as controls. The mutational landscape was assessed with next generation sequencing. The Kaplan-Meier method was used for the assessment of recurrence-free survival (RFS).

**Results:** In total, 55 p53abn stage I low-grade EEC were identified. Following pathology review, 17 (30.9%) cases were assigned as not low-grade EEC by all of the expert pathologists, while 38 (69.1%) and 26 (47.3%) were assigned low-grade EEC by ≥1

and ≥3 pathologists, respectively. Two representative cases are illustrated in figure 1. Clustering cases by agreement on low-grade EEC histology showed no significant differences in mutational landscape, with a low prevalence of *PTEN* and *PIK3CA* mutations in all cases (figure 2). 5-year RFS was higher with increasing agreement on low-grade EEC histology, with a 5-year RFS of 61.9%, 72.8% and 76.5% for cases assigned as low-grade EEC by none, ≥1 and ≥3 pathologists, respectively.

**Figure 1 - 982**

**Figure 1.** Representative H&E and p53 immunohistochemistry images of a case which none of the expert pathologists classified as low-grade endometrioid endometrial carcinoma (EEC) (A, B) and a case assigned as low-grade EEC by 5 out of 6 expert pathologists (C, D). All images taken at x10 magnification.

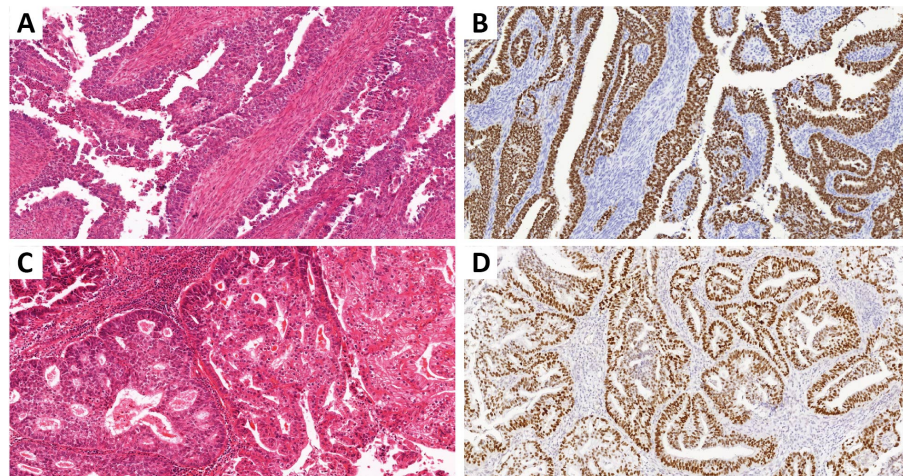
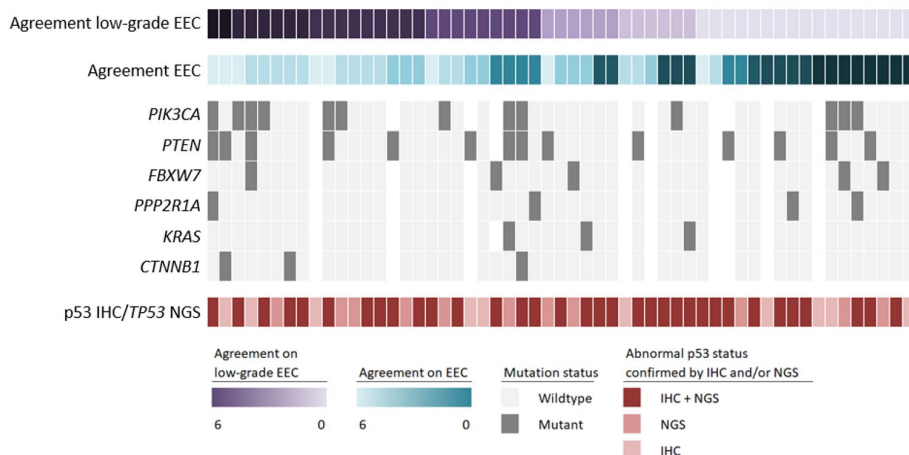


**Figure 2 - 982**

**Figure 2.** Molecular landscape of 55 stage I p53-abnormal endometrioid endometrial carcinomas (EEC), clustered by the degree of agreement on low-grade EEC histology by expert pathologists.



**Conclusions:** A subset of p53abn endometrial carcinomas are morphologically low-grade endometrioid with a molecular landscape that is similar to prototypical p53abn endometrial carcinomas. The risk of recurrence for patients with stage I low-grade p53abn EEC is higher compared to the risk of recurrence of stage I low-grade EEC in literature. Our results may support performing molecular classification on all endometrial carcinomas.

## 983 Over-Expression of EGFR Is Associated with Poor Prognosis in High Grade Ovarian Carcinoma

Duc Vo<sup>1</sup>, Yan Liu<sup>1</sup>, Anil Sood<sup>1</sup>, Katy Rezvani<sup>1</sup>, Amir Jazaeri<sup>1</sup>, Jinsong Liu<sup>1</sup>

<sup>1</sup>The University of Texas MD Anderson Cancer Center, Houston, TX

**Disclosures:** Duc Vo: None; Yan Liu: None; Anil Sood: None; Katy Rezvani: None; Amir Jazaeri: None; Jinsong Liu: None

**Background:** Epidermal growth factor receptor (EGFR) is a receptor tyrosine kinase protein that has been reported to be overexpressed in a subset of ovarian cancers. This protein not only offers a promising target for targeted therapy and but also may offer a new target for immunotherapy because of its membranous location. We analyzed the association between EGFR expression and clinical and pathologic parameters in ovarian cancer to determine the prognostic significance and guide future immunotherapy.

**Design:** We created tissue microarrays of high-grade ovarian epithelial tumors from patients diagnosed at The University of Texas MD Anderson Cancer Center. EGFR expression was examined in the microarrays by immunohistochemistry analysis using the EGFR antibody clone 31G7 (Abnova). Results were categorized as either negative (no staining or nonspecific staining) or positive (weak to strong membranous staining). For each patient, we collected age, AJCC stage, ascites, and family history of cancer; these data were summarized using descriptive statistics and compared by EGFR status using chi-square test. Kaplan-Meier analysis was used to analyze overall survival by EGFR status. GraphPad Prism v.8.4.3 was used for all statistical analysis.

**Results:** Patient data were analyzed in two cohorts. Cohort 1 contained 234 patients: 43 (18%) were positive for EGFR and 191 (82%) were negative. EGFR-negative status was associated with better overall survival ( $p<0.0001$ ). Cohort 2 contained 249 patients, with a similar pattern of EGFR positivity (18 [7%] were positive and 231 [93%] were negative) and a similar overall survival benefit for EGFR-negative status ( $p=0.0153$ ). A family history of cancer was associated with EGFR-positive status ( $p=0.01$ ). Other clinical factors, including age (>51 years vs ≤51 years), AJCC stage (stage I/II vs stage III/IV), and ascites (present vs not present), were not associated with EGFR status ( $p>0.05$ ).

Figure 1 - 983

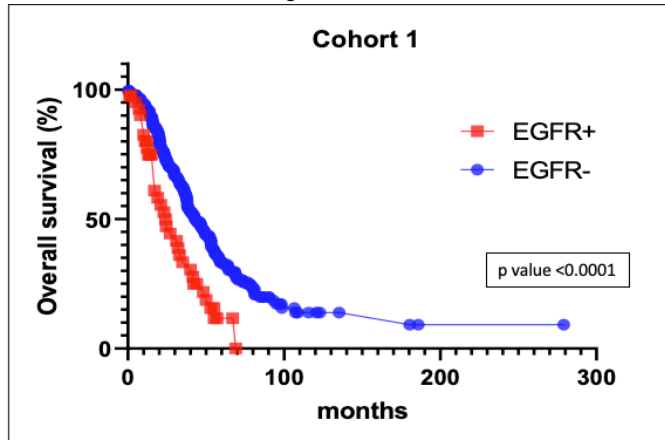
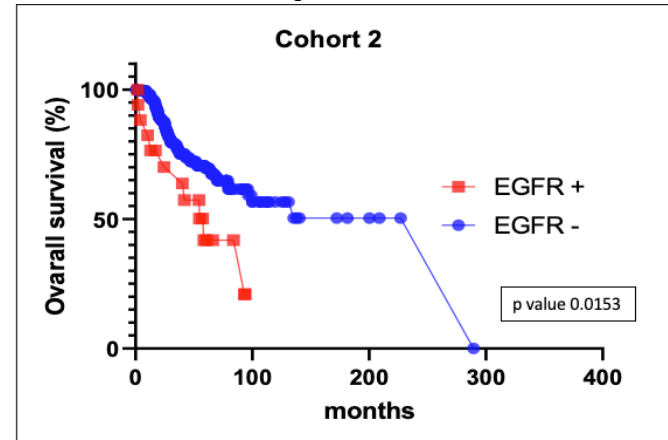


Figure 2 - 983



**Conclusions:** Our data indicate that overexpression of EGFR is associated with poor overall survival in patients with high-grade serous ovarian cancer. The data also provide a strong rationale for the development of EGFR inhibitors and offer a new potential target for immunotherapy.

## 984 Evidence-Based Strategies for Tissue Sampling to Detect Occult STIC/HGSC in Salpingo-Oophorectomies Performed for Hormone Suppression of Estrogen Receptor Positive Breast Cancer: Balancing Genetic Risks and Laboratory Resource Utilization

Anjali Walia<sup>1</sup>, Julie Mak<sup>1</sup>, Nicholas Ladwig<sup>1</sup>, Joseph Rabban<sup>1</sup>

<sup>1</sup>University of California, San Francisco, San Francisco, CA

**Disclosures:** Anjali Walia: None; Julie Mak: None; Nicholas Ladwig: None; Joseph Rabban: None

**Background:** Evidence-based guidelines remain to be defined for tissue sampling to detect occult serous tubal intraepithelial carcinoma (STIC) / high grade serous carcinoma (HGSC) in bilateral salpingo-oophorectomy (BSO) performed for hormone suppression of estrogen receptor (ER) positive breast cancer. In concept, examination of the entire ovaries and fallopian tubes (SEE-Fim protocol) is merited for patients with a pathogenic variant in any hereditary ovarian cancer gene (HOC-PV); otherwise representative sectioning of the ovaries and non-fimbriated tube is appropriate, along with complete examination of the fimbriae. This study evaluated tissue sampling, genetic risks, occult cancer and post BSO outcome in order to develop tissue sampling guidelines in this setting.

**Design:** 166 consecutive cases of BSO for hormone suppression of ER positive breast cancer were identified in our pathology archives. Germline genetic test results for HOC genes (as defined by the 2022 NCCN guidelines) were obtained from our genetic

counseling division. The prevalence of post-BSO pelvic HGSC was determined from outcome surveillance data from our institutional Cancer Registry.

**Results:** Tissue sampling was complete in 78% (129/166) specimens, resulting in a 2.5 x higher number of tissue cassettes than for representatively sampled specimens, as expected (Table 1). No cases contained STIC or HGSC but 10% (16/166) had ovarian metastasis of breast cancer and a higher prevalence of benign alterations was reported in cases completely submitted. Genetic test status was not documented in the medical records of 38% (63/166) patients. Among 103 patients with documented testing, none had a HOC-PV but 7% (7/103) had a HOC variant of unknown significance (VUS) (2 BRCA1/2, 2 RAD51C/D, 2 ATM, 1 MSH2). No patients developed post-BSO pelvic HGSC.

	Complete sampling (129)	Representative sampling (37)
Median patient age	46 yrs	45 y
Median # of cassettes per ovary:	6	2
Median # of cassettes per tube:	4	2
Germline genetic test result:		
Pathogenic variant	0	0
Variant of unknown significance	7% (7/103)	0
Not documented	39% (50/129)	35% (13/37)
STIC	0	0
HGSC (tubal or ovarian)	0	0
Other ovarian pathology		
Metastatic breast cancer	10% (13/129)	8% (3/37)
Endometriosis	15% (19/129)	5% (2/37)
Follicle cysts	16% (21/129)	8% (3/37)
Serous cystadenoma	5% (7/129)	8% (3/37)
Mucinous cystadenoma	2% (2/129)	0
Other tubal pathology		
Paratubal cysts	47% (70/149)	35% (6/17)
Adenomatoid tumor	0.7% (1/149)	0
Salpingitis isthmica nodosum	0.7% (1/149)	0
Hydrosalpinx	1% (2/149)	0

**Conclusions:** Representative sampling of grossly normal ovaries is reasonable in ER positive breast cancer patients undergoing surgical hormone suppression with confirmed negative testing for HOC-PV. However, in our institution there are significant communication gaps regarding genetic test results, leading to higher lab resource utilization than necessary. Although we did not identify any patients with a HOC-PV in this cohort, a more robust risk estimate requires a larger study size. Specimen management in patients with HOC-VUS remains to be defined.

## 985 TROP2 Expression is A Favorable Prognostic Marker in Patients with Advanced High Grade Ovarian Carcinoma

Guoliang Wang<sup>1</sup>, Yan Liu<sup>1</sup>, Preetha Ramalingam<sup>1</sup>, Anais Malpica<sup>1</sup>, Elizabeth Euscher<sup>1</sup>, Barrett Lawson<sup>1</sup>, Nadia Hameed<sup>1</sup>, Anil Sood<sup>1</sup>, Hind Rafei<sup>1</sup>, Rafet Basar<sup>1</sup>, Katy Rezvani<sup>1</sup>, Amir Jazaeri<sup>1</sup>, Jinsong Liu<sup>1</sup>

<sup>1</sup>The University of Texas MD Anderson Cancer Center, Houston, TX

**Disclosures:** Guoliang Wang: None; Yan Liu: None; Preetha Ramalingam: None; Anais Malpica: None; Elizabeth Euscher: None; Barrett Lawson: None; Nadia Hameed: None; Anil Sood: None; Hind Rafei: None; Rafet Basar: None; Katy Rezvani: None; Amir Jazaeri: None; Jinsong Liu: None

**Background:** Patients with high grade ovarian epithelial carcinoma (HGOvCa) have poor prognosis, especially at advance stages (stage III and IV). TROP2 is a cell-surface glycoprotein and has been reported to be overexpressed in various adenocarcinomas. As TROP2 expression is located on the membrane surface and thus represent an ideal target for immunotherapy. Here we examined the expression TROP2 in HGOvCa and its correlation with the survival and other clinical data.

**Design:** Tissue microarrays of 234 cases of HGOvCa diagnosed at MD Anderson Cancer Center were immunohistochemical stained for TROP2. TROP2 expression was scored using the HER2 reporting criteria. Recorded information included age, histotype, AJCC stage, surgical treatment, chemotherapy, clinical response, disease free survival (DFS) and overall survival (OS). Descriptive statistics, Kaplan Meier curves, and survival analysis were performed in GraphPad Prism v.8.4.3 (La Jolla, CA).

**Results:** Histotypes were as follows: high grade serous carcinoma, high grade endometrioid adenocarcinoma, clear cell carcinoma, carcinosarcoma, mixed high grade carcinoma, and undifferentiated carcinoma. TROP2 expression was scored into four groups: positive (Score 3+) in 24 patients (10.2%), equivocal (Score 2+) in 55 patients (23.5%), negative (Score 1+) in 84 patients

(35.9%), and negative (Score 0) in 71 patients (30.3%). We found a significant overall survival benefit in patients with positive TROP2 expression versus equivocal ( $p=0.0367$ ), negative (Score 1+) ( $p=0.031$ ), and negative (Score 0) ( $p=0.0102$ ). Meanwhile, tumors with TROP2 expression (combined score 1+, 2+, and 3+) showed a trend towards better clinical response as compared to TROP2 negative (Score 0) ( $p=0.0502$ ). However, there is no significant difference in disease free survival among the groups. A significant overall survival benefit in stage III-IV high-grade serous carcinoma patients with positive TROP2 expression versus equivocal ( $p=0.0084$ ), negative (Score 1+) ( $p=0.0462$ ), and negative (Score 0) ( $p=0.0270$ ) was also illustrated.

**Conclusions:** Our study showed that HGOvCa with positive TROP2 expression had a significant better overall survival as compared to patients with equivocal or negative TROP2 expression. This overall survival benefit may be due to better clinical response. These results indicate that TROP2 may be a prognostic marker for better survival and potential targets for immunotherapy.

## 986 DNA Methylation Profiling Accurately Classifies Primitive Neuroectodermal Tumors in the Gynecologic Tract

Lucy Wang<sup>1</sup>, Jonathan Serrano<sup>2</sup>, Cristina Antonescu<sup>1</sup>, Robert Soslow<sup>3</sup>, Esther Oliva<sup>4</sup>, Nadeem Abu-Rustum<sup>1</sup>, Marc Rosenblum<sup>1</sup>, Matija Snuderl<sup>2</sup>, Sarah Chiang<sup>1</sup>, Ivy Tran<sup>5</sup>, Varshini Vasudevaraja<sup>6</sup>

<sup>1</sup>Memorial Sloan Kettering Cancer Center, New York, NY, <sup>2</sup>New York University, New York, NY, <sup>3</sup>Memorial Sloan Kettering Cancer Center/Weill Medical College of Cornell University, New York, NY, <sup>4</sup>Massachusetts General Hospital, Harvard Medical School, Boston, MA, <sup>5</sup>NYU Langone Health, New York, NY, <sup>6</sup>New York University Medical Center, New York, NY

**Disclosures:** Lucy Wang: None; Jonathan Serrano: None; Cristina Antonescu: None; Robert Soslow: None; Esther Oliva: None; Nadeem Abu-Rustum: None; Marc Rosenblum: None; Matija Snuderl: None; Sarah Chiang: None; Ivy Tran: None; Varshini Vasudevaraja: None

**Background:** Gynecologic (GYN) primitive neuroectodermal tumors (PNET) consist of central (cPNET) and peripheral/Ewing sarcoma (ES) types. GYN ES frequently harbor EWSR1 fusion like its bone and soft tissue counterpart. GYN cPNET resemble primary central nervous system (CNS) tumors. By DNA methylation profiling, CNS tumors previously considered PNET are now reclassified as common CNS neoplasms or embryonal tumors with specific genotypes. The utility of methylation profiling in classifying on GYN PNET is unknown.

**Design:** DNA methylation profiling was performed on 16 GYN PNET that were histologically confirmed and classified as cPNET or ES based on morphology, immunohistochemistry, and EWSR1 FISH. Primary site and associated tumor were noted. Whole genome DNA methylation was analyzed using EPIC array (Illumina, CA). DNA methylation data were analyzed and tumors classified using clinically validated CNS tumor and sarcoma Random Forest classifiers. Copy numbers were analyzed using conumee package.

**Results:** GYN PNET included 13 cPNET and 3 ES arising in the ovary (n=8), uterus (n=7) and vulva (n=1). Only cPNET (n=8/13, 61%) was associated with another tumor, including teratoma (n=4), endometrioid carcinoma (n=1), adenosarcoma (n=1) and carcinosarcoma (n=2). The CNS tumor classifier matched 87% of GYN PNET (n=14/16) with a CNS tumor, including medulloblastoma (n=6), embryonal tumor with multilayered rosettes (ETMR, n=3), ES (n=2), intraocular medulloepithelioma (n=1), pediatric-type diffuse high grade glioma (n=1) and ependymoma (n=1). The sarcoma classifier confirmed both ES (n=2) and identified high-grade endometrial stromal sarcoma (HGESS, n=1). Only 1 GYN PNET remained unclassified by both classifiers.

**Conclusions:** DNA methylation profiling successfully classified >90% GYN PNET as known CNS tumor or sarcoma entities, supporting the utility of methylation-based tumor classification in the diagnostic evaluation of these rare lesions. These findings raise consideration of CNS tumor-specific treatment modalities in GYN cPNET. Given reclassification of most GYN cPNET as distinct CNS tumor and sarcoma entities, modification of PNET terminology in GYN tumors should be considered.

## 987 Fumarate Hydratase Deficient Uterine Leiomyoma: A Clinicopathological and Molecular Analysis of 85 Cases

Xiaoxi Wang<sup>1</sup>, Yan Liu<sup>2</sup>, Congrong Liu<sup>3</sup>

<sup>1</sup>Peking University Third Hospital, Beijing, China, <sup>2</sup>School of Basic Medical Sciences, Third Hospital, Peking University Health Science Center, Beijing, China <sup>3</sup>Peking University Third Hospital, Beijing, China

**Disclosures:** Xiaoxi Wang: None; Yan Liu: None; Congrong Liu: None

**Background:** Hereditary leiomyomatosis and renal cell carcinoma (HLRCC) is caused by germline variants of *fumarate hydratase* (*FH*) and presents with multiple uterine leiomyomas, multiple cutaneous leiomyomas, and renal cell carcinoma. Uterine and cutaneous leiomyomas are considered as sentinel tumors in HLRCC patients. Uterine leiomyomas caused by somatic variants of *FH* can also present with severe symptoms. Although many studies have analyzed the clinicopathological characteristics of *FH*-deficient uterine leiomyoma, there are few reports on how to integrate them with *FH* immunohistochemistry and *FH* gene

sequencing. We aimed to analyze the clinicopathological and molecular characteristics of FH-deficient uterine leiomyoma, so as to explore the pathological diagnosis strategy.

**Design:** 85 cases of FH-deficient uterine leiomyoma were diagnosed from April 2018 to September 2022. Whole exons (exon 1-10) Sanger sequencing of *FH* gene were performed on tumor tissues of all cases and matched non tumor tissues/peripheral blood, and FH immunohistochemistry were performed in 79 cases.

**Results:** Patients' age ranged from 18 to 54 (36.1±7.3) years, more than 60% of them had clinical symptoms, exhibiting multiple and large leiomyomas (average maximum diameter was 7.68cm). Four or more of the seven histological features, including staghorn vasculature, alveolar-pattern oedema, bizarre nuclei, oval nuclei arranged in chains, prominent eosinophilic nucleoli with perinucleolar haloes and eosinophilic intracytoplasmic globules were observed in 95.9% (70/73) patients. The sensitivity of FH immunohistochemistry was 82.3% (65/79). According to the results of Sanger sequencing of *FH*, the cases were divided into germline variant group (31 cases, of which 5 cases had variants of unknown significance), somatic variant group (34 cases) and no pathogenic variant group (20 cases). Only 69.0% (20/29) of the patients with *FH* germline variant had clear family history.

**Conclusions:** Clinical features, histological morphology, FH immunohistochemistry and *FH* Sanger sequencing have their own significance and limitations in differentiating FH-deficient uterine leiomyoma. In order to ensure the accurate pathological diagnosis and timely selection of patients with HLRCC, detailed clinicopathological features, FH immunohistochemistry and *FH* gene sequencing results should be fully integrated in clinical practice.

## 988 Morphologic Responses Correlate Aberrant Biomarker Expression for Endometrioid Precancers in Post-Progestin Treated Endometrial Biopsies

Yiying Wang<sup>1</sup>, Ruijiao Zhao<sup>1</sup>, Li Li<sup>2</sup>, Yan Wang<sup>3</sup>, Yue Wang<sup>4</sup>

<sup>1</sup>Henan Provincial People's Hospital, Zhengzhou, China, <sup>2</sup>School of Basic Medical Sciences, Shandong University, Jinan, China, <sup>3</sup>UT Southwestern Medical Center, Dallas, TX, <sup>4</sup>Henan Provincial People's Hospital, People's Hospital of Zhengzhou University, School of Clinical Medicine, Henan University, Zhengzhou, China

**Disclosures:** Yiying Wang: None; Ruijiao Zhao: None; Li Li: None; Yan Wang: None; Yue Wang: None

**Background:** Progestin is a treatment option for atypical endometrial hyperplasia (AEH). Presence or absence of residual disease (RD) is a common challenging question for pathologists. This is because progestin induces a spectrum of morphologic changes in AEH samples. Based on morphologic classifications (PMIDs: 32931681, 34782217) by the gynecologic pathology group at UTSW medical center, the morphologic changes can be largely divided into three groups: none or poor response (NR), partial response (PR), and complete response (CR). The relationship between progestin induced morphologic changes and RD status remains clarified. It is known that the biomarkers, PTEN, Pax2, and β-catenin (PPB), are useful to aid AEH diagnosis in both pre- and post-progestin treated samples. The study aimed to correlate the biomarker aberrancy with different morphologic responses in those post-treated samples in order to better define RD.

**Design:** 120 patients from 2018 to 2021 were studied. IHC staining using antibody against PTEN, Pax2, and β-catenin was performed on 120 post-progestin treated samples at either the first 3-month or the second 6-month F/U. Each sample contained more than 1 responding area. After reviewing all samples, different morphologic responses were recorded and summarized. Aberrant expression of either of the 3 PPB markers in any F/U sample was considered as RD. The marker aberrancy was individually calculated from different responsive areas. Results of the stain were analyzed by using Fisher exact test.

**Results:** Among 120 post progestin-treated cases with at least 2 F/Us, RD was identified in 58 (48.3%) samples. Morphologic responses were 76 NR, 132 PR, and 140 CR. Aberrant markers were expressed in 68 (89.4%) NR, 60 (48.5%) PR, and 0 (0%) CR. Detailed data is summarized in Table 1. Within the PR areas, more complex architecture and less stromal decidualization was associated with more marker aberrancy. Interesting to note that higher association of aberrant β-catenin was associated with glands showing morules.

Table 1. Biomarker aberrancy in relation with different progestin induced morphologic responding areas

Different Responses and Aberrant Rates		<i>p</i> Values		
	NR (%)	PR (%)	CR (%)	
# Responsive Areas	76	132	140	
Any Marker aberrancy	68 (89.4)	60 (48.5)	0 (0)	<0.001
PTEN	41 (53.9)	29 (21.9)	0 (0)	<0.001
Pax2	53 (69.7)	52 (39.4)	0 (0)	<0.001
β-catenin	28 (36.8)	11 (8.3)	0 (0)	<0.001

# ABSTRACTS | GYNECOLOGIC AND OBSTETRIC PATHOLOGY

Note: The p values listed represented the comparisons between NR and PR. All comparisons, either NR or PR vs CR, were statistically significant with  $p < 0.001$ .

**Conclusions:** Morphologically NRs mostly represent RD in progestin treated samples, while PRs contain a mixture of residual and non-residual diseases. The more NR areas or more complex architecture in PRs, the more likely the residual diseases. CR areas represent optimally treated without any RD. It is recommended to quantify different progestin induced different responses in the pathology report, particularly when biomarkers are not available to aid diagnosis.

## 989 Gene Mutation Patterns in Uterine Leiomyoma and Variants

Jian-Jun Wei<sup>1</sup>, Yue Feng<sup>2</sup>, Serdar Bulun<sup>1</sup>, J. Julie Kim<sup>1</sup>

<sup>1</sup>Northwestern University, Chicago, IL, <sup>2</sup>Feinberg School of Medicine/Northwestern University, Chicago, IL

**Disclosures:** Jian-Jun Wei: None; Yue Feng: None; Serdar Bulun: None; J. Julie Kim: None

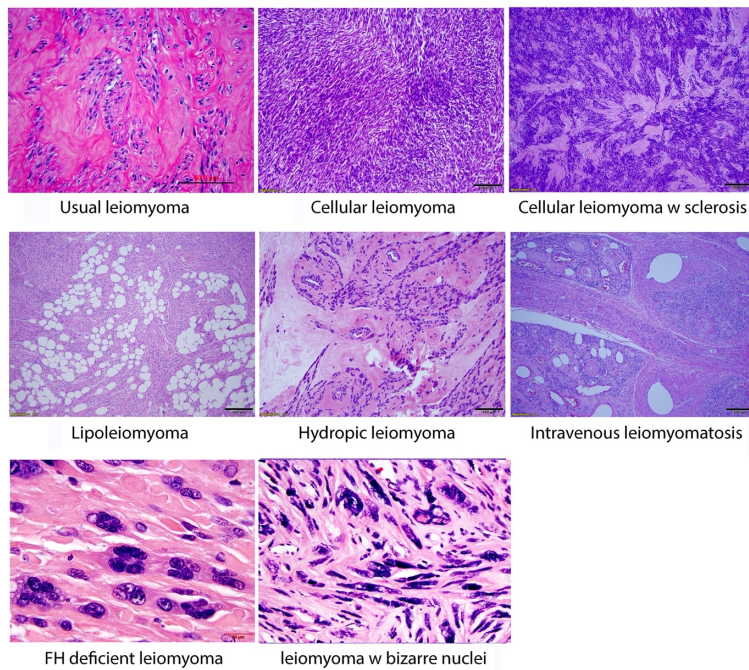
**Background:** Uterine leiomyoma (LM) is the most common benign neoplasm in reproductive age women with a prevalence of over 70% in women. About 25% patients with LM show symptoms and many are subject to surgical treatment and histologically evaluated by pathologist. Recent advantages of molecular biology uncover the specific gene mutations/alterations in LM, but molecular changes in association with LM variants remain to be fully elucidated.

**Design:** A total 716 leiomyomas from 496 patients were collected at Northwestern Prentice Hospital with either consented patients or waivered by IRB exemption. Cases included 526 usual type LM (ULM), 22 cellular LM (CLM), 52 cellular leiomyoma with sclerosis (CLMS), 24 hydropic LM (HLM), 9 lipoleiomyoma (LLM), 3 intravenous leiomyomatosis (IVLM), 40 fumarate hydratase deficient LM (FH-BN), and 37 leiomyoma with bizarre nuclei (LM-BN) (Figure 1). MED12 mutations were performed by Sanger sequencing, HMGA2 overexpression and FH deficiency were examined by immunohistochemistry (IHC).

**Results:** In a total of 716 LM and variants, MED12 mutations were detected in 56%, HMGA2 overexpression in 22% and FH deficiency in 6%. About 16% of LM and variants did not detect any mutation/alteration (Table 1). MED12 mutations were detected in 74% of ULM, and none in other variants except for CLM and LM-BN. HMGA2 overexpression was enriched in CLMS, HLM, LLM, and IVLM in a range of 75-100%. LM variants with HMGA2 overexpression showed some similar cytohistologic features, including small round-oval nuclei, hypercellularity with sclerotic matrix, increased vessels, and organized growth patterns. FH deficiency LM were selected based on the characteristic histologic features and they are frequently associated remarkable nuclear atypia. As high as 78% of LMBN and 68% of CLM did not harbor mutations of these three genes (Table 1). HMGA2, MED12 and FH alterations are mutually exclusive in all examined LM (Table 1).

	No. of Cases	MED12 mutations	HMGA2 overexpression (IHC)	FH deficiency (IHC)	Unknown
Usual LM	529	74.86% (396/529)	12.67% (67/529)	0.76% (4/529)	11.72% (62/529)
Cellular LM	22	14% (3/22)	18.2% (4/22)	0 (0/22)	68.18% (15/22)
Cellular LM with sclerosis	52	0 (0/36)	96.15% (50/52)	0 (0/52)	3.85% (2/52)
Hydropic LM	24	0 (0/21)	75.0% (18/24)	0 (0/24)	25.0% (6/24)
Lipo LM	9	0 (0/9)	100% (9/9)	0 (0/9)	0
Intravenous LM	3	-	100% (3/3)	0 (0/3)	0
FH LM	40	0 (0/25)	0 (0/40)	100% (40/40)	0
LM-BN	37	13.51% (5/37)	8.11% (3/37)	0 (0/37)	78.38% (29/37)
total	100% (716/716)	56.42% (404/716)	21.51% (154/716)	6.15% (44/716)	15.92% (114/716)

Figure 1 - 989



**Conclusions:** Overall, >85% of examined leiomyomas harbor one of three known gene mutations. HMGA2 overexpression is common in several LM variants, including CLMS, HLM, LLM and IVLM. These variants show some overlapping cytohistologic features. Immunostains for HMGA2 and FH can be used in aid of differential diagnosis of certain LM variants. More molecular studies on CLM and LMBN are needed to explore the associated genetic alterations.

**990 A Comprehensive Population-Based Study of Malignant Ovarian Tumors, including Histologic and Immunohistochemical Review, in Girls 0-19 Years in Sweden between 1970 and 2014**

Sandra Wessman<sup>1</sup>, Joseph Carlson<sup>2</sup>, Tirzah Braz Petta<sup>2</sup>, Georgia Kokaraki<sup>2</sup>

<sup>1</sup>Karolinska Institutet and Karolinska University Hospital, Stockholm, Sweden, <sup>2</sup>Keck School of Medicine of USC, Los Angeles, CA

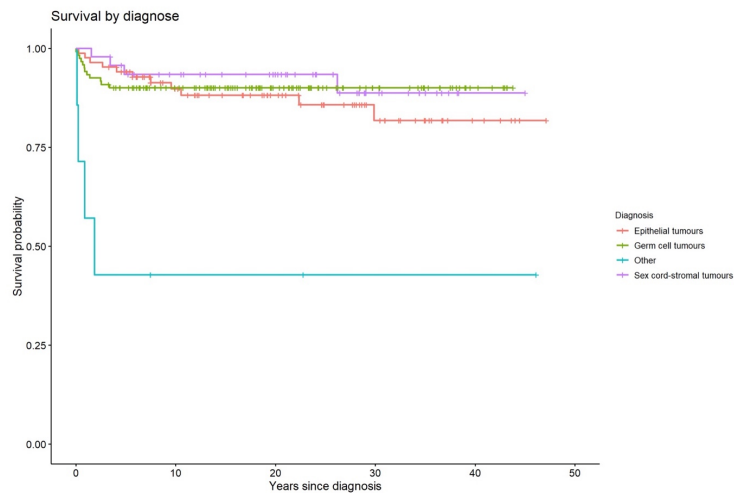
**Disclosures:** Sandra Wessman: None; Joseph Carlson: None; Tirzah Braz Petta: None; Georgia Kokaraki: None

**Background:** Ovarian tumors in the pediatric population are very rare. The overall incidence and frequency of subtypes differs between children and adults, as well as between different age groups within the pediatric population. Although not all tumors are aggressive, they may still lead to morbidity secondary to therapy. Some entities, for example, Sertoli-Leydig cell tumor, are associated with cancer predisposition syndromes. A deepened knowledge of what tumor types to expect in the pediatric population and in different age groups within this population, may aid when diagnosing these tumors. The goal of this study was a comprehensive review of malignant ovarian tumors in children.

**Design:** Individuals were identified through a search in the Swedish cancer registry using appropriate ICD-10 codes, limited for ages 0-19 between 1970 and 2014. Clinical data, such as original diagnosis, year of diagnosis, age at diagnosis, region etc. was extracted from the registry. Regional biobanks were contacted and stored material, either FFPE blocks or microscopy slides, were collected and reviewed.

**Results:** A total of 345 individuals were included. The majority were between 15-19 years old at time of diagnosis (70.7%). Median age at diagnosis was 16 years. No differences in incidence over time or geographic location were identified. The mean follow up time was 21.1 years. A total of 51 patients (14.8%) died during follow up, 45 (13%) due to their malignant ovarian tumor. New cases per year ranged from 2 to 13. 260 cases were available for slide review, resulting in 85 epithelial tumors, 121 germ cell tumors, 47 sex cord-stromal tumors and 7 other. For age 0-4 years sex cord-stromal tumors dominated, for 5-9 as well as 10-14 years germ cell tumors was the dominating category, and for the oldest age group 15-19 years epithelial tumors dominated. Kaplan Meier curves for overall survival are shown in Figure 1. The original diagnoses were known in 225 cases. Review diagnosis and original diagnosis had a complete correspondence in 182 cases (80.8%). Statistical analyses indicated that there was a strong agreement between review diagnose and original diagnose (Cohen's k 0.944). Differentiating between entities within the sex cord-stromal group posed the biggest diagnostic challenge.

Figure 1 - 990



**Conclusions:** Pediatric ovarian tumors are rare and distinct from their adult counterparts. There was a strong concurrence between original and review diagnosis. The greatest diagnostic difficulty was within the sex cord-stromal group.

### 991 Uterine Leiomyosarcoma with Heterologous (“Divergent”) Differentiation: A Pathologic and Molecular Study of 6 Cases

Erik Williams<sup>1</sup>, Roberto Ruiz-Cordero<sup>2</sup>, Andrew Rosenberg<sup>3</sup>, Douglas Lin<sup>4</sup>, Andre Pinto<sup>5</sup>

<sup>1</sup>University of Miami, Miami, FL, <sup>2</sup>Jackson Memorial Hospital/University of Miami Hospital, Miami, FL, <sup>3</sup>University of Miami Health System, Miami, FL, <sup>4</sup>Foundation Medicine, Inc., Cambridge, MA, <sup>5</sup>University of Miami Health System, Miami Beach, FL

**Disclosures:** Erik Williams: Employee: Foundation Medicine, Inc.; Roberto Ruiz-Cordero: None; Andrew Rosenberg: None; Douglas Lin: Employee: Foundation Medicine, Inc.; Andre Pinto: None

**Background:** Uterine leiomyosarcoma (uLMS) frequently harbors mutations in *TP53*, *ATRX*, *RB1*, and *PTEN*. Rarely, uLMS shows focal heterologous (“divergent”) differentiation, including rhabdomyosarcoma (RMS), chondrosarcoma (CS) and osteosarcoma (OS) - the underlying molecular aberrations of these tumors are not well characterized. This study analyzes the genomics of a cohort of uLMS with heterologous features.

**Design:** Two index cases of uLMS with RMS differentiation were retrospectively identified at our institution, and each component was microdissected for independent molecular characterization using a pan-cancer capture-based next generation sequencing assay with a total footprint of 2.8 Mb (479 cancer genes and select introns of 47 genes). Subsequently, the FoundationOne Heme® database was searched for uLMS samples showing divergent differentiation (both components analyzed in the same test). The molecular findings, pathology reports, and archived histopathology images were reviewed for each case.

**Results:** Four additional cases from a cohort of 1354 uLMS (0.3%) contained heterologous differentiation with supportive immunohistochemical findings, present in at least 10% of each sequenced sample. The final cohort consisted of tumors with RMS (4), CS (1) and OS (1) components. In 2/6 recurrent tumors, the metastatic focus demonstrated non-LMS elements only (1 CS, 1 OS). No carcinoma component was identified in any of the tumors- this helped exclude carcinosarcoma. Tumors were microsatellite stable and exhibited low tumor mutational burden. The two index cases displayed shared alterations between the LMS and RMS components, with the first harboring a shared *ATRX* alteration in the LMS and RMS components, and the second displaying a shared *TP53* and two *RB1* alterations in both components. The most frequently and recurrently mutated genes for the four cases from the F1H database included *TP53* (100%), *RB1* (50%), *ATRX* (100%), and *PTEN* (25%), at prevalence rates generally similar to the remainder of the uLMS cohort (70% *TP53*, 54% *RB1*, 29% *ATRX*, and 18% *PTEN*-mutant; p=0.33, 1.0, 0.007, 0.55, respectively). *PAX3* fusions or *IDH1* mutations, indicative of pure rhabdomyosarcoma or chondrosarcoma, were not identified in any of the six tumors.

**Conclusions:** uLMS with heterologous differentiation shows genomic overlap with conventional uLMS with similar driver alterations. Comprehensive genomic profiling of uLMS with aberrant differentiation can help diagnose and improve tumor classification.

**992 Detection of Incidental Serous Tubal Intraepithelial Carcinoma (STIC) in Women Without Known Risk for Hereditary Ovarian Cancer Undergoing Surgery Unrelated to Tubo-ovarian Cancer: Tissue Sampling Triage Strategies Based on Patient Age for Resource-Limited Practices**Rebecca Wolsky<sup>1</sup>, Oluwole Fadare<sup>2</sup>, Joseph Rabban<sup>3</sup><sup>1</sup>University of Colorado, Denver, CO, <sup>2</sup>UC San Diego School of Medicine, La Jolla, CA, <sup>3</sup>University of California, San Francisco, San Francisco, CA**Disclosures:** Rebecca Wolsky: None; Oluwole Fadare: None; Joseph Rabban: None

**Background:** Pathologic detection of STIC has been reported in rare women without known risk of a germline pathogenic variant of a hereditary ovarian cancer gene (HOC-PV) who are undergoing surgery unrelated to tubo-ovarian cancer. While it is well-established that complete examination of the fimbriae and non-fimbriated fallopian tube is required to detect occult STIC in women with HOC-PV, this is a time and resource-intensive protocol. Whether this protocol is justified in women without HOC-PV remains to be defined but is relevant to laboratory resource utilization. We hypothesize that patient age could serve to triage which specimens merit complete versus representative examination of the fimbriae. We report the largest series of incidental STIC in women without HOC-PV undergoing surgery unrelated to tubo-ovarian cancer and, integrating similar cases in the literature, provide practical guidelines for resource-limited practices.

**Design:** Cases of incidental STIC in women at presumed low risk for HOC-PV undergoing surgery unrelated to tubo-ovarian cancer were collected from 3 academic cancer-referral centers. Diagnostic confirmation by aberrant p53 immunohistochemistry was established in each case. A PubMed search was conducted for similar cases.

**Results:** 54 cases were identified in the 3 academic centers. Median age was 64.5 years. Only 1.8% (1/54) were under age 40; 22% (12/54) were under age 50. The youngest was 36 years, undergoing salpingectomy for ectopic pregnancy and found to have STIC and tubal high grade serous carcinoma (HGSC). Overall, pure STIC was present in 65% (35/54). Tubal HGSC was present in 24% (13/54). Ovarian HGSC accompanied STIC/tubal HGSC in 11% (6/54). The major surgical indications were a.) hysterectomy for endometrioid carcinoma (24%), atypical hyperplasia (5%), uterine prolapse (13%) menorrhagia (7%) or leiomyomas (5%) and b.) oophorectomy for serous cystadenoma/borderline tumor (11%) or mucinous cystadenoma (9%). No cases were identified in salpingectomy for sterilization. Among 84 similar cases published as case reports/series (Table 1), the youngest was 38 years, none involving salpingectomy for sterilization.

Authors	PMID	Number of occult STIC cases in presumed low risk women	Youngest age (years) at STIC diagnosis
Current study		54	36
Morrison et al	25517955	22	39
Gilks et al	25517954	21	38
Chay et al	26807643	17	43
Meserve et al	28479065	6	51
Samimi et al	31360879	5	42
Rabban et al	24820399	4	43
Gao et al	23465279	4	40
Seidman et al	26630221	3	55
Chong et al	32034117	1	62
Semmel et al	19407856	1	69

**Conclusions:** Complete examination of the fallopian tube fimbriae is the ideal method to maximize detection of occult STIC in women without known genetic risk for tubo-ovarian cancer. However, in resource-limited practices, young patient age could serve as a triage tool for representative sampling as occult STIC has not been reported below age 35.

**993 Glandular Crowding Sub-Diagnostic of Endometrial Intraepithelial Neoplasia (Atypical Endometrial Hyperplasia): Prevalence and Value of PAX2, PTEN and Beta-Catenin Immunohistochemistry in Predicting Neoplastic Outcome**Nicolas Wyveldens<sup>1</sup>, George Mutter<sup>2</sup>, Marisa Nucci<sup>1</sup>, David Kolin<sup>2</sup>, Carlos Parra-Herran<sup>1</sup><sup>1</sup>Brigham and Women's Hospital, Harvard Medical School, Boston, MA, <sup>2</sup>Brigham and Women's Hospital, Boston, MA**Disclosures:** Nicolas Wyveldens: None; George Mutter: None; Marisa Nucci: None; David Kolin: None; Carlos Parra-Herran: None

**Background:** The diagnosis of Endometrial Intraepithelial Neoplasia (EIN) is primarily morphologic. However, it has been demonstrated that aberrant PAX2, PTEN and/or beta-catenin (BCAT) staining by immunohistochemistry (IHC) is 92% sensitive in identifying bona fide EIN lesions. In practice, areas of endometrial gland crowding (GC), suspicious but not definitive for EIN are

often encountered. Our aim is to explore the outcome predictive value of the above markers in patients with GC in endometrial biopsy.

**Design:** Samples with GC between 2001 and 2021 with at least one follow-up biopsy and no prior history of endometrial neoplasia were retrieved. In our institution, diagnosis of GC is followed by a note recommending repeated biopsy in 3 to 6 months. Diagnosis at follow-up biopsy was categorized as benign vs neoplastic (EIN or endometrioid carcinoma). IHC for PAX2, PTEN and BCAT was performed on biopsies from patients with a neoplastic outcome and a representative selection of age-matched patients with benign outcome. Loss of PAX2 or PTEN staining and nuclear BCAT staining were scored as aberrant. IHC review was blinded to outcome. Sensitivity, specificity, positive and negative predictive values (PPV, NPV) of aberrant staining results for a neoplastic outcome were calculated.

**Results:** A total of 430 patients diagnosed with GC and follow-up biopsy were identified. Of these, 70 had a subsequent diagnosis of neoplasia (16%). Median interval between GC and neoplasia was 8 months. Median follow-up for patients with benign outcome was 53 months. IHC was successfully applied to 52 cases with neoplastic, and 63 cases with benign outcome. Individual marker performance was suboptimal, as all were frequently aberrant in both groups (Table 1). Normal staining for all markers in GC areas was seen in 46% of patients with benign vs 15% with neoplastic outcome, corresponding to 85% sensitivity and 94% NPV for neoplasia when  $\geq 1$  aberrant marker is considered positive.

	Aberrant PAX2	Aberrant PTEN	Aberrant BCAT	Aberrant any marker	Aberrant 2 markers	Aberrant all markers
GC with neoplastic follow-up (n=52)	30 (58%)	18 (35%)	28 (54%)	44 (85%)	24 (46%)	7 (13%)
GC with benign follow-up (n=63)	18 (29%)	22 (35%)	22 (35%)	34 (54%)	22 (35%)	7 (11%)
Sensitivity	58%	35%	54%	85%	46%	13%
Specificity	71%	65%	65%	46%	65%	89%
PPV	28%	16%	23%	23%	20%	19%
NPV	90%	84%	88%	94%	86%	84%

**Conclusions:** Endometrial GC, worrisome but sub-diagnostic for EIN, is associated with subsequent neoplasia in 16% of patients, justifying a clinical recommendation for follow-up sampling. Aberrant expression of PAX2, PTEN and/or BCAT has limited predictive value since it is seen in a significant number of cases with benign follow-up. However, IHC may help inform management decisions as normal staining identifies women with a low (6%) likelihood of neoplastic outcome.

## 994 Effect of PD-L1 and the Hypoxia Related Markers (HIF1 $\alpha$ , CAIX) on the Outcome of Endometrioid Carcinoma Treated with Mirena IUD

Bei Yang<sup>1</sup>, Jack Chen<sup>2</sup>, Devi Jeyachandran<sup>3</sup>, Mohamed Desouki<sup>3</sup>

<sup>1</sup>University at Buffalo, Buffalo, NY, <sup>2</sup>University of Rochester, Rochester, NY, <sup>3</sup>Roswell Park Comprehensive Cancer Center, Buffalo, NY

**Disclosures:** Bei Yang: None; Jack Chen: None; Devi Jeyachandran: None; Mohamed Desouki: None

**Background:** Mirena IUD is an alternative treatment for endometrial endometrioid carcinoma (EEC) in some clinical scenarios, especially for patients with fertility demand. However, the efficacy is limited and differs from patient to patient. Hypoxia plays a role in endocrine therapy resistance in some cancers, and crosstalk between hormone and hypoxia pathways has been reported. PD-L1 has been found to correlate with hypoxia markers in other cancers. The role of hypoxia and PD-L1 in endocrine therapy resistance in EEC has not been well studied, and this study aims to examine the effect of PD-L1 and hypoxia related markers (HIF1 $\alpha$ , CAIX) expression on Mirena IUD treatment outcome.

**Design:** A retrospective study of 62 patients (26 hyperplasia and 36 EEC) with 166 specimens were included. Tissue microarray blocks were made and stained for PD-L1, HIF1 $\alpha$ , ER, PR, and CAIX. PD-L1 IHC expression was evaluated by combined positive score (CPS) with 1% positive as cut off. Clinicopathological data was collected and analyzed. The efficacy of IUD therapy was evaluated based on pathological examination and classified as complete response (CR), partial response (PR), no response, and progression (hyperplasia to atypia/carcinoma and/or tumor upgrade). Chi square and Fisher's exact tests were used for statistics ( $p < 0.05$  is significant).

**Results:** The response rate (CR+PR) is 23/26 (88%) in hyperplasia and 15/36 (42%) in EEC ( $p=0.01$ ). ER is expressed in 86/92 (93%) EEC biopsies while positive in 71/71 (100%) hyperplasia biopsies ( $p=0.03$ ). PR is expressed in 70/92 (76%) EEC biopsies while positive in 55/72 (76%) hyperplasia biopsies ( $p=0.88$ ). HIF1 $\alpha$  expression in EEC biopsies (42/88, 48%) is higher than it in the hyperplasia (23/67, 34%) ( $p=0.1$ ). The CAIX expression in EEC biopsies (25/89, 28%) is higher than it in hyperplasia (8/69, 12%) ( $p=0.02$ ). PD-L1 expression showed no difference between hyperplasia (5/70, 7%) and EEC biopsies (11/93, 12%) ( $p=0.4$ ). EEC (hyperplasia excluded) with response (CR+ PR) are classified as group 1 while with no response or progression are classified as group 2. Table 1 summarizes the expression of HIF1 $\alpha$ , CAIX and PD-L1 in the two groups on the follow up.

Table 1: HIF1a, CAIX, PD-L1 expression in EEC with Mirena IUD treatment

	Increased HIF1a	Increased CAIX	PD-L1 (mean CPS)
Group 1	5/15 (33%)	3/15 (20%)	6%
Group 2	8/13 (62%)	11/14 (79%)	20%
P value	0.2	0.002	0.001

**Conclusions:** Increased PD-L1 and CAIX in EEC are associated with no response or progression with Mirena IUD treatment, while increased HIF1a has no significant difference. Larger sample size is needed to further validate the findings

**995 Genomic Catastrophe (Chromothripsis) in Early and Advanced High-grade Serous Carcinoma**

Ju-Yoon Yoon<sup>1</sup>, David Chapel<sup>2</sup>, Azra Ligon<sup>3</sup>, Rebecca Ramesh<sup>4</sup>, Aarti Sharma<sup>5</sup>, Grace Neville<sup>6</sup>, Amir Dehghani<sup>6</sup>, Christopher Crum<sup>3</sup>

<sup>1</sup>Unity Health Toronto, Toronto, ON, <sup>2</sup>Michigan Medicine, University of Michigan, Ann Arbor, MI, <sup>3</sup>Brigham and Women's Hospital, Boston, MA, <sup>4</sup>Perelman School of Medicine at the University of Pennsylvania, Philadelphia, PA, <sup>5</sup>Hospital for Special Surgery, Boston, MA, <sup>6</sup>Brigham and Women's Hospital, Harvard Medical School, Boston, MA

**Disclosures:** Ju-Yoon Yoon: None; David Chapel: None; Azra Ligon: None; Rebecca Ramesh: None; Aarti Sharma: None; Grace Neville: None; Amir Dehghani: None; Christopher Crum: None

**Background:** High-grade serous carcinomas (HGSC) presumably arise via clonal *TP53* mutations in fallopian tube (FT) epithelial cells. Excluding incidentally discovered serous tubal intraepithelial carcinomas (STICs) in risk reduction specimens, most HGSCs are typically advanced when discovered, many without a recognizable FT precursor. Such scenarios challenge the traditional step-wise model of carcinogenesis and frustrate efforts at early detection. Chromothripsis, which defines a presumed single catastrophic event with extensive genomic chromosomal rearrangement, contrasts with the step-wise model and has been reported in ovarian cancer. This study determined the frequency of chromothripsis in HGSC and its relationship to clinical-pathologic parameters.

**Design:** DNAs from FFPE tumors obtained locally were analyzed by the Affymetrix Oncoscan Array, a whole genome SNP microarray with 217,611 probes. Chromothripsis was defined as a minimum of 10 continuous segments/copies along the length of the chromosome, presumably altered in tandem. Retrospective analysis of a subset of TCGA cases, including CNV assessment, was performed using CNViz.

**Results:** 55 cases (17 local and 38 TCGA) included 7 FIGO stage I/II, and 48 stage III/IV cases. Chromothripsis was identified in 11/17 (65%) local cases by microarray, and 22/38 (58%) TCGA cases by DNA sequencing. Frequency of chromothripsis in stages I/II (4/7) and III/IV (26/48) was similar. Acrocentric chromosomes (13, 14, 15, 21, 22) were less frequently involved vs. metacentric and sub-metacentric chromosomes. Among the non-acrocentric chromosomes, chromosome 9 (6% of 33 cases) was least involved, followed by chromosomes 17 (9%) and 20 (9%). Among the local cases, STIC was present in 6/17 (35%); STIC or tumor distribution favored a FT primary in 12/17 (71%). Frequency of chromothripsis was similar irrespective of tumor primary (8/12 tubal 5/7 non-tubal).

**Conclusions:** The distal FT remains the principal host for the "cell of origin" for HGSC, but catastrophic chromosomal rearrangements could accelerate HGSC development in vulnerable cells, either in the tube or following escape into the peritoneal cavity. The potential for rapid onset underscores the importance of 1) timing salpingectomy to maximize HGSC prevention, 2) thorough pathologic exam of FTs to assess recurrence risk following salpingectomy (SEE-FIM dissection protocol) and 3) developing management strategies to mitigate recurrence risk when a STIC has been discovered.

**996 Challenges in Evaluating Post-Neoadjuvant Specimens of Endometrial Cancer: Histotype Designation, Chemotherapy Response Score and Molecular Phenotype Associations**

Valentina Zanfagnin<sup>1</sup>, Joseph Carlson<sup>2</sup>, Saloni Walia<sup>2</sup>

<sup>1</sup>University of Southern California, Keck School of Medicine of USC, LAC+USC Medical Center, Los Angeles, CA, <sup>2</sup>Keck School of Medicine of USC, Los Angeles, CA

**Disclosures:** Valentina Zanfagnin: None; Joseph Carlson: None; Saloni Walia: None

**Background:** Neoadjuvant chemotherapy (NACT) is now used more frequently in advanced stage endometrial carcinoma. In the presence of residual tumor, post treatment changes might affect histotype and grade (G) designation. Here, we investigated histotype and grade concordance rates between preoperative biopsies and post-NACT specimens; and association between chemotherapy response score (CRS) and p53 molecular phenotype.

# ABSTRACTS | GYNECOLOGIC AND OBSTETRIC PATHOLOGY

**Design:** Cases were identified from institutional electronic medical database (2015 to 2022). Clinicopathologic parameters were recorded as well as ancillary studies, if available. CRS was assigned to omental and adnexal metastases, and categorized as no/minimal (CRS1), partial (CRS2), and complete/near-complete (CRS3).

**Results:** 23 cases were identified, mean age at diagnosis was 55 years. 16 (70%) patients were clinically staged as FIGO III, and 7(30%) FIGO IV. The rationale for NACT was: locally advanced disease (26%), carcinomatosis (22%), extensive nodal involvement (22%), distant metastasis (30%). Preoperative histotype / grade were: endometrioid G1 (3, 13%), G2 (3, 13%), G3 (2, 9%), serous (5, 22%), clear cell (4, 17%), carcinosarcoma (1, 4%), poorly differentiated (3, 13%), and mixed histologies (2, 9%). 17 (74%) patients received carboplatin/paclitaxel as regimen of NACT. Preoperative diagnosis was based on endometrial biopsies in 22 (95%) cases, and pleural fluid in 1 case (5%). Overall concordance between pre-op biopsies and resection specimen was 70% (Table 1). Clear-cell features led to ambiguity in histotype determination and were discordant in 2 cases (1 G1 endometrioid and 1 serous); other major discordance was in pre-op and final grading of endometrioid carcinoma. CRS1 was noted in 4 cases, CRS2 in 3 cases and CRS3 in 13 cases (3 were not available for review). p53 IHC was available in 14 cases, lower response to NACT (CRS1/2) was more frequent in p53mut tumors (4/5, 80%), and CRS3 was seen in 3/9 p53 mut tumors (33%).

Biopsy		EEC G1	EEC G2	EEC G3	SEROUS	CCC	Poorly Diff	CS	Mixed
Post-NACT		1(44.0)					1(33.0)		
EEC G1		1(44.0)							
EEC G2	2(66.0)		2(66.0)						
EEC G3		1(44.)		2(100.0)		1(25.0)			
SEROUS					4(80.0)	1(25.0)	1(33.0)		
CCC						2(50.0)			
Poorly									
Diff							1(33.0)		
CS								1(100.0)	1(50.0)
Mixed									1(50.0)
No residual tumor					1(20.0)				
Total	3(100)	3(100)	2 (100)	5(100)	4(100)	3(100)	1(100)	2 (100)	

Abbreviations: CCC: clear cell carcinoma; CS=carcinosarcoma; EEC: endometrioid endometrial cancer, NACT: neoadjuvant chemotherapy.

Red highlights concordance in grade and histotype.

**Conclusions:** NACT did not affect the histotype and grade designation. Poorly differentiated tumors, especially those with clear cell features showed poor diagnostic correlation between pretreatment biopsy and resection. p53mut tumors showed minimal response to NACT irrespective of histologic subtype. Molecular genetic analysis may improve diagnostic accuracy and prognostically relevant classification of these tumors.

## 997 Diagnostic Utility of GATA3 Expression in Vulvar Lesions: Differential Patterns of Expression in Vulvar Inflammatory Dermatoses, Putative Dysplasias, and Pre-Malignant Lesions

Somaye Zare<sup>1</sup>, Elmira Vaziri Fard<sup>2</sup>, Oluwole Fadare<sup>3</sup>

<sup>1</sup>University of California, San Diego, La Jolla, CA, <sup>2</sup>UC San Diego Health, San Diego, CA, <sup>3</sup>UC San Diego School of Medicine, La Jolla, CA

**Disclosures:** Somaye Zare: None; Elmira Vaziri Fard: None; Oluwole Fadare: None

**Background:** GATA-binding protein 3 (GATA3) immunohistochemistry (IHC) has recently been reported to be of utility in the pathologic classification of vulvar intraepithelial neoplasia and in their distinction from inflammatory dermatoses (ID). The purpose of the current study is to assess the expression patterns of GATA3 in a large cohort of vulvar ID, putative dysplasias, and pre-malignant

**Design:** IHC studies for GATA3, p16 and p53 were performed on 128 vulvar tissues classified as differentiated VIN [dVIN] (n=25), vulvar altered maturation (VAM; n=11), HSIL (VINIII; n=44), and 49 ID [25 lichen sclerosus (LS), 13 spongiotic dermatitis (SD), 6 lichen simplex chronicus (LSC), 2 lichen planus (LP), 3 non-specific interface dermatitis (NSID)]. GATA3 expression was assessed

using the criteria of Goyal et al [PMID: 29434343]: Pattern 0 (no basal loss), Pattern 1 (25-75% basal staining) and Pattern 2 (<25% basal expression). Parabasal expression was also reviewed and documented separately

**Results:** The consistently observed pattern of GATA3 expression in normal vulvar epidermis was strong staining in the basal and parabasal layers, extending to at least the mid stratum spinosum. In the dermatoses cohort, moderate to strong GATA3 expression similar to non-neoplastic epidermis was observed in all cases of SD, LSC, LP, and NSID. Only one case of LS showed pattern 2 of GATA3 expression. dVIN cases showed partial/complete loss of GATA3 expression in the basal layer (with or without loss in the suprabasal layers) in 23 of 25 (92%) of cases, with the majority of these cases showing a significant loss of expression (Pattern 2 in 19 cases, 76%). Ninety percent of VAM cases (9 cases) also showed some degree of GATA3 basal loss, of which 2 (20%) showed a significant loss (Pattern 2) and 7 demonstrated moderate loss of expression (70%). In the VINIII cohort, some degree of GATA-3 loss was observed in 15.9% (1 pattern 1 and 6 pattern 2), but all other cases were Pattern 0. (Table 1)

	GATA3 staining patterns			p53 IHC results		p16 IHC results		Total
	Pattern 0	Pattern 1	Pattern 2	Wild type	Abnormal	Positive	Negative	
<b>DVIN</b>	2	4	19	1	24 (mutational)	0	10	25
<b>VAM</b>	1	7	2	9	1	0	10	10
<b>VINIII</b>	37	1	6	44	0	44	0	44
<b>Dermatoses</b>								
<i>LS</i>	23	1	1	23	2 (strong basal)	0	25	25
<i>LSC</i>	6	0	0	6	0	0	6	6
<i>SD</i>	13	0	0	13	0	0	13	13
<i>LP</i>	2	0	0	2	0	0	2	2
<i>NSID</i>	3	0	0	3	0	0	3	3
<b>Total</b>	115	13	28	101	27	44	84	128

**Conclusions:** GATA3 expression is diagnostically useful in the distinction of dVIN (76% Pattern 2) from ID such as lichen sclerosus (96% Pattern 0: no basal loss). The putative dysplastic lesion VAM, which is definitionally p53-wild type and HPV independent, also frequently displays loss of GATA3 expression. VINIII generally shows intact GATA3 expression; however, it is notable that some cases (15.9%) show basal loss. Our findings supports the theory that GATA3 basal loss is an early event in the malignant transformation of vulvar epithelium

## 998 High-Grade Transformation of Ovarian Serous Borderline Tumors: A Series and Literature Review, Emphasizing Distinctive Morphology with Abundant Dense Eosinophilic Cytoplasm, Driver Mutations, and Extremely Dismal Prognosis

Xiaoming Zhang<sup>1</sup>, Kelly Devereaux<sup>2</sup>, Emily Ryan<sup>3</sup>, Fei Fei<sup>4</sup>, Christian Kunder<sup>4</sup>, Teri Longacre<sup>3</sup>

<sup>1</sup>Stanford University School of Medicine, Stanford, CA, <sup>2</sup>NYU Grossman School of Medicine, NY, <sup>3</sup>Stanford University, Stanford, CA, <sup>4</sup>Stanford Medicine/Stanford University, Stanford, CA

**Disclosures:** Xiaoming Zhang: None; Kelly Devereaux: None; Emily Ryan: None; Fei Fei: None; Christian Kunder: None; Teri Longacre: None

**Background:** Ovarian serous borderline tumors (SBT) generally have a favorable prognosis but rare cases associated with a high-grade (HG) component have been reported. Here we report the features of 6 SBTs with the presence of a morphologically unique HG component with an associated extremely dismal prognosis.

**Design:** The 6 cases were collected from our pathology archives (1992-2022). Targeted gene panel was performed in 4 cases. A comprehensive literature review was conducted and a total of 26 cases with the development of HG carcinoma from SBT/low-grade serous carcinoma (LGSC) were identified (Table). To compare survival, the follow-up data for 45 conventional high-grade serous carcinomas (HGSC) from TCGA and 16 advanced/recurrent SBTs from a previously published study were utilized.

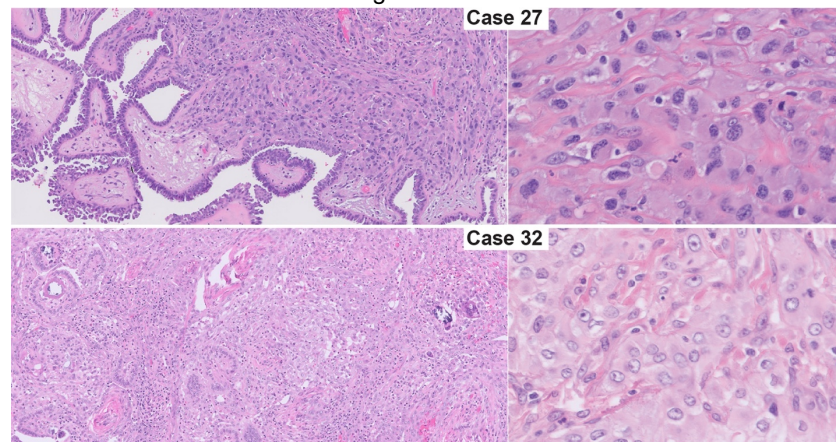
**Results:** The HG component of all 6 cases demonstrated a proliferation of epithelioid cells with abundant dense eosinophilic cytoplasm (AEC) and variable pleomorphism – each of which presented a challenging differential diagnosis that included clear cell carcinoma, mesothelioma, microinvasive SBT or LGSC, epithelioid sarcoma, and a histiocytic proliferative process (Fig. 1). Identical driver mutations were identified in both HG and SBT components in 3 cases (*BRAF* in 2, *KRAS* in 1), confirming clonality (Fig. 2). The remaining case showed *KRAS* mutation in SBT (sequencing failed in HG due to inadequate DNA). Additionally, both HG and SBT in one case harbored *TERT* promoter mutation, which has been previously reported in a case of carcinosarcoma arising from LGSC. All patients in our series with available follow-up data died within 1-9 months of diagnosis. Integrated survival analysis showed that patients with HG transformation of SBT/LGSC (n=21) had a significantly worse prognosis than conventional HGSCs or advanced/recurrent SBTs ( $P <0.05$ ), with cases showing unique AEC morphology being the worst (Fig. 2).

**Table. Summary of high-grade neoplasms in association with ovarian low-grade serous neoplasms, including prior published and current studies**

No.	Age	Stage	Original tumor	Recurrence	AEC in HG	Outcome	Authors
1	49	I	SBT+UC (MN)	NA	UK	DOD 5 mo	Clarke et al, 1987
2	72	IV	SBT+CS (MN)	NA	UK	DOD 8 d	
3	41	I	SBT+SC (MN)	SC 3 mo	UK	DOD 6 mo	De Rosa et al, 1991
4	49	I	SBT+SC (MN)	SC 8 mo	UK	DOD 32 mo	Andrews et al, 2008
5	49	III	SBT+HGSC	NA	UK	DOD 10 mo	Malpica et al, 2004
6	50	I	SBT	HC 27 mo	UK	DOD 16 mo	Parker et al, 2004
7	61	III	SBT	SC 18 mo	UK	AWD 6 mo	
8	43	III	SBT+HGSC	NA	UK	UK	
9	49	III	SBT+HGSC	NA	UK	UK	
10	55	III	LGSC+HGSC	NA	UK	UK	
11	39	III	LGSC+HGSC	NA	UK	UK	Dehari et al, 2007
12	31	II	LGSC+HGSC	NA	UK	UK	
13	67	I	SBT+HGSC	NA	UK	UK	
14	23	III	SBT/LGSC+HGSC	HGSC 16 mo	UK	UK	Quddus et al, 2009
15	54	III	SBT+SC(MN)	NA	Present	NED 7 mo	Gungor et al, 2010
16	22	II	SBT	SC 10 yr	UK	DOD 12 mo	
17	47	I	SBT	SC 3 yr	UK	DOD 6 mo	Garg et al, 2012
18	35	III	SBT/LGSC	CS 3 yr	UK	AWD 12 mo	
19	52	III	SBT/LGSC	LGSC+UC 4 yr	Present	DOD 1 mo	
20	41	VI	SBT/LGSC+UC	NA	Present	DOD 6 mo	
21	34	III	LGSC+HGSC	NA	UK	AWD 17 mo	
22	63	I	SBT/LGSC	HGSC 5 yr	UK	DOD 12 mo	Boyd et al, 2012
23	78	III	SBT+HGSC	NA	UK	AWD 36 mo	
24	52	I	SMBT	HGSC 1 yr	UK	UK	
25	63	III	SBT+HGSC	UK	UK	UK	
26	67	III	SBT/LGSC	CS 18 mo	UK	DOD 2 mo	Tavallaei et al, 2019
27	78	III	SBT+HC AEC	NA	Present	DOD 1 mo	
28	62	III	SBT+HC AEC	NA	Present	DOD 4 mo	
29	79	I	SBT/LGSC+ HC AEC	UK	Present	UK	
30	23	III	SBT	HC AEC 4 mo	Present	UK	
31	50	I	SBT	HC AEC	Present	DOD 9 mo	

Abbreviations: AEC, abundant dense eosinophilic cytoplasm; AWD, alive with disease; CS, carcinosarcoma; HC, high-grade carcinoma; HG, high-grade tumor; HGSC, high-grade serous carcinoma; LGSC, low-grade serous carcinoma; MN, mural nodule; NA, not applicable; NED, no evidence of disease; SBT, serous borderline tumor; SMBT, seromucinous borderline tumor; SC, sarcomatoid carcinoma; UC, undifferentiated carcinoma; UK, unknown

**Figure 1 - 998**

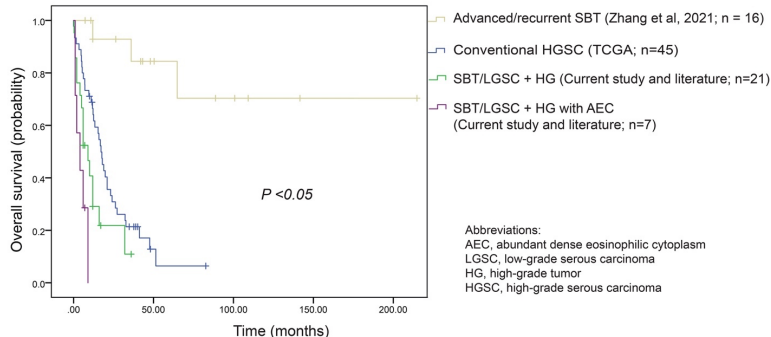
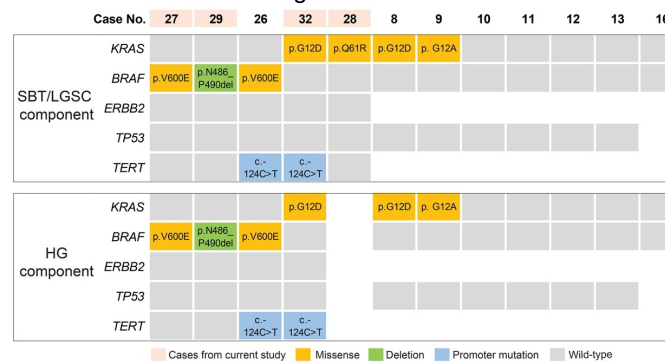


Immunohistochemical results of the high-grade carcinoma

Case	CK7	CK20	PAX8	P16	P53	ER	PR	Napsin	WT1	Calretinin	D2-40	MOC31	BeREP4	INI
27	+	-	+	+(F)	Het	-	-	-	-	-	-	+(P)	-	Intact
28	+	+(F)	+	-	Het	-	-	-	-	+(F)	-	+(P)	+(F)	Intact
29	+	-	+	-	NA	-	-	-	-	-	-	+(F)	-	Intact
30	+	-	+	+(patchy)	Het	-	-	-	-	-	-	+(P)	-	Intact
31	NA	NA	NA	NA	NA	NA	NA	NA	NA	NA	NA	NA	NA	NA
32	+	-	+	-	Het	-	NA	NA	+ (P)	-	NA	+(P)	NA	Intact

Abbreviations: F, focal; Het, heterogeneous (wild-type) pattern; P, patchy; NA, not assessed

Figure 2 - 998



**Conclusions:** Our study confirmed that ovarian SBT may occasionally undergo transformation to a high-grade tumor, which tends to be more clinically aggressive than conventional HGSCs. In particular, cases with unique AEC morphology, some of which may be deceptively bland looking, exhibited an extremely dismal prognosis. Importantly, we found *BRAF* as well as *KRAS* mutations were enriched in these high-grade transformed SBTs with AEC morphology, which questions the notion that *BRAF* is associated with improved outcome in SBTs. In addition, the role of *TERT* promoter mutation deserves further investigation in these tumors.

## 999 Limited ER Expression and Mixed Sarcomatous Histology are not Uncommon in Mesonephric-type Malignancy of the Gynecologic Tract: A Clinicopathological Review of 22 Cases

Zitong Zhao<sup>1</sup>, Yen Yeo<sup>2</sup>, Sangeeta Mantoo<sup>1</sup>

<sup>1</sup>Singapore General Hospital, Singapore, Singapore, <sup>2</sup>KKH, Singapore, Singapore

**Disclosures:** Zitong Zhao: None; Yen Yeo: None; Sangeeta Mantoo: None

**Background:** Mesonephric adenocarcinoma (MA) and mesonephric-like adenocarcinoma (MLA) are uncommon neoplasms of the gynecologic tract, share similar morphology and immunoprofiles, usually ER negative and p53 wild type. MAs originate from mesonephric remnants, while MLAs are from Mullerian epithelium with mesonephric transdifferentiation and maybe associated with endometriosis-related pathology. Mixed sarcomatous component is rarely reported.

**Design:** A search of the laboratory information system for MA/MLAs in two local institutions between January 2010 and July 2022 was performed. Clinicopathological characteristics and available molecular results were reviewed (Table 1).

**Results:** A total of 10 biopsies and 23 resection specimens from 22 patients were identified. The mean age was 57.5 years (range: 39 - 73 years). Most common primary sites include ovary, endometrium and cervix. One case had lung metastasis and 2 cases had tumor recurrence. Macroscopically, MA/MLAs often showed greyish fleshy appearance with focal hemorrhage and necrosis. In the ovary, focal cystic component was a common finding and the average tumor size was 12.9cm (range: 4 - 23cm), with frequent ovarian capsular disruption (9/11, 81.8%). Microscopically, they generally displayed admixed tubules with eosinophilic secretions, solid and papillary patterns, featuring mild to moderate cytologic atypia. Lymphovascular invasion (6/22), nodal (3/15) and peritoneal (7/22) disease were sometimes seen. Associated endometriosis and/or adenomyosis were frequently present (16/22, 72.7%). Mixed carcinomatous component, such as clear cell and endometrioid carcinomas, was identified in 5 cases. Interestingly, one MLA derived from ovarian high grade adenosarcoma (Figure 1), and one MLA was a component of endometrial carcinosarcoma (Figure 2). Variable TTF1, GATA3 and CD10 positivity was present in 72.7% (16/22), 100% (21/21) and 81.0% (17/21) cases. ER expression was observed in 33.3% (7/21) cases, mostly focal and weak. Immunohistochemistry of DNA

mismatch repair proteins was performed in 9 cases and all showed normal expression, confirmed with microsatellite stability in 5 cases. KRAS or NRAS mutations were identified in 3 cases by next generation sequencing.

	Feature	No. of cases with feature (%)
Primary tumour site	ovary	11/22 (55.0%)
	endometrium	6/22 (27.3%)
	others (cervix, vagina and posterior uterine wall)	5/22 (22.7%)
Mixed malignancy within the tumour	clear cell carcinoma	3/22 (13.6%)
	endometrioid carcinoma	2/22 (9.1%)
	sarcoma	2/22 (9.1%)
Other malignancy in ovarian cases	synsynchronous, low grade endometrioid carcinoma in the contralateral ovary	1/22 (4.5%)
	synsynchronous, mesonephric like adenocarcinoma in the contralateral ovary	1/22 (4.5%)
	synsynchronous, low grade endometrioid carcinoma in the endometrium	1/22 (4.5%)
Endometriosis-related pathology	endometriosis / adenomyosis	16/22 (72.7%)
	borderline endometrioid tumor	2/22 (9.1%)
	seromucinous adenofibroma	1/22 (4.5%)
Immunohistochemistry	TTF1, variable expression	16/22 (72.7%)
	GATA3, variable expression	21/21 (100%)
	CD10, luminal staining	17/21 (81.0%)
	ER, variable expression	7/21 (33.3%)
	DNA mismatch repair proteins, no loss	9/9 (100%)
Molecular analysis	KRAS mutation	2/3 (66.7%)
	NRAS mutation	1/3 (33.3%)
	microsatellite stable	5/5 (100%)

Figure 1 - 999

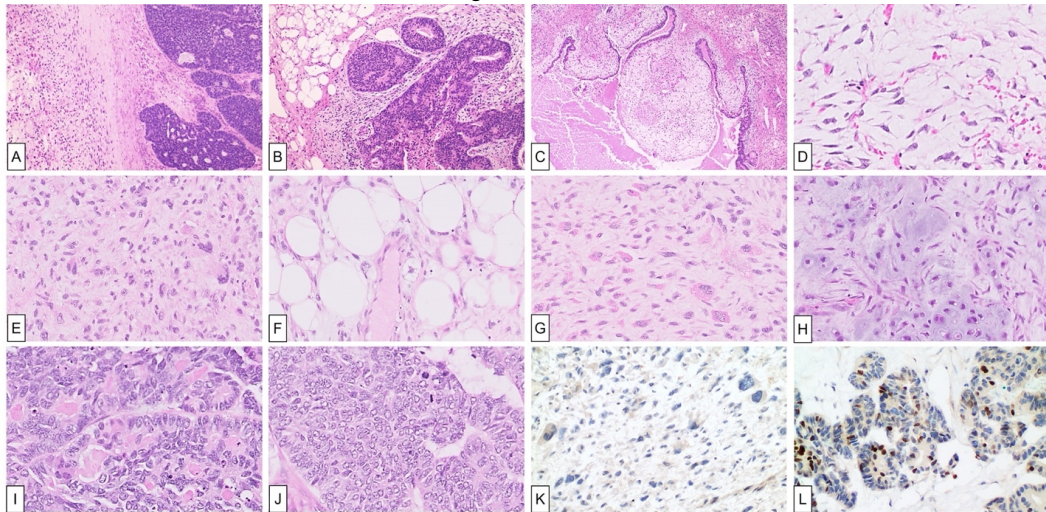


Figure 1. Histologic features of a mesonephric-like adenocarcinoma arising from high grade adenosarcoma of the ovary. Carcinomatous and sarcomatous components were arranged with abrupt transition (A), closely intermingled (B), and partly cystic epithelial component with phyllodes-like pattern (C). High grade sarcomatous component displayed a divergent morphology including myxoid areas (D), pleiomorphic spindle and epithelioid cells (E), liposarcomatous differentiation (F), as well as rhabdomyosarcoma (G) and chondrosarcoma-like areas (H). Carcinomatous elements with back-to-back small tubules containing eosinophilic secretions (I) and solid areas (J). P53 immunostain showed mutant type (null pattern) expression in sarcomatous component (K), and wild type expression in carcinomatous component (L).

Figure 2 - 999

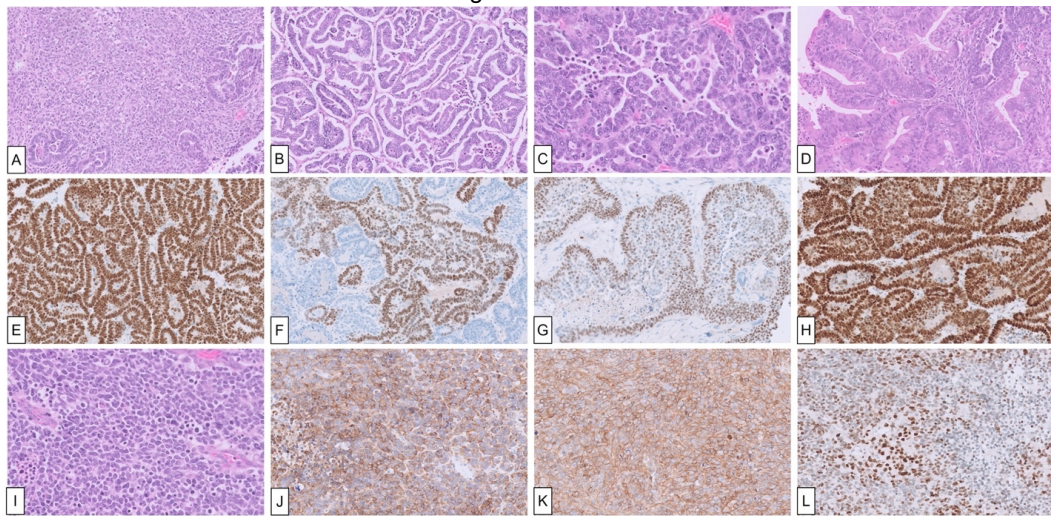


Figure 2. Histologic features of a mesonephric-like adenocarcinoma as part of an endometrial carcinosarcoma.

Carcinomatous and sarcomatous components were closely intermingled (A). Mesonephric-like adenocarcinoma (MLA) showed predominantly tubuloglandular growth (B), with focal serous-like papillary pattern and nuclear pleomorphism (C). There was focal mixed low grade endometrioid carcinoma component (D). MLA was diffusely positive for GATA3 (E), patchily positive for TTF1 (F), with focal weak ER expression (G), and mutant type (diffuse nuclear staining) expression of p53 (H). High grade sarcomatous component displayed a significant portion of discohesive sheets of round cell morphology, with diffuse reaction for synaptophysin (J) and CD99 (K), as well as wild type expression (heterogenous nuclear staining) of p53 (L).

**Conclusions:** MA/MLAs are clinically aggressive and may present with high stage disease. Mixed carcinomatous, and rarely sarcomatous component can be seen. The occasional presence of ER expression implies the potential therapeutic target in selected cases.

#### 1000 Inflammatory Myofibroblastic Tumor of Female Genital Tract: A Clinicopathological, Immunohistochemical, and Molecular Analysis of 47 Cases

Ke Zuo<sup>1</sup>, Meng-yuan Shao<sup>2</sup>, Xiaoan Zhang<sup>1</sup>, Lin Yu<sup>2</sup>, Qianlan Yao<sup>3</sup>, Gang Ji<sup>3</sup>, Qianming Bai<sup>1</sup>, Yufan Cheng<sup>1</sup>, Rui Bi<sup>3</sup>, Xiaoyu Tu<sup>1</sup>, Dan Huang<sup>4</sup>, Bin Chang<sup>3</sup>, Xiaoyan Zhou<sup>3</sup>, Wentao Yang<sup>1</sup>, Jian Wang<sup>2</sup>

<sup>1</sup>Fudan University Shanghai Cancer Center, Shanghai, China, <sup>2</sup>Fudan University Shanghai Cancer Center, Fudan University, Shanghai, China, <sup>3</sup>Fudan University Shanghai Cancer Center, Shanghai Medical College, Fudan University, Shanghai, China, <sup>4</sup>Fudan University Shanghai Cancer Center, Fudan University Shanghai Medical College, Shanghai, China

**Disclosures:** Ke Zuo: None; Meng-yuan Shao: None; Xiaoan Zhang: None; Lin Yu: None; Qianlan Yao: None; Gang Ji: None; Qianming Bai: None; Yufan Cheng: None; Rui Bi: None; Xiaoyu Tu: None; Dan Huang: None; Bin Chang: None; Xiaoyan Zhou: None; Wentao Yang: None; Jian Wang: None

**Background:** Inflammatory myofibroblastic tumor of the female genital tract (FGT-IMT) is extremely rare. Herein, we reported the largest series of FGT-IMT to further investigate its clinicopathological, immunohistochemical and molecular features.

**Design:** We collected 47 cases of FGT-IMT diagnosed in the Department of Pathology, Fudan University Shanghai Cancer Center since 2015. Clinical and follow-up data were reviewed. Immunohistochemistry (IHC), fluorescence in situ hybridization (FISH) and RNA-sequencing were performed.

**Results:** The median age at diagnosis was 43 years (range,23-65y). 39 cases occurred in the uterine corpus, 5 cases in the uterine cervix and 3 cases in the abdominal and pelvic cavity. 44 cases were consultation cases and 3 cases were diagnosed and treated in our center. The original pathological diagnosis for consultation was mainly confused with myxoid smooth muscle tumors and endometrial stromal tumors. Histologically, the tumors mainly showed loose myxoid and/or fascicular pattern. Tumor cells were spindled with mild nuclear atypia and variable mitotic figures were found. Epithelioid cells were present in some areas. The density and distribution of the inflammatory cells varied among cases, even could be inconspicuous. Tumor cells were positive for desmin, SMA, ALK, ER, PR and Ki-67(median,10%). 87.9% (29/33) of cases showed ALK rearrangement by FISH tests. RNA-seq was performed in 16 cases. The gene fusion pattern included IGFBP5-ALK(n=6), FN1-ALK(n=2), TIMP3-ALK(n=2), THBS1-ALK(n=2), TNS1-ALK(n=1), ROS1-TFG(n=1) and ROS1-FN1(n=1). Interestingly, 1 case harbored 3 different fusions (IGFBP5-ALK, TWIST2-COL6A3 and ACTN4-AKT2). 41 patients had follow-up information (range,1.2-86.5mo.; median,30.97mo.). 6 patients experienced local recurrence and 3 of them received Crizotinib as subsequent treatment, 2 patients died of the disease and 1 patient died due to high grade serous carcinoma.

# ABSTRACTS | GYNECOLOGIC AND OBSTETRIC PATHOLOGY

Clinicopathological and molecular characteristics of 48 case of IMT in the female genital tract	
Age	23-65y (median,43y)
Location	
Uterine corpus	39/47 (83.0%)
Uterine cervix	5/47 (10.6%)
Abdominal and pelvic cavity	3/47(6.4%)
Immunohistochemical staining	
ALK	43/47 (91.5%)
SMA	30/38 (78.9%)
Desmin	42/46 (91.3%)
ER	18/28 (64.3%)
PR	24/32 (75.0%)
H-caldesmon	13/35 (37.1%)
CD10	14/31 (45.2%)
Ki-67	2-40% (median,10%)
FISH test	
ALK-positive	29/33 (87.9%)
ROS1-positive	1/33 (3.0%)
RNA-seq	IGFBP5-ALK, FN1-ALK, TIMP3-ALK, THBS1-ALK, TNS1-ALK, ROS1-TFG, ROS1-FN1, TWIST2-COL6A3, ACTN4-AKT2
Follow-up (range: 1.3-86.5mo.; median: 30.97mo.)	
No evidence of disease	33/41 (80.5%)
Local recurrence	6/41 (14.6%)
Dead of the disease	2/41 (4.9%)

**Conclusions:** IMT in the female genital tract has been increasingly recognized in recent years. ALK IHC or FISH test can help to distinguish them from those morphologically similar tumors. A small number of uterine IMT have ROS1 translocation, and our study reported a new ROS1-TFG gene fusion in uterine IMT. For ALK negative tumors, it is important to perform ROS1 IHC and/or molecular analysis. Since aggressive behavior can be presented in some IMTs, recognition of this rare mesenchymal neoplasm is crucial.